METHODS IN PHARMACOLOGY AND TOXICOLOGY

Methods in Biological Oxidative Stress

Edited by

Kenneth Hensley

Robert A. Floyd

HUMANA PRESS

Methods in Biological Oxidative Stress

METHODS IN PHARMACOLOGY AND TOXICOLOGY

Mannfred A. Hollinger, ***PhD*** *SERIES EDITOR*

Methods in Biological Oxidative Stress
edited by ***Kenneth Hensley*** *and* ***Robert A. Floyd,*** *2003*

Apoptosis Methods in Pharmacology and Toxicology: Approaches to Measurement and Quantification
edited by ***Myrtle A. Davis,*** *2002*

Ion Channel Localization: Methods and Protocols
edited by ***Anatoli N. Lopatin*** *and* ***Colin G. Nichols,*** *2001*

METHODS IN PHARMACOLOGY AND TOXICOLOGY

Methods in Biological Oxidative Stress

Edited by

Kenneth Hensley

Robert A. Floyd

Free Radical Biology and Aging Research Program
Oklahoma Medical Research Foundation
Oklahoma City, OK

Humana Press  **Totowa, New Jersey**

999 Riverview Drive, Suite 208
Totowa, NJ 07512

www.humanapress.com

Cover design by Patricia F. Cleary.

For additional copies, pricing for bulk purchases, and/or information about other Humana titles, contact Humana at the above address or at any of the following numbers: Tel.: 973-256-1699; Fax: 973-256-8341; E-mail: humana@humanapr.com or visit our website: http://humanapress.com

This publication is printed on acid-free paper. ∞
ANSI Z39.48-1984 (American National Standards Institute) Permanence of Paper for Printed Library Materials.

Printed in the United States of America. 10 9 8 7 6 5 4 3 2 1

Library of Congress Cataloging-in-Publication Data

Methods in biological oxidative stress / edited by Kenneth Hensley, Robert A. Floyd.
p. cm.
Includes bibliographical references and index.
ISBN 0-89603-815-7 (alk. paper); E-ISBN 1-59259-424-7
1 . Active oxygen in the body--Laboratory manuals. 2. Oxidation, Physiological--Laboratory manuals. 3. Stress (Physiology)--Laboratory manuals. I. Hensley, Kenneth. II. Floyd, Robert A., 1940-

RB170 .M48 2003
616.07--dc21

2002033397

Foreword

Oxidative damage appears to play a central role in the development of a wide range of tissue pathology, including neurodegenerative disease, drug side-effects, xenobiotic toxicity, carcinogenesis, and the aging process, to name just a few.

Because of the centrality of oxidative processes to normal and abnormal tissue function, it has become imperative to develop appropriate analytical techniques to facilitate the quantitation of significant reactants. Without advances in methodology, corresponding advances in our knowledge of underlying biochemical events will be necessarily limited.

Drs. Hensley and Floyd have done an outstanding job of assembling the work of world-class experts into *Methods in Biological Oxidative Stress*. The contributors have presented concise, yet thorough, descriptions of the state-of-the-art methods that any investigator working in the field needs to access.

Mannfred A. Hollinger

Preface

Free radicals and reactive oxidizing agents were once ignored as biochemical entities not worth close scrutiny, but are now recognized as causes or contributing factors in dozens, if not hundreds, of disease states. In addition, free radical metabolisms of xenobiotics have become increasingly important to pharmacologists. Accordingly, the need has arisen to accurately quantify reactive oxygen species and their byproducts.

Methods in Biological Oxidative Stress is practical in scope, providing the details of up-to-date techniques for measuring oxidative stress and detecting oxidizing agents both in vitro and in vivo. The contributors are recognized experts in the field of oxidative stress who have developed novel strategies for studying biological oxidations.

The chapters of *Methods in Biological Oxidative Stress* cover widely used standard laboratory techniques, often developed by the authors, as well as HPLC–electrochemical measurement of protein oxidation products, particularly nitrotyrosine and dityrosine, and HPLC–electrochemical detection of DNA oxidation products. Additionally, recently developed techniques are presented to measure lipid oxidation and nitration products such as 5-NO_2-γ-tocopherol and isoprostanes, using HPLC-electrochemical/photodiode array methods and mass spectrometry as well as electron paramagnetic resonance (EPR) techniques.

In scope, presentation, and authority therefore, *Methods in Biological Oxidative Stress* was designed to be an invaluable manual for clinical laboratories and teaching institutions now conducting routine measurements of biological oxidants and biological oxidative stress or implementing new programs in this vital area of research. As a reference work, this collection of techniques and methods will prove useful for many years to come.

Kenneth Hensley
Robert A. Floyd

Contents

Part II DNA, Protein, and Amino Acids

Contributors

Ian N. Acworth • *ESA Inc., Chelmsford, MA*
Joe A. Archangelo • *ESA Inc., Chelmsford, MA*
Nathalie Bernoud-Hubac • *Departments of Pharmacology and Medicine, Vanderbilt University, Nashville, TN*
Olivier Boutaud • *Departments of Pharmacology and Medicine, Vanderbilt University, Nashville, TN*
Cynthia J. Brame • *Departments of Pharmacology and Medicine, Vanderbilt University, Nashville, TN*
D. Allan Butterfield • *Sanders-Brown Center on Aging, Center of Membrane Sciences, Department of Chemistry, University of Kentucky, Lexington, KY*
Jaeman Byun • *Department of Medicine, Washington University School of Medicine, St. Louis, MO*
Alessandra Castegna • *Sanders-Brown Center on Aging, Center of Membrane Sciences, Department of Chemistry, University of Kentucky, Lexington, KY*
Alexander Christov • *Department of Pathology, University of Oklahoma Health Sciences Center; Oklahoma Center for Neuroscience, Oklahoma City, OK*
Sean S. Davies • *Departments of Pharmacology and Medicine, Vanderbilt University, Nashville, TN*
Jennifer Drake • *Sanders-Brown Center on Aging, Center of Membrane Sciences, Department of Chemistry, University of Kentucky, Lexington, KY*
Scott Ferrell • *Free Radical Biology and Aging Program, Oklahoma Medical Research Foundation, Oklahoma City, OK*
Joshua P. Fessel • *Departments of Pharmacology and Medicine, Vanderbilt University, Nashville, TN*
Robert A. Floyd • *Free Radical Biology and Aging Program, Oklahoma Medical Research Foundation, Oklahoma City, OK*
Paul H. Gamache • *ESA Inc., Chelmsford, MA*
Joseph P. Gaut • *Department of Medicine, Washington University School of Medicine, St. Louis, MO*

Paula Grammas • *Department of Pathology, University of Oklahoma Health Sciences Center; Oklahoma Center for Neuroscience, Oklahoma City, OK*
Ladan Hamdheydari • *Department of Pathology, University of Oklahoma Health Sciences Center; Oklahoma Center for Neuroscience, Oklahoma City, OK*
Jay W. Heinecke • *Department of Medicine, Washington University School of Medicine, St. Louis, MO*
Kenneth Hensley • *Free Radical Biology and Aging Program, Oklahoma Medical Research Foundation, Oklahoma City, OK*
Mark M. Huycke • *The Muchmore Laboratories for Infectious Diseases Research; Research Service, Department of Veterans Affairs Medical Center; Department of Medicine, University of Oklahoma Health Sciences Center, Oklahoma City, OK*
Yashige Kotake • *Free Radical Biology and Aging Program, Oklahoma Medical Research Foundation, Oklahoma City, OK*
Mark A. Lovell • *Sanders-Brown Center on Aging, Department of Chemistry, University of Kentucky, Lexington, KY*
William R. Markesbery • *Sanders-Brown Center on Aging, Departments of Pathology and Neurology, University of Kentucky, Lexington, KY*
Danny R. Moore • *Department of Pharmacology and Toxicology, College of Pharmacy, University of Oklahoma, Oklahoma City, OK*
Jason D. Morrow • *Departments of Medicine and Pharmacology, Vanderbilt University, Nashville, TN*
Shenyun Mou • *Free Radical Biology and Aging Research Program, Oklahoma Medical Research Foundation, Oklahoma City, OK*
Jun Nakamura • *Department of Environmental Sciences and Engineering, University of North Carolina, Chapel Hill, NC*
Chava Pocernich • *Sanders-Brown Center on Aging, Center of Membrane Sciences, Department of Chemistry, University of Kentucky, Lexington, KY*
Quentin N. Pye • *Free Radical Biology and Aging Program, Oklahoma Medical Research Foundation, Oklahoma City, OK*
Lester A. Reinke • *Department of Pharmacology and Toxicology, College of Pharmacy, University of Oklahoma, Oklahoma City, OK*
L. Jackson Roberts, II • *Departments of Pharmacology and Medicine, Vanderbilt University, Nashville, TN*
Hong Sang • *Free Radical Biology and Aging Program, Oklahoma Medical Research Foundation, Oklahoma City, OK*

KIMIHIKO SATOH • *Department of Organic Function, Hirosaki University School of Health Sciences, Hirosaki, Japan*
JAMES A. SWENBERG • *Department of Environmental Sciences and Engineering, University of North Carolina, Chapel Hill, NC*
KOJI UCHIDA • *Laboratory of Food and Biodynamics, Graduate School of Bioagricultural Sciences, Nagoya University, Nagoya, Japan*
PAUL A. ULLUCCI • *ESA Inc., Chelmsford, MA*
KELLY S. WILLIAMSON • *Free Radical Biology and Aging Program, Oklahoma Medical Research Foundation, Oklahoma City, OK*

I

Lipids

1

Measurement of Fat-Soluble Vitamins and Antioxidants by HPLC With Electrochemical Array Detection

Paul H. Gamache, Paul A. Ullucci, Joe A. Archangelo, and Ian N. Acworth

1. INTRODUCTION

Fat-soluble vitamins and antioxidants (FSVAs) are a structurally diverse group of compounds (Fig. 1) that play important roles in a wide spectrum of biochemical and physiological processes, e.g., photoreception (vitamin A, retinol); plasma calcium homeostasis (vitamin D2, ergocalciferol; vitamin D3, cholecalciferol); and blood clotting (vitamin K1, phylloquinone). Of considerable interest is the involvement of some FSVAs in oxidative metabolism and the prevention of damage by reactive oxygen species (ROS) *(1,2)*. For example, α-tocopherol (vitamin E) is the primary antioxidant species in the membrane. Here it intercepts lipid peroxyl radicals, thereby inhibiting lipid peroxidation, a self-perpetuating chain reaction, and preventing catastrophic membrane damage. α-Tocopherol is thought to be regenerated from the resulting α-tocopheryl radical by reaction with reduced coenzyme Q10 (CoQ10) (the ubiquinone/ubiquinol system) also located within the membrane, or with cytosolic ascorbic acid (or glutathione) at the cytoplasm-membrane interface *(1,2)*. Another form of vitamin E, γ-tocopherol, readily reacts with reactive nitrogen species (RNS) such as peroxynitrite to form 5-nitro-γ-tocopherol, a marker of RNS production *(3)*.

Tissue levels of FSVAs can be measured following HPLC separation by a variety of detectors either alone (e.g., ultraviolet [UV], photodiode array [PDA], fluorescence) or in combination (absorbance-fluorescence, absorbance-electrochemical, electrochemical-fluorescence) *(4,5)*. Electrochemi-

From: *Methods in Pharmacology and Toxicology: Methods in Biological Oxidative Stress*
Edited by: K. Hensley and R. A. Floyd © Humana Press Inc., Totowa, NJ

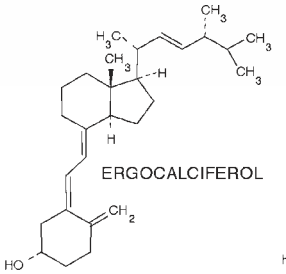

ERGOCALCIFEROL

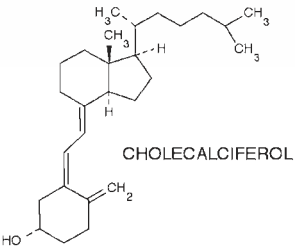

CHOLECALCIFEROL

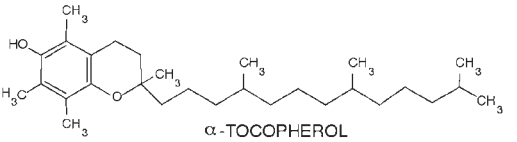

α-TOCOPHEROL

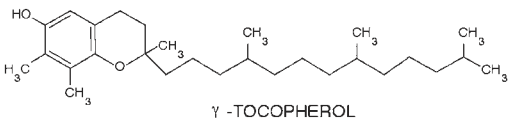

γ -TOCOPHEROL

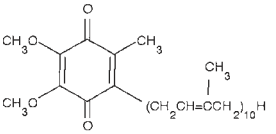

UBIQUINONE-10

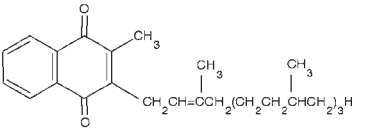

PHYLLOQUINONE

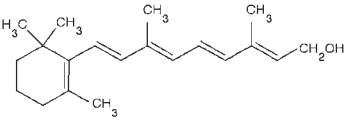

ALL-TRANS RETINOL

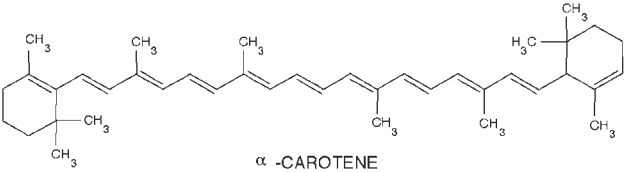

α -CAROTENE

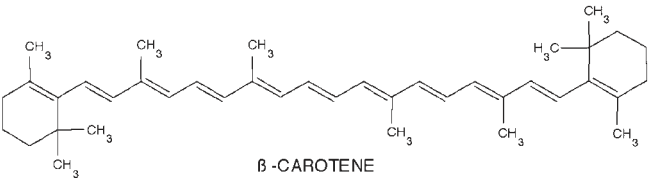

ß -CAROTENE

cal detection (ECD) is typically chosen for its enhanced selectivity and sensitivity, especially when trying to measure low levels of analytes (e.g., K1, CoQ10) in low volume-low level samples (e.g., fasting or neonatal plasma). Single- and dual-channel ECDs are typically used at settings that are suitable for only a few analytes at the expense of others' whereas multi-component analyses are limited by the poor compatibility of thin-layer amperometric electrodes with gradient elution chromatography *(6)*.

An alternate electrochemical approach uses a serial array of highly efficient (coulometric) flow-through graphite working electrodes maintained at different but constant potentials, each optimal for a given analyte or class of analytes (the CoulArray® - ESA Inc.) *(7,8)*. When combined with gradient HPLC, a three-dimensional chromatogram is generated that identifies an analyte by both retention time and electrochemical (hydrodynamic voltammetric) behavior. The latter, like a photodiode array spectrum, can be used to verify analyte authenticity or to identify co-eluting or misnamed analytes. This approach is finding great use in the field of oxidative metabolism for the measurement of water- and fat-soluble antioxidants, DNA adducts, and protein oxidation products *(2,3,9–11)*.

Presented here are three methods using HPLC-coulometric array detection:

1. Method 1: A global method capable of measuring vitamins A, and E as well as CoQ10, retinoids and carotenoids in plasma and serum.
2. Method 2: A second global method that also includes vitamins D2 and D3 for the analysis of milk sample.
3. Method 3: A method for the measurement of carotenoid isomers in plasma and serum.

2. MATERIALS

1. The analytical system for Methods 1 and 2 consisted of a model 5600 CoulArray 8-channel system with two model 582 pumps, a high pressure gradient mixer, a PEEK® pulse dampener, a model 540 autosampler, a CoulArray thermostatic chamber and a serial array of eight coulometric electrodes (all from ESA, Inc.) The apparatus for Method 3 was the same as the other methods, but used a single pump.
2. Standards for Methods 1 and 2 were obtained from Sigma Chemical Co. (St. Louis, MO). Stock standards were made by dissolving approx 10 mg of each compound in 10 mL of ethanol (EtOH) with the exception of the carotenoids and Q10. For these more lipophilic compounds, ~1.0 mg were dissolved in 5.0 mL of hexane followed by dilution with 15 mL EtOH. Stock solutions were

Fig. 1. The chemical structures of some fat-soluble vitamins and antioxidants.

then assayed spectrophotometrically and assigned a concentration value prior to the addition of 10 mg/L butylated hydroxyanisole (BHA) as a preservative. Stock solutions were stored at –20°C for up to six mo. Dilutions were made weekly in EtOH containing 10 mg/L BHA and stored protected from light at –20°C. Standards for Method 3 were prepared by dissolving ~1 mg/10 mL chloroform followed by dilution in ethanol. Concentration determination, protection, storage, and dilution are the same as for the other methods.

3. The mobile phases and columns were:
   a. Method 1. Phase A: methanol, 0.2 *M* ammonium acetate, pH 4.4 (90:10 v/v). Phase B: methanol, propan-1-ol, 1 *M* ammonium acetate, pH 4.4 (78:20:2 v/v/v). MD 150 C18 (150 × 3 mm; 3 μm particle) (ESA, Inc.).
   b. Method 2. Phase A: acetonitrile, water (containing 20 m*M* sodium perchlorate and 5 m*M* perchloric acid) (90:10 v/v). Phase B: acetonitrile, propan-1-ol (containing 20 m*M* sodium perchlorate and 10 m*M* perchloric acid) (65:35 v/v). Betasil Basic C18 (250 × 4.6 mm; 5 μm) (Keystone).
   c. Method 3. Methanol: methyl-tert-butyl ether, 1.0 *M* ammonium acetate, pH 4.4 (63:35:2 v/v/v). Carotenoid C30 (250 × 4.5 mm; 5 μm) (ESA, Inc.).

3. METHODS

1. Gradient profiles, flow rate, temperature, and applied potentials:
   a. Method 1. Gradient profile, 10 min linear gradient from 0–80% B. A 10-min linear gradient from 80–100% B. 7 min isocratic 100% B before returning to initial conditions for 5 min for a total run time of 32 min. The flow rate was 0.8 mL/min and the temperature – +37°C. The applied potentials were +200, +400, +500, +700, +800, –1000, –1000, and +500 mV (vs palladium reference).
   b. Method 2. Gradient profile, 20 min linear gradient from 10–100%B followed by a 5 min hold at 100% B before returning to initial conditions for 5 min. The total run time was 30 min. The flow rate was 1.5 mL/min and the temperature was 32°C. The applied potentials were –700 mV, +100, +250, +400, +550, +800 and +850mV.
   c. Method 3. The assay was isocratic with a flow rate of 1.0 mL/min. The temperature was 28°C and the applied potentials were +100, +160, +220, +280, +340, +400, +460, and +520 mV.
2. Sample preparation.
   a. Method 1. Reference sera were obtained from the National Institute of Standards and Technology (NIST, Gaithersburg, MD). A 0.2 mL volume of serum (or plasma) or standard mixture was vortexed (1 min) with 0.2 mL diluent and 10 μL of 10 μg/mL retinyl acetate as internal standard; 1.0 mL of hexane was added and the resulting mixture was vortexed (10 min) and centrifuged (4000*g*, 10 min). Supernatant (0.8 mL) was withdrawn and the sample was re-extracted, as above, with an additional 1.0mL of hexane. Combined extracts were evaporated under nitrogen, the residue was dissolved in 0.2mL diluent.

b. Method 2. Milk samples (unsaponified): A 1.0 mL volume, augmented with 10 μL of 1.0 μg/mL D2 (internal standard), was thoroughly mixed with 3.0 mL diluent and 0.1 g magnesium sulfate. The resulting mixture was extracted two times with 4.0 mL hexane. Combined hexane extracts were evaporated under a stream of nitrogen and residue was dissolved in 1.0 mL of diluent. The solution was centrifuged as in Method 1. Milk samples (saponified): a 1.0 mL volume of milk was mixed with 1.75 mL 85% aqueous EtOH containing 75 mg/mL potassium hydroxide and 0.25 mg/mL ascorbic acid. The sample was then placed in a heated water bath for 45 min at 95°C. Saponified samples were then extracted as for unsaponified milk samples.
c. Method 3. A 0.5 mL volume of serum or standard was mixed with 0.5 mL ethanol/10 mg/L BHA. After mixing for 1 min, 1.5 mL of hexane was added and after mixing for an additional 10 min was centrifuged (4,000*g*, 10 min). Approx 1.0 mL of supernatant was withdrawn and the remaining sample extracted with an additional 1.5 mL of hexane. Combined hexane extracts were evaporated to dryness under a stream of nitrogen. Finally, the residue was dissolved in 0.25 mL of mobile phase.

4. RESULTS AND DISCUSSION

The global method (Method 1) combines the resolution of gradient HPLC with coulometric array detection to separate and identify FSVAs in under 30 min [Fig. 2A, 2B; extracted standards and a typical NIST (National Institute Science and Technology) control human serum, respectively]. The RNS marker, 5-nitro-γ-tocopherol, eluted at 31 min (data not shown) *(see ref. 3)*. The tocopherols were the most easily oxidized and were measured on channel 1 (200 mV) of the array. The carotenoids responded on channel 2 (400 mV) while the retinoids were the highest oxidizing compounds and reacted mainly on channel 4 (700 mV). Vitamin K1 (not shown) and CoQ10 only responded after their reduction at –1000 mV on channel 6 followed by facile oxidation at +200 mV on channel 7.

The assay had a sensitivity in the low picogram range (e.g., retinol [all-*trans*], α-tocopherol, and CoQ10 were 3.8, 5.1, and 7.5 pg on column, respectively) and was linear from 0–10 μg/mL. Ratio accuracies, indicators of analyte authenticity, were >0.850 *(6,7)*. The levels of analytes determined by this method correlated well with NIST published values (Table 1).

The chromatography and electrochemical array conditions used in Method 2 were optimized for a wide range of FSVAs, including vitamins D2 and D3 (Fig. 3). The first electrode in the array was set to –700 mV to reduce vitamin K1 and CoQ10, these were then measured oxidatively on sensors 2 and 3, respectively.

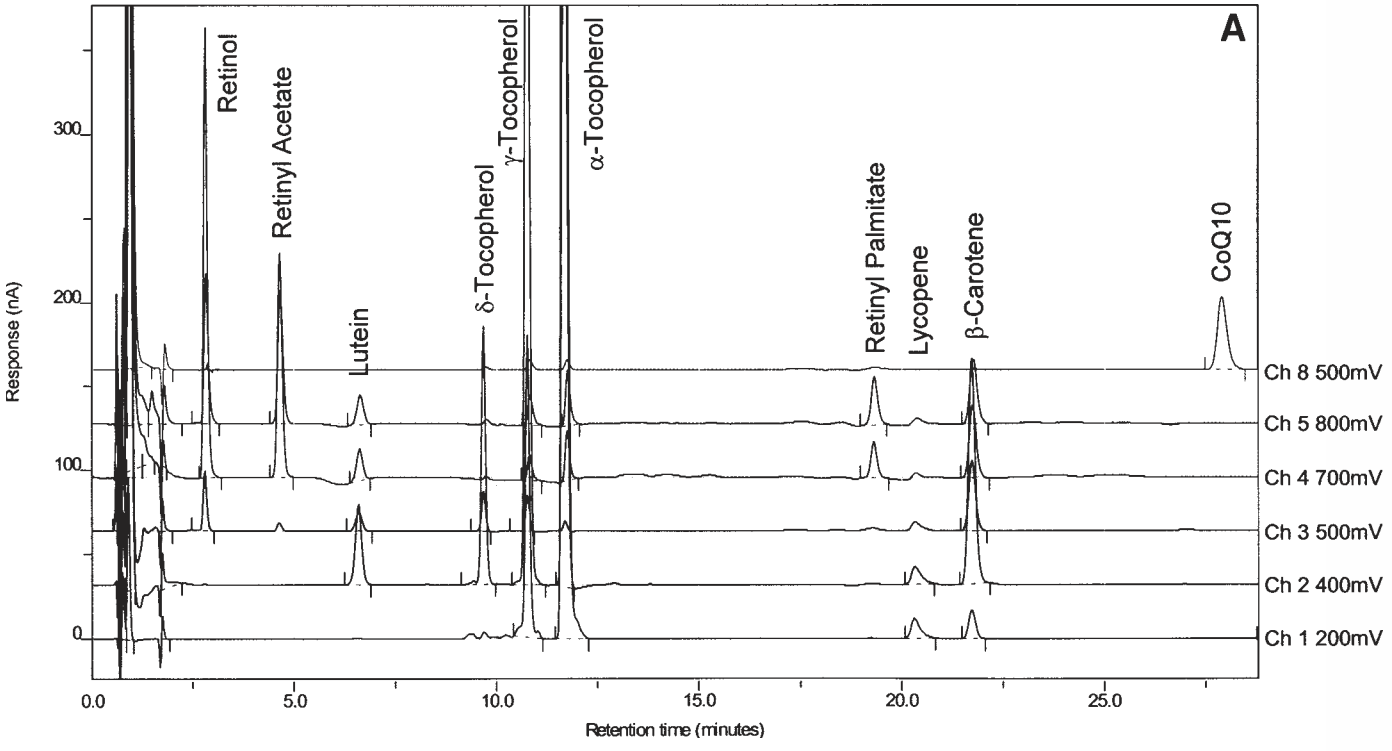

Fig. 2. Gradient HPLC–coulometric array chromatograms of (**A**) extracted standards and (**B**) NIST control plasma sample. Signal from the reduction channels (6 and 7) is not included.

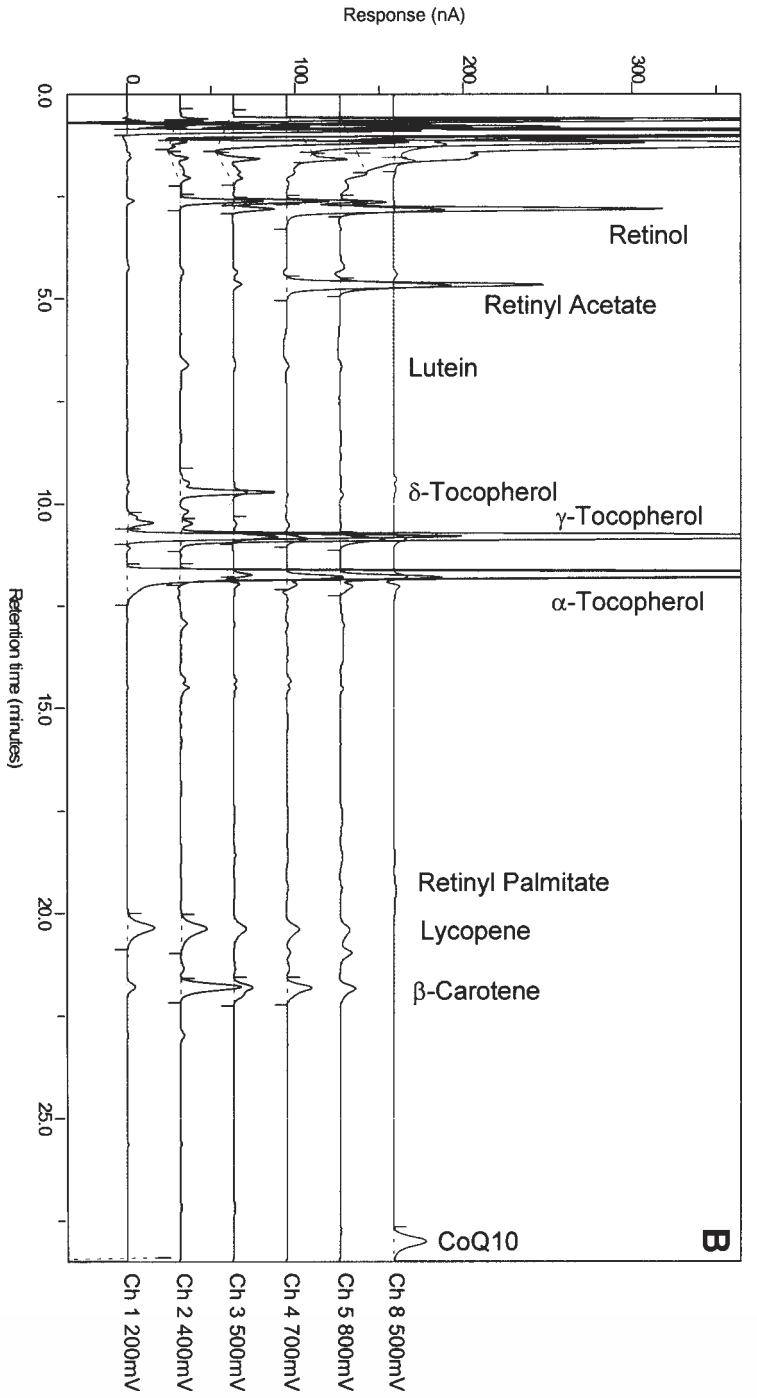
Response (nA)
0
100
200
300
0.0
5.0
10.0
15.0
20.0
25.0
Retention time (minutes)
Retinol
Retinyl Acetate
Lutein
δ-Tocopherol
γ-Tocopherol
α-Tocopherol
Retinyl Palmitate
Lycopene
β-Carotene
CoQ10
B
Ch 1 200mV
Ch 2 400mV
Ch 3 500mV
Ch 4 700mV
Ch 5 800mV
Ch 8 500mV

Table 1
Fat-Soluble Vitamin Performance Data in μg/L (from NIST Round Robin XLVII)

	Example 1		Example 2		Example 3	
Vitamin/Antioxidant	NIST	ESA	NIST	ESA	NIST	ESA
trans-β-Carotene	222 ± 39	262	300 ± 32	346	208 ± 27	216
Coenzyme Q10*	606	606	816	816	550	484
Lutein	107 ± 30	96	210 ± 33	194	100 ± 18	91
trans Lycopene	183 ± 34	214	228 ± 44	228	169 ± 19	179
trans-Retinol	599 ± 34	582	690 ± 71	742	558 ± 55	547
Retinyl Palmitate	118 ± 21	118	114 ± 37	110	121 ± 29	95
α-Tocopherol	11,900 ± 1090	12,730	18,560 ± 1830	20,140	11,150 ± 1000	11,810
δ-Tocopherol	115 ± 64	112	77 ± 95	70	70 ± 86	63
γ-Tocopherol	2340 ± 240	2200	1120 ± 130	1010	2180 ± 320	2040

[a]Note: For Q10, only three labs reported data. Data from refs. *(14–16)*.

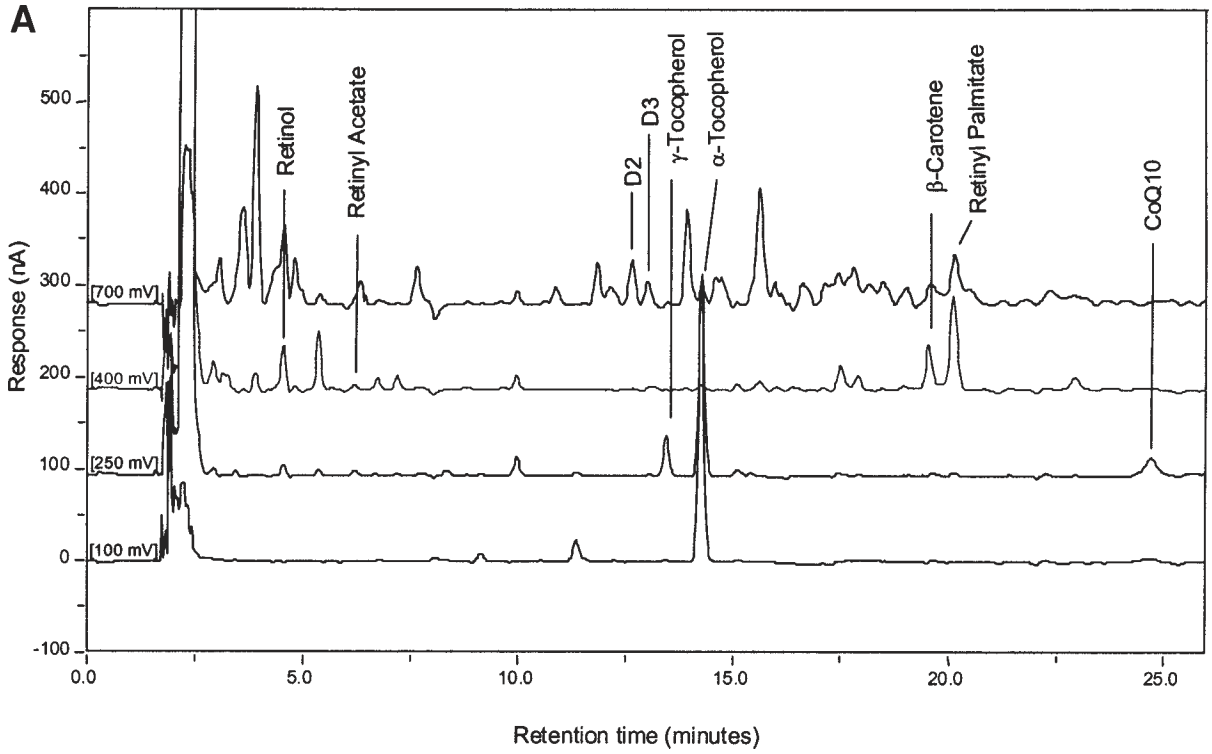

Fig. 3. Gradient HPLC–coulometric array chromatogram of a standard mixture (**A**) and an unsaponified fortified low-fat milk sample (**B**).

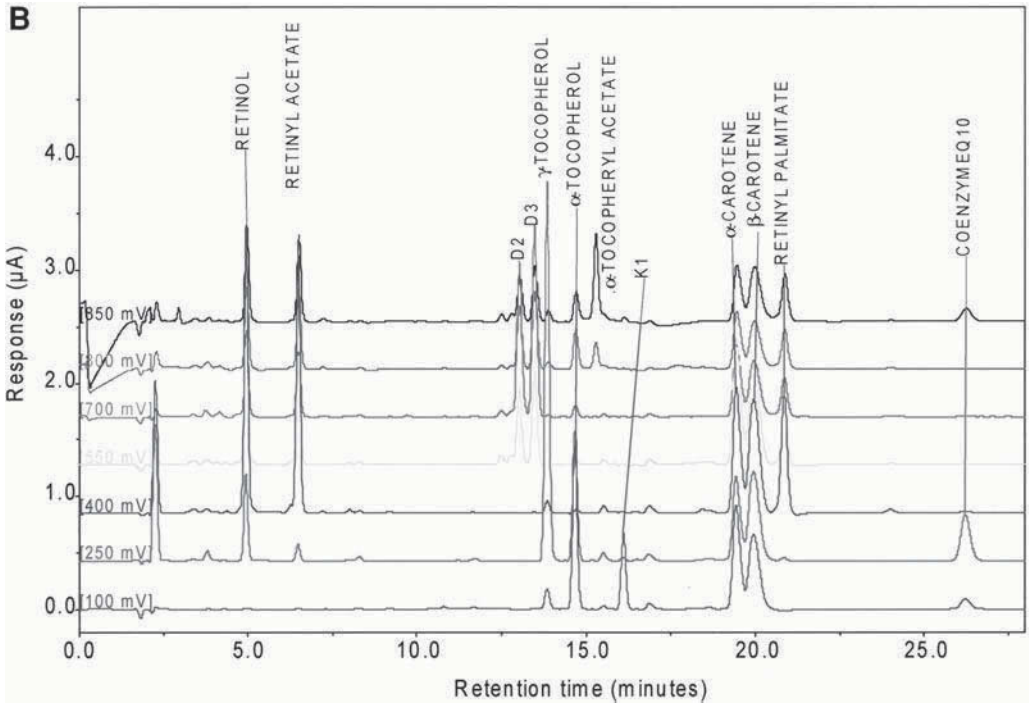
B
RETINOL
RETINYL ACETATE
D2
D3
γ-TOCOPHEROL
α-TOCOPHEROL
α-TOCOPHERYL ACETATE
K1
α-CAROTENE
β-CAROTENE
RETINYL PALMITATE
COENZYMEQ10
[850 mV]
[800 mV]
[700 mV]
[550 mV]
[400 mV]
[250 mV]
[100 mV]
Response (μA)
4.0
3.0
2.0
1.0
0.0
0.0
5.0
10.0
15.0
20.0
25.0
Retention time (minutes)

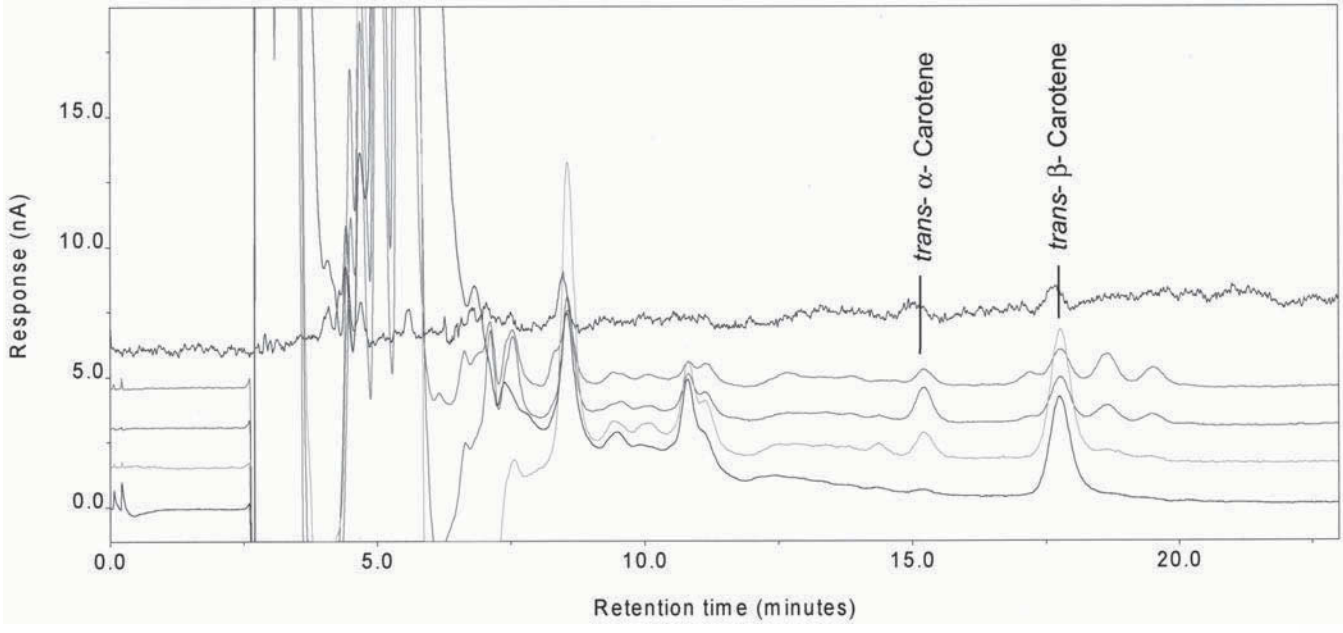

Fig. 4. Isocratic HPLC–coulometric array chromatogram of a low-level human serum sample. We are grateful to Drs. S. Schwartz, M. Ferruzzi, and M. Nguyen (Dept. Food Science and Technology, Ohio State University) for their collaboration in this study.

Fig. 3B shows the feasibility of the method for the determination of vitamins A (as retinol) and D3 (D2 used as an internal standard) in unsaponified fortified low fat (2%) milk. Although the detection of vitamins D2 and D3 is more readily achieved in saponified milk samples, this leads to the loss of carotenoids, tocopherols, and CoQ10 (data not shown) so is unsuitable as part of a global method.

The use of a C30 column in Method 3 enables the separation of a number of carotenoid isomers *(12,13)*. The assay was completed in 25 mins. (Fig. 4). It was linear from 0.1–500 ng (on column) and had a sensitivity of ~20 pg on column (s/n 3:1). A modification of this method has been used to measure carotenoid isomers in different biological microsamples *(13)*.

ACKNOWLEDGMENTS

We are grateful to Drs. S. Schwartz, M. Ferruzzi, and M. Nguyen (Dept. Food Science and Technology, Ohio State University) for their collaboration in this study.

REFERENCES

1. Halliwell, B. and Gutteridge, J. M. C. (1999) *Free Radicals in Biology and Medicine*. Oxford University Press, Oxford, UK.
2. Acworth, I. N., McCabe, D. R., and Maher, T. J. (1997) The analysis of free radicals, their reaction products, and antioxidants, in *Oxidants, Antioxidants and Free Radicals* (Baskin, S. I. and Salem, H., eds.), Washington, DC, Taylor and Francis, pp. 23–77.
3. Hensley, K., Williamson, K. S., Maidt, M. L., Gabbita, S. P., Grammas, P., and Floyd, R. A. (1999) Determination of biological oxidative stress using high performance liquid chromatography with electrochemical detection. *J. High Resol. Chromatogr.* **22,** 429–437.
4. Bui, M. H. (1994) Simple determination of retinol, α-tocopherol and carotenoids (lutein, all-*trans*-lutein, α- and β-carotene) in human plasma by isocratic liquid chromatography. *J. Chromatogr. B* **654,** 129–133.
5. Edlund, P. O. (1988) Determination of coenzyme Q10, a-tocopherol and cholesterol in biological samples by coupled-column liquid chromatography with coulometric and ultraviolet detection. *J. Chromatogr. B* **425,** 87–97.
6. Acworth, I. N. and Bowers, M. (1997) An introduction to HPLC-based electrochemical detection: from single electrode to multi-electrode arrays, in *Coulometric Electrode Array Detectors for HPLC. Progress in HPLC-HPCE*. 6. (Acworth, I. N., Naoi, M., Parvez, H., and Parvez, S., eds.), VSP, The Netherlands, pp. 3–50.
7. Acworth, I. N., Naoi, M., Parvez, H., and Parvez, S., eds. From single electrode to multi-electrode arrays, in *Coulometric Electrode Array Detectors for*

HPLC. Progress in HPLC-HPCE. 6. (Acworth, I.N., Naoi, M., Parvez, H., and Parvez, S., eds.), VSP, The Netherlands.

8. Svendsen, C. N. (1993) Multi-electrode array detectors in high-performance liquid chromatography: a new dimension in electrochemical analysis. *Analyst* **118,** 123–129.
9. Acworth, I. N., Bailey, B. A., and Maher, T. J. (1998) The use of HPLC with electrochemical detection to monitor reactive oxygen and nitrogen species, markers of oxidative damage and antioxidants: application to the neurosciences, in *Neurochemical Markers of Degenerative Nervous Diseases and Drug Addiction. Progress in HPLC-HPCE*. 7. (Qureshi, G. A., Parvez, H., Caudy, P., and Parvez, S., eds.), VSP, The Netherlands, pp. 3–56.
10. Gamache, P. H., Freeto, S. M., and Acworth, I. N. (1999) Coulometric array HPLC analysis of lipid-soluble vitamins and antioxidants. *Am. Clin. Lab.* **18,** 18–19.
11. Gamache, P. H., McCabe, D. R., Parvez, H., Parvez, S., and Acworth, I. N. (1997) The measurement of markers of oxidative damage, anti-oxidants and related compounds using HPLC and coulometric array detection, in *Coulometric Electrode Array Detectors for HPLC. Progress in HPLC-HPCE*. 6. (Acworth, I.N., Naoi, M., Parvez, H., and Parvez, S., eds.), VSP, The Netherlands. pp. 99–126.
12. Emenhiser, C., Sander, L. C., and Schwartz, S. J. (1995) Capability of a polymeric C30 stationary phase to resolve *cis-trans* carotenoid isomers in reversed-phase liquid chromatography. *J. Chromatogr. A* **707,** 205–216.
13. Ferruzzi, M. G., Sander, L. C., Rock, C. L., and Schwartz, S. J. (1998) Carotenoid determination in biological microsamples using liquid chromatography with a coulometric electrochemical array. *Anal. Biochem.* **256,** 74–81.
14. Brown, T. J. and Sharpless, K. E., eds. (1995) *Methods for Analysis of Cancer Chemopreventive Agents in Human Serum*. NIST Special Publication 874. Washington, DC, US Government Printing Office.
15. Duewer et al. (1997) *NIST/NCI Micronutrients Measurement Quality Assurance Program:* Measurement reproducibility, repeatability, stability, and relative accuracy for fat-soluble vitamin-related compounds in human sera. *Anal. Chem.* **69,** 1406–1413.
16. Duewer et al. (1999) *Micronutrients Measurement Quality Assurance Program:* Helping participants use interlaboratory comparison exercise results to improve their long-term measurement performance. *Anal. Chem.* **71,** 1870–1878.

2

Analysis of Aldehydic Markers of Lipid Peroxidation in Biological Tissues by HPLC with Fluorescence Detection

Mark A. Lovell and William R. Markesbery

1. INTRODUCTION

Increasing evidence supports a role for oxidative stress in the neuronal degeneration observed in a spectrum of neurological disorders including stroke, amyotrophic lateral sclerosis (ALS), Parkinson's disease (PD), head trauma, and Alzheimer's disease (AD) (reviewed in ref. *1*). Of particular interest is the role of lipid peroxidation and the aldehydic by-products of lipid peroxidation in the pathogenesis of neuron degeneration in these diseases. Peroxidation of lipids leads to aldehyde formation including C_3–C_{10} straight-chain aldehydes and a series of α,β-unsaturated aldehydes including acrolein and 4-hydroxynonenal (HNE). Although the straight-chain aldehydes have no discernable toxicity, acrolein and HNE are neurotoxic and could potentially play a role in the pathogenesis of AD among other diseases. The most common methods of measuring lipid peroxidation center around measurement of aldehydic by-products, including the use of ultraviolet (UV)-Vis spectrometry to measure the heat mediated-condensation products of aldehydes with thiobarbituric acid in the thiobarbituric acid-reactive substances (TBARs) assay. Although this method will provide an overall measure of aldehyde levels, including malondialdehyde (MDA), it is plagued with interferences from nonlipid derived aldehydes from sugars, amino acids, and DNA, and species resulting from chemical interaction of thiobarbituric acid with nonlipid molecules during the assay *(2)*. Another method that allows measurement of aldehydes is through the use of high pressure liquid chromatography (HPLC) for separation and UV-Vis or fluorescence detection to

From: *Methods in Pharmacology and Toxicology: Methods in Biological Oxidative Stress*
Edited by: K. Hensley and R. A. Floyd © Humana Press Inc., Totowa, NJ

analyze the individual aldehydes. For use with UV-Vis, aldehydic by-products are reacted with 2,4 dinitrophenylhydrazine (2,4 DNPH), whereas detection by fluorescence uses derivatization with 1,3 cyclohexanedione. Comparison of the two detection methods indicates that use of HPLC with fluorescence detection provides the greatest sensitivity and detection limits for aldehydic markers of lipid peroxidation.

2. MATERIALS

1. HEPES buffer, pH 7.4, containing 137 m*M* NaCl, 4.6 m*M* KCl, 1.1 m*M* KH_2PO_4, 0.6 m*M* $MgSO_4$, (0.7 μg/mL) pepstatin, (0.5 μg/mL) leupeptin, (0.5 μg/mL) aprotinin, and (40 μg/mL) phenylmethylsulfonyl fluoride (PMSF) for tissue homogenization.
2. 1.43 μ*M* heptanal in HPLC-grade methanol (internal standard).
3. Cyclohexanedione reagent consisting of 10 g ammonium acetate, 10 mL glacial acetic acid, and 0.25 g 1,3 cyclohexanedione dissolved in 100 mL distilled/deionized water.
4. C_{18} Sep-Pak Plus solid-phase extraction columns preconditioned with 10 mL HPLC-grade methanol followed by 10 mL distilled/deionized water.
5. HPLC-grade chloroform.
6. Dual-pump HPLC system equipped with a C_{18} analytical column and a fluorescence detector operated at an excitation wavelength of 380 nm and an emission wavelength of 446 nm.
7. HPLC-grade tetrahydrofuran (THF) and filtered distilled/deionized water both thoroughly degassed.
8. Pierce bicinchoninic (BCA) or Lowry protein-detection kit.
9. Tissue samples for aldehyde analysis should be frozen immediately after autopsy and be stored at –80°C.

3. METHODS

1. Tissue homogenization: 100 mg frozen tissue is homogenized in 5 mL N_2-purged HEPES buffer using a modified Potter-Elvehjem motor-driven homogenizer or a chilled Dounce homogenizer. The homogenization is carried out on ice and all samples are maintained on ice. Use of 5 mL of homogenization buffer allows a large enough volume for enzyme assays from the same sample of tissue.
2. The method of aldehyde determination is that of Yoshino et al. *(3)* with modification *(4)*. Duplicate 500 μL aliquots of homogenate are added to glass test tubes (to prevent leaching of potential interferences from plastic) along with 500 μL 1.43 μ*M* heptanal in HPLC-grade methanol. Heptanal was chosen as an internal standard because there is no detectable heptanal present in samples analyzed. The samples are vortexed for 30 s to extract aldehydes from the tissue homogenate and are centrifuged at 850*g* for 10 min. Aliquots (20 μL) of

tissue homogenate are taken for protein content determination using the Pierce BCA method (Sigma).
3. After centrifugation, 500 μL of supernatant is mixed with 1 mL of 1,3 cyclohexanedione reagent and heated 1 h in a 60°C water bath.
4. After cooling to room temperature, 1 mL of the reaction mixture is added to preconditioned Sep-Pak C_{18} solid-phase extraction columns using virgin 1- mL plastic syringes.
5. The columns are washed with 2 mL distilled/deionized water to remove excess ammonium acetate and the derivatized aldehydes are eluted with 2 mL HPLC-grade methanol.
6. The samples are evaporated to dryness using a speed-vac or freeze-dryer.
7. Samples are dissolved in 1 mL HPLC-grade chloroform and centrifuged at 800*g* for 5 min to pellet any remaining ammonium acetate.
8. An 800-μL aliquot of the supernatant is removed and evaporated to dryness.
9. Before HPLC analysis, the residue is redissolved in 500 μL 50/50 HPLC grade methanol/water and 250 μL subjected to HPLC analysis using a dual-pump system equipped with a C_{18} analytical column. The elution conditions are 10:90 THF/water to 40:60 THF/water from time 0–30 min followed by 40:60 THF/water to 100% THF from 30–40 mins. THF (100%) is maintained for 5 min and initial elution conditions are reestablished from 46–49 min.
10. Detection of derivatized aldehydes is via fluorescence detection at an excitation wavelength of 380 nm and an emission wavelength of 446 nm.
11. Quantification of aldehyde levels is based on comparison of the peak area of interest to the peak area of heptanal (internal standard).
12. Identification of chromatographic peaks is by comparison to chromatograms of authentic standard compounds.
13. Results of the analyses are calculated as nmol aldehyde/mg protein, based on initial protein content measurements.

4. DISCUSSION

The elution conditions described previously are a modification of those used by Yoshino et al. *(3)* and allow the separation of straight chain and α,β-unsaturated aldehydic by-products of lipid peroxidation in biological samples. Fig. 1 shows a representative chromatogram of a mixture of standards including propanal, butanal, pentanal, hexanal, heptanal, and HNE and demonstrates adequate chromatographic separation of the individual aldehydes. Minimum detection limits of HNE are approx 0.1 pmol with shot to shot reproducibility of a standard HNE solution of 3–5%. The signal-to-noise ratio is on the order of 50 for standard solutions of HNE. Generally there are no significant interferences observed using this method, provided glass test tubes and HPLC-grade solvents are used for the derivatization reactions and chromatography. It is possible that fluorogenic compounds may be leached from plastics if used during derivatization. Based on the

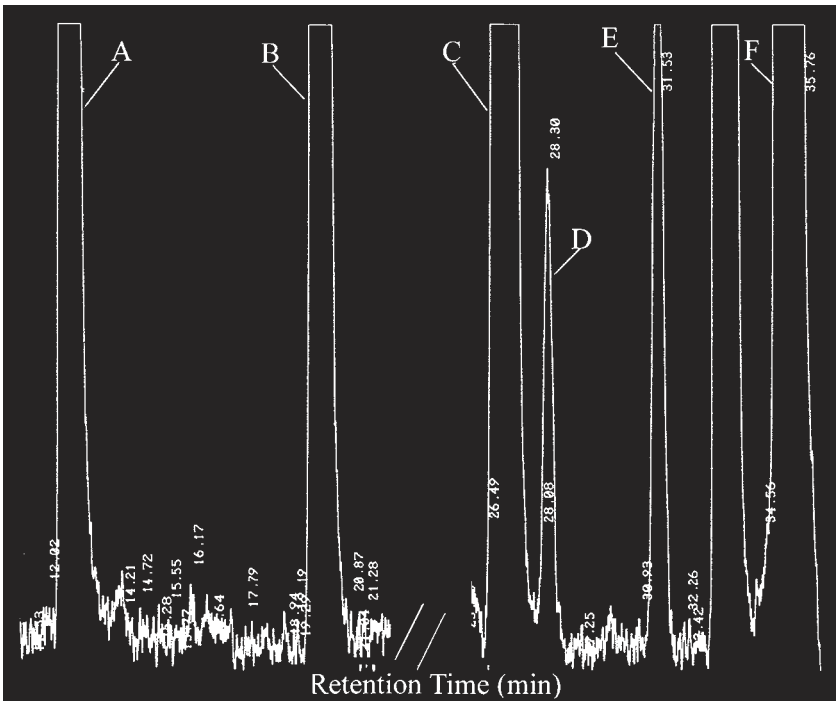

Fig. 1. Representative HPLC of a mixture of standard aldehydes. *A* Propanal. *B* Butanal. *C* Pentanal. *D* 4-hydroxynonenal. *E* Hexanal. *F* Heptanal.

extraction procedure described earlier, it is likely that the results of the assay reflect levels of both free and protein-bound aldehydes.

Another potential problem associated with the use of HPLC with optical detection is the coelution of other compounds with the aldehydes of interest. Because the derivatization process is dependent on the reaction between the aldehydic group and 1,3 cyclohexanedione (Fig. 2), it is unlikely that other compounds without aldehydic groups would be derivatized. Additionally, the possible aldehydic products are well-separated as shown in Fig. 1.

Overall, HPLC with fluorescence detection provides an effective analytical approach for the measurement of levels of the aldehydic by-products of lipid peroxidation.

ACKNOWLEDGMENTS

This work was supported by NIH grants 5P01-AG05119 and 5-P50-AG05144 and by a grant from the Abercrombie Foundation. The authors thank Paula Thomason for editorial assistance.

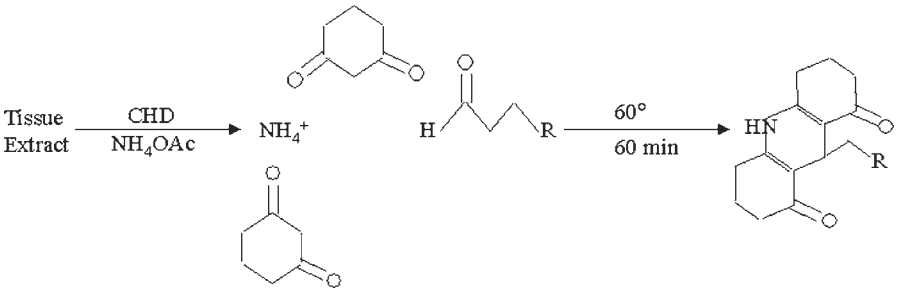

Fig. 2. Reaction of 1,3 cyclohexanedione with a generic aldehyde.

REFERENCES

1. Markesbery, W. R., Montine, T. J., and Lovell, M. A. (2001) Oxidative alterations in neurodegenerative diseases, in *The Pathogenesis of Neurodegenerative Disorders* (Mattson, M. P., ed.), Humana Press, Totowa, NJ, pp. 21–51.
2. Janero, D. R. (1990) Malondialdehyde and thiobarbituric acid-reactivity as diagnostic indices of lipid peroxidation and peroxidative tissue injury. *Free Radic. Biol. Med.* **9,** 515–540.
3. Yoshino, K., Matsuura, Y., Sano, M., Saito, S.-I., and Tomita, I. (1986) Fluorometric liquid chromatographic determination of aliphatic aldehydes arising from lipid peroxides. *Chem. Pharm. Bull.* **34,** 1694–1700.
4. Markesbery, W. R. and Lovell, M. A. (1998) Four-hydroxynonenal, a product of lipid peroxidation, is increased in the brain in Alzheimer's disease. *Neurobiol. Aging* **19,** 33–36.

3

Measurement of Isofurans by Gas Chromatography–Mass Spectrometry/ Negative Ion Chemical Ionization

Joshua P. Fessel and L. Jackson Roberts, II

1. INTRODUCTION

Many methods have been developed to assess oxidative stress status in vivo, which include products of lipid, protein, and DNA oxidation. However, it has long been recognized that most of these methods are unreliable because they lack specificity, sensitivity, or are too invasive for human investigation *(1)*. In 1990, Roberts and Morrow described formation of prostaglandin F_2-like compounds, F_2-isoprostanes (F_2-IsoPs), in vivo by nonenzymatic free radical-induced peroxidation of arachidonic acid *(2)*. Measurement of F_2-IsoPs by gas chromatography–mass spectrometry/negative ion chemical ionization (GC–MS/NICI) has since emerged as one of the most sensitive and reliable approaches to assess lipid peroxidation and oxidative stress status in vivo *(3,4)*.

Despite the utility of measurement of F_2-IsoPs as a marker of oxidative stress, this approach has one potential limitation related to the influence of oxygen tension on the formation of IsoPs. The formation of IsoPs during oxidation of arachidonic acid in vitro under increasing oxygen tensions up to 100% O_2 has been found to plateau at 21% O_2 *(5)*. However, evidence suggests that reactive oxygen species (ROS) are involved in the pathogenesis of disorders associated with high oxygen tension, such as hyperoxic lung injury *(6)*. Thus, measurement of F_2-IsoPs may provide an insensitive index of oxidative stress and the extent of lipid peroxidation in settings of increased oxygen tension. The molecular basis for why IsoP formation becomes disfavored at high oxygen tensions is shown in Fig. 1. In the path-

From: *Methods in Pharmacology and Toxicology: Methods in Biological Oxidative Stress*
Edited by: K. Hensley and R. A. Floyd © Humana Press Inc., Totowa, NJ

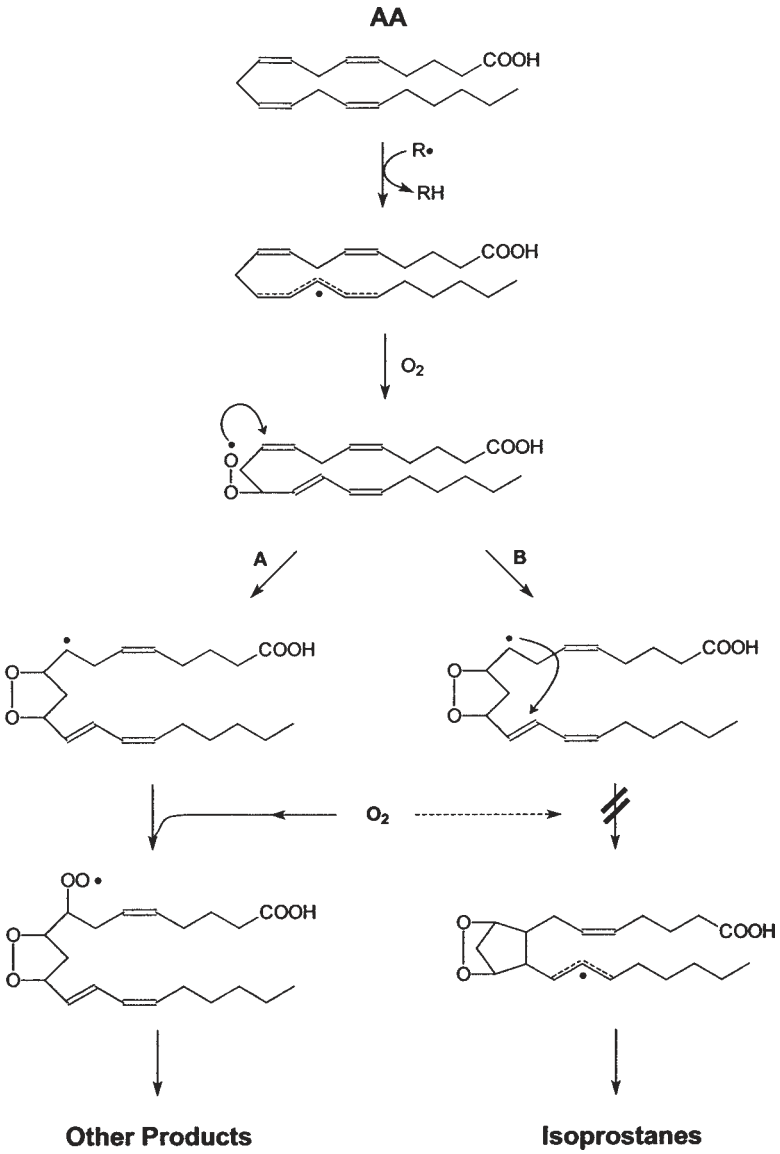

Fig. 1. Mechanistic basis for the favored formation of IsoFs and the disfavored formation of F_2-IsoPs as a function of oxygen tension. As O_2 tension increases, addition of molecular O_2 (pathway A) competes with the endocyclization (pathway B) required for IsoP formation, thus shunting the total product distribution away from IsoPs and in favor of other products.

way of formation of IsoPs is a carbon centered radical. To form IsoPs, this carbon-centered radical must undergo intramolecular attack to form the bicyclic endoperoxide intermediate. However, competing with this endocyclization is attack of the carbon-centered radical by O_2. Thus, as oxygen tension increases, the formation of IsoPs would be expected to be disfavored, while other products formed as a result of attack of the carbon centered radical by O_2 would become favored.

We recently discovered a series of novel isomeric compounds containing a substituted tetrahydrofuran ring, termed isofurans (IsoFs), formed as a result of attack of oxygen on the carbon-centered radical intermediate *(7)*. Two pathways are involved in the formation of IsoFs. In one pathway (cyclic peroxide cleavage pathway), all four oxygen atoms are incorporated from molecular oxygen and in the other (epoxide hydrolysis pathway), three atoms are incorporated from molecular oxygen and one atom from water, resulting in the formation of eight regioisomers, each of which is comprised of sixteen racemic diastereomers (Fig. 2). As hypothesized, the formation of IsoFs during oxidation of arachidonic acid in vitro was found to increase strikingly as oxygen tension is increased from 21 to 100%, whereas, as found previously, no further increase in the formation of IsoPs occurs above 21% O_2. This suggests that measurement of IsoFs may provide a much more reliable indicator of the oxidative stress and the extent of lipid peroxidation than F_2-IsoPs in settings of elevated oxygen tension.

2. MATERIALS

1. Ultrapure water and high purity organic solvents. Use water that has been triply distilled and passed over a Chelex ion-exchange resin (100 mesh, Bio-Rad Laboratories), and wash all plastic and glassware with ultrapure water. Use chromatography-grade methanol, chloroform (with ethanol added as a preservative), ethyl acetate, heptane, and acetonitrile (Burdick and Jackson brand, Baxter Diagnostics, Inc.).
2. Tetradeuterated internal standard, $[^2H]_4$ 8-iso-$PGF_{2\alpha}$, (Cayman Chemical Co.) dissolved in ethanol to a final concentration of approx 100 pg/µL. The exact concentration of the internal standard is determined by co-derivatization and analysis of an aliquot of accurately weighed unlabelled 8-iso-$PGF_{2\alpha}$ standard (Cayman Chemical Co.).
3. C18 and silica SepPak cartridges (Waters).
4. Pentafluorobenzyl bromide (PFBB; Sigma Chemical Co.) made as a 10% solution in acetonitrile.
5. *N*,*N* - Diisopropylethylamine (DIPE; Sigma Chemical Co.) made as a 10% solution in acetonitrile.

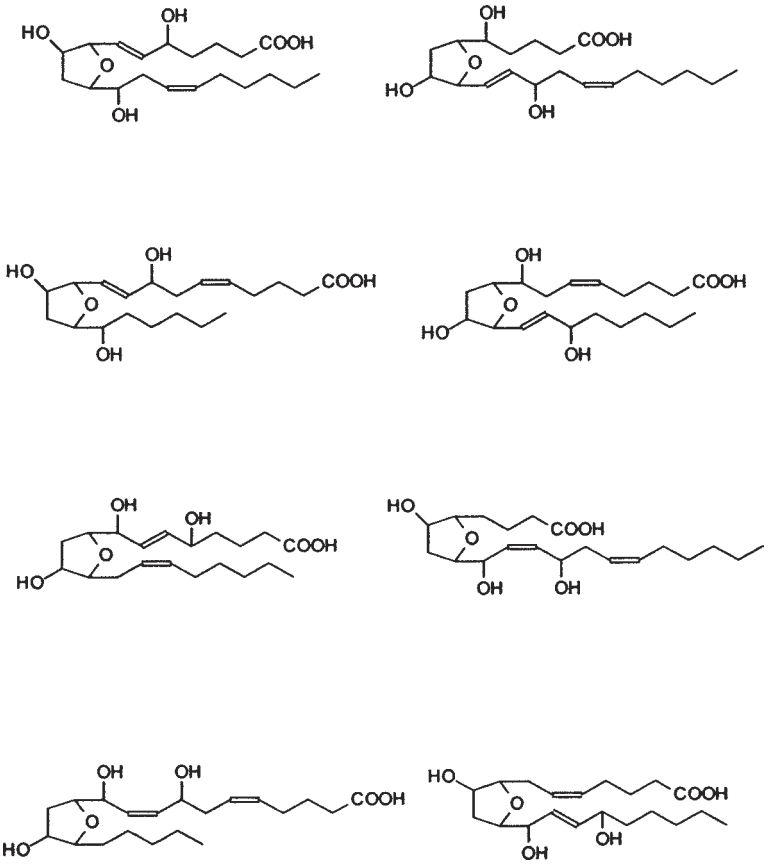

Fig. 2. Eight IsoF regioisomers are formed by two distinct mechanisms, each of which are comprised of 16 racemic diastereomers. For simplicity, stereochemistry is not shown.

6. Butylated hydroxytoluene (BHT); Sigma Chemical Co.) as a 0.005% solution in methanol. This is most easily made as 25 mg BHT dissolved in 500 mL methanol.
7. 15% solution of KOH (final concentration of 2.7 *M*).
8. *N,O*-Bis(trimethylsilyl)trifluoroacetamide (BSTFA, Supelco, Inc.) in 100 µL ampules.
9. Dimethylformamide (DMF, Aldrich Chemical Co.) and undecane dried over calcium hydride.
10. 5 × 20 cm, channeled thin-layer chromatography (TLC) plates (LK6D silica, Whatman) with a 250-µm silica film.
11. The methyl ester of $PGF_{2\alpha}$ (Cayman Chemical Co.) at a concentration of 1 mg/mL in ethanol for use as a TLC standard.

12. Phosphomolybdic acid (Sigma Chemical Co.) to visualize the TLC standard.
13. Miscellaneous labware: glass Hamilton syringe (10 mL, Hamilton), conical centrifuge tubes (50 mL), microcentrifuge tubes, 17 × 100 mm plastic tubes, glass scintillation vials, reactivials (5 mL, Supelco, Inc.), disposable plastic syringes with Luer lock tips, hydrochloric acid (ACS reagent), sodium sulfate, CaH_2 course granules (Aldrich Chemical Co.).
14. Sample to be analyzed. For tissue samples, 200–500 mg pieces are ideal. For cells in culture, a suspension in 1X phosphate-buffered saline (PBS) yielding a protein concentration of approx 1 mg/mL is desirable. For fluids (cell media, plasma, urine, etc.), a volume of 1–3 mL should be used, with the amount varying based on the fluid to be analyzed.

3. EQUIPMENT

1. Gas chromatograph–mass spectrometer capable of negative ion chemical ionization with selected ion monitoring and equipped with a DB-1701 column (15 m length, 0.25 mm i.d., 0.25 μm film). Helium is used as the carrier gas, and methane is the ionization gas.
2. Blade homogenizer-PTA 10s generator (Brinkman Instruments), table top centrifuge, analytical evaporation unit (such as a Meyer N-Evap, Organomation), nitrogen tank, microcentrifuge, 37°C water bath.

4. METHODS

1. For tissue samples, homogenize tissue in 10 mL Folch solution (2:1 chloroform:methanol) containing 0.005% BHT using a blade homogenizer. For cells, wash pellet with 1X PBS, resuspend in 500 μL 1X PBS, and proceed with base hydrolysis (*see* step 6). For fluids to be assayed for free compound, begin at step 7.
2. Allow homogenate to sit at room temperature, capped and under nitrogen, for 1 h, vortexing every 10–15 min.
3. Add 2 mL of 0.9% NaCl solution, vortex, and centrifuge at 2000 rpm for 3–5 min.
4. Carefully aspirate off the top (aqueous) layer. Decant the bottom (organic) layer into a 50-mL conical tube, being sure to leave behind the precipitated protein.
5. Evaporate to dryness under nitrogen.
6. Add 1 mL methanol + 0.005% BHT and swirl. Add 1 mL 15% KOH and swirl. If the sample is a cell pellet, remove an aliquot for protein analysis prior to adding the methanol. Brief sonication may be necessary for cell pellets to facilitate homogenization. Cap sample and place at 37°C for 30 min.
7. Bring pH of the sample to approx 3.0. For tissue and cell samples, add a volume of 1 N HCl equal to ~2.5 times the volume of 15% KOH used. For fluids, dilute the sample in a few mL of deionized water, then add 1 N HCl to bring pH to 3.0. This step is to ensure protonation of the compounds.

8. Add 10 μL of the $[^2H]_4$-8-iso-$PGF_{2\alpha}$ internal standard using a Hamilton syringe. For cells and tissue, dilute the sample to 20 mL, with pH 3.0 water (deionized water brought to a pH of 3.0 with HCl) prior to adding the standard.
9. Prepare a C18 SepPak by attaching to a 12 mL Luer lock syringe and washing with 5 mL methanol followed by 7 mL pH 3.0 water.
10. Add the sample over the SepPak at a flow rate of approx 1 mL/min.
11. Wash the sample with 10 mL pH 3.0 water followed by 10 mL heptane.
12. Elute the sample into a scintillation vial with 10 mL 1:1 ethyl acetate:heptane.
13. Add sodium sulfate to the sample to remove water.
14. Prepare a silica SepPak by washing with 5 mL ethyl acetate.
15. Add the sample over SepPak, being careful to exclude sodium sulfate.
16. Wash with 5 mL ethyl acetate.
17. Elute with 5 mL 1:1 ethyl acetate:methanol.
18. Evaporate to dryness under nitrogen. Add 40 μL 10% PFBB solution and 20 μL of 10% DIPE solution. Vortex and place at 37°C for 20 min.
19. Evaporate to dryness under nitrogen. Dissolve the sample in 50 μL 3:2 methanol:chloroform for TLC.
20. Spot the sample on a TLC plate. On a separate plate, spot 5 mL of the $PGF_{2\alpha}$ methyl ester TLC standard.
21. Run the plates in a freshly made solvent system of 93:7 chloroform:ethanol. Run until the solvent front is 13 cm from the origin, giving an Rf $\approx$ 0.15 for the methyl ester standard.
22. Spray the standard plate with a light layer of phosphomolybdic acid. Heat until a single dark band appears approx 2 cm from the origin.
23. Scrape the sample lane at a distance 1 cm below to 1 cm above the center of the standard band (a typical scrape beginning 1 cm above the origin and ending 3 cm above the origin). Place in 1 mL ethyl acetate in a microcentrifuge tube and vortex to extract compounds.
24. Centrifuge in a microcentrifuge at maximum speed for 2 min. Pipet off ethyl acetate into a clean microcentrifuge tube.
25. Evaporate to dryness under nitrogen. Add 8 μL dry DMF (DMF stored over CaH_2 course granules) and 20 μL BSTFA. Cap and place at 37°C for 5–10 min.
26. Evaporate to dryness under nitrogen. Add 20 μL dry undecane (undecane stored over CaH_2 course granules), vortex, and place in a sealed vial for GC–MS analysis.
27. Analyze by GC–MS at an injection temperature of 250°C, a source temperature of 270°C, an interface temperature of 260–270°C, and a temperature gradient from 190–300°C at 20°C/min. Using negative ion chemical ionization with selected ion monitoring, monitor *m/z* 569 for the IsoPs, *m/z* 573 for the internal standard, and *m/z* 585 for the IsoFs. The amount of IsoFs in the sample is calculated by comparing the integrated areas representing all of the IsoF peaks with that of the internal standard peak (*see* next subheading).

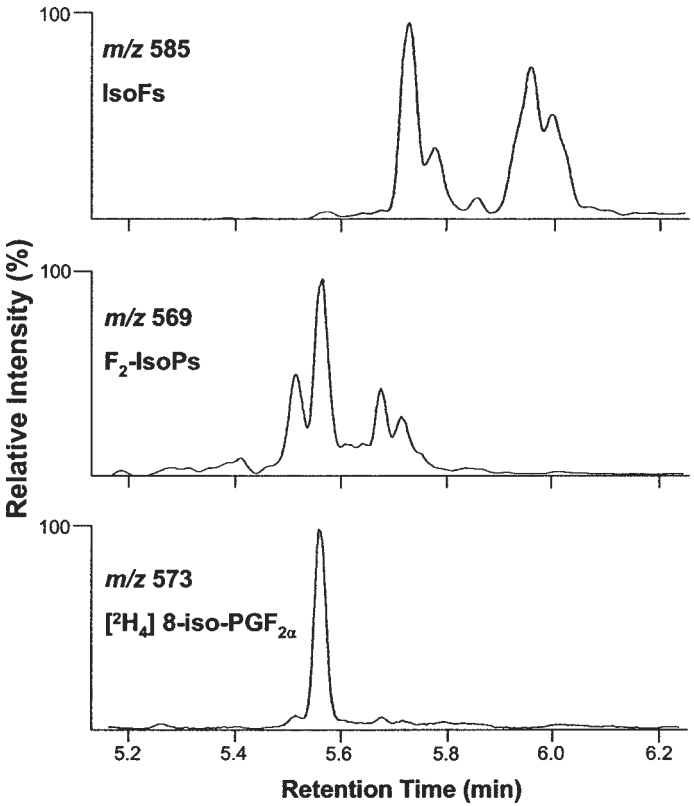

Fig. 3. Representative selected ion-monitoring chromatograms of F_2-IsoPs and F_2-IsoFs generated from the in vitro oxidation of arachidonic acid. The formation of multiple isomers accounts for the series of peaks seen for the IsoPs and IsoFs.

5. ANALYSIS

A representative selected ion current chromatogram obtained from an assay for IsoFs and F_2-IsoPs during oxidation of arachidonic acid in vitro is shown in Fig. 3. In the upper *m/z* 585 ion-current chromatogram is seen a series of intense peaks representing IsoFs eluting at a slightly longer retention time from the GC column than the $[^2H_4]$ 8-iso-$PGF_{2\alpha}$ internal standard peak shown in the bottom *m/z* 573 ion-current chromatogram. Shown in the middle *m/z* 569 ion-current chromatogram are a series of peaks representing F_2-IsoPs. The finding that IsoFs have a slightly longer GC retention time is expected owing the fact that they contain an additional oxygen atom. The ratio of the area under the IsoF peaks is compared to the ratio under the internal standard peak to determine the amount of IsoFs in the sample.

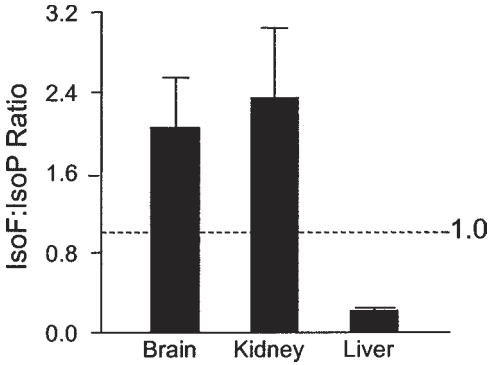

Fig. 4. Isofuran to isoprostane ratio (IsoF:IsoP) measured in the brain, kidney, and liver of normal rats (n = 4, 6, and 3 for the respective tissues).

6. DISCUSSION

The discovery of IsoFs represents a valuable adjunct to our approach to assess oxidant injury, in particular in settings of elevated oxygen tension where the formation of F_2-IsoPs becomes disfavored. As such, the combined use of measurements of F_2-IsoPs and IsoFs likely provides a more accurate assessment of the severity of lipid peroxidation under all settings of oxygen tension than either measure in isolation. In this regard, the method of analysis detailed earlier allows for the simultaneous measurement of both IsoFs and F_2-IsoPs in a single assay.

Moreover, preliminary data we have obtained suggests that measurement of the F_2-IsoP:IsoF ratio shows promise as a physiological "O_2 sensor" in vivo. Every cell is exposed to a chronic low level of oxidative stress as a consequence of mitochondrial respiration, which generates superoxide anions *(8)*. F_2-IsoPs are present at readily detectable levels in all normal biological fluids and tissues, indicating that lipid peroxidation is also an ongoing process in all normal tissues and organs in the body. However, the ratio of the formation of F_2-IsoPs and IsoFs in normal organs would be expected to differ depending on the degree of oxygenation of various organs in the body, which varies substantially. For example, kidneys and brain have a rich arterial blood supply, whereas the liver is perfused primarily with venous blood from the portal vein. Therefore, one would hypothesize that the IsoF:F_2-IsoP ratio would be high in the brain and kidney, but low in the liver. As shown in Fig. 4, that is precisely what was found. This finding suggests that in addition to utilizing measurements of IsoFs and F_2-IsoPs to assess enhanced oxidant injury, determination of the ratio of IsoFs:F_2-IsoPs in various patho-

logic situations may provide additional useful information on the oxygenation state of a tissue/organ, e.g., in vascular disease, and allow an assessment of therapeutic or surgical interventions to improve tissue oxygenation.

ACKNOWLEDGMENTS

This work was supported by grants GM42056, GM15431, DK22657, and CA68485 and by Medical Scientist Training Program grant 5-T32GM07437-22 (JPF) from the National Institutes of Health.

REFERENCES

1. Halliwell, B. and Grootveld, M. (1987) The measurement of free radical reactions in humans. Some thoughts for future experimentation. *FEBS Lett.* **213,** 9–14.
2. Morrow, J. D., Hill, K. E., Burk, R. F., Nammour, T. M., Badr, K. F., and Roberts, L.J., 2nd (1990) A series of prostaglandin F_2-like compounds are produced in vivo in humans by a non-cyclooxygenase, free radical-catalyzed mechanism. *Proc. Natl. Acad. Sci. USA* **87,** 9383–9387.
3. Roberts, L. J. and Morrow, J. D. (2000) Measurement of $F(_2)$-isoprostanes as an index of oxidative stress in vivo. *Free Radic. Biol. Med.* **28,** 505–513.
4. Pryor, W. (2000) Oxidative stress status: the sec set. *Free Radic. Biol. Med.* **28,** 503–504.
5. Longmire, A. W., Swift, L. L., Roberts, L. J., 2nd, Awad, J. A., Burk, R. F., and Morrow, J. D. (1994) Effect of oxygen tension on the generation of F_2-isoprostanes and malondialdehyde in peroxidizing rat liver microsomes. *Biochem. Pharmacol.* **47,** 1173–1177.
6. Stogner, S. W. and Payne, D. K. (1992) Oxygen toxicity. *Ann. Pharmacother.* **26,** 1554–1562.
7. Fessel, J. P., Porter, N. A., Moore, K. P., Sheller, J. R., and Roberts, L. J., II (2002) Discovery of lipid peroxidation products formed in vivo with a substituted tetrahydrofuran ring (isofurans) that are favored by increased oxygen tension. *Proc. Natl. Acad. Sci. USA* **99,** 16,713–16,718.
8. Richter, C., Park, J. W., and Ames, B. N. (1988) Normal oxidative damage to mitochondrial and nuclear DNA is extensive. *Proc. Natl. Acad. Sci. USA* **85,** 6465–6467.

4

Analysis of F_2-Isoprostanes by Gas Chromatography–Mass Spectrometry/ Negative Ion Chemical Ionization

L. Jackson Roberts, II and Jason D. Morrow

1. INTRODUCTION

Numerous methods have been developed to assess oxidative stress/injury in vivo in humans, which include products of oxidation of lipids, proteins, and DNA. However, it has long been recognized that most methods are unreliable because they measure products that are not specific products of free radical-induced oxidation, because the method is not specific for the oxidation product being measured, or because the method is too invasive for use in humans *(1)*. Thus, it has long been recognized that there has been a need for a reliable method to assess oxidative stress status in vivo in humans.

In 1990, we discovered the formation of F_2-isoprostanes F_2-IsoPs *(2)*, and measurement of F_2-IsoPs has emerged over the years as one of the most sensitive and reliable approaches to assess oxidative stress status in vivo *(3,4)*. F_2-IsoPs are prostaglandin-like compounds produced nonenzymatically by free radical-induced oxidation of arachidonic acid. The pathway of the formation of F_2-IsoPs is shown in Fig. 1. Four regioisomers of F_2-IsoPs are formed, each comprised of eight racemic diastereomers. An important concept regarding measurement of F_2-IsoPs is that they are initially formed in situ esterified to phospholipids and subsequently released in free form by phospholipase action *(5)*. Thus, F_2-IsoPs can be measured in free form in biological fluids, e.g., plasma, to assess total endogenous IsoP production but levels esterified in phospholipids can be utilized to localize F_2-IsoP formation in key tissues of interest. F_2-IsoPs are remarkably stable molecules. E- and D-ring IsoPs are also produced by the IsoP pathway *(6)*, but these

From: *Methods in Pharmacology and Toxicology: Methods in Biological Oxidative Stress*
Edited by: K. Hensley and R. A. Floyd

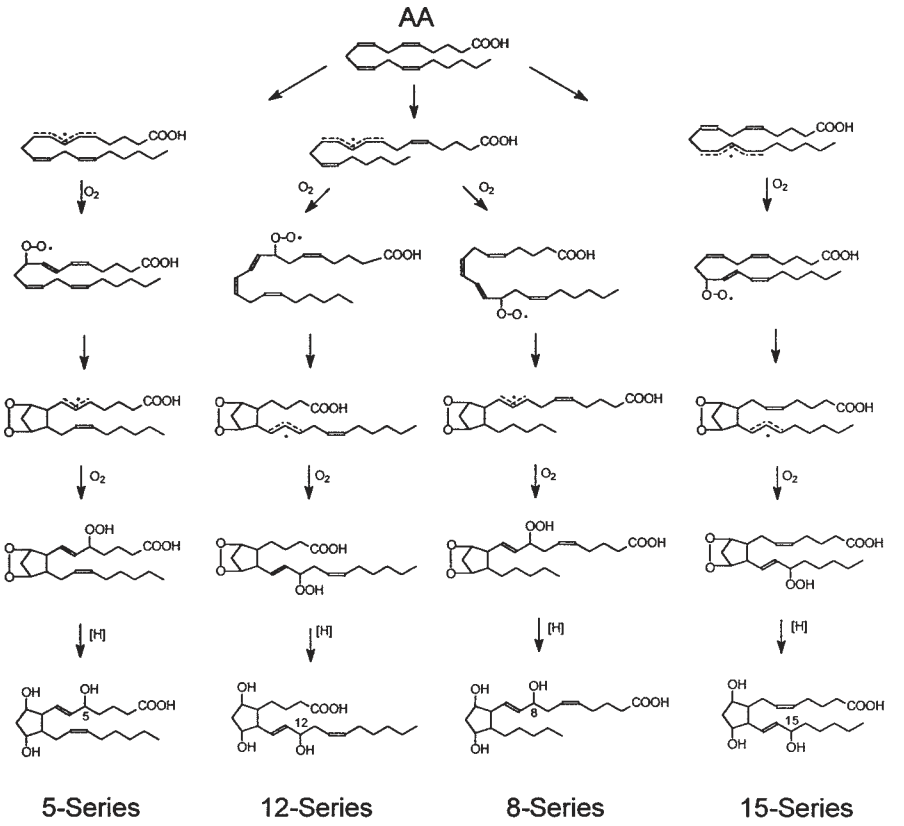

Fig. 1. Pathway and mechanism of the formation of F_2-IsoPs. Four regioisomers are formed, each comprised of eight racemic diastereomers.

compounds are labile compounds and therefore are not as suitable as F_2-IsoPs to measure to assess oxidant stress.

Although somewhat labor-intensive and expensive, gas chromatography–mass spectrometry (GC–MS) has proven to be the most reliable method to measure IsoPs. Commercial labs have developed and marketed immunoassays for F_2-IsoPs but the accuracy and reliability of the immunoassays is frequently compromised by the presence of interfering substances in complex biological fluids and tissues.

Another important issue with measuring IsoPs in tissues and some biological fluids involves artifactual generation of IsoPs by autoxidation. This can occur in all tissues and in plasma, but it is not a problem in urine because of the low amount of arachidonic acid in urine. Generation of IsoPs by autoxidation can occur at –20°C *(7)*. To prevent autoxidation, samples

must be stored at –70°C or lower. At this temperature, samples can be stored for at least 6 mo without the occurrence of autoxidation. In addition, butylated hydroxytoluene (BHT) and/or triphenylphosphine is used in some extraction solvents to prevent autoxidation during sample processing (*see* Subheading 4.2.).

2. MATERIALS

1. Ultrapure water. We use water that has been triply distilled (or its equivalent) and subsequently passed over a column containing the ion-exchange resin Chelex (100 mesh; Bio-Rad Laboratories) to remove trace metals. In addition, all glass- and plasticware should be hand washed and rinsed with ultrapure water prior to use.
2. High-purity organic solvents: methanol, choloroform (with ethanol added as a preservative), ethyl acetate, heptane, acetonitrile (Burdick and Jackson brand, Baxter Diagnostics, Inc.).
3. BHT, triphenylphosphine (Aldrich Chemical Co.), HCL (reagent ACS), phosphomolybdic acid (Sigma Chemical Co.), Na_2SO_4, $MgCl_2$.
4. Derivatizing reagents: pentafluorobenzyl bromide (PFBB), *N,N*'-diisopropylethylamine (DIPE), and undecane (Aldrich Chemical Co.), *N,O*-bis(trimethylsilyl)trifluoroacetamide (BSTFA) (Supelco, Inc.), diazomethane.
5. [$^2H_4$] 8-iso-$PGF_{2\alpha}$ internal standard (Cayman Chemical Co.), C-18 and silica Sep Pak cartridges (Millipore Corp.), thin-layer chromatography (TLC) plates (LK6D silica (Whatman), precise glass syringe (10 μL) (Hamilton).
6. Conical glass centrifuge tubes (40 mL), microcentrifuge tubes, 17 × 100 mm plastic tubes, glass scintillation vials, reactivials (5 mL), disposable plastic syringes (10 mL).

3. EQUIPMENT

1. Blade homogenizer-PTA 10s generator (Brinkman Instruments), table-top centrifuge, analytical evaporation unit (such as Meyer N-Evap, Organomation), tank of nitrogen, microcentrifuge, 37°C water bath.
2. Gas chromatography negative ion chemical ionization mass spectrometry instrument.

4. METHODS

4.1. Extraction, Purification, and Derivatization of F_2-IsoPs from Plasma or Urine

1. Add 1–5 pmol of [$^2H_4$] 8-iso-$PGF_{2\alpha}$ internal standard (stored in ethanol) to a few mL of ultrapure water using a Hamilton syringe.
2. Add 1–3 mL of plasma or 250 μL of urine to the water containing the internal standard.

3. Acidify to pH 3.0 with 1 *M* HCI and vortex.
4. Precondition Sep Pak connected to a 12 mL plastic syringe by pushing 5 mL methanol followed by 5 mL of pH 3 water through the cartridge.
5. Apply the sample to the preconditioned C18 Sep Pak cartridge at a rate of 1–2 mL/min.
6. Wash column with 10 mL pH 3.0 water and then 10 mL heptane.
7. Elute F_2-IsoPs from column with 10 mL ethyl acetate:heptane (50:50, v/v) into a 20-mL glass scintillation vial.
8. Add 5 g anhydrous Na_2S0_4 to vial and swirl gently to remove any residual water from the eluate.
9. Apply eluate to silica Sep Pak preconditioned with 5 mL methanol and 5 mL ethyl acetate.
10. Wash cartridge with 5 mL ethyl acetate.
11. Elute F_2-IsoPs from silica Sep Pak with ethyl acetate:methanol (50:50, v/v) into a 5-mL reactivial.
12. Evaporate eluate under nitrogen.
13. To convert F_2-IsoPs into pentafluorobenzyl esters add 40 μL 10% (v/v) PFBB in acetonitrile and 20 μL 10% (v/v) DIPE in acetonitrile to residue, vortex, and let stand for 30 min at room temperature.
14. Dry reagents under nitrogen and resuspend in 50 :l methanol.
15. Apply mixture to a lane on a silica TLC plate (LKBB) that has been prewashed with methanol. Chromatograph to 13 cm in a solvent system of chloroform:ethanol (93:7, v/v). For a TLC standard, apply approx 2–5 μg of the $PGF_{2\alpha}$ methyl ester standard to another TLC lane. Visualize the TLC standard by spraying the lane with a 10% solution of phosphomolybdic acid in ethanol and heating.
16. Scrape silica from the TLC plate in the sample lane in a region of the methyl ester of the $PGF_{2\alpha}$ standard (Rf 0.15) and adjacent areas 1 cm above and below. The methyl ester of $PGF_{2\alpha}$ is used rather than a PFB-ester of 8-iso-$PGF_{2\alpha}$ to avoid any contamination of the standard in the sample lane because of the high concentration used.
17. Place silica in microcentrifuge tube and add 1 mL ethyl acetate. Vortex vigorously for 20 s.
19. Pour off ethyl acetate into another microcentrifuge tube, taking care not to disrupt silica pellet.
20. Dry organic layer under nitrogen.
21. To convert F_2-IsoPs into trimethylsilylether ether derivatives, add 20 :l BSTFA and 6 μL DMF to residue.
22. Vortex well and incubate tube at 37°C for 5 min.
23. Dry reagents under nitrogen.
24. Add 10 μL undecane (which has been stored over calcium hydride to prevent water accumulation). Sample is now ready for mass spectrometric analysis.

4.2. Extraction and Hydrolysis of F_2-IsoPs Esterified in Tissue Lipids

1. Weigh out 0.05–1 g of either fresh tissue or tissue frozen at –70°C.

2. Add tissue to 20 mL of ice-cold Folch solution (chloroform/methanol; 2:1 v/v) containing 0.005% BHT in a 40-mL glass centrifuge tube.
3. Homogenize tissue with blade homogenizer at full speed for 30 s.
4. Purge airspace in centrifuge tube with nitrogen and cap. Let solution stand at room temperature for 1 h to effect maximum extraction of lipids from ground tissue. Shake tube occasionally during this time period.
5. Add 4 mL aqueous NaCl (0.9%) and vortex vigorously for 30 s.
6. Centrifuge 800*g* for 10 min at room temperature.
7. After centrifugation, carefully pipet off top aqueous layer and discard. Remove the lower organic layer carefully from under the intermediate semisolid proteinaceous layer and transfer it to another tube and evaporate under nitrogen.
8. Add methanol containing 5 mg/100 mL BHT (add 4 mL if beginning tissue weight was >100 mg and 0.5 mL if weight is <100 mg) and an equal volume of 15% aqueous KOH. Vortex and heat to 30o C for 30 min.
9. Acidify solution to pH 3.0 with 1 *M* HCL
10. Dilute methanolic KOH solution 20-fold or greater with pH 3.0 water.
11. Then proceed with extraction, purification, and derivatization as in Subheading 4.1.

5. ANALYSIS

A representative selected ion current chromatogram of *m*/*z* 569 (endogenous F_2-IsoPs) and *m*/*z* 573 [$^2H_4$] 8-iso-$PGF_{2\alpha}$ from analysis of plasma is shown in Fig. 2. All of the peaks in the m/z 569 ion current chromatogram represent different F_2-IsoP isomers. The peak we measure is the one that is starred (*). The peak area or peak height is compared to that of the known amount of the [$^2H_4$] 8-iso-$PGF_{2\alpha}$ internal standard for quantitation. This peak contains 8-iso-$PGF_{2\alpha}$ but HPLC analysis has indicated that there are at least three additional isomers co-eluting with 8-iso-$PGF_{2\alpha}$ *(8)*. The other large peak denoted (+) should not be included in any measurements of F_2-IsoPs. This peak does contain a F_2-IsoP isomer(s) but cyclooxygenase-derived $PGF_{2\alpha}$ also coelutes perfectly with this peak. Thus, when measuring free F_2-IsoPs in biological fluids, it cannot be ascertained to what extent $PGF_{2\alpha}$ contributes to the intensity of this peak. Using only a single peak in the *m*/*z* 569 ion-current chromatogram for quantitation can provide an accurate index of formation of all F_2-IsoPs, because all isomers increase or decrease proportionally when IsoP formation varies. This GC–MS assay is highly accurate. The precision of the assay is ±6% and the accuracy is 96% *(9)*.

6. DISCUSSION

The GC–MS assay described herein for measurement of F_2-IsoPs is highly accurate and can be applied to virtually any biological fluid or tissue. The

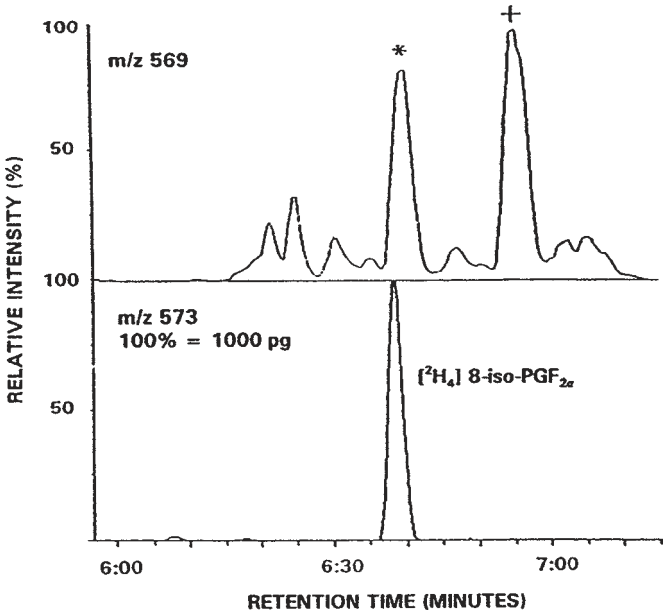

Fig. 2. Representative selected ion chromatogram obtained from analysis of F_2-IsoPs in plasma. Seen in the lower *m/z* 573 channel is a peak representing the deuterated internal standard, [$^2H_4$] 8-iso-$PGF_{2\alpha}$. Seen in the upper m/z 569 channel are a series of peaks representing different F_2-IsoP isomers. The peak denoted by a (*) is the peak that is used for quantitation. The peak denoted by (+) contains F_2-IsoP isomers but also perfectly co-chromatographs with cyclooxygenase-derived $PGF_{2\alpha}$. Therefore, as discussed in the text, this peak should not be used for quantitation of F_2-IsoPs.

sensitivity is also high (lower limits of detection in the low pg range), allowing measurements to be made in very small volumes of fluids or small amounts of tissue, as low as ~30 mg. Notably, the assay is more labor-intensive than immunoassays and requires a mass spectrometer, which is expensive. The throughput has been improved considerably over the last few years with the advent of auto-injectors on mass spectrometers, which drastically lowers the time technicians spend actually running samples. With experienced technicians, approx 20 samples can be purified for analysis in a single d with the analyses performed overnight with the use of an auto-injector.

ACKNOWLEDGMENTS

This work was supported by GM42056, GM15431, DK22657, and CA68485 from the National Institutes of Health.

REFERENCES

1. Halliwell, B. (1987) The measurement of free radical reactions in humans. *FEBS Lett.* **213,** 9–14.
2. Morrow, J. D., Hill, K. E., Burk, R. F., Nammour, T. M., Badr, K. F., and Roberts, L. J. II (1990) A series of prostaglandin F_2-like compounds are produced *in vivo* in humans by a non-cyclooxygenase free radical catalyzed mechanism. *Proc. Natl. Acad. Sci. USA* **87,** 9383–9387.
3. Roberts, L. J. II and Morrow, J. D. (2000) Measurement of F_2-isoprostanes as an index of oxidative stress *in vivo*. *Free Rad. Biol. Med.* **28,** 505–513.
4. Pryor, W. (2000) Oxidative stress status: the sec set. *Free Rad. Biol. Med.* **28,** 503–504.
5. Morrow, J. D., Awad, J. A., Boss, H. J., Blair, I. A., and Roberts, L. J. II (1992) Non-cyclooxygenase derived prostanoids (F_2-isoprostanes) are formed in situ on phospholipids. *Proc. Natl. Acad. Sci. USA* **89,** 10721–10725.
6. Morrow, J. D., Minton, T. A., Mukundan, C. R., Campbell, M. D., Zackert, W. E., Daniel, V. C., et al. (1994) Free radical induced generation of isoprostanes *in vivo*: Evidence for the formation of D-ring and E-ring isoprostanes. *J. Biol. Chem.* **269,** 4317–4326.
7. Morrow, J. D., Harris, T. M., and Roberts, L. J. II (1990) Non- cyclooxygenase oxidative formation of a series of novel prostaglandins: Analytical ramifications for measurement of eicosanoids. *Anal. Biochem.* **184,** 1–10.
8. Morrow, J. D., Badr, K. F., and Roberts, L. J. II (1994) Evidence that the F_2-isoprostane, 8-epi-$PGF_{2\alpha}$, is formed *in vivo*. *Biochim. Biophys. Acta.* **1210,** 244–248.
9. Morrow, J. D. and Roberts, L. J. II (1998) Mass spectrometric quantification of F_2-isoprostanes in biological fluids and tissues as a measure of oxidant stress. *Methods Enzymol.* **300,** 3–12.

5

Measurement of F_4-Neuroprostanes by Gas Chromatography–Mass Spectrometry/ Negative Ion Chemical Ionization

Nathalie Bernoud-Hubac and L. Jackson Roberts, II

1. INTRODUCTION

Oxidative damage has been strongly implicated in the pathogenesis of a number of neurodegenerative diseases including Alzheimer's disease (AD), Parkinson's disease (PD), amyotrophic lateral sclerosis (ALS), and Huntington's disease (HD) *(1–9)*. Several years ago, we reported the discovery of the formation of F_2-isoprostanes (F_2-IsoPs), which are prostaglandin F_2-like compounds formed in vivo nonenzymatically as products of free radical-induced oxidation of arachidonic acid *(10)*. More recently we described the formation of IsoP-like compounds in vivo from free radical-induced oxidation of docosahexaenoic acid (DHA) *(5)*. DHA is a fatty acid that is uniquely enriched in the brain, particularly the gray matter, where it comprises approx 25–35% of the total fatty acids in aminophospholipids *(11,12)*. Our motive for exploring whether IsoP-like compounds are formed from oxidation of DHA derives from our hypothesis that measurement of such compounds may provide a unique and sensitive biomarker of oxidative neuronal injury in the brain. Accordingly, we have termed these compounds neuroprostanes (NPs).

The mechanism by which NPs are formed is shown in Fig. 1. Initially, five docosahexaenoyl radicals are generated, which are then converted to eight peroxyl radicals following addition of oxygen. These peroxyl radicals undergo endocyclization to yield endoperoxide intermediates, which are then reduced to form eight F_4-NP regioisomers. The eight regioisomers are

From: *Methods in Pharmacology and Toxicology: Methods in Biological Oxidative Stress*
Edited by: K. Hensley and R. A. Floyd

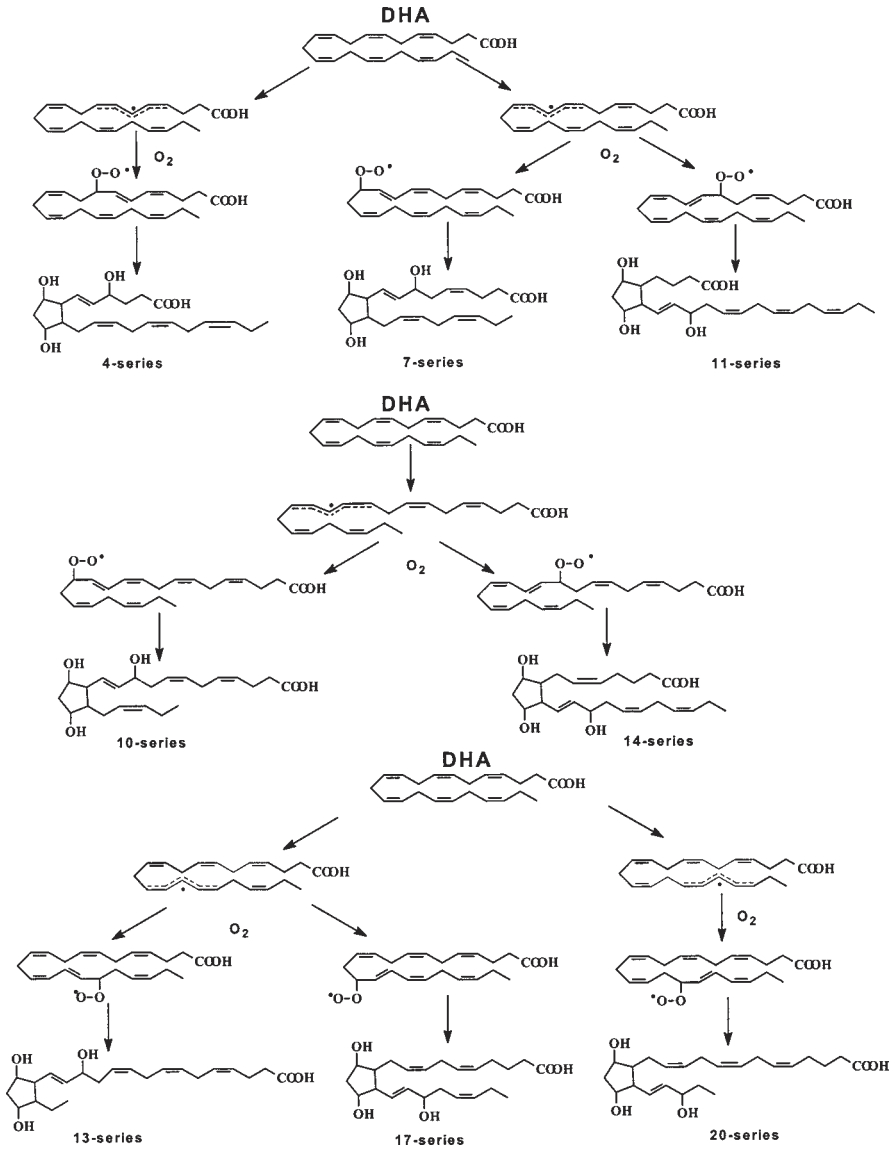

Fig. 1. Mechanism of the formation of F_4-NPs by nonenzymatic free radical-induced peroxidation of DHA.

designated by the carbon number on which the side-chain hydroxyl is located in accordance with the nomenclature system for IsoPs approved by the Eicosanoid Nomenclature Committee *(13)*.

2. MATERIALS

1. DHA, pentafluorobenzyl bromide (PFBB), diisopropylethylamine (DIPE), dimethylformamide (DMF), undecane (Sigma-Aldrich, St. Louis, MO).
2. *N,O*-bis(trimethylsilyl)trifluoroacetamide (BSTFA; Supelco, Bellefonte, PA).
3. Organic solvents (Baxter Healthcare, Burdick & Jackson Brand, McGaw Park, Il).
4. C-18 Sep-Paks (Waters Associates, Milford, MA).
5. 60ALK6D thin-layer chromatography (TLC) plates (Whatman, Maidstone, UK).
6. $[^2H_4]PGF_{2\alpha}$ (Cayman Chemical, Ann Arbor, MI).

3. EQUIPMENT

1. Blade homogenizer-PTA 10s generator (Brinkman Instruments), microfuge, water bath, analytical evaporation unit (such as Meyer N-Evap, Oganomation).
2. Negative ion chemical ionization gas chromatograph mass spectrometer.

4. METHODS

4.1. Analysis of Free F_4-NPs in Cerebrospinal Fluid

1. To a few mL (1.2–1.3 mL) of deionized water in a 17 × 100 mm plastic tube, add 5 μL of $[^2H_4]PGF_{2\alpha}$ internal standard (0.125 ng/μL) and vortex.
2. Add at least 1 mL of cerebrospinal fluid (CSF) to this tube and vortex.
3. Adjust pH to 3.0 with 1 N HCl.
4. Extract F_4-NPs using a C-18 Sep-Pak cartridge. Place C18 Sep-Pak onto 12-cc syringe and precondition the column with 5 mL methanol and 7 mL pH 3.0 water. Load the sample slowly (1–2 mL/min is recommended). Wash the column with 10 mL pH 3.0 water and 10 mL heptane. Elute the sample slowly with 10 mL 1:1 ethyl acetate:heptane into a 20 mL scintillation vial.
5. Remove any remaining water by adding a small scoop of sodium sulfate.
6. Add the sample slowly to a silica Sep-Pak pre-rinse with 5 mL ethyl acetate. Wash the sample with 5 mL 75:25 ethyl acetate:heptane and elute it slowly from silica Sep-Pak with 5 mL 1:1 ethyl acetate:methanol into a 5-mL reactivial.
7. Dry the sample and convert it to a pentafluorobenzylester by adding 40 μL of 10% PFBB solution in acetonitrile and 20 μL of 10% diisopropylethylamide in acetonitrile. Cap, vortex, and place at 37°C for 20 min.
8. Dry the sample under nitrogen and reconstitute in 50 μL of 3:2 methanol:chloroform.
9. Purify F_4-NPs by TLC using the solvent chloroform/ethanol (93/7). Scrape the region from 1 cm below to 3 cm above a $PGF_{2\alpha}$ methyl ester standard. Pour silica into a bullet tube containing 1 mL of ethyl acetate. Centrifuge for 2 min in a microfuge and pipet off carefully the ethyl acetate into another bullet tube. Repeat this operation.

10. Dry the sample under nitrogen and then convert NPs to a trimethylsilyl ether derivated by adding 8 μL of dry dimethylformamide and 20 μL of BSTFA. Vortex and place at 37°C for 5 min.
11. Dry the sample under nitrogen and reconstitute in 4 μL undecane.

4.2. *Analysis of Esterified F_4-NPs in Brain*

1. Prepare Folch solution (2:1 chloroform/methanol) with butylated hydroxytoluene (BHT) (5 mg/100 mL).
2. Add 5 mL Folch solution to a plastic test tube (2 tubes for 1 sample brain) and place on ice.
3. Weigh out the sample as much as of possible and record number of grams.
4. Homogenize brains with a blade homogenizer in the 5-mL Folch solution.
5. Rinse homogenizer in 5 mL Folch solution in another tube, then combine tubes.
6. Allow sitting under nitrogen at room temperature in sealed tubes for 30 min, mixing every 10 min.
7. Add 4 mL 0.9% NaCl.
8. Vortex vigorously and centrifuge 2–3 min.
9. Discard upper phase (methanol/saline).
10. Add 1 mL acetonitrile and 10 μL of $[^2H_4]PGF_{2\alpha}$ internal standard (0.125 ng/μL) in lower phase and remove this phase to Falcon tubes.
11. Evaporate the sample and add 1 mL methanol (containing 5 mg BHT/100 mL). Sonicate to break up any residue left on the side of the tube and then add 1 mL of 15% KOH.
12. Place in water bath for 30 min at 37–40°C.
13. Adjust pH to 3.0 with 1 N HCl using approx 2.5 times the volume of 15% KOH.
14. Centrifuge 2–3 min and dilute to 40–80 mL with pH 3.0 water so that the volume of methanol is <5% of the total volume).
15. Proceed as described above for the analysis of F_4-NPs in cerebrospinal fluid (*see* steps 4–11). Reconstitute in 10 μL undecane.

5. ANALYSIS

NPs are quantified by gas chromatography–mass spectrometry/negative ion chemical ionization (GC–MS/NICI) using $[^2H_4]$ $PGF_{2\alpha}$ as an internal standard. The M-$^{\bullet}CH_2C_6F_5$ ions are monitored for quantification (*m*/*z* 573 for $[^2H_4]$ $PGF_{2\alpha}$, *m*/*z* 593 for F_4-NPs). The ratio of integrated areas under the peaks for F_4-NPs and the internal standard is calculated to quantify the total amount of NPs formed.

A representative ion current chromatogram obtained from the analysis of F_4-NPs formed during oxidation of DHA in vitro is shown in Fig. 2. The peak in the lower *m*/*z* 573 ion-current chromatogram represents the internal standard $[^2H_4]$ $PGF_{2\alpha}$. In the upper *m*/*z* 593 ion-current chromatogram are a series of chromatographic peaks eluting over an approximate 60-s period representing F_4-NPs. F_4-NPs would be expected to have a longer GC reten-

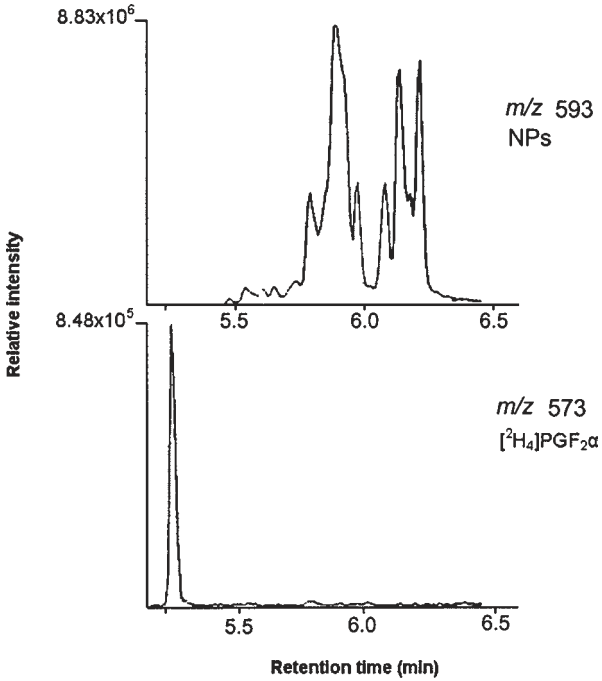

Fig. 2. Selected ion current chromatograms obtained from GC–MS/NICI analysis for F_4-NPs formed during iron/ADP/ascorbate-induced oxidation of DHA in vitro. The series of peaks in the *m*/*z* 593 chromatogram represent F_4-NPs analyzed as a pentafluorobenzyl ester, *O*-methyloxime, trimethylsilyl ether derivative; and the *m*/*z* 573 chromatogram represents the $[^2H_4]PGF_{2\alpha}$ internal standard.

tion time than $PGF_{2\alpha}$ because the former compounds contain two additional carbon atoms. Similar chromatograms are obtained from in vivo studies except that the pattern of peaks representing F_4-NPs in vivo differ somewhat from the pattern of F_4-NPs formed from oxidation of DHA in vitro. This may be explained by our previous observation that there appears to be a steric influence of phospholipids on the formation of different isomers from esterified substrate.

6. DISCUSSION

F_4-NPs can be readily detected esterified in normal brain lipids and levels are substantially higher than levels of F_2-IsoPs in areas of brain rich in gray matter *(5)*. Interestingly, we have found that levels of F_4-NPs, but not F_2-IsoPs, are increased in diseased areas of brain from patients with AD compared to

age- and sex-matched controls *(9)*. This finding supports the hypothesis that measurement of F_4-NPs may provide a more sensitive biomarker of oxidative neuronal injury than F_2-IsoPs. Moreover, CSF contains detectable concentrations of F_4-NPs and levels have also been found to be increased in CSF from patients with AD *(5)*. These findings suggest that measurement of F_4-NPs can provide a unique and sensitive approach to assess oxidative injury in the brain. This approach can be utilized to explore the role of free radicals in neurodegenerative diseases, as well as the pathogenesis of other disorders involving the brain in which free radicals are thought to be involved. In addition, measurement of F_4-NPs in CSF may prove useful in assessing the efficacy of future therapies attempting to suppress oxidant injury in the brain in living patients.

ACKNOWLEDGMENTS

This work was supported by GM42056, GM15431, DK26657, and CA68485 from the National Institutes of Health.

REFERENCES

1. Markesbery, W. R. (1997) Oxidative stress hypothesis in Alzheimer's disease. *Free Radic. Biol. Med.* **23,** 134–147.
2. Markesbery, W. R. (1999) The role of oxidative stress in Alzheimer disease. *Arch. Neurol.* **56,** 1449–1452.
3. Simonian, N. A. and Coyle, J. T. (1996) Oxidative stress in neurodegenerative diseases. *Annu. Rev. Pharmacol. Toxicol.* **36,** 83–106.
4. Perry, G., Nunomura, A., Hirai, K., Takeda, A., Aliev, G., and Smith, M. A. (2000) Oxidative damage in Alzheimer's disease: the metabolic dimension. *Int. J. Dev. Neurosci.* **18,** 417–421.
5. Roberts, L. J., 2nd, Montine, T. J., Markesbery, W. R., Tapper, A. R., Hardy, P., Chemtob, S., et al. (1998) Formation of isoprostane-like compounds (neuroprostanes) in vivo from docosahexaenoic acid. *J. Biol. Chem.* **273,** 13,605–13,612.
6. Montine, T. J., Markesbery, W. R., Morrow, J. D., and Roberts, L. J. (1998) Cerebrospinal fluid F2-isoprostane levels are increased in Alzheimer's disease. *Ann. Neurol.* **44,** 410–413.
7. Montine, T. J., Beal, M. F., Cudkowicz, M. E., O'Donnell, H., Margolin, R. A., McFarland, L., et al. (1999) Increased CSF F2-isoprostane concentration in probable AD. *Neurology* **52,** 562–565.
8. Montine, T. J., Beal, M. F., Robertson, D., Cudkowicz, M. E., Biaggioni, I., O'Donnell, H., et al. (1999) Cerebrospinal fluid F2-isoprostanes are elevated in Huntington's disease. *Neurology* **52,** 1104–1105.

9. Reich, E. E., Markesbery, W. R., Roberts, L. J., Swift, L. L., Morrow, J. D., and Montine, T. J. (2001) Brain regional quantification of F-ring and D-/E-ring isoprostanes and neuroprostanes in Alzheimer's disease. *Am. J. Pathol.* **158,** 293–297.
10. Morrow, J. D., Hill, K. E., Burk, R. F., Nammour, T. M., Badr, K. F., and Roberts, L. J., 2nd (1990) A series of prostaglandin F2-like compounds are produced in vivo in humans by a non-cyclooxygenase, free radical-catalyzed mechanism. *Proc. Natl. Acad. Sci. USA* **87,** 9383–9387.
11. Salem, N., Jr., Kim, H.-Y., and Yergery, J.A. (1986) Docosahexaenoic acid: membrane function and metaolism, in *Health Effects of Polyunsaturated Fatty Acids in Seafoods* (Simopoulos, A. P., Kifer, R. R., and Martin, R. E., eds.), Academic Press, Orlando, FL, pp. 263–317.
12. Skinner, E. R., Watt, C., Besson, J. A., and Best, P. V. (1993) Differences in the fatty acid composition of the grey and white matter of different regions of the brains of patients with Alzheimer's disease and control subjects. *Brain* **116,** 717–725.
13. Taber, D. F., Morrow, J. D., Roberts, L. J., 2nd (1997) A nomenclature system for the isoprostanes. *Prostaglandins* **53,** 63–67.

6

Immunoassays for Lipid Peroxidation End Products

One-Hour ELISA for Protein-Bound Acrolein and HNE

Kimihiko Satoh and Koji Uchida

1. INTRODUCTION

Unsaturated aldehydes such as acrolein and hydroxyalkenals are produced in vivo through lipid peroxidation chain reactions under conditions of oxidative stress or carcinogenic insult, and are causally involved in the pathogenesis of numerous diseases *(1,2)*. The ability of cytotoxic and genotoxic compounds to inactivate various biologically important macromolecules has been well documented *(3–5)*. For enzymes and proteins, lysine, cysteine, histidine, and other amino acid residues that play key roles in their functionings are preferentially modified. The complicated chemistry and biochemistry of the reactive molecules occurring in vivo in micro- or ultramicroquantities remain unclear, because direct determination of such unstable compounds is problematic. An alternative approach is the immunochemical quantification of reaction products accumulating in vivo, for which monoclonal antibodies (MAbs) specific for the acrolein-modified lysine and 4-hydroxy-2-nonenal (HNE)-modified histidine epitopes have been prepared (Fig. 1) *(6,7)*. However, several difficulties are encountered with enzyme-linked immunosorbent assay (ELISA) determination of haptenic molecules. One is the low avidity of MAbs against the small epitopes in general. The other is that the most widely used sandwich method is unapplicable to the quantitation because monovalent antigens are undetectable in principle. Here, we report a very simple, rapid, and sensitive ELISA method for quantitation of the modified proteins through attachment of epitopes to hydrophobic blocking matrices, together with the finding of diffusion-controlled rapid reaction rates in the binding of epitope-bound matrices, MAbs, and polyclonal sec antibodies *(8)*.

From: *Methods in Pharmacology and Toxicology: Methods in Biological Oxidative Stress*
Edited by: K. Hensley and R. A. Floyd

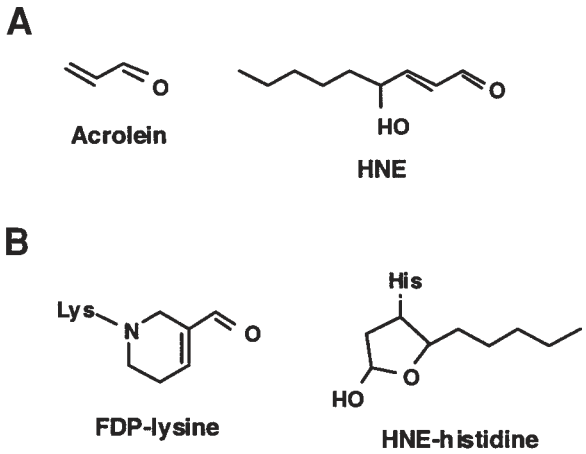

Fig. 1. Structures of acrolein and HNE (**A**) and their amino acid adducts (**B**).

2. MATERIALS

1. Acrolein (Aldrich), HNE (Cayman Chemical) and casein (bovine milk, technical, Sigma) are commercially available.
2. Epitope-attached casein. Add a 500-µL portion of acrolein (2 mmoles), which has been diluted five-fold with water (final conc. 250 m*M*), or a 320-µL portion of HNE (10 mg/mL in hexane, final conc. 5 m *M*) to casein mixture dissolved in 8 mL of 50 m*M* NaH_2PO_4, pH 7.4 (1 mg/mL). Let stand for 2–3 d at room temperature (R.T.), and the resultant modified caseins are diluted 10-fold with water, and then subjected to ELISA without removal of unreacted aldehydes.
3. Aldehyde-modified proteins. Incubate bovine serum albumin (BSA), ovalbumin, or myoglobin (2 or 4 mg/mL) in 50 m*M* NaH_2PO_4, pH 7.4 with appropriate aldehyde above. Modified proteins are then purified by gel filtration on a PD-10 column (Pharmacia LKB) with phosphate-buffered saline (PBS).
4. Authentic FDP (3-formyl-3, 4-dehydropiperidino)-lysine (Fig. 1) *(9)*. Incubate 100 m*M* N^{α}-acetyllysine with 50 m*M* acrolein in 50 m*M* sodium phosphate buffer (pH 7.2, 10 mL), and let stand for 24 h at 37°C under stirring. The acrolein-N^{α}-acetyllysine adduct formed can be analyzed/purified with a reverse-phase (RP) HPLC column of Develosil ODS-HG-5 (8 × 250 mm) (Nomura Chemicals) with 5% methanol/0.1% trifluoroacetic acid (TFA) as eluant at a flow rate of 2.5 mL/min and monitoring at 227 nm.
5. Authentic HNE-histidine adduct (Fig. 1) *(4)*. Incubate 10 m*M* N^{α}-acetylhistidine with 10 m*M* HNE in 10 mL of 50 m*M* sodium phosphate buffer, pH 7.2, and let stand for 24 h at 37°C under stirring. HNE-N^{α}-acetylhistidine adduct can be purified similarly with 25% methanol /0.1% TFA as eluant and monitoring at 215 nm.

6. MAbs: anti-acrolein-lysine MAb (mAb5F6, NOF Co. Ltd, Japan) *(7)*; anti-HNE-histidine monoclonal antibody (mAbHNEJ2, NOF Co. Ltd, Japan) *(6)*. Dilute with PBS containing casein (approx 0.5 mg/mL).
7. Peroxidase-conjugated goat anti-mouse IgG (H+L) (Bio-Rad, Hercules, CA). Dilute 1,000-fold with PBS/casein (0.5 mg/mL).
8. TMBZ (3,3'5,5'-tetramethylbenzidine) color developing kit (Sumitomo Chemical Ind., Akita, Japan).

3. METHODS

1. Precoat/block microtiter plate wells with 150-μL-portions of epitope-attached casein (15 μg/well) for 3 min and then wash 4 times with 200-μL portions of PBS/0.05% Tween-20/0.25 mg/mL casein. The coating and the initial washing should be performed in a hood. Eight-tipped micropipet (e.g., Gilson 8 × 200) is efficient and essential for washing.
2. Take 60 μL-aliquots of serially diluted samples and equal volumes of antibody solution in polypropylene microtubes (500-μL), mix well and let stand for 3 min.
3. Apply 100-μL portions of the mixture to each well, let stand 3 min, and then wash 4 times with the PBS buffer.
4. Add an aliquot (100 μL) of peroxidase-conjugated goat anti-mouse IgG to each well, let stand for 7 min, and wash 4 times.
5. Apply TMBZ reagent (100 μL) to each well and develop color for 2–5 min.
6. Terminate with 1 N H_2SO_4 (100 μL) and measure at 450 nm with a microplate reader.

4. ANALYSIS

Typical dilution patterns of urine and serum samples of rat and man are shown in Fig. 2. Coating plate wells with aldehyde-modified BSA or with MAb for sandwich ELISA did not allow detection of immunoreactive components with the same samples. Anti-acrolein reactive component levels in human and rat urine samples are easily quantifiable and the values for five human individuals are shown in Table 1, in which No. 5 was the highest, being two- to three-fold higher than others. The dilution factor (fold) is the degree of dilution for a sample to give 50% inhibition of the MAb binding, and the amount of immunoreactive component can then be calculated from ([FDP concentration to give 50% inhibition] × dilution factor), with FDP as a tentative standard. The amounts of immunoreactive components contained in the sera of rat and man were approx 1/10 to 1/20 those contained in urine samples of either species. Anti-HNE reactive component levels in the sera and urine samples were much lower than those of anti-acrolein reactive ones (Fig. 2B). Statistically significant differences were observed between sera

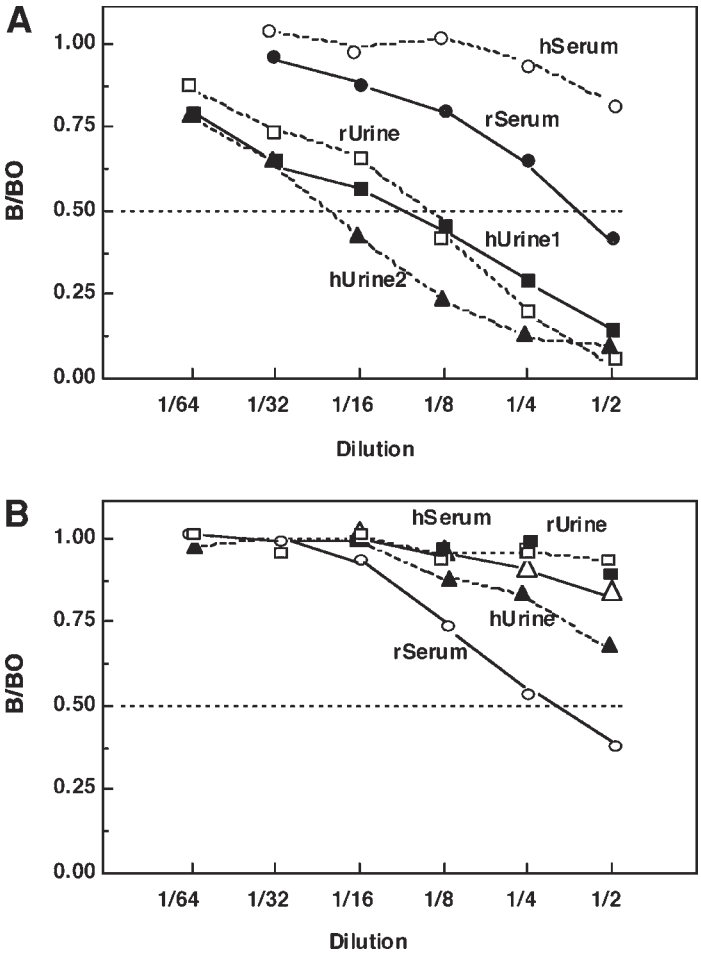

Fig. 2. Detection of immunoreactive components in serum and urine samples of rat and man. (**A**) and (**B**) are dilution patterns of samples examined with mAb5F6 (0.25 μg/well) and mAbHNEJ2 (0.05 μg/well) antibodies.

from normal individuals and patients with renal diseases by the HNE-assay (data not shown).

5. DISCUSSION

ELISA is one of the most widely used immunochemical techniques in biological sciences. Antigen coating, blocking, and first and sec antibody bindings are the major steps that take overnight, 1, 1, and 1.5 h, respec-

Table 1
Anti-acrolein Antibody-Reactive Components in Human Urine Samples

Sample no.	Dilution factor[a]	m*M*[b]
1	5.5	0.41
2	5.0	0.37
3	6.8	0.50
4	6.1	0.45
5	16.8	1.24

[a]Degree of dilution (fold) for a sample fluid to give 50% inhibition of competition i.e., (1/2)B/B_0 value corresponding to 74 μ*M* FDP under the assay conditions.
[b]FDP-equivalent concentration.

tively, for routine determinations. Various improvements have been achieved in the present 1-h assay for acrolein and HNE-modified proteins. First, epitopes were directly attached to the blocking matrices of the casein mixture, allowing for coating and blocking simultanously. This follows from the effective blocking ability of milk proteins according to Duhamel and Johnson *(10)*. The epitope-attachment modification is simple and efficient, and the matrix protein binding to the plate well is strong enough to hold the antibodies in place. The first two steps have been found to be very fast and akin to the diffusion-controlled rate limiting reactions characteristic of hydrophobic interaction *(11,12)*. In addition, the third step (sec antibody binding) has also been noted to be much faster than expected. Thus, minimal reaction times required for the coating/blocking, and the first and sec antibody binding, are 3, 3, and 7 min, or less, respectively. As the solid-phase binding process, i.e., antigen coating for ordinary ELISA and/or antibody coating for the sandwich method, usually requires overnight incubation, the rapid binding rates of the epitope-bound casein matrices are most time-saving. The antigen/antibody binding reaction is composed of primary and secary reactions *(13)*. Whereas the former monovalent binding is a rapid diffusion-controlled reaction, the latter divalent binding is slow a reaction as to take 1- or 2-wk for completion. Differing from polyclonal antibodies (PAbs), monoclonal species are completely homogenous in structure and avidity, and the binding to the solid-phase epitopes is practically a primary reaction. In addition, the sec antibody binding was also found to be fast enough, as was the case for primary reaction. Since all the antibody/antigen reactions are reversible in nature and all the components are fairly soluble in water in principle, the faster for the ELISA procedure the better in order to avoid the loss of bound materials on prolonged incubation. In the present approach, 5–10 samples were quantifiable within 30 min, including

color development and spectrophotometric measurement. With precoated plates, a 30-min ELISA is much more readily accomplished.

On quantitation of the aldehyde-modified protein components in body fluids such as serum and urine, it should be borne in mind that the products are highly heterogenous, differing from ordinary homogenous antigens. Aldehyde-modified authentic proteins must also be different from molecule to molecule. Despite of the low antigenicities of low molecular-weight compounds, haptenic FDP-lysine and HNE-histidine were tentatively used as standards in the present study. For comparison of immunoreactive components in biomaterials, it may be more practical simply to estimate the dilution factor that gives 50% inhibition of competition, because MAbs are highly stable as to give reproducible results. The present rapid method could be employed efficiently in identification of the structural and immunogenic features of the major antigen(s) in combination with appropriate chromatographic fractionations. It was also noteworthy that the kinetic processes of ovalbumin modification with acrolein was conveniently characterized by the 1-h ELISA. As the present determination is rapid, sensitive, and convenient, it may have advantages in various aspects of oxidative stress and carcinogenic insult *(1,2)*. Quantitation and identification of reaction products might thus allow elucidation of the molecular mechanisms underlying the adverse effects of aldehydic compounds. Present epitope-attachment methodology may also be applicable to various other haptenic molecules of bilogical importance.

REFERENCES

1. Hallwell, B. and Gutteridge, J. M. C. (1998) Free Radicals in Biology and Medicine, 3rd ed. Oxford Science Publ. Great Clarendon.
2. Esterbauer, H., Schaur, R. J., and Zollner, H. (1991) Chemistry and biochemistry of 4-hydroxynonenal, malonaldehyde and related aldehydes. *Free Radic. Biol. Med.* **11,** 81–128.
3. Benedetti, A., Comporti, M., and Esterbauer, H. (1980) Identification of 4-hydroxynonenal as a cytotoxic product originating from the peroxidation of liver microsomal lipids. *Biochim. Biophys. Acta* **620,** 281–296.
4. Uchida, K. and Stadtman, E. R. (1992) Modification of histidine residues in proteins by reaction with 4-hydroxynonenal. *Proc. Natl. Acad Sci. USA* **89,** 4544–4548.
5. Satoh, K., Kitahara, A., Soma, Y., Inaba, Y., Hatayama, I., and Sato, K.(1985) Purification, induction, and distribution of placental glutathione transferase: a new marker enzyme for preneoplastic cells in the rat chemical hepatocarcinogenesis. *Proc. Natl. Acad. Sci. USA* **82,** 3964–3968.

6. Toyokuni, S., Miyake, N., Hiai, H., Hagiwara, M., Kawakishi, S., Osawa, T., and Uchida, K. (1995) The monoclonal antibody specific for the 4-hydroxy-2-nonenal histidine adduct. *FEBS Lett.* **359,** 189–191.
7. Uchida, K., Kanematsu, M., Sakai, K., et al. (1998) Protein-bound acrolein: potential markers for oxidative stress. *Proc. Natl. Acad. Sci. USA* **95,** 4852–4887.
8. Satoh, K., Yamada, S., Koike, Y., et al. (1999) A 1-hour enzyme-linked immunosorbent assay for quantitation of acrolein- and hydroxynonenal-modified proteins by epitope-bound casein matrix method. *Anal. Biochem.* **270,** 323–328.
9. Uchida, K., Kanematsu, M., Morimitsu, Y., Osawa, T., Noguchi, N., and Niki, E.(1998) Acrolein is a product of lipid peroxidation reaction. Formation of free acrolein and its conjugate with lysine residues in oxidized low density lipoproteins. *J. Biol. Chem.* **273,** 16,058–16,066.
10. Duhamel, R. C. and Johnson, D. A. (1985) Use of nonfat dry milk to block nonspecific nuclear and membrane staining by avidin conjugates. *J. Histochem. Cytochem.* **33,** 711–714.
11. Froese, A., Sehon, A. H., and Eigen, M. (1962) Kinetic studies of protein-dye and antibody-hapten interactions with the temperature-jump method. *Canad. J. Chem.* **40,** 1786–1797.
12. Day, L. A., Sturtevant, J. M., and Singer, S. J. (1962) The kinetics of the reactions between antibodies to the 2,4 dinitrophenyl group and specific haptens. *Ann. N. Y. Acad. Sci.* **103,** 611–625.
13. Kabat, E. A. and Mayer, N. M. (1961) *Experimental immunochemistry*, 2nd ed., Charles C. Thomas Publ., Springfield, IL, pp. 22–96.

7

Fluorometric and Colorimetric Assessment of Thiobarbituric Acid-Reactive Lipid Aldehydes in Biological Matrices

Kelly S. Williamson, Kenneth Hensley, and Robert A. Floyd

1. INTRODUCTION

The thiobarbituric acid (TBA) assay was developed to quantitatively determine lipid peroxidation for aldehydic compounds in biological matrices. Kohn and Liversedge introduced this methodology in 1944 *(1,2)*. Since its introduction, the TBA assay has generated widespread interest in providing valuable information in the assessment of free radical-mediated damage owing to various disease pathologies as well as peroxidation of fatty acids, foods from plant and animal sources, cell membranes *(2–4)*, and rat-liver microsomes *(3–5)*. A biological marker that indicates oxidative stress with respect to lipid peroxidation in body fluids or cells is malondialdehyde (MDA). MDA is a byproduct of the arachidonate cycle, as well as lipid peroxidation *(6–8)* and is detectable in quantifiable amounts employing the TBA assay. TBA and MDA react to form a schiff base adduct (illustrated in Fig. 1) under high temperature/acidic conditions to produce a chromogenic/fluorescent product that can be easily measured employing various analytical techniques such as spectrophotometric *(7,9–11)* or fluorometric methods *(6,12–14)*. Incorporating HPLC with ultraviolet (UV)/fluorometric detection or gas chromatography–mass spectrometry (GC–MS) have also been used previously to determine TBA-MDA adducts *(2–3,5,15–17)* but those methodologies are beyond the scope of this investigation. Our laboratory has developed a quick, simple, and reliable bioanalytical assay using a fluo-

From: *Methods in Pharmacology and Toxicology: Methods in Biological Oxidative Stress*
Edited by: K. Hensley and R. A. Floyd

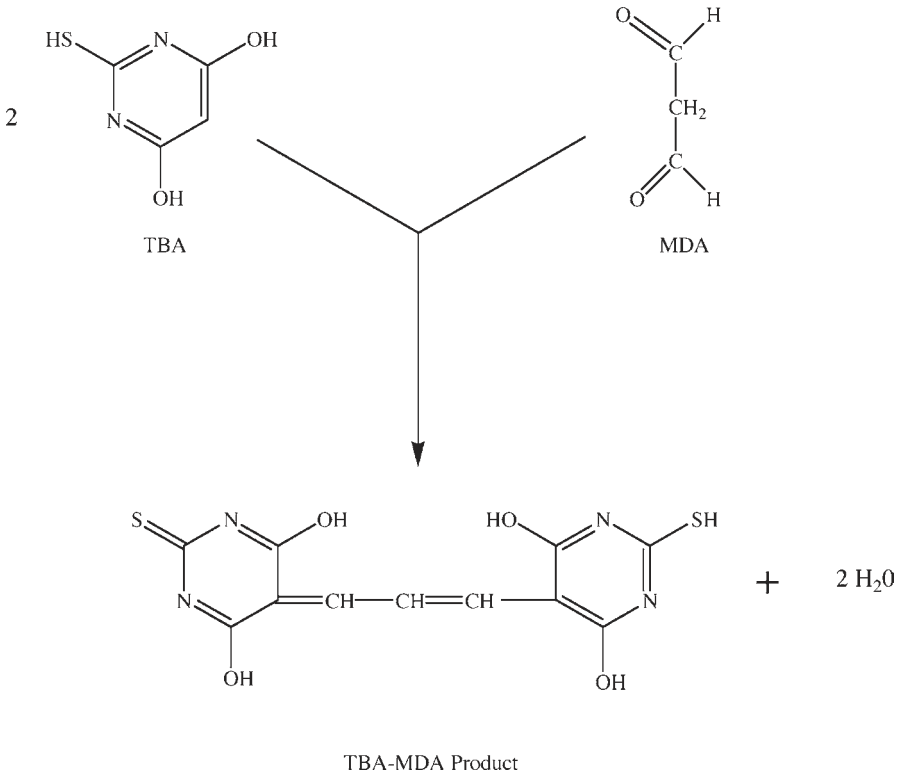

Fig. 1. The chemical reaction between TBA and MDA to yield the TBA-MDA adduct as discussed in the text.

rescence microplate reader in the detection, as well as quantification of the TBA-MDA adduct (lipid peroxidation product) in rat liver microsomes, which we describe here.

2. MATERIALS

Unless otherwise stated, all reagents were purchased from Fisher Scientific (Pittsburgh, PA) or Sigma Chemical Company (St. Louis, MO).

1. TBA Reagents. 0.25 *N* HCl, 15% trichloroacetic acid (TCA), 2.5 m*M* butylated hydroxytoluene (BHT) in absolute ethanol, 0.375% 2-thiobarbituric acid (TBA), 8.1% sodium dodecyl sulfate (SDS) were prepared.
2. IEC HN-SII Benchtop Centrifuge (International Equipment Co., Needham Hts., MA).
3. Vortex-Genie (Scientific Industries, Inc., Bohemia, NY).

4. Pierce Reacti-Therm III™ Heating Module (Pierce, Rockford, IL).
5. Beckman Coulter™ Du® 640B UV Spectrophotometer (Beckman Coulter, Fullerton, CA).
6. Fluorescence Microplate Reader (Fmax, Molecular Devices Corp., Sunnyvale, CA).
7. THERMOmax™ UV Microplate Reader (Molecular Devices Corp., Sunnyvale, CA).
8. Standard. MDA or 1,1,3,3-tetraethoxypropane was purchased from Sigma Chemical Co., prepared at a stock concentration of 10 m*M* in absolute ethanol, and checked by UV spectrophotometry *(11)*.

3. METHODS

1. The TBA method employed by Chirico et al. *(5)* and Lapenna et al. *(10)* was modified and consisted of removing the liver from a sacrificed rat and sonicating it in 10 mL of phosphate-buffered saline-1X (PBS). A 0.100-mL aliquot of the liver homogenate was put aside for a Lowry protein assay to determine the protein concentration. 100 m*M* ascorbic acid in PBS (adjust pH between 7.0–7.5) and 10 m*M* $FeCl_3$ solutions were prepared. Triplicate sample treatments of the liver homogenates were designated in the following manner:
   a. Control-liver homogenate only;
   b. 100 μ*M* ascorbic acid;
   c. 100 μ*M* ascorbic acid + 100 μ*M* $FeCl_3$.
2. Transfer 0.500-mL aliquots of each of the prepared microsome homogenates into individual, 15-mL centrifuge tubes. The following volumes of each reagent were added to the sample/standard: 250 μL of 15% TCA, 250 μL of 0.25 *N* HCl, 250 μL of 2.5 m*M* BHT in absolute ethanol, 250 μL of 0.375% TBA, and 100 μL of 8.1% SDS. Vortex mix each sample for approx 1 min and minimize light exposure as much as possible. Incubate samples at 37°C for 30 min, add 0.005 mL of 100 m*M* BHT in absolute ethanol, and the final volume of treated rat-liver microsomal homogenates was approx 0.500 mL.
3. The mixture was incubated for 60 min at 95°C. After heating, the tubes were placed on ice to stop the reaction and to cool the samples. As the rat-liver homogenates are heated, A reddish-pink color will evolve, demonstrating the TBA-MDA homolog has been generated. Centrifuge samples at 4,000 rpm on an IEC HN-SII benchtop centrifuge, at ambient temperature for 10 min. Remove 200 μL from each calibration standard/sample and transfer to a 96-well plate for fluorometric microplate-reader analysis.
4. The detection limits of the TBA assay were determined to demonstrate instrument efficiency. A calibration curve consisting of 0.500 mL MDA standards were prepared at varying concentrations in PBS to run inconjunction with the liver homogenate samples and submitted to the aforementioned TBA protocol (steps 1–3) for processing/analysis. Sample and reagent blanks were also processed and analyzed, as previously mentioned in steps 1–3 for background determination.

4. SPECTROPHOTOMETRIC VS FLUOROMETRIC MICROPLATE READER ANALYSIS

For comparative purposes between a UV spectrophotometric and fluorometric microplate reader, a UV spectrophotometric and fluorometric microplate reader were used to generate calibration curves using the TBA assay with MDA standards. This was done to demonstrate the sensitivity differences between the spectrophotometric and fluorometric microplate readers. Serial dilutions of the stock 10 m*M* MDA standard were performed, run through the TBA assay to form the TBA-MDA adduct, and analyzed by both microplate readers at (UV: 540/560 nm; fluorescence excitation: 544 nm; fluorescence emission: 590 nm). Fig. 2 and 3 illustrate representative calibration curves of serial dilutions consisting of the TBA-MDA adduct after processing. Concentrations and recoveries of TBA-MDA standards employing both detection techniques are shown in Tables 1 and 2. Fluorometric detection generated a minimum quantifiable limit (MQL) of 50 n*M* whereas spectrophotometric detection produced a MQL of 100 n*M*. The results concluded that fluorometric detection is much more sensitive than spectrophotometric detection.

NOTE: Our laboratory is interested in evaluating a bioanalytical/screening assay for generating a high throughput of samples using the aforementioned assay. In order to streamline and custom-tailor our protocol from other TBA methods used to sequester the TBA-MDA adduct, previous publications reported using n-butanol as an extraction solvent. In this protocol, samples were processed using the TBA assay with and without n-butanol and no discrepancies in the TBA-MDA homolog concentrations were determined.

5. ANALYSIS

The optimized fluorescence microplate reader parameters used are as follows:

- Wavelength: excitation: 544 nm; emission: 590 nm
- Assay Type: endpoint read
- Integration time: 20 ms
- Concentration units: μ*M*
- AUTOmix: On
- Autocalibrate: On
- Plate pre-read: Off
- Plate blank subtract: On

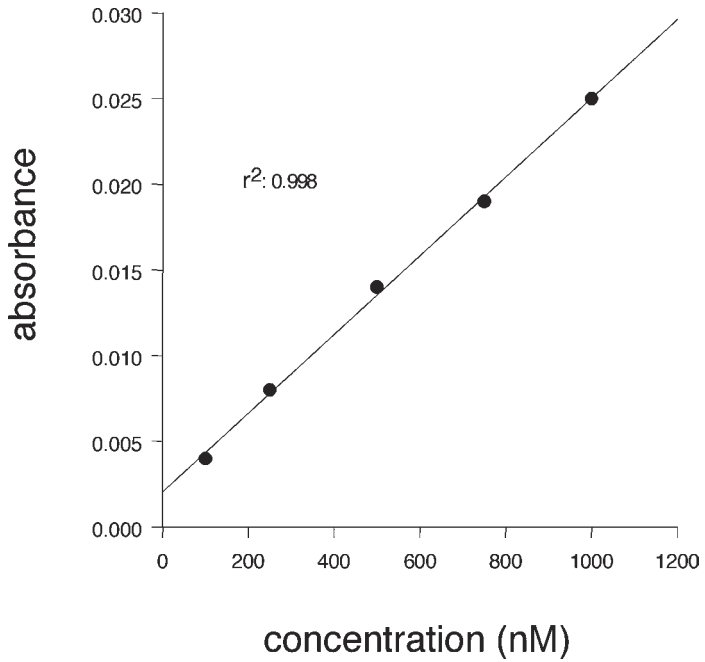

Fig. 2. Representative UV spectrophotometric microplate reader-calibration curve using the TBA assay with MDA standards only.

Quantification of standards/samples was determined by fluorometric microplate reader analysis. Linear-regression analysis and the correlation coefficient (r^2) were calculated to demonstrate linearity of each calibration curve generated. TBA-MDA concentrations of rat liver microsomes were determined to be in the submicromolar range as depicted in Table 3.

6. DISCUSSION

An overall assessment employing the TBA assay as a bioanalytical tool to accurately quantify lipid peroxidation in rat-liver microsomes was shown. The MQL for the TBA-MDA adduct was reported to be 50 n*M* via fluorometric microplate-reader analysis. Other biological matrices, such as serum or plasma, can be analyzed by this method as a quick-screening TBA assay, but there is still some debate, as well as drawbacks *(2–6,11,14–16)* on the accuracy and reliability. Instrumentation consisting of HPLC coupled with spectrophotometric or fluorometric detection and GC–MS are also excellent analytical screening techniques used to analyze aldehydic compounds in bio-

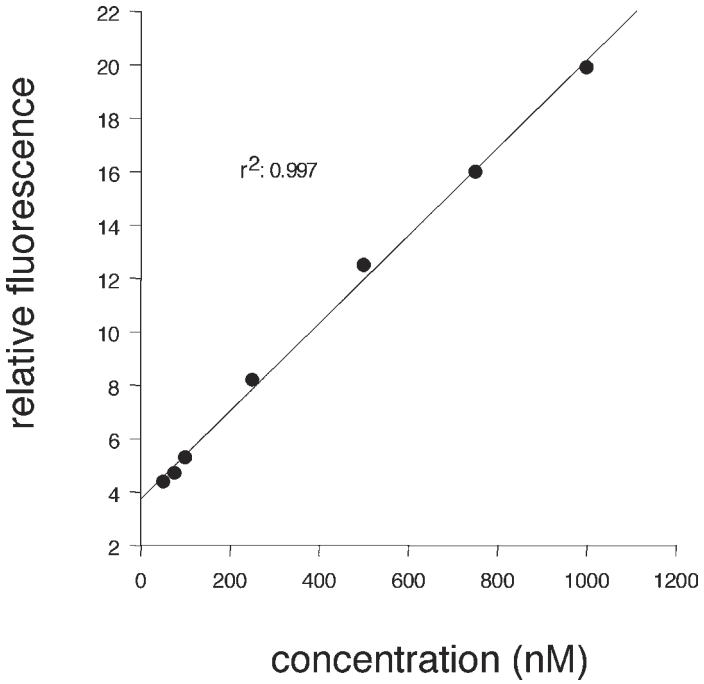

Fig. 3. Representative fluorometric microplate reader-calibration curve of serial dilutions consisting of the TBA-MDA adduct after employing the TBA assay.

Table 1
Concentrations and Recoveries of TBA-MDA Standards Employing Spectrophotometric Detection

Standard I.D.	Nominal concentration (n*M*)	Absorbance	Actual concentration (n*M*)	Percent recovered (%)
Vial #1	100	0.004	105.9	105.9
Vial #2	250	0.008	282.2	112.9
Vial #3	500	0.014	513.6	102.7
Vial #4	750	0.019	733.9	97.9
Vial #5	1000	0.025	998.2	99.8

logical matrices. In order to get a true and accurate measure of lipid peroxidation in different biological samples, the user should employ additional bioanalytical methodologies and techniques for comparative purposes, as well as to attempt to alleviate any possible ambiguities between bioassays.

Table 2
Concentrations and Recoveries of TBA-MDA Standards Employing Fluorometric Detection

Standard I.D.	Nominal concentration (n*M*)	Mean relative fluorescence units (MRFUs)	Actual concentration (n*M*)	Percent recovered (%)
Vial #1	50	4.39	43.3	86.6
Vial #2	75	4.72	63.6	84.8
Vial #3	100	5.30	98.5	98.5
Vial #4	250	8.20	274.1	109.6
Vial #5	500	12.5	537.2	107.4
Vial #6	750	16.0	747.0	99.6
Vial #7	1000	19.9	979.3	97.9

Table 3
TBA-MDA Concentrations of Rat-Liver Microsomes Using Fluorometric Detection

Vial number	Standard I.D.	Actual concentration (μ*M*)
Vial #1	Control homogenate	3.94
Vial #2	Control homogenate	3.82
Vial #3	Control homogenate	3.61
Vial #4	100 μ*M* Ascorbic acid	3.72
Vial #5	100 μ*M* Ascorbic acid	3.67
Vial #6	100 μ*M* Ascorbic acid	3.94
Vial #7	100 μ*M* Ascorbic acid + 100 μ*M* $FeCl_3$	9.76
Vial #8	100 μ*M* Ascorbic acid + 100 μ*M* $FeCl_3$	8.62
Vial #9	100 μ*M* Ascorbic acid + 100 μ*M* $FeCl_3$	7.65

ACKNOWLEDGMENTS

This work was supported by the National Institute of Health (NIH NS35747) and the Oklahoma Center for the Advancement of Science and Technology (OCAST H967067).

REFERENCES

1. Kohn, H. I. and Liversedge, M. (1944) New aerobic metabolite whose production by brain is inhibited by apomorphine, emetine, ergotamine, epinephrine, and menadione. *J. Pharmacol. Exp. Ther.* **82,** 292–300.
2. Chirico, S. (1994) High-performance liquid chromatography-based thiobarbituric acid tests. *Methods Enzymol.* **233,** 314–318.
3. Esterbauer, H., Lang, J., Zadravec, S., and Slater, T. F. (1984) Detection of malonaldehyde by high-performance liquid chromatography. *Methods Enzymol.* **105,** 319–328.
4. Halliwell, B. and Gutteridge, J. M. C. (1999) Free Radicals in Biology and Medicine, 3rd ed. Oxford Press, New York, NY.
5. Chirico, S., Smith, C., Marchant, C., Mitchinson, M. J., and Halliwell, B. (1993) Lipid peroxidation in hyperlipidaemic patients. A study of plasma using an HPLC-based thiobarbituric acid test. *Free Radic. Res. Commun.* **19,** 51–57.
6. Wasowicz, W., Nève, J., and Peretz, A. (1993) Optimized steps in fluorometric determination of thiobarbituric acid-reactive substances in serum: importance of extraction pH and influence of sample preservation and storage. *Clin. Chem.* **39,** 2522–2526.
7. Jain, S. K. (1988) Evidence for membrane lipid peroxidation during in vivo aging of human erythrocytes. *Biochem. Biophys. Acta.* **937,** 205–210.
8. Bird, R. P. and Draper, H. H. (1984) Comparative studies of different methods of malondialdehyde determination. *Methods Enzymol.* **105,** 299–305.
9. Hoving, E. B., Laing, C., Rutgers, H. M., Teggeler, M., Van Doormaal, J. J., and Muskiet, F. A. J. (1992) Optimized determination of malondialdehyde in plasma lipid extracts using 1,3-diethyl-2-thiobarbituric acid: Influence of detection method and relations with lipids and fatty acids in plasma from healthy adults. *Clin. Chim. Acta.* **208,** 63–76.
10. Lapenna, D., Ciofani, G., Pierdomenico, S. D., Giamberardino, M. A., and Cuccurullo, F. (2001) Reaction conditions affecting the relationship between thiobarbituric acid reactivity and lipid peroxides in human plasma. *Free Radic. Biol. Med.* **31,** 331–335.
11. Jentzsch, A. M., Bachmann, H., Fürst, P., and Biesalski, H. K. (1996) Improved analysis of malondialdehyde in human body fluids. *Free Radic. Biol. Med.* **20,** 251–256.
12. Conti, M., Morand, C., Levillain, P., and Lemmonnier, A. (1991) Improved fluorometric determination of malondialdehyde. *Clin. Chem.* **37,** 1273–1275.
13. Hendriks, T. and Assmann, R. T. F. A. (1988) On the fluorometric assay of circulating lipoperoxides. *Clin. Chem. Acta.* **174,** 263–270.
14. Richard, M. J., Portal, B., Meo, J., Coudray, C., Hadjian, A., and Favier, A. (1992) Malondialdehyde kit evaluated for determining plasma and lipoprotein fractions that react with thiobarbituric acid. *Clin. Chem.* **38,** 704–709.
15. Largillière, C. and Mélancon, S. B. (1988) Free malondialdehyde determination in human plasma by high-performance liquid chromatography. *Anal. Biochem.* **170,** 123–126.

16. Uchiyama, M. and Mihara, M. (1978) Determination of malonaldehyde precursor in tissues by thiobarbituric acid test. *Anal. Biochem.* **86,** 271–278.
17. Yeo, H. C., Helbock, H. J., Chyu, D. W., and Ames, B. N. (1994) Assay of MDA in biological fluids by GC-MS. *Anal. Biochem.* **220,** 391–396.

8

HPLC With Electrochemical and Photodiode Array Detection Analysis of Tocopherol Oxidation and Nitration Products in Human Plasma

Kelly S. Williamson, Kenneth Hensley, and Robert A. Floyd

1. INTRODUCTION

Advances in analytical methodologies in the isolation, characterization, and quantitation of lipid-soluble antioxidants, such as vitamin E, have evolved since its discovery in 1922 *(1)*. The primary purpose of vitamin E (tocopherol) and its tocopherol homologs is to act as free radical scavengers to control lipid oxidation in the body *(2)*. The physiological and biochemical processes lipid-soluble vitamins possess are beneficial in preventing a number of degenerative diseases and conditions such as Alzheimer's disease and Parkinson's disease *(3–7)*, cardiovascular disease *(8–10)*, and cancer *(11–13)*. Pharmaceutical, medical, as well as industrial disciplines have been interested in the clinical outcomes of tocopherol studies. Thus, a critical need exists to measure multiple tocopherols and their oxidation products simultaneously in human tissue *(2,14–19)*. Our laboratory is interested in studying lipid nitration products in biological matrices primarily as biomarkers to determine the level of oxidative stress and tissue damage. 3-Nitrotyrosine has been determined to be a useful protein biomarker employed to measure oxidative stress based in previous publications (20–26). The most commonly measured nitrated tocopherol compound of interest is 5-NO_2-γ-tocopherol *(2,19,27,28)*. This and other tocopherol congeners of interest are depicted in Fig. 1. High performance liquid chromatography (HPLC) with combined electrochemical and photo-

From: *Methods in Pharmacology and Toxicology: Methods in Biological Oxidative Stress*
Edited by: K. Hensley and R. A. Floyd

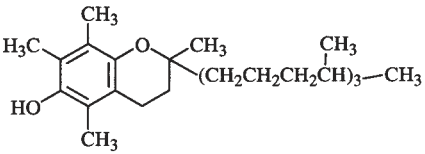

α-tocopherol

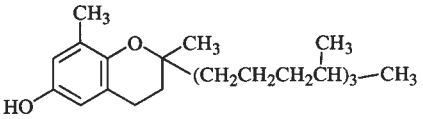

δ-tocopherol

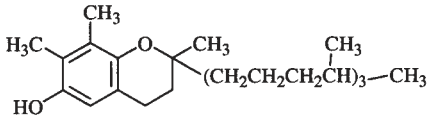

γ-tocopherol

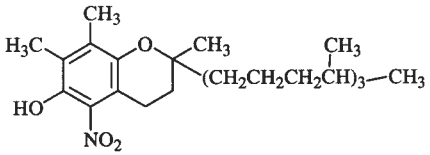

5-nitro-γ-tocopherol

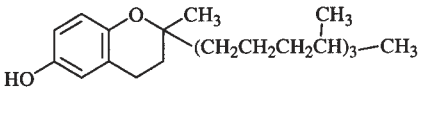

tocol

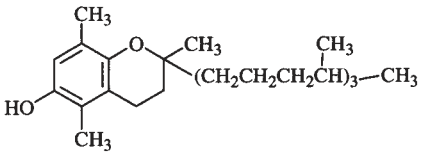

β-tocopherol

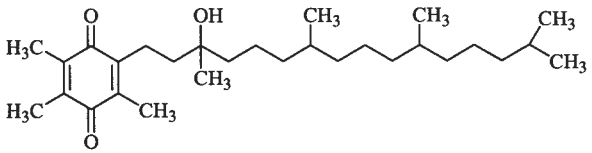

α-tocopheryl quinone

Fig. 1. The chemical structures of the different tocopherol congeners discussed in the text.

diode array detection (HPLC–ECD–PDA) is a relatively new, versatile and reliable chromatographic technique employed to generate high sensitivity and selectivity, reproducibility, and accuracy in the determination of tocopherol homologs. HPLC–ECD–PDA generates chromatograms that provide information on both the electrochemical properties and spectral properties of resolved analytes. The instrumental principles of HPLC–ECD–PDA have been previously discussed *(2,19)*. Therefore, the primary focus of this chapter is to discuss the bioanalytical methodologies and techniques used to analyze 5-NO_2-γ-tocopherol as well as its tocopherol variants in human plasma samples.

2. MATERIALS

Unless otherwise stated, all reagents and HPLC-grade solvents were purchased from Fisher Scientific (Pittsburgh, PA) or Sigma Chemical Company (St. Louis, MO).

1. HPLC grade hexane, methylene chloride, methanol, and acetonitrile.
2. Ethanol-absolute-200 proof (AAPER Alcohol and Chemical Co., Shelbyville, KY).
3. 10 mg/mL ethanolic butylated hydroxtoluene (BHT).
4. IEC HN-SII benchtop centrifuge (International Equipment Co., Needham Hts., MA).
5. Vortex-Genie (Scientific Industries, Inc., Bohemia, NY).
6. UV Spectrophotometer (Beckman DU® 65 Series Spectrophotometer, Fullerton, CA).
7. 13-mm, 0.2-μm Pall Gelman® Acrodisks LC PVDF syringe filters.
8. Mobile Phase: 30 m*M* lithium acetate, 83% HPLC grade acetonitrile, 12% HPLC grade methanol, 0.2% HPLC-grade acetic acid and 50 μL/L reagent MB (ESA, Chelmsford, MA).
9. Standards. α-tocopherol, β-tocopherol, δ-tocopherol, γ-tocopherol, were purchased from Sigma Chemical Co., (St. Louis, MO). α-Tocol was purchased from Matreya Lipids, Inc., (Pleaseant Gap, PA). α-Tocopheryl quinone was purchased from Research Organics Inc., (Cleveland, OH). 5-γ-NO_2-tocopherol was prepared as per Hensley et al. (2) and Cooney et al. (27). Briefly, an ethanolic solution containing 10 mg/mL of γ-tocopherol is briefly sparged with NO_2 (g). The resulting sample is separated across a silica column with a mobile phase containing 99% methylene chloride, 1% methanol. The red fraction eluting near the solvent front contains the nitration product; the yellow fraction eluting at $R_f = 0.6$ contains quinone products. Identification of 5-γ-NO_2-tocopherol was confirmed by mass spectrometry (MS) and UV spectroscopy. Concentrations of each standard were prepared, measured, and quantified by using a UV spectrophotometer. Molar extinction coefficients are listed in Table 1. Serial dilutions of mix standards were prepared by diluting all tocopherol homologs at varying concentrations in order to generate a six-point calibration curve and demonstrate linearity.
10. HPLC–ECD–PDA Equipment. ESA Model 5600 CoulArray HPLC (ESA, Chelmsford, MA) that is equipped with a binary gradient elution system (only an isocratic system was needed), 84 vial autosampler with a column oven, and 12 electrochemical cells operating in the oxidative mode. Analyte separation was conducted on a TosoHaas (Montgomeryville, PA) reverse-phase ODS-TM C_{18} analytical column (4.6 × 250 mm, 5 μm particle size). The photodiode array detector (PDA) used was a Waters 996 PDA detector (Waters Corporation, Milford, MA) equipped with its own data acquisitioning system. The software used to acquire and process chromatograms for this application was the Millenimum 32, version 2.10. Table 2 lists the optimal cell potentials for chromatographic analysis using HPLC–ECD–PDA detection. Hydrodynamic voltammograms were generated for each standard to determine the assign-

Table 1
Molar Extinction Coefficients for Tocopherol Homologs

Homolog	λ max	$M^{-1}cm^{-1}$
α-tocopherol	294 nm	3060
β-tocopherol	298 nm	3600
γ-tocopherol	298 nm	3966
δ-tocopherol	298 nm	3677
tocol	298 nm	3389
5-NO_2-γ-tocopherol	302 nm	6750
α-tocopheryl quinone	260 nm	15839

Table 2
Optimal Cell Potentials for Electrochemical Array Detection of Tocopherols Using a 12-Channel Instrument

Cell number	Cell potential (mV)	Cell number	Cell potential (mV)
1	200	7	650
2	300	8	675
3	400	9	700
4	525	10	750
5	600[a]	11	825
6	625	12	900

[a]Optimal cell potential for tocopherol analytes.

ment of chromatographic peaks, as well as determining the optimal oxidation potential for each analyte. This was done by preparing a plot of the fractional percentage of the cumulative current response versus the cell potential (mV).

3. METHODS

1. Aliquot 0.500 mL of human plasma into a 15 mL centrifuge tube, add 0.500 mL of 200 proof ethanol, 13 µL of ethanolic BHT, vortex each sample for approx 1 min, and sonicate sample (15 dips with the sonicator tip). Minimize light exposure as much as possible.
2. Transfer 6 mL of HPLC-grade hexane to each sample, vortex mix again for approx 1 min, and sonicate again as in step 1.
3. Centrifuge plasma samples at 4,000 rpm using a IEC HN-SII benchtop centrifuge, at ambient temperature for 20 min. Remove and transfer each supernant into labeled, individual 16 × 125 mm borosilicate glass culture tubes. The aqueous layer is discarded.

4. Concentrate samples to dryness with high purity nitrogen gas (heat was not used to concentrate samples-thermal degradation could result) and reconstitute in 0.500 mL HPLC-grade methanol. Transfer supernatant into appropriate sample containers.
5. Filter each sample through a 0.2-μm, 13-mm Pall Gelman® LC PVDF acrodisks prior to HPLC–ECD–PDA analysis. This is done to remove any particulate matter that might obstruct the HPLC–ECD–PDA system. Only filter and analyze samples that can be run during one sample sequence to minimize sample loss via filtration. Lipids and proteins tend to fall out of solution if stored in –20°C freezer overnight with or without filtration. It is strongly recommended that the user filter samples on the day a HPLC–ECD–PDA run sequence is initiated, otherwise, precipitation will result and possibly clog up the HPLC–ECD–PDA system.
6. As previously stated, standard mixes consisting of all 7 tocopherol congeners were prepared at different concentrations (six-point calibration curve) and interspersed among the plasma samples for HPLC–ECD–PDA autoanalysis.

4. ANALYSIS

The optimized HPLC–ECD–PDA parameters used are as follows:

- Photodiode array wavelength settings: λ_1 260 nm; λ_2 302 nm
- ECD array electrode settings: See Table 2.
- Flow rate: 2.0 mL/min
- Injection volume: 60 μL
- Column temperature: ambient
- Autosampler temperature: 4°C

All other chromatographic conditions were previously mentioned in the HPLC–ECD–PDA equipment section. Figure 2 represents a typical chromatogram of tocopherol homologs separated and detected by reverse phase HPLC–ECD after extraction from human plasma. Figure 3 compares the hydrodynamic voltamograms of the 5-NO_2-γ-tocopherol peaks between a standard and an actual plasma sample. Figure 4 illustrates the photodiode array chromatogram used to determine α-tocopheryl quinone, which is not very electrochemically active under the conditions employing the above analysis. In general, the products of tocopherol oxidation should be expressed as a ratio to their precursors. That is to say, one should report the ratio of α-tocopheryl quinone/α-tocopherol and 5-NO_2-γ-tocopherol/γ-tocopherol. Reference values for six tocopherol analytes are listed in Table 3, based on 81 samples of fresh plasma analyzed from a random population of presumptively healthy subjects in Oklahoma City, OK, USA.

It should be noted that β-tocopherol and γ-tocopherol are structural isomers that coelute on reverse phase HPLC columns. A normal phase method will

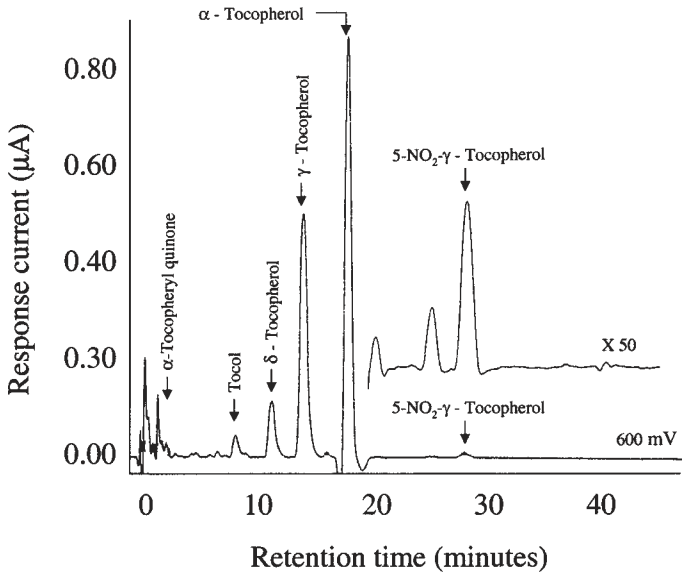

Fig. 2. A typical HPLC–ECD separation of tocopherol homologs extracted from the plasma of a presumptively normal individual; only the 600 mV channel is illustrated, for clarity.

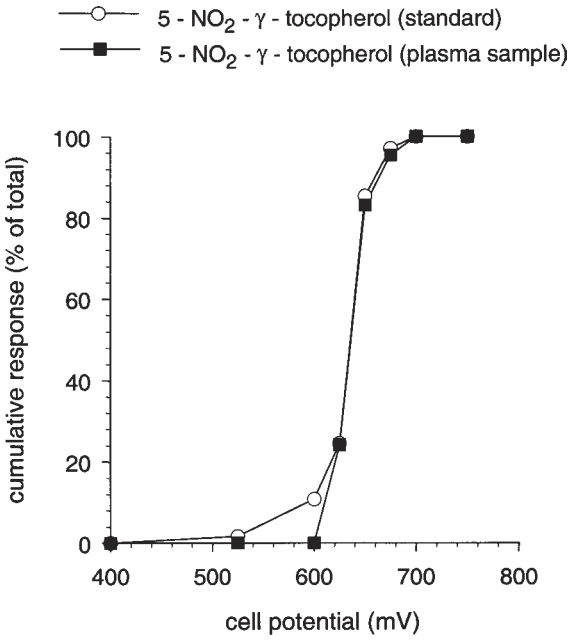

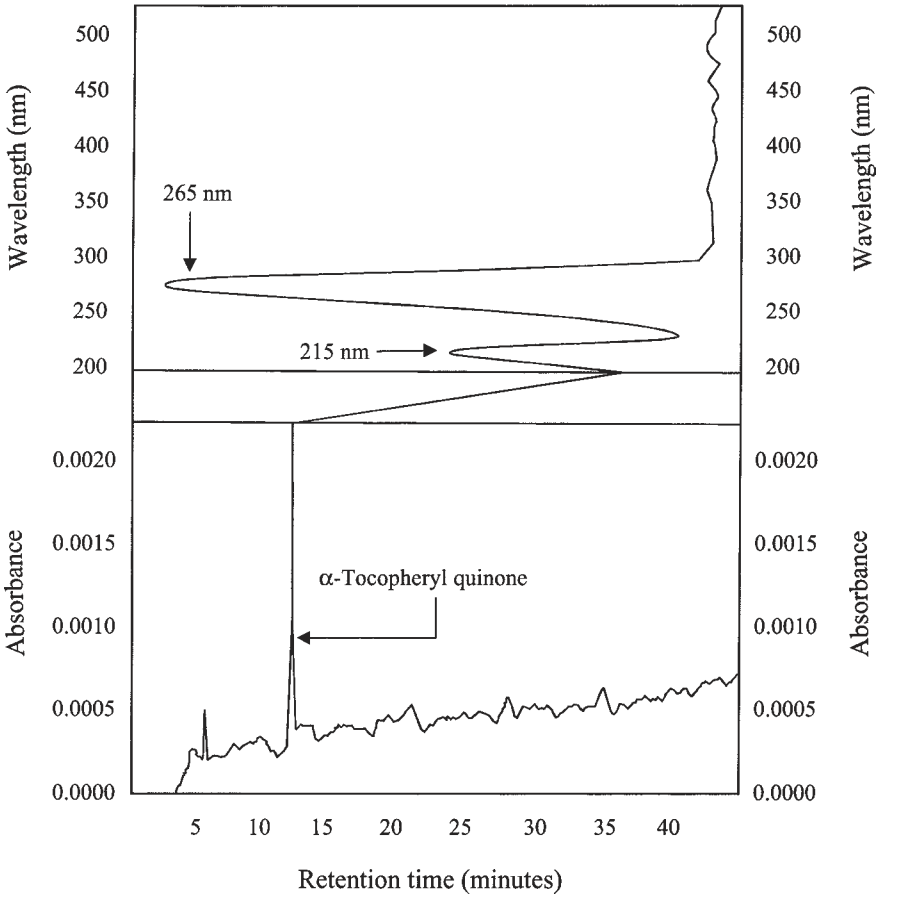

Fig. 4. Photodiode array chromatogram of a-tocopheryl quinone (the a-tocopherol oxidation product).

separate the two isomers but electrochemical detection cannot be employed since the mobile phase would strictly be a non-polar solvent of low ionic strength, e.g.. hexane. Normally the plasma ratio of β-tocopherol/γ-tocopherol is less than 0.1, so this is not a serious consideration in the analysis.

Fig. 3. *(opposite page)* Representative hydrodynamic voltammograms consisting of 5-γ-NO_2-tocopherol standard and a presumptive 5-γ-NO_2-tocopherol peak in a human plasma extract. The plots generated are a fractional percentage of the cumulative current response versus the cell potential (mV). The data collected from the chromatographic run to generate the voltammograms was done using a 12-channel coulometric array as discussed in the text.

Table 3
Reference Values for Tocopherol Concentrations in Normal Human Plasma

Congener	Concentration in normal plasma (mean ± SEM, $N = 81$)
α-tocopherol	37.9 ± 4.5 μ*M*
γ-tocopherol	2.25 ± 0.28 μ*M*
δ-tocopherol	325 ± 27 n*M*
tocol	125 ± 8 n*M*
5-NO_2-γ-tocopherol	19.5 ± 2.6 n*M*
α-tocopheryl quinone	47.4 ± 8.1 n*M*

5. DISCUSSION

HPLC–ECD–PDA is an effective, quantitative method used to study lipid oxidation and nitration products in biological matrices such as plasma samples. The detection limit determined for 5-NO_2-γ-tocopherol and its tocopherol homologs, using this method, was approx 1 n*M*. These methods are amenable to automation and may be widely applicable to basic and applied research and clinical medicine.

ACKNOWLEDGMENTS

This work was supported by the National Institute of Health (NIH NS35747) and the Oklahoma Center for the Advancement of Science and Technology (OCAST H967067).

REFERENCES

1. Serbinova, E. A. and Packer, L. (1994) Antioxidant properties of α-tocopherol and α-tocotrienol. *Methods Enzymol.* **234,** 354–366.
2. Hensley, K., Williamson, K. S., and Floyd, R. A. (2000) Measurement of 3-nitrotyrosine and 5-nitro-γ-tocopherol by high-performance liquid chromatography with electrochemical detection. *Free Radic. Biol. Med.* **28,** 520–528.
3. Sano, M., Ernesto, C., Thomas, R. G., Klauber, M. R., Schafer, K., Grundman, M., et al. (1997) A controlled trial of selegiline, alpha-tocopherol, or both as treatment for Alzheimer's disease. *N. Engl. J. Med.* **336,** 1216–1222.
4. Jiménez-Jiménez, F. J., Bustos de, F., Molina, J. A., Benito-León, J., Tallón-Barranco, A., Gasalla, T., et al. (1997) Cerebrospinal fluid levels of alpha-tocopherol (vitamin E) in Alzheimer's disease. *J. Neural Transm.* **104,** 703–710.

5. Metcalfe, T., Bowen, D. M., and Muller, D. P. R. (1989) Vitamin E concentrations in human brain of patients with Alzheimer's disease, fetuses with Down's syndrome, centenarians, and controls. *Neurochem. Res.* **14,** 1209–1212.
6. Grundman, M. (2000) Vitamin E and Alzheimer's disease: the basis for additional clinical trials. *Am. J. Clin. Nutr.* **71 (suppl),** 630S–636S.
7. Adams, Jr., J. D., Klaidman, L. K., Odunze, I. N., Shen, H. C., and Miller, C. A. (1991) Alzheimer's and Parkinson's disease: Brain levels of glutathione, glutathione disulfide, and vitamin E. *Mol. Chem. Neuropathol.* **14,** 213–226.
8. Janero, D. R. (1991) Therapeutic potential of vitamin E in the pathogenesis of spontaneous atherosclerosis. *Free Radic. Biol. Med.* **11,** 129–144.
9. Rimm, E. B., Stampfer, M. J., Ascherio, A., Giovannucci, E., Colditz, G. A., and Willett, W.C. (1993) Vitamin E consumption and the risk of coronary heart disease in men. *N. Engl. J. Med.* **328,** 1450–1456.
10. Armstrong, N. C., Paganga, G., Brunner, E., Miller, N. J., Nanchahal, K., Shipley, M., et al. (1997) Reference values for α-tocopherol and β-carotene in the Whitehall II Study. *Free Rad. Res.* **27,** 207–219.
11. Gridley, G., McLaughlin, J. K., Block, G., Blot, W.J., Gluch, M., and Fraumeni, Jr., J. F. (1992) Vitamin supplement use and reduce risk of oral and pharyngeal cancer. *Am. J. Epidemiol.* **135,** 1083–1092.
12. Wald, N. J., Boreham, J., Hayward, J. L., and Bulbrook, R. D. (1984) Plasma retinol, β-carotene, and vitamin E levels in relation to the future risk of breast cancer. *Br. J. Cancer.* **49,** 321–324.
13. Bostick, R. M., Potter, J. D., McKenzie, D. R., Sellers, T. A., Kushi, L. H., Steinmetz, K. A., and Folsom, A. R. (1993) Reduced risk of colon cancer with high intake of vitamin E: the Iowa's women health study. *Cancer Res.* **53,** 4230–4237.
14. Simon, E., Paul, J. L., Atger, V., Simon, A., and Moatti, N. (2000) Study of vitamin E net mass transfer between α-tocopherol-enriched HDL and erythrocytes: application to asymptomatic hypercholesterolemic men. *Free Radic. Biol. Med.* **28,** 815–823.
15. Schüep, W. and Rettenmaier, R. (1994) Analysis of vitamin E homologs in plasma and tissue: high-performance liquid chromatography. *Methods Enzymol.* **234,** 294–302.
16. Zaman, Z., Fielden, P., and Frost, P. G. (1993) Simultaneous determination of vitamins A and E and carotenoids in plasma by reverse-phase HPLC in elderly and younger subjects. *Clin. Chem.* **39,** 2229–2234.
17. Stahl, W., Graf, P., Brigelius-Flohé, R., Wechter, W., and Sies, H. (1999) Quantification of the α- and γ-tocopherol metabolites 2,5,7,8-tetramethyl-2-(2'-carboxyethyl)-6-hydroxychroman and 2,7,8-trimethyl-2-(2'-carboxyethyl)-6-hydroxychroman in human serum. *Anal. Biochem.* **275,** 254–259.
18. Katsanidis, E. and Addis, P. B. (1999) Novel HPLC analysis of tocopherols, tocotrienols, and cholesterol in tissue. *Free Radic. Biol. Med.* **27,** 1137–1140.
19. Hensley, K., Williamson, K. S., Maidt, M. L., Gabbita, S. P., Grammas, P., and Floyd, R. A. (1999) Determination of biological oxidative stress using high performance liquid chromatography with electrochemical detection (HPLC-ECD). *J. High Res. Chromatogr.* **22,** 429–437.

20. Hensley, K., Maidt, M. L., Pye, Q. N., Stewart, C. A., Wack, M., Tabatabaie, T., and Floyd, R. A. (1997) Quantitation of protein-bound 3-nitrotyrosine and 3,4-dihyroxyphenylalanine by high-performance liquid chromatography with electrochemical array detection. *Anal. Biochem.* **251,** 187–195.
21. Hensley, K., Maidt, M. L., Yu, Z. Q., Sang, H., Markesbery, W. R., and Floyd, R. A. (1998) Electrochemical analysis of protein nitrotyrosine and dityrosine in the Alzheimer brain reveals region-specific accumulation. *J. Neurosci.* **18,** 8126–8132.
22. Maruyama, W., Hashizume, Y., Matsubara, K., and Naoi, M. (1996) Identification of 3-nitro-l-tyrosine, a product of nitric oxide and superoxide, as an indicator of oxidative stress in the human brain. *J. Chromatogr. B Biomed. Appl.* **676,** 153–158.
23. Shigenaga, M. K. (1999) Quantitation of protein-bound 3-nitrotyrosine by high-performance liquid chromatography with electrochemical detection. *Methods Enzymol.* **301,** 27–40.
24. Kaur, H., Lyras, L., Jenner, P., and Halliwell, B. (1998) Artefacts in HPLC detection of 3-nitrotyrosine in human brain tissue. *J. Neurochem.* **70,** 2220–2223.
25. Evans, P., Kaur, H., Mitchinson, M. J., and Halliwell, B. (1996) Do human atherosclerotic lesions contain nitrotyrosine. *Biochem. Biophys. Res. Commun.* **226,** 346–351.
26. Herce-Pagliai, C., Kotecha, S., and Shuker, D. E. (1998) Analytical Methods for 3-nitrotyrosine as a marker of exposure to reactive nitrogen species: a review. *Nitric Oxide* **2,** 324–336.
27. Cooney, R. V., Harwood, P. J., Franke, A. A., Narala, K., Sundström, A. K., Berggren, P. O., and Mordan, L. J. (1995) Products of γ-tocopherol reaction with NO_2 and their formation in rat insulinoma (RINm5F) cells. *Free Radic. Biol. Med.* **19,** 259–269.
28. Williamson, K. S., Gabbita, S. P., Mou, S., West, M., Pye, Q. N., Markesbery, W. R., et al. (2002) The nitration product 5-nitro-γ-tocopherol is increased in the Alzheimer brain. *Nitric Oxide* **6,** 221–227.

II

DNA, Protein, and Amino Acids

9

Electron Paramagnetic Resonance Spin-Labeling Analysis of Synaptosomal Membrane Protein Oxidation

D. Allan Butterfield

1. INTRODUCTION

Synaptosomal protein oxidation, most often indexed by increased protein carbonyl content *(1,2)*, is one biomarker of oxidative stress in brain *(2)*. Protein carbonyls are detected by UV-Vis spectrometric, fluorescence, or immunochemical methods *(2)*, and are increased in a variety of oxidative stress disorders of the brain. Among the latter are Alzheimer's disease (AD) *(3)* and animal models of AD *(4)*, Huntington's disease (HD) *(5,6)*, and accelerated aging *(7)*.

In addition to measurement of protein carbonyl levels, protein oxidation has been monitored by electron paramagnetic resonance (EPR) in conjunction with protein-specific spin labels. Spin labeling is an EPR technique in which a relatively stable paramagnetic species (usually a nitroxide) is covalently attached to the system of interest *(8)*. In contrast to spin labels, spin probes are non-covalently attached to the system of interest, e.g., stearic acid nitroxide spin probes of the lipid bilayer. In most biological samples, including synaptosomes, the system is EPR silent; thus, the EPR signal arises from the introduced spin label *(8)*. The protein-specific spin label, 2,2,6,6-tetramethyl-4-piperidin-1-oxyl (MAL-6), is selective for cysteine sulfhydryl (SH) groups in proteins *(8)*. MAL-6 binds to at least two classes of SH groups distinguishable by the motion of the bound spin label: strongly (S) and weakly (W) immobilized (Fig. 1). Those MAL-6 spin labels covalently bound to SH groups located on the surface of proteins are relatively unhindered in their rotational motion, and consequent relatively narrow resonance

From: *Methods in Pharmacology and Toxicology: Methods in Biological Oxidative Stress*
Edited by: K. Hensley and R. A. Floyd

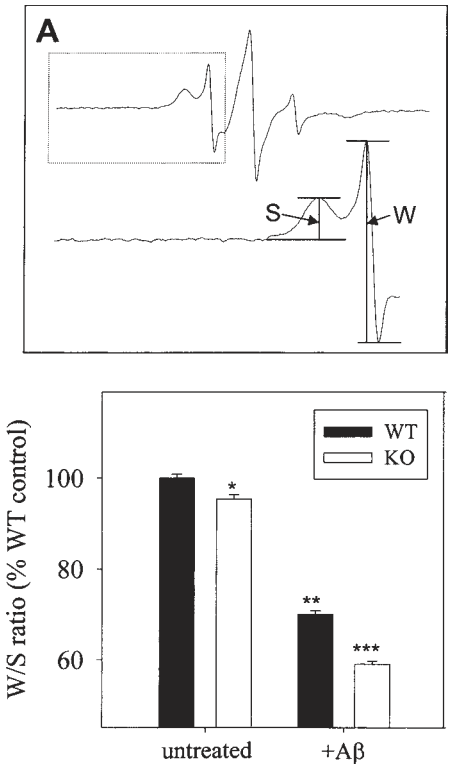

Fig. 1. (**A**) A typical EPR spectrum of MAL-6-labeled synaptosomal membrane proteins. The box outlines the low-field resonance lines depicting the W and S components, which are indicated in the lower part of (**A**). (**B**) An example of the decreased W/S ratio of MAL-6 in synaptosomal membranes undergoing oxidative stress is indicted. Synaptosomal membranes from apolipoprotein E knockout mice (KO) mice have altered protein conformations and are susceptible to further change induced by treatment with amyloid β-peptide [Aβ(1-40)]. Indicated by a decrease in the W/S ratio, synaptosomal membrane proteins isolated from apolipoprotein E KO mice have altered conformations under basal conditions. After a 3-h incubation at 37°C with 5 μ*M* Aβ(1-40), a decrease in the W/S ratio occurs in apolipoprotein E KO synaptosomal membrane proteins that is greater than the decrease observed in wild-type synaptosomal membrane proteins. Data are the mean and SEM from 4–6 preparations (*$p < 0.02$ vs WT basal, **$p < 0.001$ vs WT basal, ***$p < 0.001$ vs KO basal and WT treated; Student's t-test). Adapted from ref. *(13)*.

lines are observed in the spectrum. These lines are separated by an isotropic hyperfine coupling constant of 17.1G, the value of this parameter for MAL-6 in aqueous solution and consistent with the location of this spin label on proteins *(8)*. In addition, MAL-6 bound to W sites of membrane proteins

can be instantly reduced to the diamagnetic hydroxylamine by negatively charged ascorbate, again consistent with the polar location of the spin label on the surface of proteins *(8)*. In contrast to W sites, S sites are located in deep crevices, pockets, or protein folds that significantly restrict the motion of MAL-6. Consequently, broad resonance lines result, which in the case of the $M_I = +1$ low-field resonance line, occurs at a lower magnetic field-resonance position than that for the W sites (Fig. 1). Because the $M_I = 0$ central W and S lines overlap and the $M_I = -1$ high-field W and S resonance lines, though separated, are of low amplitude as a consequence of the quantum mechanics of nitroxides *(9)*, analysis of the EPR spectrum is confined to the low-field resonance lines. The relevant parameter, the W/S ratio, is lowered, reflecting slower spin-label motion, when membrane protein–protein interactions increase, protein crosslinking occurs, or with decreased segmental motion of proteins *(8)*. As discussed below, the W/S ratio of MAL-6 in synaptosomal membranes is decreased in oxidative stress conditions.

2. MATERIALS

MAL-6 is obtained from Sigma-Aldrich, as are all buffer materials used. Spectra are obtained using a Bruker EMX EPR spectrometer operating at X-band frequency (9.5 GHz) and employing a TM mode resonant cavity.

3. METHODS

3.1. Synaptosome Isolation

1. Synaptosomes are obtained from human or rodent brain by differential centrifugation methods *(10,11)*.
2. Cortical synaptosomes are prepared as described following. Briefly, cortices isolated from rodent or human brain are homogenized in isolation buffer (0.32 *M* sucrose, 4 μg/mL leupeptin, 4 μg/mL pepstatin, 5 μg/mL aprotinin, 20 μg/mL trypsin inhibitor, 0.2 m*M* phenylmethylsulfonyl fluoride [PMSF], 2 m*M* ethylenediamine tetracecetic acid [EDTA], 2 m*M* (ethylene bis(oxonitrilo)tetraacetic acid [EGTA], and 20 m*M* 4-(2-hydroxyethyl)-l-piperazinetranesulfonic acid [HEPES]) by 12 passes with a motorized teflon pestle.
3. The homogenate is centrifuged at 3,800 rpm (1,500*g*) for 10 min at 4°C.
4. The supernatant is collected and centrifuged at 14,800 rpm (20,000*g*) for 10 min at 4°C.
5. The resulting pellet is mixed in a small volume of cold isolation buffer and layered onto discontinuous sucrose gradients containing 10 mL each of 1.18 *M*, 1.0 *M*, and 0.85 *M* sucrose solutions each with 2 m*M* EDTA, 2 m*M* EGTA, and 10 m*M* HEPES (pH 8.0 for 0.85 *M* and 1.0 *M* solutions, pH 8.5 for 1.18 *M* solution).

6. The gradients are centrifuged in an ultracentrifuge at 22,000 rpm (82,500*g*) for 2 h at 4°C.
7. The resulting purified synaptosomal vesicles are removed from the 1.18 *M*/1.0 *M* interface and subsequently washed twice in phosphate buffered saline (PBS).
8. Protein concentrations are determined by the Pierce BCA method and all samples are adjusted to a concentration of 3–4 mg/mL.

3.2. MAL-6 Spin Labeling of Synaptosomal Membranes

1. Spin labeling with MAL-6 using 50 μ*M* MAL-6, a concentration sufficiently low to prevent possible protein extraction of membrane proteins by SH agents *(8,12)*, is performed as previously described *(3–7,10,11,13)*. Briefly, for protein conformational studies in synaptosomal membranes MAL-6 is dissolved in 100 μL of acetonitrile and diluted to a final concentration of 200 μM in 50 mL of lysing buffer (2 m*M* EDTA, 2 m*M* EGTA, 10 m*M* HEPES, pH 7.4).
2. Synaptosomal membrane samples are labeled by incubating 12.5 μg MAL-6/mg of protein (50 μ*M* final concentration) overnight at 4°C *(8)*.
3. Synaptosomes are pelleted in a refrigerated Eppendorf table-top centrifuge.
4. The supernatant is discarded and replaced with fresh lysing buffer.
5. After mixing, the cycle is repeated.
6. Samples are washed six times to ensure complete removal of all unbound spin label before acquiring EPR spectra.
7. EPR spectra are acquired on a Bruker EMX spectrometer with the following instrumental parameters: microwave power, 20 mW; microwave frequency, 9.77 GHz; modulation amplitude, 0.3 G; modulation frequency, 100 KHz; receiver gain, 1×10^5; time constant, 0.64 ms.

4. ANALYSIS

As is well-known the signal-to-noise ratio increases with the square root of the number of spectral accumulations *(8)*. Hence, repeated scans are accumulated to lead to a signal with exceptional signal-to-noise ratio. In addition, using the computer controlled EPR spectrometer, the instrument identifies the maximum and minimum resonance positions of the W-line. Similarly, either the computer associated with the instrument or the investigator identifies the maximum in the S-line of the $M_I = +1$ resonance. Noting that the low-field resonance lines are Lorentzian in shape, it is imperative to obtain a true baseline from which the S height is measured; hence, recording of the baseline at a position at least 5 half-widths of the S line on the low-field side of the $M_I = +1$ S-line is needed. In this way, a true baseline unencumbered by overlap of the tail of the S resonance line can be obtained.

Using this approach, the W/S ratio of MAL-6 covalently bound to synaptosomal membranes is highly significantly lowered in oxidative stress con-

Table 1
Oxidative Stress Conditions in Which Increased Protein Carbonyls are Found and in Which the W/S Ratio of MAL-6 Covalently Bound to Synaptosomal Membrane Proteins Is Lowered Relative to Their Respective Controls

Oxidative stress condition	Inhibited by antioxidants?	References
Hydroxyl free radical attack	Yes, glutathione	*(10,14)*
Alzheimer's disease	Not determined	*(3)*
Amyloid β-peptide addition	Yes, vitamin E	*(15,13)*
In vivo 3-nitropropionic acid model of Huntington's Disease	Yes, the spin trap DEPMPO and glutathione	*(5,6)*
Ischemia/reperfusion injury	Yes, the spin trap PBN	*(16–19)*
Addition of 4-Hydroxy-2-nonenal, a reactive product of lipid peroxidation	Yes, glutathione	*(20)*
Addition of acrolein, A reactive product of lipid Peroxidation	Yes, glutathione	*(21)*
Peroxynitrite, formed by superoxide and nitric oxide	Yes, glutathione	*(22,23)*
Rodent accelerated aging, a model of progeria and Werner's syndrome	Yes, the spin trap PBN	*(7)*
Hyperoxia	Yes, the spin trap PBN and the spin label, tempol	*(24)*
Apolipoprotein E knock-out mice	Not determined	*(13)*

ditions (Table I), showing that this EPR method is a good monitor of synaptosomal membrane-protein oxidation.

Another use of EPR and protein-specific spin labels is possible in favorable cases. As an example, the SH groups of the oxidatively prone enzyme, glutamine synthetase (GS), can be spin labeled exclusively using the SH-specific spin label (1-oxyl-2,2,5,5-tetramethyl-Δ^3-pyrroline-3-methyl)methanethiosulfonate (MTS). In this procedure, GS is oxidized by Fenton chemistry and the rate of incorporation of MTS into the oxidized and unoxidized protein is compared *(25)*. The rate of incorporation of MTS

into GS is monitored by progressive line broadening owing to the increasingly restricted motion of the spin label once bound to the numerous SH groups of this high molecular-weight protein. The linewidth and peak-to-peak amplitude of the three resonance lines of MAL-6, each of equal integrated intensity, are related by:

$$I = kAW^2$$

where k is a constant peculiar to particular lineshapes (e.g., Lorentzian), A is the peak-to-peak amplitude, and W is the peak-to-peak width. Hence, as the spin label moves from solution, where extremely narrow lines exist, to the protein, increased linewidths with correspondingly decreased amplitudes are observed *(8,25)*. The rate of MTS incorporation into GS or other oxidatively prone protein can be compared in the oxidized and unoxidized case. When GS was examined in this manner, a significantly decreased rate of MTS incorporation was found in oxidized GS *(25)*. A similar result was found in purified GS from AD brain compared to GS from neurologically normal brain and in GS oxidized by amyloid β-peptide *(25)*. This result, probably owing to a compaction of the protein upon oxidation as suggested by circular dichroism (CD) studies *(25)*, is consistent with the notion that GS is oxidized in AD brain and may account for the decreased activity of this enzyme in AD brain *(3)*.

5. DISCUSSION

Thus far, in all oxidative stress conditions examined the W/S ratio of MAL-6 covalently bound to synaptosomal membrane proteins is always decreased. No exceptions to this generality have thus far been found. Consequently, in conjunction with other indices of protein oxidation *(1,2)*, EPR using MAL-6 monitors protein oxidation in brain synaptosomal membranes. Spin labeling, whether of synaptosomal membranes or of oxidatively prone proteins, provides a unique way to monitor protein oxidation in oxidative stress conditions. Continued exploitation of this technique in AD, HD, and other neurodegenerative disorders is ongoing in our laboratory.

ACKNOWLEDGMENTS

This work was supported in part by grants from NIH.

REFERENCES

1. Stadtman, E. R. (1992) Protein oxidation and aging. *Science* **257,** 1220–1224.
2. Butterfield, D. A. and Stadtman, E. R. (1997) Protein oxidation processes in aging brain. *Adv. Cell Aging Gerontol.* **2,** 161–191.

3. Hensley, K., Hall, N., Subramaniam, R., Cole, P., Harris, M., et al. (1995) Brain regional correspondence between Alzheimer's disease histopathology and biomarkers of protein oxidation. *J. Neurochem.* **65,** 2146–2156.
4. Yatin, S. M., Link, C. D., and Butterfield, D. A. (1999) *In-vitro* and *in-vivo* oxidative stress associated with Alzheimer's amyloid β-peptide (1-42). *Neurobiol. Aging* **20,** 325–330.
5. La Fontaine, M. A., Geddes, J. W., Banks, A., and Butterfield, D. A. (2000) 3-Nitropropionic acid induced *in-vivo* protein oxidation in striatal and cortical synaptosomes: insights into Huntington's disease. *Brain Research* **858,** 356–362.
6. La Fontaine, M. A., Geddes, J. W., Banks, A., and Butterfield, D. A. (2000) Effect of exogenous and endogenous antioxidants on 3-nitropropionic acid-induced in-vivo oxidative stress and striatal lesions: insights into Huntington's disease. *J. Neurochem.* **75,** 1709–1715.
7. Butterfield, D. A., Howard, B. J., Yatin, S., Allen, K. L., and Carney, J. M. (1997) Free radical oxidation of brain proteins in accelerated senescence and its modulation by N-tert-butyl-α-phenylnitrone. *Proc. Natl. Acad. Sci. USA* **94,** 674–678.
8. Butterfield, D. A. (1982) Spin labeling in disease. *Biol. Mag. Reson.* **4,** 1–78.
9. McConnell, H. M. and McFarland, B. G. (1970) Physics and chemistry of spin labels. *Q. Rev. Biophys.* **3,** 91–136.
10. Hensley, K., Carney, J., Hall, N., Shaw, W., and Butterfield, D. A. (1994) Electron paramagnetic resonance investigations of free radical-induced alterations in neocortical synaptosomal membrane protein infrastructure. *Free Radic. Biol. Med.* **17,** 321–331.
11. Umhauer, S. A., Isbell, D. T., and Butterfield, D. A. (1992) Spin labeling of membrane proteins in mammalian brain synaptic plasma membranes: partial characterization. *Anal. Lett.* **25,** 1201–1215.
12. Matsumoto, N., Shiomura, T., Ishihara, T., Adachi, H., and Miwa, S. (1976) Extraction of erythrocyte membrane proteins by sulfhydryl inhibitors. *Tohoku J. Exp. Med.* **120,** 365–376.
13. Lauderback, C. M., Hackett, J. M., Keller, J. N., Varadarajan, S., Sweda, L., Kindy, M., et al. (2001) Vulnerability of synaptosomes from apoE knock-out mice to structural and oxidative modifications induced by Aβ(1-40): Implications for Alzheimer's disease. *Biochemistry* **40,** 2548–2554.
14. Pocernich, C. B., La Fontaine, M., and Butterfield, D. A. (2000) *In-vivo* glutathione elevation protects against hydroxyl free radical-induced protein oxidation in rat brain. *Neurochem. Int.* **36,** 185–191.
15. Subramaniam, R., Koppal, T., Green, M., Yatin, S., Jordan, B., and Butterfield, D.A. (1998) The free radical antioxidant vitamin E protects cortical synaptosomal membrane proteins from amyloid β-peptide (25-35) toxicity but not from hydroxynonenal toxicity: relevance to the free radical hypothesis of Alzheimer's disease. *Neurochem. Res.* **23,** 1403–1410.
16. Hall, N. C., Carney, J. M., Cheng, M. S., and Butterfield, D. A. (1995) Ischemia/reperfusion induced changes in membrane proteins and lipids of gerbil cortical synaptosomes. *Neuroscience* **64,** 81–89.
17. Hall, N. C., Carney, J. M., Cheng, M., and Butterfield, D. A. (1995) Prevention of ischemia/reperfusion-induced alterations in synaptosomal membrane-associated

proteins and lipids by N-tert-butyl-α-phenylnitrone and difluoromethylornithine. *Neuroscience* **69,** 591–600.
18. Hall, N. C., Dempsey, R. J., Carney, J. M., Donaldson, D. L., and Butterfield, D. A. (1995) Structural alterations in synaptosomal membrane-associated proteins and lipids by transient middle cerebral artery occulusion in the cat. *Neurochem. Res.* **20,** 1161–1169.
19. Hall, N. C., Carney, J. M., Plante, O. J., Cheng, M., and Butterfield, D. A. (1997) Effect of 2-cyclohexene-1-one-induced glutathione diminution on ischemia/reperfusion-induced alterations in the physical state of brain synaptosomal membrane proteins and lipids. *Neuroscience* **77,** 283–290.
20. Subramaniam, R., Roediger, F., Jordan, B., Mattson, M. P., Keller, J. N., Waeg, G., and Butterfield, D. A. (1997) The lipid peroxidation product, 4-hydroxy-2-trans-nonenal, alters the conformation of cortical synaptosomal membrane proteins. *J. Neurochem.* **69,** 1161–1169.
21. Pocernich, C. B., Cardin, A. L., Racine, C. L., Lauderback, C. M., and Butterfield, D. A. (2001) Glutathione elevation and its protective role in acrolein-induced protein damage in synaptosomal membranes: relevance to brain lipid peroxidation in neurodegenerative disease. *Neurochem. Int.* **39,** 141–149.
22. Koppal, T., Drake, J., Yatin, S., Jordan, B., Varadarajan, S., Bettenhausen, L., and Butterfield, D. A. (1999) Peroxynitrite-induced alterations in synaptosomal membrane proteins: insight into oxidative stress in Alzheimer's disease. *J. Neurochem.* **72,** 310–317.
23. Koppal, T., Drake, J., and Butterfield, D. A. (1999) *In-vivo* modulation of rodent glutathione and its role in peroxynitrite-induced neocortical synaptosomal membrane protein damage. *Biochim. Biophys. Acta* **1453,** 407–411.
24. Howard, B. J., Yatin, S., Hensley, K., Allen, K. L., Kelly, J. P., Carney, J., and Butterfield, D. A. (1996) Prevention of hyperoxia-induced alterations in synaptosomal membrane-associated proteins by N-Tert-Butyl-α-phenylnitrone (PBN) and 4-hydroxy-2,2,6,6-tetramethylpiperidine-1-oxyl (Tempol). *J. Neurochem.* **67,** 2045–2050.
25. Butterfield, D. A., Hensley, K., Cole, P., Subramaniam, R., Aksenov, M., Aksenova, M., et al. (1997) Oxidatively-induced structural alteration of glutamine synthetase assessed by analysis of spin labeled incorporation kinetics: relevance to Alzheimer's disease. *J. Neurochem.* **68,** 2451–2457.

10

Gas Chromatography–Mass Spectrometric Analysis of Free 3-Chlorotyrosine, 3-Bromotyrosine, *Ortho*-Tyrosine, and 3-Nitrotyrosine in Biological Fluids

Joseph P. Gaut, Jaeman Byun, and Jay W. Heinecke

1. INTRODUCTION

Reactive oxidants are thought to protect the host by destroying invading microbes *(1)*. However, owing to their indiscriminate nature, reactive oxidants might also damage the host if generated inappropriately. Indeed, they have been implicated in a wide array of pathologies *(2–4)*.

Because reactive oxidants are proposed to have wide-ranging biological effects, it has become critical to develop appropriate methods for their detection and quantification. This is not a trivial issue. Owing to their high reactivity, the reactive species themselves are inherently difficult to detect. To circumvent this problem, we have designed mass-spectromectric techniques to detect stable end products of reactive oxidant production. In particular, 3-chlorotyrosine, 3-bromotyrosine, and 3-nitrotyrosine are end products of tyrosine chlorination, bromination, and nitration, respectively (Fig. 1). Similarly, ortho-tyrosine is an end product of phenylalanine hydroxylation (Fig. 1). Using gas chromatography/mass spectrometry (GC–MS) to detect and quantify these molecules provides several distinct advantages over other techniques. First, GC–MS is highly sensitive, capable of detecting less than 100 attomoles of material in a single analysis. Second, GC–MS provides specific structural information about the molecule of interest; thus, a more reliable measure of a specific molecule can be made. Third, stable heavy isotope-labeled internal standards that are chemically identical to the molecule of interest can be used to provide accurate quantitative data.

From: *Methods in Pharmacology and Toxicology: Methods in Biological Oxidative Stress*
Edited by: K. Hensley and R. A. Floyd

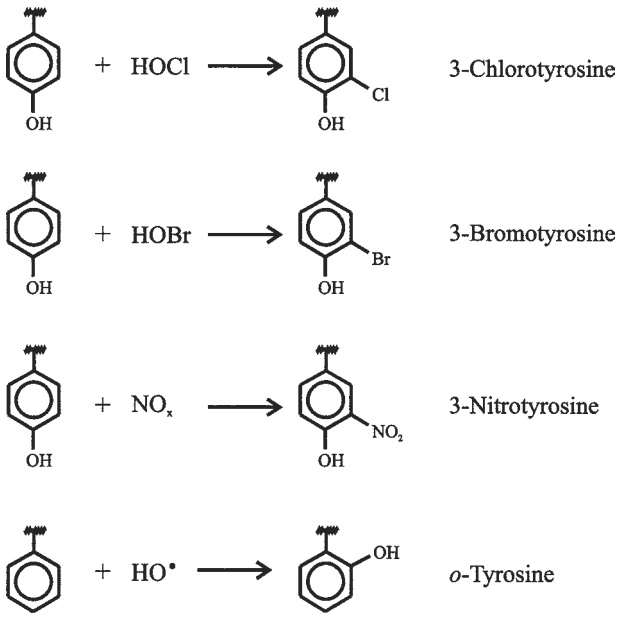

Fig. 1. Schematic representation of various oxidation products and their proposed mechanisms of generation.

A critical issue that must be acknowledged when quantifying trace amounts of oxidative biomarkers is the potential for artifact generation during the sample preparation and analysis. GC–MS provides the distinct advantage in allowing monitoring and quantification of artifact production throughout the analysis.

2. MATERIALS

1. Isotope-labeled internal standards: L-*ortho*[$^{13}C_6$]tyrosine, L-3-chloro[$^{13}C_6$]tyrosine, L-3-bromo[$^{13}C_6$]tyrosine, L-3-nitro[$^{13}C_6$]tyrosine, L-[$^{13}C_6$]tyrosine, L-[$^{13}C_9$, ^{15}N]tyrosine, and L-[$^{13}C_6$]phenylalanine. Isotope-labeled L-tyrosine and L-phenylalanine are purchased from Cambridge Isotope Laboratories (Andover, MA). The biomarkers are synthesized and purified by reverse-phase high-performance liquid chromatography (RP-HPLC) as described previously *(5)*.
2. Antioxidant buffer containing: phosphate-buffered saline (PBS; 0.01 *M* phosphate, 0.138 *M* NaCl, 0.0027 *M* KCl, pH 7.4) supplemented with 50 μ*M* butylated hydroxytoluene, 100 μ*M* diethylenetriaminepentaacetic acid (DTPA), 1 m*M* sodium azide, and 10 m*M* aminotriazole.
3. Solid-phase extraction apparatus, columns, and solvents. The solid-phase apparatus and columns can be purchased from Supelco (Bellefonte, PA). Two

columns are utilized: C18 (3 mL) and Chrom P (3 mL). Solvents used for extraction are 0.1% trifluoroacetic acid (TFA), pH 5.0, methanol, 25% methanol, 1% TFA, pH 4.0, 1% methanol, and 50% methanol.

4. Derivatization solvents and reagents: ethyl heptafluorobutyrate (Aldrich), *N*-methyl-*N*-(*t*-butyldimethylsilyl)-trifluoroacetamide + 1% trimethylchlorosilane (MtBSTFA) (Regis, Morton Grove, IL), and undecane (Aldrich, Milwaukee, WI).
5. HPLC system with an ultrasphere octadecylsilicic (ODS) reverse-phase column, bath sonicator, nitrogen evaporator, and a mass spectrometer capable of negative chemical ionization and on-column injection interfaced with a gas chromatograph.

3. METHODS

1. Collect fluid sample. The fluid may be frozen at –80°C prior to workup and analysis. Add internal standards. It is important to perform some preliminary experiments to determine the amount of internal standard to add to a particular sample. Ideally, the internal standard should equal the amount of endogenous analyte in the sample. This will ensure more precise quantitative results. Generally, in 1 mL of plasma, 0.5–1 pmol of internal standard is sufficient for 3-chlorotyrosine, 3-bromotyrosine, and 3-nitrotyrosine, 3–5 pmol for *ortho*-tyrosine, and 5–50 nmol for tyrosine and phenylalanine. It is important to add L-[$^{13}C_9$, ^{15}N]tyrosine as opposed to L-[$^{13}C_6$]tyrosine, because this will allow for monitoring of artifact during the analysis. Centrifuge in microfuge (4°C) for 10 min at 16,000*g* to pellet cellular debris. Transfer supernatant to a separate tube.
2. Solid-phase extraction *(5–7)*. Samples are brought to 2 mL with 0.1% TFA, pH 5.0. The pH is brought to 5.0 with a minimum volume of acetic acid. Prior to applying the sample to the C18 column, the column is first conditioned with 2 mL of 100% methanol and washed with 8 mL of 0.1% TFA. The sample is added and washed with 2 mL of water. Analytes are eluted with 2 mL of 25% methanol and dried under nitrogen. Unfortunately, biological samples contain contaminants that migrate closely to 3-nitrotyrosine and 3-bromotyrosine when analyzed by GC–MS. Therefore a second solid-phase extraction step is recommended to remove these impurities. The Chrom P column is conditioned with 2 mL of methanol and washed with 8 mL of 1.0% TFA. Samples are resuspended in 1.0% TFA, pH 4.0, applied to the column, washed once with 2 mL of 1.0% methanol, and eluted with 2 mL of 50% methanol. Samples are then dried under anhydrous N_2 and stored at –20°C until analysis.
3. Derivatization *(5–7)*. Because the derivatizing reagents are highly sensitive to moisture, it is important to remove excess water by resuspending the samples in 50 µL dimethylformamide (DMF) and drying under nitrogen. Once dry, add 200 µL DMF and 40 µL diisopropylethylamine. Cool samples by placing on ice for 5 min. Add 40 µL ethyl heptafluorobutyrate and leave on ice for 30 min. Drive the reaction to completion by sonicating in a water bath sonicator for 1 h at room temperature. Dry samples under nitrogen. React with 30 µL

MtBSTFA for 30 min at room temperature. Dry under nitrogen and resuspend in 50 µL undecane containing 25% MtBSTFA.

4. GC–MS *(5–7)*. One µL of sample is analyzed using selected ion monitoring in the electron capture-negative ion chemical ionization mode. All samples are manually injected using an on-column inlet (room temperature) and are separated using a 15 m DB-5ms column (J&W Scientific). The injector, transfer line, and source temperatures are initially set at 183°C, 300°C, and 250°C, respectively. The injector and transfer-line temperatures are set to increase incrementally with the temperature gradient (180°C to 300°C at 40°C/min). *Ortho*-tyrosine, 3-chlorotyrosine, 3-bromotyrosine, and 3-nitrotyrosine are quantified using the respective ions at *m/z* 407 ([M–COO^-–*t*-butyl-dimethylsilyl]$^-$), 489 ([M–halide–*t*-butyl-dimethylsilyl]$^-$), and 518 ([M–O–*t*-butyl-dimethylsilyl]$^-$) and their isotopically labeled [$^{13}C_6$]-internal standards (*m/z* 413, 495, and 524). Potential artifact formation during sample work-up is monitored as any appearance of ions at *m/z* 499 (chlorination and bromination artifact) or *m/z* 528 (nitration artifact) derived from L-[$^{13}C_9$, ^{15}N]tyrosine. Either all eight ions can be monitored simultaneously or in three stages in order of elution: stage 1, *ortho*-tyrosine (*m/z* 407 and 413); stage 2, 3-chlorotyrosine and 3-bromotyrosine (*m/z* 489, 495, 499); stage 3, 3-nitrotyrosine (*m/z* 518, 524, 528). Because L-phenylalanine and L-tyrosine are present at 10,000–100,000-fold excess compared to the oxidation products, a 1:100 dilution is made, and a separate injection is performed for these amino acids. L-Phenylalanine and L-tyrosine are quantified using the ions at *m/z* 277 ([M–COO^-–*t*-butyl-dimethylsilyl]$^-$) and 407 ([M–COO^-–*t*-butyl-dimethylsilyl]$^-$) and the ions derived from L-[$^{13}C_6$]phenylalanine and L-[$^{13}C_9$, ^{15}N]tyrosine at *m/z* 283 and 416.

4. ANALYSIS

A standard curve must be generated using authentic analyte and its respective internal standard (Fig. 2). The result should yield an accurate linear regression. The ratio of the peak areas of the endogenous material and the internal standard is then obtained and the amount calculated using the standard curve. In the event of artifact formation, the artifact is quantified by dividing the artifact peak area by the corresponding internal standard peak area and multiplying by the peak area ratio of L-[$^{13}C_9$, ^{15}N]tyrosine to L-tyrosine. This value is subtracted from the endogenous value. Values can be reported as mol/mol tyrosine or phenylalanine (in the case of *ortho*-tyrosine), or as absolute concentration.

5. DISCUSSION

GC–MS provides a highly sensitive, accurate, and quantitative means of measuring a variety of oxidation products in a single analysis. It is critical,

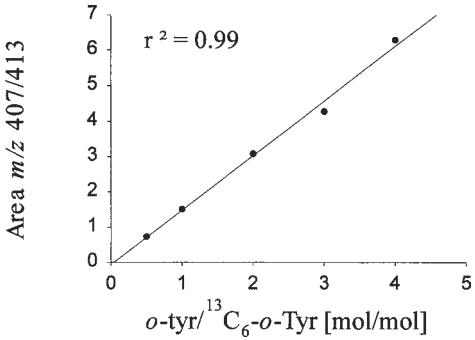

Fig. 2. Standard curve for the analysis of *ortho*-tyrosine.

however, to keep in mind the possibility of artifact formation during sample preparation. For instance, acidic conditions in the presence of nitrite and tyrosine will generate 3-nitrotyrosine *(8,9)*. Fortunately, GC–MS is unique in that it allows for monitoring of artifact during the analysis. If, for example, nitration artifact is formed, the tyrosine present in the sample will be converted into 3-nitrotyrosine *(8,9)*. A proportional amount of the tyrosine internal standard will also be converted to artifact. Because the isotopically labeled tyrosine differs from the tyrosine used to synthesize the internal standards, we can monitor the production of artifact relatively easily (Fig. 3).

If a large quantity of samples are to be analyzed, it would be advantageous to automate the GC–MS system. Although theoretically possible, automation of this technique has proven difficult because the samples are injected using an on-column inlet. However, this injection system is only necessary for analysis of 3-nitrotyrosine. We have found that if 3-nitrotyrosine is not going to be analyzed, a conventional split/splitless inlet coupled to an autosampler will suffice.

REFERENCES

1. Klebanoff, S. J. (1970) Myeloperoxidase: contribution to the microbicidal activity of intact leukocytes. *Science* **169,** 1095–1097
2. Ames, B. N., Gold, L. S., and Willett, W. C. (1995) The causes and prevention of cancer. *Proc. Natl. Acad. Sci. USA* **92,** 5258–5265
3. Heinecke, J. W. (1997) Pathways for oxidation of low density lipoprotein by myeloperoxidase: tyrosyl radical, reactive aldehydes, hypochlorous acid and molecular chlorine. *Biofactors* **6(2),** 145–155.
4. Weiss, S. J. (1989) Tissue destruction by neutrophils. *N. Engl. J. Med.* **320,** 365–376.

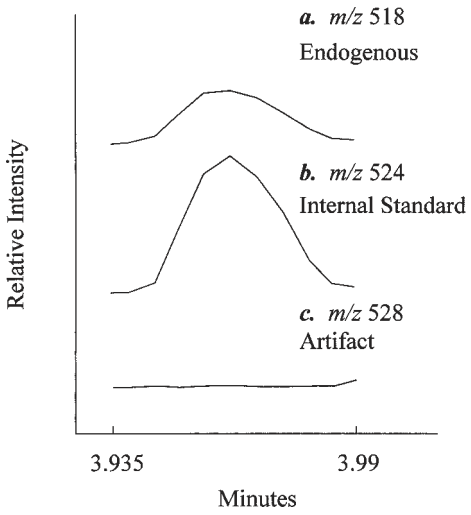

Fig. 3. GC–MS analysis of mouse peritoneal lavage fluid for (**A**) endogenous 3-nitrotyrosine (*m/z* 518), (**B**) heavy isotope-labeled internal standard of 3-nitrotyrosine (*m/z* 524), and (**C**) artifactual 3-nitrotyrosine (*m/z* 528).

5. Heinecke, J. W., Hsu, F. F., Crowley, J. R., Hazen, S. L., Leeuwenburgh, C., Mueller, D. M., et al. (1999) Detecting oxidative modification of biomolecules with isotope dilution mass spectrometry: sensitive and quantitative assays for oxidized amino acids in proteins and tissues. *Methods Enzymol.* **300,** 124–134.
6. Frost, M. T., Halliwell, B., and Moore, K. P. (2000) Analysis of free and protein-bound nitrotyrosine in human plasma by a gas chromatography/mass spectrometry method that avoids nitration artifacts. *Biochem. J.* **345,** 453–458.
7. Gaut, J. P., Byun, J., Tran, H. D., and Heinecke, J. W. (2002) Artifact-free quantification of free 3-chlorotyrosine, 3-bromotyrosine, and 3-nitrotyrosine in human plasma by electron capture-negative chemical ionization gas chromatography mass spectrometry and liquid chromatography-electrospray ionization tandem mass spectrometry. *Anal. Biochem.* **300,** 252–259.
8. Oury, T., Tatro, L., Ghio, A., and Piantadosi, C. (1995) Nitration of tyrosine by hydrogen peroxide and nitrite. *Free Radic. Res.* **23(6),** 537–547.
9. Gaut, J. P., Byun, J., Tran, H. D., et al. (2002) Myeloperoxidase produces nitrating oxidants in vivo. *J. Clin. Invest.* **109,** 1311–1319.

11

Isotope Dilution Gas Chromatography–Mass Spectrometric Analysis of Tyrosine Oxidation Products in Proteins and Tissues

Jay W. Heinecke

1. INTRODUCTION

Oxidative reactions that modify proteins have been implicated in the pathogenesis of aging and disease *(1)*. It has been difficult to identify the physiologically relevant pathways, however, because the reactive intermediates are short-lived. We attempt to determine which oxidative pathways damage proteins in vivo by first identifying stable end products of potential pathways through in vitro experiments. We then analyze normal and diseased tissues for those compounds. For example, two stable isomers of *p*-tyrosine—*ortho*-tyrosine and *meta*-tyrosine—appear after hydroxyl radical modifies protein-bound phenylalanine residues *(2–4)*. In contrast, *o*,*o*'-dityrosine forms when hydroxyl radical crosslinks tyrosine residues. *o*,*o*'-Dityrosine also appears when free or protein-bound tyrosine is attacked by tyrosyl radical *(5)*, which is produced from tyrosine and H_2O_2 by the heme enzyme myeloperoxidase *(6,7)*. Tyrosyl radical does not generate *ortho*-tyrosine and *meta*-tyrosine, however *(2–5)*. Another oxidant, hypochlorous acid (HOCl), produces 3-chlorotyrosine when it reacts with tyrosine *(8,9)*. HOCl is generated only by myeloperoxidase, which requires H_2O_2 and Cl^- to perform the reaction. Thus, determining relative levels of *ortho*-tyrosine, *meta*-tyrosine, *o*,*o*'-dityrosine, and 3-chlorotyrosine can indicate which pathway might have inflicted protein damage in vivo in a particular tissue. These amino acid products are useful markers because they are stable to acid hydrolysis, an essential analytical step.

From: *Methods in Pharmacology and Toxicology: Methods in Biological Oxidative Stress*
Edited by: K. Hensley and R. A. Floyd

We have developed sensitive and quantitative assays for measuring *ortho*-tyrosine, *meta*-tyrosine, *o*,*o*'-dityrosine, and 3-chlorotyrosine in proteins and tissues *(2–9)*. The methods combine gas chromatography (GC) with isotope dilution negative-ion electron capture mass spectrometry (MS). GC–MS analysis permits the use of a stable, isotopically labeled internal standard that, apart from its heavy isotope, is structurally identical to the target analyte and therefore behaves identically during extraction, processing, and chromatographic analysis. Including such a standard corrects for analyte loss during processing and increases the precision of quantitative measurements.

2. TISSUE COLLECTION

Tissue resected at surgery or autopsy is immediately placed in ice-cold antioxidant buffer (100 μ*M* diethylenetriaminepentaacetic acid (DTPA), 1 m*M* butylated hydroxytoluene, 1% (v/v) ethanol, 140 m*M* NaCl, 10 m*M* sodium phosphate, pH 7.4) and then frozen at –80°C until analysis. DTPA (prepared as a 10 m*M* stock solution, pH 7.4) and butylated hydroxytoluene (BHT; prepared as a 100 m*M* stock solution in 95% ethanol) are included to respectively inhibit metal-catalyzed oxidation reactions and lipid peroxidation. Depending on the oxidation products of interest, the antioxidant buffer is supplemented with inhibitors of other pathways. For example, 10 m*M* 3-aminotriazole can be included to inhibit myeloperoxidase.

3. PROTEIN HYDROLYSIS

We use two procedures to prepare tissue for hydrolysis. Most tissues (50–100 mg wet weight) are suspended (1:10, w/v) in ice-cold homogenization buffer [50 m*M* sodium phosphate, pH 7.4, supplemented with 100 μ*M* DTPA and 1 m*M* BHT, 1% (v/v) ethanol (from the stock solution of BHT in 95% ethanol)]. We then homogenize the tissue, using a motor-driven Teflon pestle in a glass receptacle. Tissue that is difficult to homogenize is frozen in liquid nitrogen and pulverized with a stainless steel mortar and pestle previously immersed in liquid nitrogen. All subsequent procedures are performed at 4°C. We suspend tissue powder (10–20 mg wet weight) in 1 mL of buffer A (100 μ*M* DTPA, pH 7.0) and dialyze the suspension for 24 h against that buffer to remove free amino acids, nitrite, and other low molecular-weight contaminants. The protein is dried under vacuum, resuspended in 0.5 mL of water, and delipidated by incubation for 10 min with 6.5 mL of H_2O/methanol/water-washed diethyl ether (1:3:7, v/v/v). If we need to analyze the preparation for 3-chlorotyrosine, we perform an additional wash with 1 mL

of water and 13 mL of methanol/water-washed diethyl ether (3:10, v/v) to remove residual chloride that might otherwise chlorinate tyrosine during acid hydrolysis. To recover tissue protein, the sample is centrifuged at 5000*g* for 10 min, the supernatant is removed, and the fluffy protein powder is delipidated again with 10 mL of water-washed diethyl ether.

We routinely use acid to hydrolyze tissues because it quantitatively releases amino acids from proteins. Therefore, the oxidation product of interest must be stable under these conditions (generally a 24-h exposure to 6 *N* HCl at 110°C). Because acid hydrolysis also can contribute to protein oxidation ex vivo, we suppress such reactions by adding phenol (0.1–1%) to the reaction mixture. Also, exposing proteins to HCl would generate low levels of 3-chlorotyrosine, which might contribute significantly to the apparent level of that compound in biological materials *(8,9)*. We avoid this artifact by using HBr for hydrolysis (see below).

4. HYDROLYSIS CONDITIONS FOR *o,o'*-DITYROSINE, *ORTHO*-TYROSINE, AND *META*-TYROSINE

After adding ^{13}C-labeled internal standards (~50 pmol oxidized amino acid and 50 nmol precursor amino acid), we concentrate the protein or tissue residue (~0.5 mg protein) to dryness under nitrogen and hydrolyze the powder at 110°C for 24 h in 0.5 mL of 6 *N* HCI (Sequenal Grade, Pierce Chemical) supplemented with 1% phenol. Prior to hydrolysis, we cap the tubes with gas-tight valves and alternately degas and purge them with argon five times.

5. HYDROLYSIS CONDITIONS FOR 3-CHLOROTYROSINE

To avoid the trace amounts of artifactual 3-chlorotyrosine that form when proteins are hydrolyzed with HCl *(8,9)*, we hydrolyze proteins with HBr and phenol. After adding internal standards (~10 pmol 3-chlorotyrosine and 100 nmol tyrosine) to the protein or tissue residue (~0.5 mg protein), we concentrate the sample to dryness under nitrogen, and hydrolyze it at 110°C for 24 h in 0.5 mL of 6 *N* HBr supplemented with 1% phenol. Prior to hydrolysis, we cap the tubes with gas-tight valves and alternately degas and purge them with argon, as described in the previous subheading. We have demonstrated that protein hydrolysis is stoichiometric under these conditions by quantita-

tively recovering a variety of amino acids (L-tyrosine, L-lysine, and L-phenylalanine), using isotope dilution GC–MS. 3-Chlorotyrosine is stable under these hydrolysis conditions and is recovered in >98 % yield, as determined by reverse-phase HPLC analysis.

6. SOLID-PHASE EXTRACTION

We isolate amino acids from protein hydrolysates by solid-phase extraction with octadecylsilicic (ODS) columns. This procedure removes contaminants that interfere with derivatization of amino acid analytes and analysis of the derivatives by negative-ion electron capture mass spectrometry. Before using ODS extraction columns (Supelclean LC-18 SPE tube, 3 mL; Supelco, Inc., Bellefonte, PA), we activate them by washing with 3 mL of methanol.

7. EXTRACTION OF *o,o'*-DITYROSINE, *ORTHO*-TYROSINE, AND *META*-TYROSINE

We condition activated ODS extraction columns before use with 10 mL of 50 m*M* sodium phosphate, pH 7.4, supplemented with 100 μ*M* DTPA. A wash with 12 mL of 0.1% trifluoroacetic acid (TFA) follows. The DTPA inhibits oxidation of phenylalanine and tyrosine during amino acid isolation. After adjusting the volume of the ~0.5 mL of amino acid hydrolysate to 2 mL with 0.1% TFA, we pass the solution over the ODS solid-phase extraction column. We then wash the column with 2 mL to 4 mL of 0. 1% TFA and elute the amino acids with 2 mL of H_2O:methanol (4:1, v/v). The amino acid solution is concentrated to dryness under vacuum, and immediately derivatized (see below). Studies with standard compounds indicate that this procedure recovers >80% of tyrosine oxidation products from ODS columns.

8. EXTRACTION OF 3-CHLOROTYROSINE

In this case, we condition the ODS extraction column with 0.1% TFA (12 mL). The volume-adjusted hydrolysate is then passed over the column and washed with 2 mL of 0.1% TFA. The amino acids are eluted with 2 mL of H_2O:methanol (1:1, v/v) containing 0.1% TFA, concentrated to dryness under vacuum, and immediately derivatized. Under these conditions, 3-chlorotyrosine liberated by HBr is recovered quantitatively *(9)*.

9. AMINO ACID DERIVATIZATION

Conversion of amino acids to their heptafluorobutyryl derivatives with heptafluorobutyric acid anhydride (HFBA) generates compounds whose

high volatility and electron-capturing properties make them suitable for negative-ion electron capture GC–MS analysis. The amino acids in the dried protein hydrolysates (~0.5 mg) are first converted to their n-propyl carboxylic acid esters by addition of 200 μL of 3.5 *M* HCl (or 3.5 *M* HBr for 3-chlorotyrosine determination) in *n*-propanol. The solution is then heated at 65°C for 1 h, and reaction products are concentrated to dryness under nitrogen. Heptafluorobutyryl (HFB) derivatives are generated by adding 50 μL of 3:1 (v/v) ethyl acetate/HFBA and incubating at 65°C for 5 min.

10. GC–MS ANALYSIS OF AMINO ACID DERIVATIVES

We use commercially available quadrupole mass spectrometers with chemical ionization sources and negative ion capabilities. Systems include the Hewlett-Packard 5988A and 5973 and the Finnigan SSQ-7000. We typically use 10–30 m, 0.2–0.3 mm i.d. fused-silica capillary columns with helium as the carrier gas for GC analysis. Both J & W Scientific, Inc. (Folsom, CA) DB-1 columns (15 m, 0.33 μm methyl silicone film thickness, 0.32 mm i.d.) and DB-17 columns (30 m, 0.25 μm phenyl methyl silicone film thickness, 0.25 mm i.d.) have proved useful. These columns provide excellent separation of amino acids that have been derivatized with HFBA. The precursor amino acids (*p*-tyrosine, phenylalanine) that are present at high concentrations in amino acid hydrolysates are injected into the GC with a 50–100:1 split to avoid overloading the column or saturating the detector of the mass spectrometer. Oxidized amino acids, which are present at low concentrations in biological materials, may be injected in the splitless mode to increase the sensitivity of the analysis. The injector temperature and transfer lines of the GC are maintained at 200°C to 250°C, and the mass spectrometer ion source temperature is 100°–150°C. The mass spectrometer is operated in the negative-ion electron capture mode with methane as the moderating gas at a source pressure of 0.6–1.0 torr. Emission current is set at 300 μA, and the electron energy is 240 ev.

In the selected ion-monitoring mode, the mass spectrometer monitors a limited number of ions with defined mass-to-charge (*m/z*) values as a function of GC retention time. This gives much greater sensitivity than the full-scan mode because a greater proportion of the instrument's duty cycle is used to detect ions of interest. The molecular ion (M^-) of HFBA-derivatized amino acids is often in low abundance, but intense ions are generally observed at M – 20 ($M^- - HF$) and M – 198 ($M^- - CF_3(CF_2)_2CHO$).

Once we have established an analyte's GC retention time and mass spectrum, we try to detect it qualitatively in biological materials. After releasing

amino acids from proteins by hydrolysis, we generate their derivative, which we analyze by negative-ion electron capture GC–MS. Structurally informative ions of high abundance that occur in the negative-ion electron capture mass spectrum of the derivatized standard compound are detected by selected ion monitoring. If multiple ions with the expected relative abundance at the appropriate GC retention time co-elute, we deduce that the compound of interest was present in the biological material. Such compounds can be identified unequivocally by comparing the GC–MS behavior of additional derivatives (e.g., pentafluoropropionyl derivatives) with that of standards.

For quantitative analysis, we construct a standard curve that enables us to determine the concentration of the analyte by isotope dilution. To derive the curve, we add a constant amount of heavy isotope-labeled internal standard and varied but known amounts of standard target analyte to a series of reaction vessels. We derivatize these materials and analyze the derivatives by negative-ion electron capture GC–MS, using selected monitoring of the analogous ions that arise from the analyte and the internal standard. We plot the ratio of the integrated ion current peaks for these ions as a function of the amount of target analyte initially added to the reaction vessel. For the analytes discussed here, the resultant regression line is typically linear over at least two orders of magnitude. To quantify analytes from biological material, we add only enough internal standard to make its blank value (which reflects its intrinsic content of unlabeled analyte) represent <5% of the total current of ions monitored. To ensure that interfering ions from extraneous substances are not co-eluting with the analyte, we generally monitor the ratio of ion currents of the two most abundant structurally informative ions of each compound and its internal standard.

11. GC–MS ANALYSIS OF PHENYLALANINE AND *p*-TYROSINE

An aliquot of derivatized amino acids is diluted 1:100 (v/v) with ethyl acetate. A 1 μL sample is injected (1:100 split) into the GC and analyzed on a 12 m DB-1 capillary column. The initial GC oven temperature of 120°C is maintained for 1 min; the temperature is increased at a rate of 10°C/min to a final reading of 220°C. The mass spectrum of the *n*-propyl-HFB derivative of phenylalanine includes a low abundance molecular ion (M^-) at *m/z* 403 and a prominent ion at *m/z* 383 ($M^- - HF$). The phenylalanine is quantified by monitoring the intensity of the ion at *m/z* 383 relative to that at *m/z* 389 (the ion for the derivatized [$^{13}C_6$]phenylalanine internal standard). The mass spectrum of the *n*-propyl-HFB derivative of *p*-tyrosine reveals prominent

ions at *m/z* 595 (M^- – HF) and *m/z* 417 (M^- – $CF_3(CF_2)_2CHO$). To quantify tyrosine relative to the derivatized [$^{13}C_6$]tyrosine internal standard, we take the ratio of the ion at *m/z* 417 to the ion at *m/z* 423.

12. GC–MS ANALYSIS OF o,o' -DITYROSINE, *ORTHO*-TYROSINE, AND *META*-TYROSINE

After preparing the *n*-propyl-HFB derivatives of amino acids, concentrating them to dryness under nitrogen, and redissolving them in 50 μL of ethyl acetate, we inject aliquots (1–2 μL) into a 12 m DB-1 capillary GC column in the splitless mode. We increase the GC oven temperature from its initial temperature of 70°C to a final temperature of 300°C at a rate of 40°C/min. The mass spectrum of the *n*-propyl-HFB derivative of *o*,*o*'-dityrosine includes a low intensity molecular ion at *m/z* 1228 (M^-) and prominent ions at *m/z* 1208 (M^- – HF) and *m/z* 1030 (M^- – $CF_3(CF_2)_2CHO$). To quantify *o*,*o*'-dityrosine relative to the derivatized *o*,*o*'-[$^{13}C_{12}$]dityrosine internal standard, we take the ratio of the ion at *m/z* 1208 to the ion at *m/z* 1220. The mass spectrum of the *n*-propyl-HFB derivative of *ortho*-tyrosine exhibits prominent ions at *m/z* 595 (M^- – HF) and *m/z* 417 (M^- – $CF_3(CF_2)_2CHO$). To quantify this analyte relative to the derivatized *o*-[$^{13}C_6$]tyrosine internal standard, we use the ratio of the ion at *m/z* 595 to the ion at *m/z* 601. The mass spectrum of the *n*-propyl-HFB derivative of *meta*-tyrosine exhibits prominent ions at *m/z* 595 (M^- – HF) and *m/z* 417 (M^- – $CF_3(CF_2)_2CHO$). In this case, we use the ratio of the ion at *m/z* 417 to the ion at *m/z* 423 (the derivatized *m*-[$^{13}C_6$]tyrosine internal standard).

13. GC–MS ANALYSIS OF 3-CHLOROTYROSINE

We analyze 3-chlorotyrosine as the *n*-propyl-per-HFB derivative. For quantification, we compare the intensities of analyte ions at *m/z* 451 (M^- – $CF_3(CF_2)_2CHO$) and *m/z* 629 (M^- – HF) to those of the analogous ions (*m/z* 457 and *m/z* 635) from the derivatized 3-[$^{13}C_6$]chlorotyrosine internal standard. We perform GC analyses on a 30 m DB-17 capillary column. Samples are diluted 50-fold with ethyl acetate and injected using a 1:50 split. The initial GC oven temperature of 150°C is increased to a final temperature of 250°C at a rate of 20°C/min.

REFERENCES

1. Shigenaga, M. K., Hagen, T. M., and Ames B. N. (1994) Oxidative damage and mitochondrial decay in aging. *Proc. Natl. Acad. Sci. USA* **91,** 10,771–10,778.

2. Pennathur, S., Wagner, J. D., Leeuwenburgh, C., Litwak, K. N., and Heinecke, J. W. (2001) A hydroxyl radical-like species oxidizes cynomolgus monkey artery wall proteins in early diabetic vascular disease. *J. Clin. Invest.* **107,** 853–860.
3. Leeuwenburgh, C., Rasmussen, J. E., Hsu, F. F., Mueller, D. M., Pennathur, S., and Heinecke, J. W. (1997) Mass spectrometric quantification of markers for protein oxidation by tyrosyl radical, copper, and hydroxyl radical in low density lipoprotein isolated from human atherosclerotic plaques. *J. Biol. Chem.* **272,** 3520–3526.
4. Pennathur, S., Jackson-Lewis, V., Przedborski, S., and Heinecke, J. W. (1999) Mass spectrometric quantification of 3-nitrotyrosine, orthortho-tyrosine, and *o*,*o*'-dityrosine in brain tissue of 1-methyl-4-phenyl-1,2,3, 6-tetrahydropyridine-treated mice, a model of oxidative stress in Parkinson's disease. *J. Biol. Chem.* **274,** 34,621–34,628.
5. Heinecke, J. W., Li, W., Francis, G. A., and Goldstein, J. A. (1993) Tyrosyl radical generated by myeloperoxidase catalyzes the oxidative cross-linking of proteins. *J. Clin. Invest.* **91,** 2866–2872.
6. Heinecke, J. W., Li, W., Daehnke, H. L. 3rd, and Goldstein, J. A. (1993) Dityrosine, a specific marker of oxidation, is synthesized by the myeloperoxidase-hydrogen peroxide system of human neutrophils and macrophages. *J. Biol. Chem.* **268,** 4069–4077.
7. Jacob, J. S., Cistola, D. P., Hsu, F. F., Muzaffar, S., Mueller, D. M., Hazen, S. L., and Heinecke, J. W. (1996) Human phagocytes employ the myeloperoxidase-hydrogen peroxide system to synthesize dityrosine, trityrosine, pulcherosine, and isodityrosine by a tyrosyl radical-dependent pathway. *J. Biol. Chem.* **271,** 19,950–19,956.
8. Hazen, S. L., Hsu, F. F., Mueller, D. M., Crowley, J. R., and Heinecke, J. W. (1996) Human neutrophils employ chlorine gas as an oxidant during phagocytosis. *J. Clin. Invest.* **98,** 1283–1289.
9. Hazen, S. L. and Heinecke, J. W. (1997) 3-Chlorotyrosine, a specific marker of myeloperoxidase-catalyzed oxidation, is arkedly elevated in low density lipoprotein isolated from human atherosclerotic intima. *J. Clin. Invest.* **99,** 2075–2081.

12

Single-Cell Gel Electrophoresis or Comet Assay of Intestinal Epithelial Cells Using Manual Scoring and Ridit Analysis

Mark M. Huycke

1. INTRODUCTION

The single-cell gel electrophoresis or comet assay was initially reported in 1984 as a novel technique to directly visualize DNA damage in individual cells *(1)*. The method was modified by adding strong alkaline conditions to denature genomic DNA and detect alkali labile lesions, greatly improving sensitivity for single-strand breaks *(2,3)*. This simple assay has come into widespread use because of its sensitivity, need for few cells, applicability to nearly all eukaryotic cells, and ease in processing numerous samples *(4)*.

The comet assay begins by suspending cells of interest in a mincing solution. Suspended cells are mixed in low melting-point agar, applied to conventional microscope slides, lysed, and denatured under alkaline conditions to unwind supercoiled genomic DNA. Dimethyl sulfoxide (DMSO) is an essential component of mincing and lysing solutions that stops oxidation of DNA during processing. Alkaline treatment is followed by electrophoresis. Comets are visualized using a fluorescent DNA stain with broken ends of negatively charged DNA fragments migrating away from the nuclei of cells as does the "tail" of a comet emanate from the head. Comet tail length increases with the degree of DNA damage, but reaches a plateau defined by electrophoresis conditions and not fragment size. Comets have been analyzed by many methods that range from simple manual scoring to sophisticated computerized-image analysis. For laboratories wishing to use comet techniques

From: *Methods in Pharmacology and Toxicology: Methods in Biological Oxidative Stress*
Edited by: K. Hensley and R. A. Floyd

but otherwise unable to afford expensive image analysis equipment and software, we tested a simple scoring technique and applied standard Ridit (relative to an identified distribution) statistical methods to analyze our results *(5)*. The alkaline comet assay described here has been adapted from techniques described by Klaude *(6)*, Tice *(7)*, and Strauss *(8)*.

2. MATERIALS

Unless otherwise stated, all reagents were purchased from Fisher Scientific (Pittsburgh, PA), Sigma Chemical Company (St. Louis, MO), or Gibco (Rockville, MD).

1. HT-29 intestinal epithelial cells were purchased from the American Type Culture Collection (Bethesda, MD) and routinely maintained in McCoy's medium containing 10% fetal calf serum (FCS) at 5% CO_2 and 37°C.
2. Mincing solution: Hanks Balanced Salt Solution (HBSS, Ca^{+2} and Mg^{+2} free) with 20 m*M* EDTA and 10% DMSO.
3. Phosphate buffered saline (PBS, Ca^{+2} and Mg^{+2} free) at pH 7.4.
4. Alkaline salt solution: 2.5 *M* NaCl, 100 m*M* EDTA, and 10 m*M* Tris base; dissolve ingredients with NaOH pellets and adjust pH to 10.0 with concentrated HCl or NaOH; store at room temperature.
5. Lysing solution: add 1% Triton X-100 (v/v) and 10% DMSO (v/v) to alkaline salt solution; refrigerate for >30 min and prepare day of use.
6. 10 *N* NaOH and 200 m*M* ethylenediaminetetraacetic acid (EDTA), pH 10.0, stocks; prepare fresh every 2 wk.
7. Electrophoresis buffer (300 m*M* NaOH and 1 m*M* EDTA): prepare prior to electrophoresis by mixing 30 mL NaOH and 5 mL EDTA stocks; q.s. to 1 L with deionized water; pH must be >13.0.
8. Neutralization buffer: 0.4 M Tris base; adjust to pH 7.5 with concentrated HCl.
9. Vital stain:
   a. Ethidium bromide solution: prepare stock by dissolving 50 mg in 1 mL 100% ethanol and add 100 µL to 4.9 mL phosphate-buffered saline (PBS); add 250 µL stock to 9.75 mL PBS before use; protect from light.
   b. 5,6-carboxyfluorescein diacetate (CFDA, Molecular Probes, Eugene, OR): prepare stock by dissolving 3 mg CFDA in 1 mL acetone; add 420 µL stock to 9.58 mL PBS before use; protect from light
   c. Vital staining solution: mix ethidium bromide and CFDA working solutions in 1:1 ratio; may refrigerate up to 6 mo.
10. DNA staining solution: add 10 µL ethidium bromide stock to 5 mL deionized water.
11. Agar: boil low melting-point agar (LMPA, 0.5%) and normal melting agar (NMA, 1%) in PBS using a microwave; 5-mL aliquots of LMPA can be refrigerated until needed, remelting prior to use.
12. Slides: label conventional microscope slides with one frosted end using a histology marking pen (ordinary markers will not work as most inks are not fast

in alkali). Dip slides into hot NMA (~80–90°C) approx halfway onto the frosted ends. Wipe undersides to remove agar and lay flat to dry. Slides can be prepared in advance and stored at room temperature in low humidity. When finished, dispose of NMA in a trash can with liner and not down the sink.

3. METHODS

1. Cell isolation. For tissue-culture cells, remove the medium and add mincing solution. Scrape cells into mincing solution and suspend to ~10^6 cells/mL. Trypsinizing cells will cause DNA damage and should be avoided. Similarly, for animal or human tissues and organs, cut samples into fine pieces, mix in mincing solution, let pieces settle, and remove cells as an aliquot of the supernatant.
2. Slide preparation. Melt an aliquot of LMPA in a microwave and cool to 37°C in a water bath. Mix ~5–10 µL of the cell suspension (~10,000 cells) in 75 µL of LMPA and pipet onto an NMA-coated slide. Spread cells in LMPA by applying a 24 × 50 mm coverslip and place on a metal tray resting on ice packs for 3–5 min to harden the agar. Remove the coverslip, add a third layer of LMPA (~75 µL) using a new coverslip, and return the slide to the tray. After the agar hardens remove the coverslip and gently insert the slide into a Coplin jar filled two-thirds full with cold, freshly prepared lysing solution. Refrigerate for at least 1 h, but no more than 4 wk. Protect from light.
3. Cell viability *(8)*. To 40 µL of a cell suspension add 10 µL of the final staining solution (ethidium bromide and CFDA), mix, and let stand for 3–5 min at 37°C. Centrifuge and remove excess staining solution. Wash twice with 1 mL of PBS. Pelleted cells may be stored briefly at 4°C until ready to score.
4. Electrophoresis. Perform electrophoresis in dim yellow light or the dark to minimize light-induced DNA damage. Carefully remove slides from Coplin jars and place side-by-side on a horizontal gel box near one end. Fill the reservoir with sufficient electrophoresis buffer to cover slides with 1–3 mm of buffer. Avoid bubbles over the agar. Allow denaturation to occur for 30 min. Electrophorese at 25 volts and 300.0 milliamperes for 20 min (PS 250 DC Power Supply, Hoefer Scientific Instruments, San Francisco, CA). Carefully adjust the current at the start by raising or lowering the buffer level; leave buffer alone for the remainder of a run. Electrophoresis times can vary between 10 and 40 min in order to produce an optimal migration of DNA into comet tails. Turn off power and transfer slides to a drip tray. Slowly drop neutralization buffer onto the slides, let stand for 5 min, drain, and repeat twice. Drain slides using a paper towel to remove excess buffer, fix in cold 100% ethanol or methanol, and dry overnight. Slides can be stored indefinitely in a dry place.

4. ANALYSIS

1. Viability assessment *(8)*. Suspend cell pellets that have been stained with CFDA and ethidium bromide in 10 µL of PBS and drop mixture on a slide.

Apply a small coverslip and score 100 cells for viability (green cytoplasm), compromise (green cytoplasm, red nucleus), or death (red nucleus) using fluorescent microscopy with FITC or acridine orange filter combination (Olympus BM-40X, Melville, NY). Greater than 90% viable cell percentage is essential before proceeding with scoring comets.

2. Manual scoring. Prior to scoring, randomize and mask slides to treatments and decode only after all slides are scored. Stain DNA by pipetting ~90 µL of ethidium bromide solution onto a slide and apply a 24 × 50 mm coverslip. Randomly score 100 cells from several areas on the slide using a fluorescent microscope (*see* Fig. 1).
3. Ridit analysis. Compare the distributions of comet scores for controls and tests using Ridit analysis, a term derived from "relative to an identified distribution" *(5)*. This statistical method assumes discrete measures, in this case comet scores, represent intervals in a continuous but unobservable distribution. This technique has broad applicability because no assumptions are made about the nature or normality of the underlying distribution. Ridits range from 0–1, and by definition a Ridit for a control distribution (e.g., cells having no treatment) is 0.50. The mean Ridit for a test distribution (e.g., cells exposed to H_2O_2) is the probability that randomly selected cells will have a score indicating greater DNA damage than randomly selected cells from the control distribution. Mean Ridits are easily calculated using a spreadsheet format (Table 1). For comet analyses, a mean ridit >0.50 indicates greater DNA damage compared to the control or identified distribution. Values <0.50 indicate lesser damage. Standard errors for mean Ridits are also easily calculated and allow assignment of *P* values to comparisons *(5)*. Frequencies for comet scores and associated Ridit values are shown in Table 2 for HT-29 cells exposed to H_2O_2 for 30 min. The degree to which catalase protects DNA against H_2O_2-mediated damage is shown in Table 3.

5. DISCUSSION

The comet assay has enjoyed popularity as a technique that can assess low levels of DNA damage and repair in eukaryotic cells following diverse in vitro or in vivo treatments *(4,9)*. We recently used this assay to study colonic epithelial cell DNA damage caused by rats colonized with the commensal prokaryotic microorganism *Enterococcus faecalis (10)*. This bacterium generates substantial extracellular superoxide, H_2O_2, and hydroxyl radical through dysfunctional respiration *(11)*. The comet assay detected subtle in vivo oxidant stress on the colonic epithelial cell DNA caused by *E. faecalis*. Application of Ridit testing to comet image analysis allows any laboratory with a fluorescent microscope to use this powerful technique with minimal additional investment of resources.

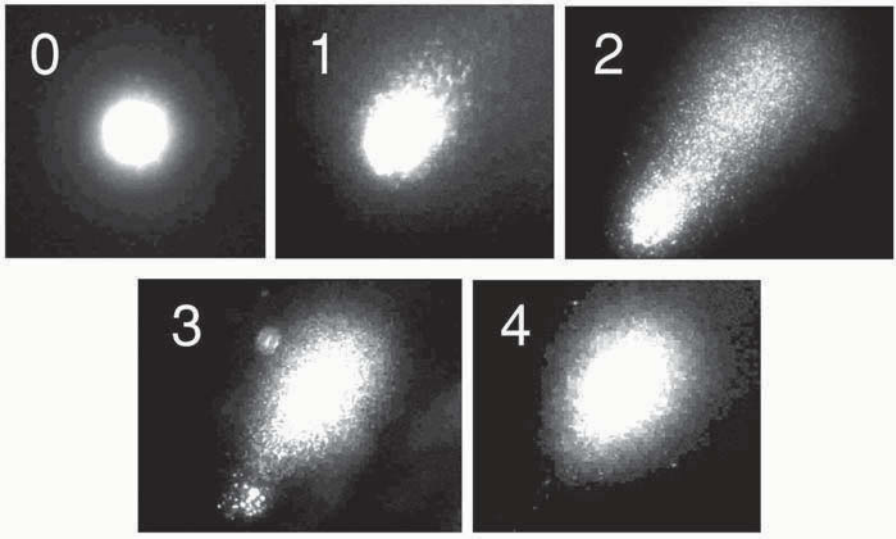

Fig. 1. Five-point scoring system for comets: *0*, no visible DNA migration from the nucleus; *1*, minimal DNA migration with an intact nucleus; *2*, moderate DNA migration with reduction in nuclear size; *3*, extensive DNA migration with only a pinpoint nucleus remaining; *4*, complete migration of DNA into a comet tail with no visible nucleus.

ACKNOWLEDGMENTS

This work was supported by a Merit Review Program from the Department of Veterans Affairs and the Frances Duffy Endowment.

REFERENCES

1. Östling, O. and Johanson, K. J. (1984) Microelectrophoretic study of radiation-induced DNA damages in individual mammalian cells. *Biochem. Biophys. Res. Commun.* **123,** 291–298.
2. Olive, P. L., Banáth, J. P., and Durand, R. E. (1990) Heterogeneity in radiation-induced DNA damage and repair in tumour and normal cells measured using the "comet" assay. *Radiat. Res.* **122,** 86–94.
3. Singh, N. P., McCoy, M. T., Tice, R. R., and Schneider, E. L. (1988) A simple technique for quantitation of low levels of DNA damage in individual cells. *Exp. Cell Res.* **175,** 184–191.
4. Fairbairn, D. W., Olive, P. L., and O'Neill, K. L.(1995) The comet assay: a comprehensive review. *Mutation Res.* **339,** 37–59.

Table 1
Sample Calculations of a Mean Ridit for Test Compared to Control Frequency[a]

Comet score	Control frequency	1	2	3	Ridit	Test frequency	5	Mean ridit
0	26	13.0	0.0	13.0	0.130	10	1.300	
1	43	21.5	26.0	47.5	0.475	22	10.450	
2	18	9.0	69.0	78.0	0.780	36	28.080	
3	11	5.5	87.0	92.5	0.925	21	19.425	
4	2	1.0	98.0	99.0	0.990	11	10.890	
Totals	100					100	70.145	0.701

[a]Comet scores range from *0* for no visible DNA migration to *4* for complete migration of DNA out of nucleus (*see* Fig. 1); the control frequency is the identified distribution and corresponds to untreated cells; column 1 is half the corresponding value for the control frequency; column 2 is the accumulated entries in column 1, but displaced one category downwards; column 3 is the sum of corresponding entries in columns 1 and 2; ridits correspond to entries in column 3 divided by the total sample size; the mean ridit is the sum of the products of test frequencies for treated cells multiplied by the corresponding ridits (column 5) divided by the total frequency; in this example, the odds are 7 to 3 more likely (= 0.701/0.299) treated cells sustained DNA damage than control cells.

Table 2
Comet Assay Measures Damaging Effect of H_2O_2 on HT-29 Intestinal Epithelial Cell DNA

Comet scores	Frequency of scores (%)[a]				
	H_2O_2 (μ*M*)				
	0	25	50	100	200
0	54	35	21	30	9
1	36	45	53	35	26
2	9	16	24	20	28
3	1	3	2	15	20
4	0	1	0	0	17
Ridit	0.50	0.61	0.68	0.67	0.84
P value	—	0.004	<0.001	<0.001	<0.001

[a]30 min incubations; assays performed twice with data combined.

Table 3
Comet Assay Measures Catalase Protection Against H_2O_2-Mediated DNA Damage for HT-29 Intestinal Epithelial Cells

Comet scores	Frequency of scores (%)[a]			
	Control	Catalase	H_2O_2	Catalase & H_2O_2
0	30	44	11	40
1	41	36	21	38
2	25	12	29	18
3	3	5	25	4
4	1	3	14	0
Ridit	0.50	0.43	0.75	0.44
P value	—	<0.001	<0.001	0.003

[a]30 min incubations; catalase, 100 U/mL; H_2O_2, 200 μM; assays performed twice with data combined.

5. Fleiss, J. L. (1981) The comparison of proportions from several independent samples: ridit analysis, in *Statistical Methods for Rates and Proportions,* 2nd ed. John Wiley & Sons, New York, pp. 150–157.
6. Klaude, M., Eriksson, S., Nygren, J., and Ahnström, G. (1996) The comet assay: mechanisms and technical considerations. *Mutation Res.* **363,** 89–96.
7. Tice, R. R. (1995) The single cell/gel comet assay: a microgel electrophoretic technique for the detection of DNA damage and repair in individual cells, in

Environmental Mutagenesis. (Phillips, D. H. and Venitt, S., eds.) Bios Scientific Publishers, Oxford, pp. 315–339.
8. Strauss, G. H. S. (1991) Non-random cell killing in cryopreservation: implications for performance of the battery of leukocyte tests (BLT), I. Toxic and immunotoxic effects. *Mutat. Res.* **252,** 1–15.
9. McKelvey-Martin, V. J., Green, M. H. L., Schmezer, P., Pool-Zobel, B. L., De Méo, M. P., and Collins, A. (1993) The single cell gel electrophoresis assay (comet assay): a European review. *Mutat. Res.* **288,** 47–63.
10. Huycke, M. M., Abrams, V., and Moore, D. R. (2002) *Enterococcus faecalis* produces extracellular superoxide and hydrogen peroxide that damages colonic epithelial cell DNA. *Carcinogenesis* **23,** 529–536.
11. Huycke, M. M., Moore, D., Shepard, L., et al. (2001) Extracellular superoxide production by *Enterococcus faecalis* requires demethylmenaquinone and is attenuated by functional terminal quinol oxidases. *Mol. Microbiol.* **42,** 729–740.

13

Detection of Aldehydic DNA Lesions Using Aldehyde Reactive Probe

Jun Nakamura and James A. Swenberg

1. INTRODUCTION

In living cells, reactive oxygen species (ROS) such as superoxide anion, hydrogen peroxide (H_2O_2), and hydroxyl radicals are constitutively produced endogenously and also induced by exogenous agents including ionizing radiation, ultraviolet (UV) light, and a various redox cycling chemicals including polycyclic aromatic hydrocarbons. Massive production of ROS that overwhelms cellular defense systems can result in serious outcomes such as cell death. H_2O_2 is produced at a relatively high rate as a product of aerobic metabolism. In the presence of transition metals (Fe^{2+} and Cu^{+}), H_2O_2 can generate hydroxyl radicals via the Fenton reaction *(1)*. The highly reactive hydroxyl radical can induce protein modification, lipid peroxidation, and DNA damage *(2,3)*. Although the heterocyclic bases of nucleic acids are important sites of free radical-mediated alteration, such as 8-hydroxyguanine (8-OHG) *(4)*, the sugar-phosphate backbone is also highly vulnerable to attack. Abstraction of a hydrogen atom from each carbon from deoxyribose produces a carbon-based sugar radical that can rearrange, resulting in scission of the nucleic acid strand, deoxyribose fragmentation, as well as formation of base loss lesions, so-called apurinic/apyrimidinic (AP) sites *(5,6)*. These deoxyribose lesions frequently contain aldehydic moieties; however, they have been difficult to examine, mainly owing to the large variety of products, as well as their chemical instability, even at mild temperatures and neutral pH *(7)*. Many oxidized sugars are very labile, because terminal sugar lesions tend to be modified spontaneously during experimental procedures.

From: *Methods in Pharmacology and Toxicology: Methods in Biological Oxidative Stress*
Edited by: K. Hensley and R. A. Floyd

We developed a sensitive aldehyde reactive probe (ARP) slot-blot (ASB) assay to detect aldehydic DNA lesions (ADLs) in DNA, which can quantitate ~2 lesions/10^7 nucleotides *(8)*. In this assay, we utilize ARP, a biotin-tagged hydroxylamine probe that reacts with ADLs including aldehydic ring-opened AP sites *(9)*. The number of biotin-tagged ADLs can then be determined colorimetrically by an enzyme-linked immunosorbent assay (ELISA)-like assay on the nitrocellulose membrane. Using ARP, we stabilized ADLs induced by ROS and detected a significant number of these lesions in naked DNA after the Fenton reaction *(10)*. In addition, we demonstrated formation of these lesions in human cancer cell lines exposed to millimolar levels of H_2O_2 *(10)*. Our current on-going experiments further show that H_2O_2 induces ADLs in human cancer cells at concentrations as low as 0.05 m*M* for 15 min (unpublished data).

2. MATERIALS

1. ARP (Dojindo Molecular Technologies, Inc.), dissolve to 10 m*M* in distilled water and freeze at –80°C (stable for at least 6 mo).
2. Streptavidin-conjugated horseradish peroxidase (BioGenix) at 4°C (stable until expired date).
3. Electrogenerated chemiluminescence (ECL) reagent at 4°C (Amersham).
4. Primary and secondary internal standard DNA is generated by incubation of calf thymus DNA pretreated with 100 m*M* methoxyamine (MX, Sigma) at 70°C in depurination buffer, for 10 and 3 min, respectively *(8)*. This DNA should contain ~100 and ~30 AP sites/10^6 nucleotides. The number of AP sites should be calibrated by another researcher or other method. DNA is frozen at –80°C (stable for at least 2 yr).
5. Blank DNA solution is prepared at 275 ng ARP-unreacted DNA/220 µL TE buffer.
6. Tris-EDTA (TE) buffer, pH 7.5.
7. 10× phosphate-buffered saline (PBS), pH 7.4.
8. Washing buffer. 0.26 M NaCl, 1 m*M* EDTA, 20 m*M* Tris-HCl, 0.1% Tween-20, pH 7.5.
9. 2 *M* ammonium acetate.
10. 5× SSC. 0.75 *M* NaCl, 75 mM trisodium citrate.
11. Hybrid mix. 20 m*M* Tris-HCl, pH 7.5, 0.1 *M* NaCl, 1 m*M* EDTA, 0.5% casein, 0.25% bovine serum albumin (BSA), 0.1% Tween-20.

3. METHODS

1. DNA extraction. Regular phenol/chloroform/sevag extraction *(8)* supplemented with 20 m*M* 2,2,6,6-tetramethylpiperidinoxyl (TEMPO; Aldrich) is recommended for DNA extraction from animal tissues *(8,10)*. For cultured cells, PureGene DNA extraction kit (Gentra Systems, Inc.) supplemented with 20 m*M*

TEMPO is appropriate to reduce background levels of ADLs. DNA extraction needs to be performed at low temperature except RNase digestion (37°C for 30 min). The extracted DNA is resuspended in distilled water with 1 or 2 m*M* TEMPO.

2. ARP reaction. Prepare DNA sample in 30–135 μL buffer containing 8 μg DNA and 1/10 volume of 10× PBS in tube on ice. Prepare the following:
   a. One primary standard containing 100 AP sites/10^6 nucleotides.
   b. Three secondary standards containing 30 AP sites/10^6 nucleotides.
   c. Unknown samples.
   After addition of 1/10 volume of 10 m*M* ARP, samples are incubated for 10–30 min at 37°C.
3. Purification. To eliminate free ARP from samples, DNA is precipitated by cold ethanol. DNA pellets are washed once by 70% ethanol and are resuspended in Tris-EDTA buffer. DNA concentration should be measured before DNA loading on the nitrocellulose (NC) membrane by a spectrophotometer.
4. Preparation of ARP-reacted loading samples and secary standard. ARP-reacted DNA samples and secary standard are prepared in 220 μL TE buffer containing 275 ng ARP-reacted DNA. DNA is then heat-denatured at 100°C for 10 min and is placed on ice.
5. Preparation of ARP-reacted primary standard. ARP-reacted primary standard DNA is prepared at concentration of 275 ng/220 μL TE buffer. After heat-denaturation of primary standard DNA and ARP-unreacted blank DNA, the primary standard is serially diluted with blank DNA on ice. Each serially diluted standard solution should contain 275 ng DNA in 220 μL TE buffer.
6. DNA loading. After mixing with an equal amount of 2 *M* ammonium acetate, the single-stranded DNA is loaded on the nitrocellulose membrane in at least duplicates. The slots are rinsed with 200 μL 1 *M* ammonium acetate. The NC membrane is soaked with 5 × SSC at 37°C for 15 min.
7. Reaction with streptavidin-conjugated horseradish peroxidase. The NC filter is dried and baked in a vacuum oven at 80°C for 30 min. The membrane is preincubated with 20 mL Hybrid Mix at room temperature for 20 min. The NC filter is then incubated in the same solution containing 2 μL streptavidin-conjugated horseradish peroxidase at room temperature for 45–60 min.
8. Chemiluminescence reaction and film exposure. After rinsing the NC membrane with washing buffer for 15 min, the enzymatic activity on the membrane is visualized by the ECL reagents. The NC filter is then exposed to X-ray film for 1–10 min.
9. Analysis. The developed film is analyzed using a Kodak Image station 440CF (Kodak). Quantitation is based on comparisons to standard curve generated by the primary internal standard DNA. Before the comparison, the standard curve is adjusted by the number of triplicated secondary standard containing 30 AP sites per 10^6 nucleotides.

4. DISCUSSION

It is noteworthy that ARP reacts not only with regular AP sites generated by either depurination/depyrimidination or by DNA glycosylase (Fig. 1),

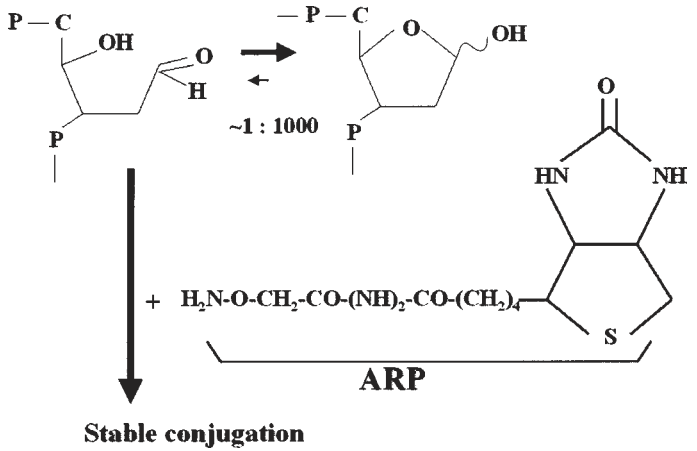

Fig. 1. Structures of regular AP site and aldehydic reactive probe.

but also with modified bases with aldehydic moieties such as formyluracil *(11)* and N2-(3-oxo-1-propenyl)-guanosine converted from M1G *(12)* and possibly many other oxidized deoxyribose (Fig. 2). Therefore, without clear evidence of biochemical characteristics or structural information using mass spectroscopy, the lesions detected by this assay should be referred as ADLs instead of AP sites. For example, naked calf thymus DNA exposed to the Fenton reaction showed $FeSO_4$ concentration-dependent increase in the number of ADLs *(9)* (Fig. 3, facing page, bottom; *see* caption this page). These ADLs appear to be sugar lesions directly oxidized by hydroxyl radicals, rather than simple AP sites generated by depurination/depyrimination.

This assay is also applicable to determine the number of oxidized purines and pyrimidines by combination with DNA glycosylases to excise base lesions and leave AP sites. The number of AP sites newly generated by the DNA glycosylase corresponds to the amount of base lesions. We established *Escherichia coli* endonuclease III- *(10)* and human 8-OHG DNA glycosylase (hOGG1)-coupled AP site assays (Fig. 4).

Fig. 3. *(opposite page)* Detection of ADLs in calf thymus DNA following the Fenton reaction by a combination of H_2O_2 (0.1 m*M*) and FeCl2 (0.625–10 μ*M*). **(A)**, scanning densitometric data of ADLs in MX-pretreated calf thymus DNA exposed to the Fenton reaction; means from duplicate slots of three individual samples; bars, SD; **(B)**, X-ray film showing formation of ADLs in calf thymus DNA induced by the Fenton reaction. DNA was loaded on a NC membrane (275 ng per slot). ►

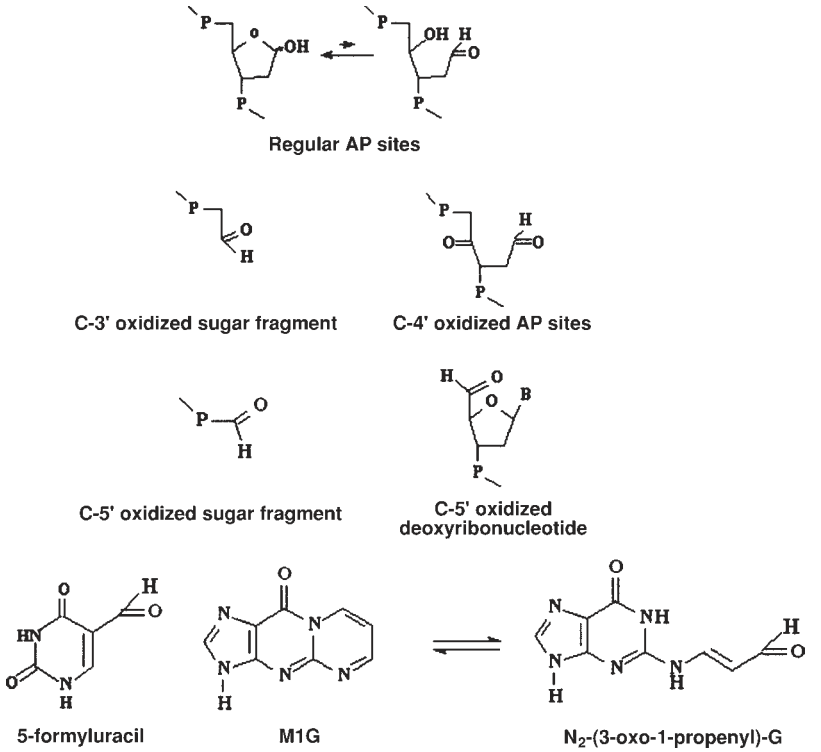

Fig. 2. Structures of aldehydic deoxyribose and base lesions.

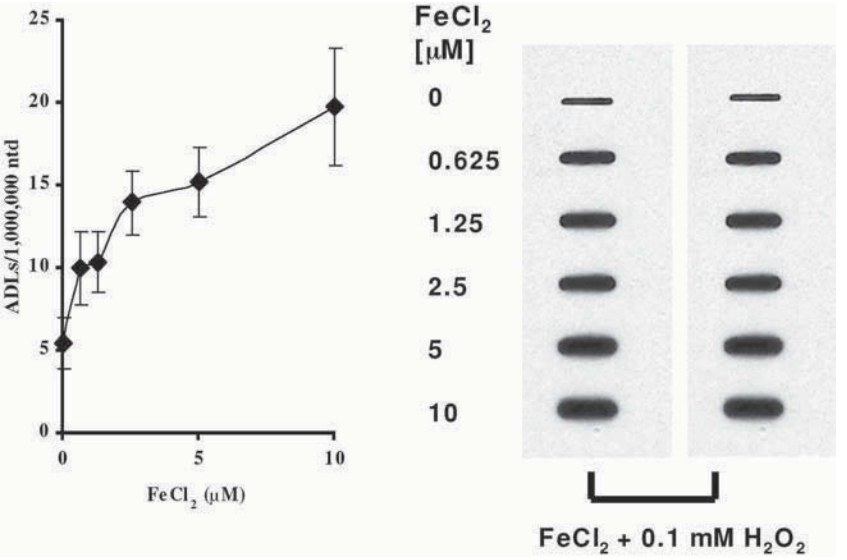

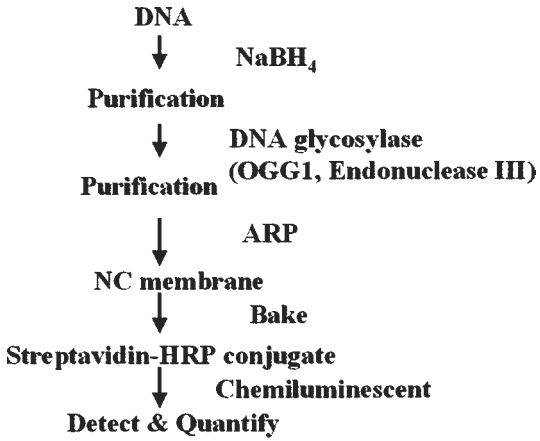

Fig. 4. Scheme of DNA glycosylase-coupled AP site assay to detect oxidized bases in DNA.

ACKNOWLEDGMENTS

This work was supported in part by grants P42-ES05948, R42-ES11746, P30-CA16086, and P30-ES10126 from the National Institutes of Health and a grant from the Coca-Cola Foundation.

REFERENCES

1. Henle, E. S. and Linn, S. (1997) Formation, prevention, and repair of DNA damage by iron/hydrogen peroxide. *J. Biol. Chem.* **272(31),** 19095–19098.
2. Kasprzak, K. S. (2002) Oxidative DNA and protein damage in metal-induced toxicity and carcinogenesis. *Free Radic. Biol Med.* **32(10),** 958–967.
3. Marnett L. J. Lipid peroxidation-DNA damage by malondialdehyde. *Mutat. Res.* **424(1-2),** 83–95.
4. Beckman, K. B. and Ames, B. N. (1997) Oxidative decay of DNA. *J. Biol. Chem.* **272,** 19,633–19,636.
5. Pogozelski, W. K. and Tullius, T. D. (1998) Oxidative strand scission of nucleic acids: routes initiated by hydrogen abstraction from the sugar moiety. *Chem. Rev.* **98,** 1089–1108.
6. Breen, A. P. and Murphy, J. A. (1995) Reactions of oxyl radicals with DNA. *Free Radic. Biol. Med.* **18,** 1033–1077.
7. Lafleur, M. V. M., Woldhuis, J., and Loman, H. (1981) Alkali-labile sites in biologically active DNA: comparison of radiation induced potential breaks and apurinic sites. *Int. J. Radiat. Biol. Relat. Stud. Phys. Chem. Med.* **39,** 113–118.
8. Nakamura, J., Walker, V. E., Upton, P. B., Chiang, S.-Y., Kow, Y. W., and Swenberg, J. A. (1998) Highly sensitive apurinic/apyrimidinic site assay can

detect spontaneous and chemically induced depurination under psychological conditions. *Cancer Res.* **58,** 222–225.
9. Kubo, K., Ide, H., Wallace, S. S., Kow, Y. W. (1992) A novel, sensitive, and specific assay for abasic sites, the most commonly produced DNA lesion. *Biochemistry* **31(14),** 3703–3708.
10. Nakamura, J., La, D. K., and Swenberg, J. A. (2000) 5'-nicked apurinic/apyrimidinic sites are resistant to β-elimination by POL-β and are persistent in human cultured cells after oxidative stress. *J. Biol. Chem.* **275,** 5323–5328.
11. Ide, H., Akamatsu, K., Kimura, Y., Michiue, K., Makino, K., Asaeda, A., et al. (1993) Synthesis and damage specificity of a novel probe for the detection of abasic sites in DNA. *Biochemistry* **32,** 8276–8283.
12. Mao, H., Schnetz-Boutaud, N. C., Weisenseel, J. P., Marnett, L. J., and Stone, M. P. (1999) Duplex DNA catalyzes the chemical rearrangement of a malondialdehyde deoxyguanosine adduct. *Proc. Natl Acad. Sci. USA* **96,** 6615–6620.

14

Analysis of Neuroketal Protein Adducts by Liquid Chromatography–Electrospray Ionization/Tandem Mass Spectrometry

Nathalie Bernoud-Hubac, Sean S. Davies, Olivier Boutaud, and L. Jackson Roberts, II

1. INTRODUCTION

A role of free radicals has been implicated in the pathogenesis of a number of neurological disorders, including amyotrophic lateral sclerosis, Huntington's disease (HD), Parkinson's disease (PD), and Alzheimer's disease (AD) *(1–9)*. Furthermore, reactive aldehydes produced as products of lipid peroxidation are thought to be key mediators of oxidant injury because of their capacity to covalently modify proteins and DNA *(10)*, and evidence suggests they may be involved in the pathogenesis of neurodegenerative diseases *(11–13)*. Aggregated cross-linked proteins are characteristic features of neurodegenerative diseases *(14)*. Isoprostanes (IsoPs) are prostaglandin-like compounds formed by free radical-induced peroxidation of arachidonic acid *(15)*. We recently identified the formation of highly reactive γ-ketoaldehydes, now termed isoketals (IsoKs), as products of the IsoP pathway *(16)*. IsoKs are orders of magnitude more reactive than other known reactive products of lipid peroxidation and exhibit a unique proclivity to cross-link proteins *(17)*. Neuroprostanes (NPs) are IsoP-like compounds formed from oxidation of docosahexaenoic acid (DHA) *(5)*, which is highly enriched in the brain *(18,19)*, and levels of neuroprostanes in cerebrospinal fluid (CFS) have been found to be increased in patients with AD *(5)*. Analogous to the formation of IsoKs via the isoprostane pathway, we recently identified the formation of another class of highly reactive γ-ketoaldehydes as products of the neuroprostane pathway, termed neuroketals (NKs) *(20)*.

From: *Methods in Pharmacology and Toxicology: Methods in Biological Oxidative Stress*
Edited by: K. Hensley and R. A. Floyd

The mechanism by which NKs are generated by free radical-induced oxidation of DHA is shown in Fig. 1. Five docosahexaenoyl radicals are initially formed and following addition of oxygen, eight peroxyl radicals are generated. These undergo endocyclization and then rearrangement to form eight D_4-NKs and eight E_4-NKs regioisomers. Each regioisomer is theoretically comprised of eight racemic diastereoisomers for a total of 256 compounds. The designation "D" and "E" refers to the location of the keto group in conformity with prostaglandin nomenclature. In accordance with the nomenclature system for IsoPs that has been approved by the Eicosanoid Nomenclature Committee, the different regioisomers are designed by the carbon number on which the side-chain hydroxyl group is located with the carbonyl carbon as C_1 *(21)*. NKs rapidly adduct to lysine residues in a time frame of secs and exhibit a remarkable proclivity to form protein cross-links. Moreover, NK-lysyl protein adducts can also be detected in vivo in normal human brain. Fig. 2 represents the proposed mechanism of formation of NK-lysyl adducts. An initial reversible Schiff base adduct is formed, which then proceeds through a pyrrole, which readily undergoes autoxidation to form stable lactam and hydroxylactam adducts. We hypothesize that NKs may participate in the formation of protein adducts and protein cross-links in neurodegenerative diseases. The primary focus of this chapter is to describe the methodologies used to characterize and quantify NK-lysyl lactam adducts in vivo.

2. MATERIALS

1. DHA (Nu-Chek-Prep, Inc., Elysian, MN).
2. *N-N*-dimethylformamide, ammonium acetate, trolox, triphenylphosphine (TPP) (Aldrich, Milwaukee, WI).
3. Butylated hydroxytoluene (BHT) (Sigma, St. Louis, MO).
4. Pronase and aminopeptidase M (Calbiochem, La Jolla, CA).
5. Oasis cartridges from Waters Associates (Milford, MA).
6. L-Lysine-U-$^{13}C_6$.HCl and [$^2H_3$]Methoxyamine HCl (Cambridge Isotope Laboratories, Inc., Andover, MA).
7. L-Lysine-[4,5-^{3}H(N)] (NEN, Boston, MA).
8. 4.6 × 250 mm Macrosphere 300 C18 column and 2.1 × 1.5 mm XDB C8 column (MacMod Analytical, Chadds Ford, PA).
9. Centrifuge tube filter (Corning Incorporate, NY).
10. Electrospray tandem mass spectrometric analysis were carried out on a Finnigan TSQ7000.

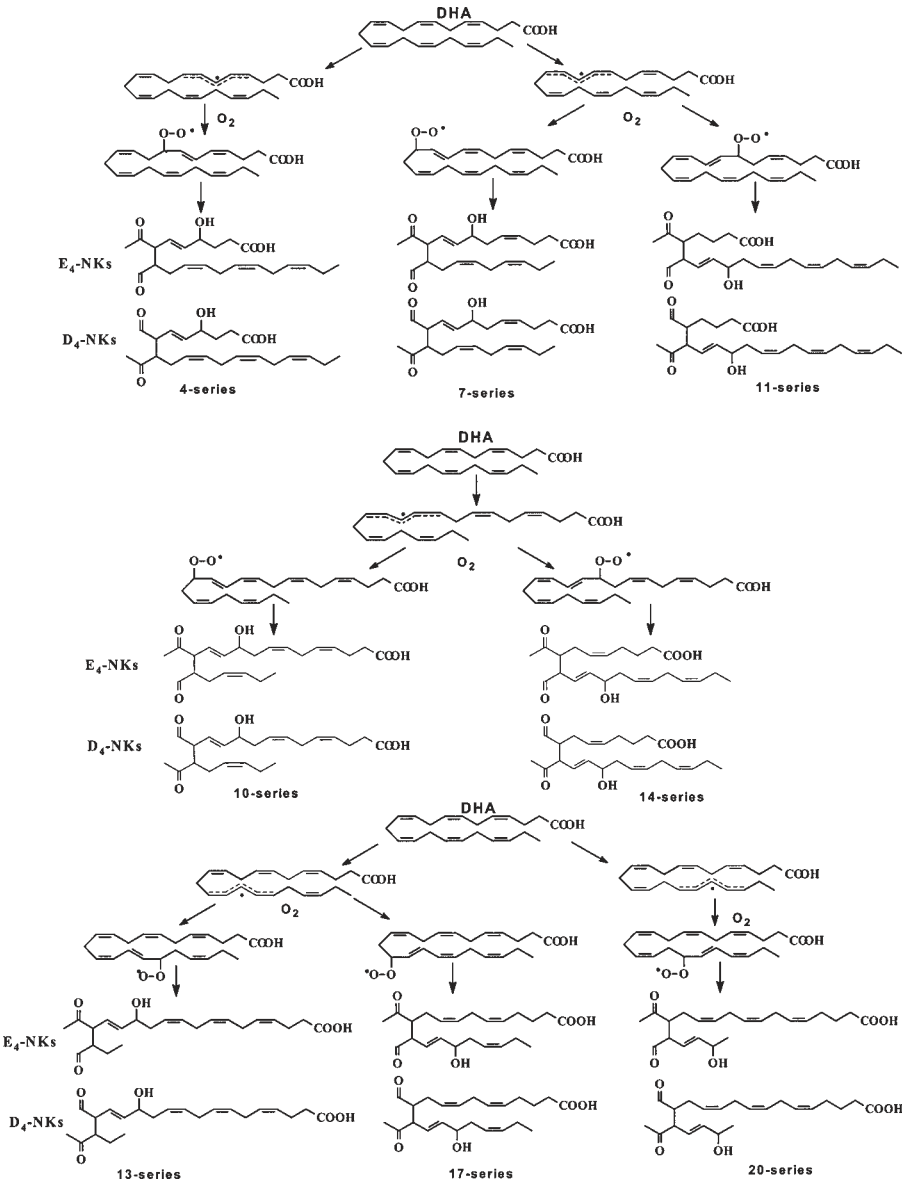

Fig. 1. Pathway for the formation of NKs by oxidation of DHA.

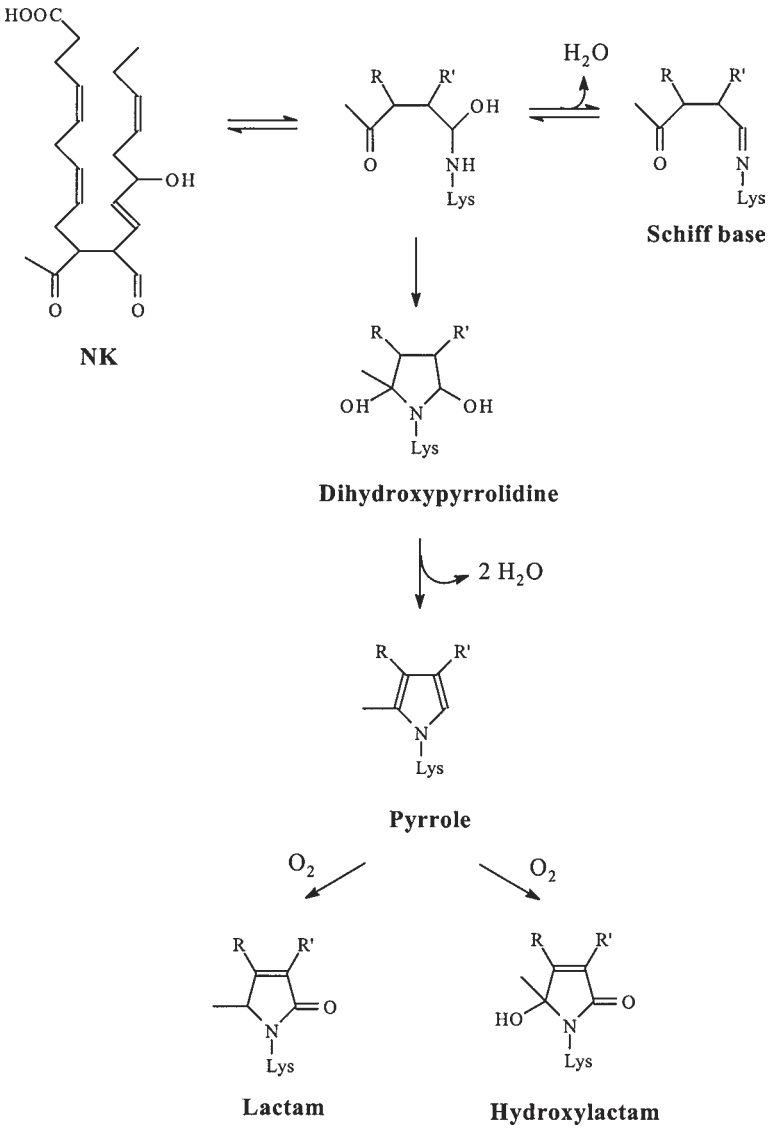

Fig. 2. Proposed mechanism of formation of NK-lysyl adducts.

3. EQUIPMENT

1. Blade homogenizer-PTA 10s generator (Brinkman Instruments), table top centrifuge, analytical evaporation unit (such as Meyer N-Evap, Oganomation), tank of nitrogen, microcentrifuge, 37°C water bath.

2. HPLC system, liquid chromatography electrospray ionization tandem mass spectrometer.

4. METHODS

4.1. NK-Lysyl Adduct Internal Standard Preparation

1. Mix equal volumes of iron (16.20 mg/mL in deionized water) and ADP (85.44 mg/mL in deionized water) and let sit 1 h at room temperature.
2. In a small flask containing 1X phosphate-buffered saline (PBS) pH 7.5, 37°C), oxidize 25 mg DHA (1 mg/mL) by adding 100 μL of iron/ADP solution and 50 μL of ascorbic acid solution (17.6 mg/mL in deionized water) in presence of [$^{13}C_6$] lysine (2 mg) and [^{3}H]lysine (50×10^6 cpm) for 2 h.
3. Apply the sample to an 1 g Oasis column that has been preconditioned with 10 mL methanol and 10 mL deionized water. Load the sample slowly and wash it with 10 mL deionized water before eluting it with 10 mL methanol into a scintillation tube.
4. Dry the eluate under nitrogen until there is less than 100 μL, but do not completely dry. Resuspend the sample in 1 mL 20 m*M* ammonium acetate in water with 0.1% acetic acid and purify it by isocratic HPLC using a 4.6 × 250 mm Macrosphere 300 C18 column. The solvent system to be employed is a gradient consisting of 20 m*M* ammonium acetate with 0.1% acetic acid (solvent A) to 5 m*M* ammonium acetate/MeOH/acetic acid (10:90:0.1, v/v/v) (solvent B). The flow rate is 1 mL/min beginning at 100% A, followed by an increase to 40% B in 5 min and 100% B in 14 min. The column is then washed with 100% B for an additional 12 min and equilibrated with 100% A for 43 min.
5. Analyze aliquots containing radioactivity by liquid chromatography electrospray ionization tandem mass spectrometry (LC-ESI-MS-MS) as described in Subheading 5.
6. Combine fractions containing the NK-lysyl adduct internal standard. Dry the sample under nitrogen and resuspend it in 1 mL methanol. Layer with argon and freeze internal standard at –80°C. Calculate the concentration from the specific activity of the [^{3}H] lysine.

4.2. Analysis of NK-Adducts In Vivo

1. For aqueous samples such as plasma, add 1 volume of 0.4 *N* KOH containing 3 m*M* Trolox for base hydrolysis, vortex sample, layer with argon, and place at 37°C for 2 h in a shaking water bath.
2. Tissue samples are homogenized using Polytron homogenizer in 3 mL of cold ethanol containing 5 mg of BHT and 50 mg of TPP (100 mL). Add up to 0.05 mL/mg tissue of ethanol to each tube and pellet precipitated proteins by centrifugation at 2000 rpm at 4°C for 10 min. Remove and discard supernatant. Resuspend sample in 3 mL of cold MeOH (containing BHT and TPP) and 3 mL of 0.4 *N* KOH (containing trolox) for the base hydrolysis, which is done as described for the aqueous samples.

3. Neutralize the sample with 1 *N* HCl.
4. Precipitate proteins in cold ethanol (containing BHT and TPP) (0.05 mL ethanol/mg tissue or 10 volumes ethanol for aqueous samples) by centrifugation at 2000 rpm at 4°C for 10 min.
5. Reprecipitate proteins in the same previous volume of cold Folch solution and wash with cold methanol (each containing BHT and TPP). All of these precipitation steps are sufficient to eliminate phospholipids. Therefore, there is no need to use an antioxidant in later steps.
6. Resuspend proteins in 1X PBS and heat samples at 95°C for 10 min.
7. After cooling, add pronase (3 mg/mg of starting protein weight) and incubate the digest overnight at 37°C in a shaking water bath.
8. Heat samples at 95°C for 10 min to inactivate the pronase.
9. After cooling, add aminopeptidase (3 μL/mg of starting protein weight) and incubate the digest 18 h at 37°C in a shaking water bath.
10. Extract the digest with a 1 g Oasis cartridge and dry it until there is less than 100 μL as described for the preparation of NK-lysyl adduct internal standard. Before purifying the digest by HPLC as described above, filter it using a centrifuge tube filter (pore size: 0.22 μm).
11. Combine HPLC fractions containing radioactivity from NK-lysyl adduct internal standard (do not pool too many fractions to obtain a cleaner signal in LC-ESI-MS-MS. In our conditions, we recommend combining fractions 20 and 21).
12. Re-extract with a 60 mg Oasis cartridge, as previously described.
13. Analyze adducts by LC-ESI-MS-MS as described below.

5. ANALYSIS

NK-lysyl lactam adducts are analyzed by LC–ESI/MS-MS in the positive ion mode. The adducts are chromatographed on a 2.1 × 15 mm XDB C8 column with a flow rate of 0.2 mL/min using a linear gradient of 10–90% acetonitrile in 5 m*M* ammonium acetate/0.1% acetic acid. The sheet gas pressure is 70 psi and the auxiliary gas pressure is 10 psi. The voltage on the capillary is 20 V and the tube lens voltage is 80 V. The capillary temperature is 200°C. Selected reaction monitoring (SRM) of fragmentation of the molecular ion to a specific daughter ion for the lactam adduct (*m/z* 503.4 to *m/z* 84.1 and *m/z* 509.4 to *m/z* 89.1 for the lactam adducts present in tissue or biological fluid and the internal standard, respectively) is performed at –36 eV with 2.6 mTorr collision gas. Quantification of the amount of NK-lysyl lactam adduct detected is performed by integration of peaks.

Fig. 3 represents a typical ion-current chromatogram from the analysis of NK-lysyl lactam adducts in cortex of human brain utilizing selected reaction monitoring of the transition of the $[MH]^+$ ions for the brain lactam adducts (*m/z* 503.4) and NK [$^{13}C_6$] lysine lactam internal standards (*m/z* 509.4) to the specific respective collision-induced dissociation ions *m/z* 84.1 and 89.1.

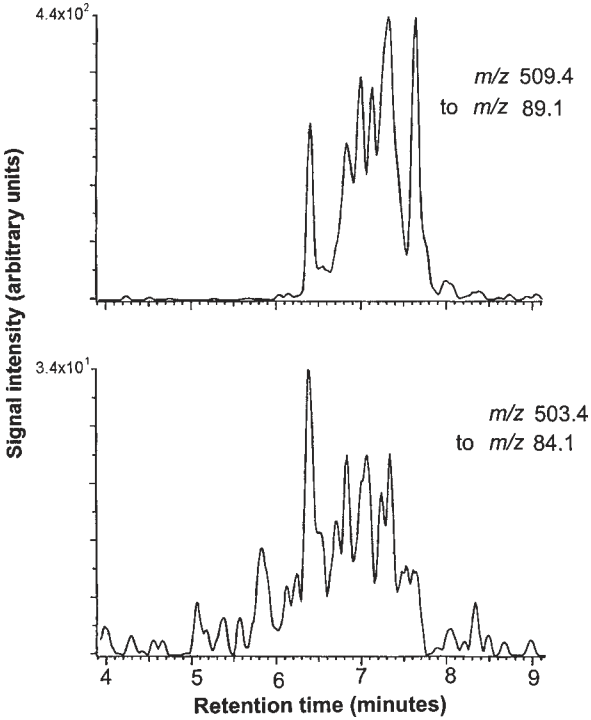

Fig. 3. Ion-current chromatograms from the LC-ESI-MS-MS analysis of NK-lysyl lactam adducts in cortex from human brain. Selected reaction monitoring of the transitions from *m/z* 509.4 to *m/z* 89.1 (NK-lysyl lactam internal standard) and *m/z* 503.4 to *m/z* 84.1 (NK-lysyl lactam protein adducts in brain) was performed. HPLC fractions 20 and 21 were combined.

This has been obtained after combining the HPLC fractions 20 and 21. Fractions 20 and 21 contain all of the peaks in the internal standard. If additional fractions are included, the tracings obtained are less than optimal because additional interfering peaks are introduced in the *m/z* 503.4 transitioned to *m/z* 84.1 channel.

6. DISCUSSION

Because of the remarkable rapidity with which NKs adduct to proteins, they exist almost exclusively as protein adducts in biological tissues, precluding their detection in free form. The LC-ESI-MS-MS assay described herein provides a sensitive and specific method to analyze NK protein adducts

in vivo as a mean to explore the pathophysiological role of these adducts in oxidative injuries to the brain in general and specifically in neurodegenerative diseases. The unique proclivity of NKs to induce protein aggregation, a characteristic feature of neurodegenerative diseases, makes them attractive as potential candidates involved in the neurodegenerative process in these diseases. In this regard, we have recently found that levels of NK adducts are significantly increased in disease affected areas of brain from patients with AD (manuscript submitted).

ACKNOWLEDGMENTS

This work was supported by National Institute of Health Grants GM42056, GM15431, CA68485, and DK26657.

REFERENCES

1. Markesbery, W. R. (1997) Oxidative stress hypothesis in Alzheimer's disease. *Free Radic. Biol. Med.* **23,** 134–147.
2. Markesbery, W. R. (1999) The role of oxidative stress in Alzheimer disease. *Arch. Neurol.* **56,** 1449–1452.
3. Simonian, N. A. and Coyle, J. T. (1996) Oxidative stress in neurodegenerative diseases. *Annu. Rev. Pharmacol. Toxicol.* **36,** 83–106.
4. Perry, G., Nunomura, A., Hirai, K., Takeda, A., Aliev, G., and Smith, M. A. (2000) Oxidative damage in Alzheimer's disease: the metabolic dimension. *Int. J. Dev. Neurosci.* **18,** 417–421.
5. Roberts, L. J., 2nd, Montine, T. J., Markesbery, W. R., Tapper, A. R., Hardy, P., Chemtob, S., et al. (1998) Formation of isoprostane-like compounds (neuroprostanes) in vivo from docosahexaenoic acid. *J. Biol. Chem.* **273,** 13605–13612.
6. Montine, T. J., Markesbery, W. R., Morrow, J. D., and Roberts, L. J. (1998) Cerebrospinal fluid F2-isoprostane levels are increased in Alzheimer's disease. *Ann. Neurol.* **44,** 410–413.
7. Montine, T. J., Beal, M. F., Cudkowicz, M. E., O'Donnell, H., Margolin, R. A., McFarland, L., et al. (1999) Increased CSF F2-isoprostane concentration in probable AD. *Neurology* **52,** 562–565.
8. Montine, T. J., Beal, M. F., Robertson, D., Cudkowicz, M. E., Biaggioni, I., O'Donnell, H., et al. (1999) Cerebrospinal fluid F2-isoprostanes are elevated in Huntington's disease. *Neurology* **52,** 1104–1105.
9. Reich, E. E., Markesbery, W. R., Roberts, L. J., Swift, L .L., Morrow, J. D., and Montine, T. J. (2001) Brain regional quantification of F-ring and D-/E-ring isoprostanes and neuroprostanes in Alzheimer's disease. *Am. J. Pathol.* **158,** 293–297.

10. Esterbauer, H., Schaur, R. J., and Zollner, H. (1991) Chemistry and biochemistry of 4-hydroxynonenal, malonaldehyde and related aldehydes. *Free Radic. Biol. Med.* **11,** 81–128.
11. Smith, R. G., Henry, Y. K., Mattson, M. P., and Appel, S. H. (1998) Presence of 4-hydroxynonenal in cerebrospinal fluid of patients with sporadic amyotrophic lateral sclerosis. *Ann. Neurol.* **44,** 696–699.
12. Lovell, M. A., Ehmann, W. D., Mattson, M. P., and Markesbery, W. R. (1997) Elevated 4-hydroxynonenal in ventricular fluid in Alzheimer's disease. *Neurobiol. Aging* **18,** 457–461.
13. Montine, K. S., Reich, E., Neely, M. D., Sidell, K. R., Olson, S. J., Markesbery, W. R., and Montine, T. J. (1998) Distribution of reducible 4-hydroxynonenal adduct immunoreactivity in Alzheimer disease is associated with APOE genotype. *J. Neuropathol. Exp. Neurol.* **57,** 415–425.
14. Kaytor, M. D., Warren, S. T. (1999) Aberrant protein deposition and neurological disease. *J. Biol. Chem.* **274,** 37,507–37,510.
15. Morrow, J. D., Hill, K. E., Burk, R. F., Nammour, T. M., Badr, K. F., and Roberts, L. J., 2nd (1990) A series of prostaglandin F2-like compounds are produced in vivo in humans by a non-cyclooxygenase, free radical-catalyzed mechanism. *Proc. Natl. Acad. Sci. USA* **87,** 9383–9387.
16. Brame, C. J., Salomon, R. G., Morrow, J. D., and Roberts, L. J., 2nd (1999) Identification of extremely reactive gamma-ketoaldehydes (isolevuglandins) as products of the isoprostane pathway and characterization of their lysyl protein adducts. *J. Biol. Chem.* **274,** 13,139–13,146.
17. Iyer, R. S., Ghosh, S., and Salomon, R. G. (1989) Levuglandin E2 crosslinks proteins. *Prostaglandins* **37,** 471–480.
18. Salem, N., Jr., Kim, H.-Y., and Yergery, J. A. (1986) Docosahexaenoic acid:Membrane function and metaolism, in *Health Effects of Polyunsaturated Fatty Acids in Seafoods* (Simopoulos. A. P., Kifer, R. R., and Martin, R. E., eds.), Academic Press, Orlando, FL, pp. 263–317.
19. Skinner, E. R., Watt, C., Besson, J. A., and Best, P. V. (1993) Differences in the fatty acid composition of the grey and white matter of different regions of the brains of patients with Alzheimer's disease and control subjects. *Brain* **116,** 717–725.
20. Bernoud-Hubac, N., Davies, S. S., Boutaud, O., Montine, T. J., and Roberts, L. J., 2nd (2001) Formation of highly reactive gamma-ketoaldehydes (neuroketals) as products of the neuroprostane pathway. *J. Biol. Chem.* **276,** 30,964–30,970.
21. Taber, D. F., Morrow, J. D., and Roberts, L. J., 2nd (1997) A nomenclature system for the isoprostanes. *Prostaglandins* **53,** 63–67.

15

Measurement of Isoketal Protein Adducts by Liquid Chromatography–Electrospray Ionization/Tandem Mass Spectrometry

Sean S. Davies, Cynthia J. Brame, Olivier Boutaud, Nathalie Bernoud-Hubac, and L. Jackson Roberts, II

1. INTRODUCTION

Oxidative stress has been increasingly implicated in the pathogenesis of a wide variety of diverse human diseases. Free radical damage to lipids, proteins, and DNA may all contribute to the pathogenesis of disease. We have recently discovered a series of highly reactive γ-ketoaldehydes that are formed by rearrangement of bicyclic endperoxide intermediates in the isoprostane (IsoP) pathway of free radical-mediated peroxidation of arachidonic acid *(1)*, which we now term isoketals (IsoKs) *(2)* (Fig. 1). IsoKs rapidly react with the ε-amine of lysyl residues on proteins to form Schiff base, lactam, and hydroxylactam adducts *(1,3,4)* (Fig. 2). The rapidity with which IsoKs adduct to proteins exceeds that of other known reactive products of lipid peroxidation, e.g., 4-hydroxynonenal, by orders of magnitude *(1)*. Adduction of proteins frequently leads to altered protein function *(5–8)*. This in turn can lead to cellular dysfunction, which may be causally linked to the pathogenesis of disease processes.

The remarkable rapidity with which IsoKs adduct to proteins precludes their detection in biological tissues as free unadducted compounds. Therefore, we developed an accurate method to detect and quantify IsoK protein adducts to explore their role in the pathogenesis of disease utilizing liquid chromatography–electrospray ionization/tandem mass spectrometry (LC–ESI/MS-MS). The basis of this method involves enzymatic digestion of proteins to individual amino acids followed by analysis of lysyl-IsoK

From: *Methods in Pharmacology and Toxicology: Methods in Biological Oxidative Stress*
Edited by: K. Hensley and R. A. Floyd

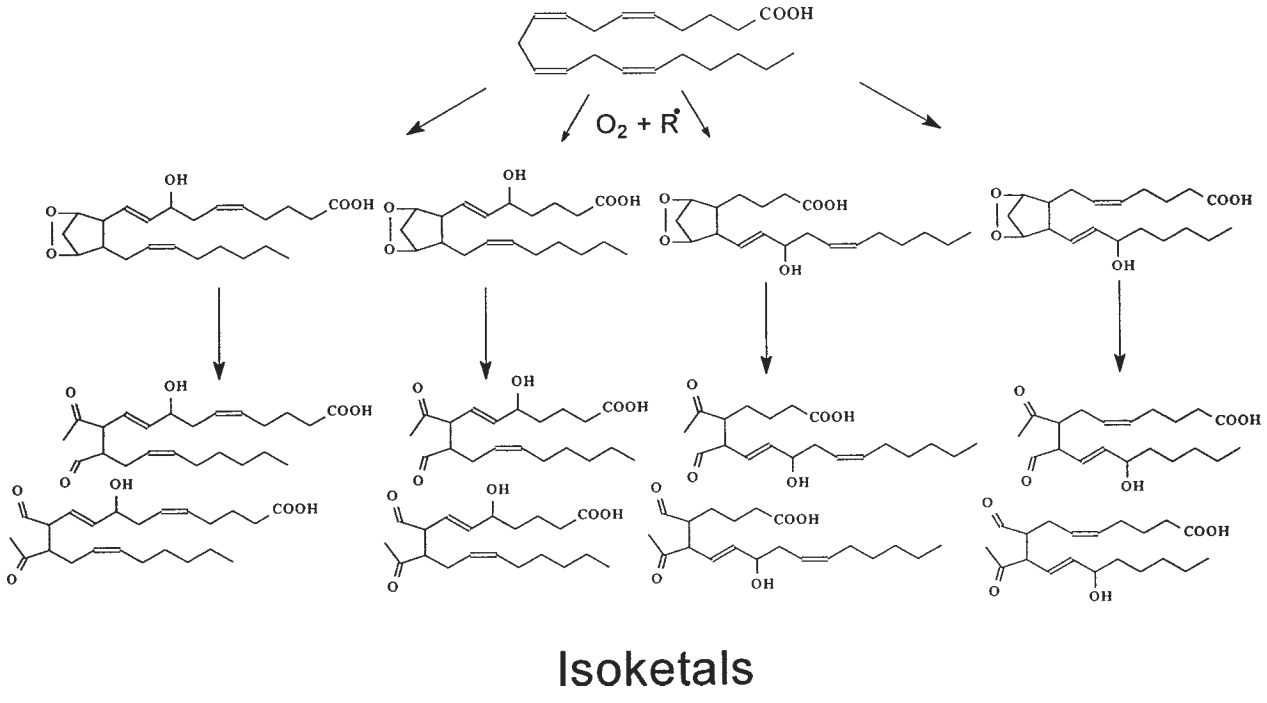

Fig. 1. Formation of isoketals. Oxidation of arachidonic acid generates a series of bicyclic endoperoxide intermediates that undergo rearrangement to form a series of γ-ketoaldehyde stereo- and regio-isomers termed isoketals.

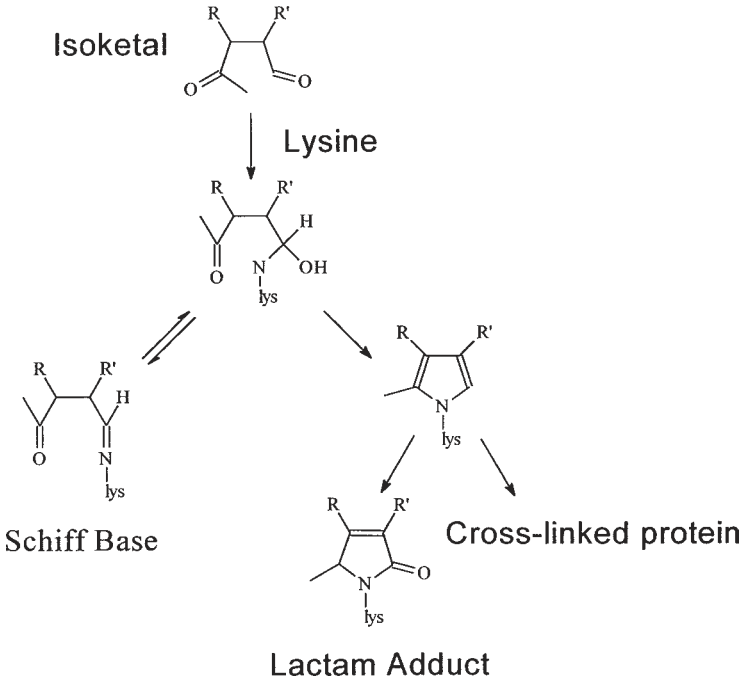

Fig. 2. Formation of lysyl-isoketal adducts. Isoketals rapidly react with the ε-amine of lysine and lysyl residues on proteins to form Schiff base adducts, lactam adducts, and crosslinks.

adducts. Enzymatic digestion of proteins is necessary because we found that adducts are not stable to acid-hydrolysis procedures commonly used to hydrolyze proteins for amino acid analysis. Stable isotope dilution LC–ESI/MS-MS currently represents the most accurate method for the quantification of IsoK adducts. This methodology also has the advantage that it can measure both Schiff base and lactam adducts, which provide different information related to the kinetics of their formation and disappearance. The initial adduct formed is the Schiff base. However, this is reversible, and then proceeds through a pyrrole, which undergoes facile autoxidation to form stable lactam adducts. During ongoing oxidation, the Schiff base is continually formed, however, upon cessation of the oxidation, it disappears over time, whereas the lactam adducts accumulate *(4)*. Therefore, measurement of Schiff base adducts provides a useful index of acute ongoing oxidative stress, whereas measurement of levels of lactam adducts provides a more sensitive indicator of chronic oxidant injury. The unstable Schiff base adduct can be measured after stabilization by reduction with $NaBH_4$.

2. MATERIALS

1. Preparation of [^{13}C]- and [^{3}H]-labeled lysine. Dissolve 22.3 mg of [U-$^{13}C_6$] lysine (Cambridge Isotope Laboratories, Andover, MA) in 30 mL phosphate buffer (Sigma, St. Louis, MO). To 1 mL of the 3.3 m*M* [$^{13}C_6$]-lysine stock, add 10^7 dpm of [^{3}H] lysine (NEN Life Science, Boston, MA). The exact amount of weight and label of the lysines are recorded.
2. IsoK is synthesized according to Salomon et. al. *(9)* and a stock solution in chloroform (1 m*M*) is prepared.
3. As an alternative to IsoK synthesis, IsoK is generated by conversion of arachidonic acid into IsoK by prostaglandin H_2 synthetase-1 (PGHS-1) (Oxford Biomedical Research, Oxford, MI) *(10)*. Prepare arachidonic acid at 10 mg/mL in EtOH. Prepare 10 m*M* phenol by dissolving 18.8 mg phenol in 20 mL water. Prepare 0.5 m*M* hematin by adding 3.17 mg porcine hematin (Sigma) in 10 mL dimethyl sulfoxide (DMSO) and sonicating until dissolved (about 30 min).
4. Prepare 100 m*M* sodium borohydride by dissolving 3.7 mg sodium borohydride in 1 mL dimethyl formamide. Prepare fresh.
5. Dissolve 25 mg of butylated hydroxyl toluene (BHT) and 250 mg triphenylphosphine (TPP) in 500 mL EtOH. Chill on ice.
6. Dissolve 25 mg of BHT and 250 mg TPP in 500 mL Folch Solution (2:1 $CHCl_3$:MeOH). Chill on ice.
7. Dissolve 25 mg BHT and 250 mg TPP in 500 mL MeOH. Chill on ice.
8. Prepare 0.4 *N* potassium hydroxide in water.
9. 10X Phosphate-buffered saline (PBS) pH 7.4 (Gibco BRL, Gaithersburg, MD) or other nonamine containing pH 7.4 buffer.
10. Aminopeptidase M from porcine kidney (Calbiochem, San Diego, CA) with specific activity of approx 65 U/mL.
11. Pronase protease (*Streptomyces griseus*) (Calbiochem), dissolved at 100 mg/mL in water. Make fresh each time.
12. 1 g and 60 mg Oasis HLB cartridges (Waters, Milford, MA).
13. Macrosphere RP 300 C18 5u 250 × 4.6 mm i.d. HPLC column (Alltech). Column must be end-capped.
14. Inertsil C8 5 × 1 mm i.d. RP-HPLC column (Micro-Tech Scientific, Sunnyvale, CA). Column must be end-capped.
15. HPLC Solvent A: Make up 1 L of 20 m*M* ammonium acetate (NH_4OAc) by adding 1.540 g of NH_4OAc to 1 L of HPLC-grade water. To 750 mL of 20 m*M* NH_4OAc, add 750 μL of glacial acetic acid. Filter and degas.
16. HPLC Solvent B: To 250 mL of 20 m*M* NH_4OAc, add 250 mL HPLC-grade methanol and 500 μL glacial acetic acid. Filter and degas.
17. HPLC Solvent C: To 20 mL of 20 m*M* NH_4OAc, add 60 mL HPLC-grade water, 720 mL of HPLC grade methanol, and 80 μL of glacial acetic acid. Filter and degas.
18. HPLC Solvent D: Prepare 5 m*M* NH_4OAc by dissolving 192.5 mg NH_4OAc in 500 mL HPLC-grade water. To 450 mL of 5 m*M* NH_4OAc, add 50 mL HPLC-grade acetonitrile, and 500 μL glacial acetic acid. Filter and degas.

19. HPLC Solvent E: To 50 mL of 5 m*M* NH_4OAc, add 450 mL HPLC-grade acetonitrile, and 500 μL glacial acetic acid. Filter and degas.
20. Biological sample to be assayed for IsoK adducts. After harvesting, sample can be used immediately or snap-frozen in liquid nitrogen and stored at –70°C. 500 mg or more (wet weight) of tissue or 5 mL of plasma is generally recommended. Adducts should be normalized to protein content or tissue weight, depending on the tissue and the appropriateness of the measurement. In order to determine the amount of digestive proteases to use, a rough estimate of the protein concentration to tissue weight is required, and can be obtained from the literature or experimentally.

3. EQUIPMENT

1. Blade homogenizer-PTA 10s generator (Brinkman Instruments), table-top centrifuge, analytical evaporation unit (such as Meyer N-Evap, Organomation), tank of nitrogen, microcentrifuge, 37°C water bath.
2. HPLC instrument with fraction collector.
3. Triple quadrupole mass spectrometer (such as Finnigan TSQ-7000) equipped with a standard API-1 electrospray ionization source outfitted with a 100 μm I.D. deactivated fused silica capillary.

4. METHODS

1. Preparation of [$^{13}C_6$] lactam adduct standard (LTM STD) and [$^{13}C_6$] reduced Schiff base adduct standard (RSB STD). Dry 250 μL IsoK stock solution under N_2, then resuspended in 10 μL methanol. Add 175 μL phosphate buffer and 75 μL of [^{3}H]/[$^{13}C_6$]-lysine solution and mix well. Incubate at 37°C for 4 h. Alternatively, to prepare standards using PGHS-1, mix 75 μL of [^{3}H]/[$^{13}C_6$]-lysine solution, 12.5 μL phenol, and 150 μL (~200 U) of PGHS-1 and incubate at 37°C for 5 min. Then add 12.5 μL hematin for at least 1 min at 37°C. Then add 10 μL arachidonic acid. Incubate at 37°C for 4 h. Purify LTM STD and RSB STD. Add 26 μL of 100 m*M* $NaBH_4$ to reaction mixture. Incubate at room temperature for 30 min. Neutralize pH using 10X PBS solution. Prequilibrate a 60 mg Oasis column with 1 mL methanol and then 1 mL water. Reaction mixture is loaded onto column, then washed with 1 mL water and eluted with 1 mL methanol. The eluant is dried to less than 100 μL volume under nitrogen, and 1 mL of HPLC solvent A is added. The eluant is injected into C18 reverse phase (RP)-HPLC gradient system at 1 mL/min beginning at 100% HPLC solvent A for 10 min, then a gradient ramp to 100% HPLC solvent B over 10 min, and held at 100% B for an additional 50 min. One min fractions are collected and 10 μL of each fraction counted by liquid scintillation. RSB STD elutes at approx 40 min and LTM STD elutes in two peaks at approx 55 min and 60 min. The presence of standard should be confirmed by LC–ESI/MS-MS as described in step 11. Combine the two LTM STD peaks. Calculate the ng RSB STD or LTM STD/μL as [^{3}H]-dpm in standard fraction/μL) × (ng [$^{13}C_6$]-lysine added/dpm of [^{3}H] lysine added).

2. Sample workup. Solid sample tissue for determination is weighed as quickly as possible to minimize exposure to air. Tissue is then placed in 20 mL of ice-cold ethanol solution containing TPP and BHT for each gram of sample tissue. Tissue is homogenized using blade homongenizer or Dounce homogenizer. For plasma or other liquid samples, 20 mL of ice cold ethanol solution is added per mL sample.
3. Homogenate is centrifuged at 2000*g* for 10 min at 4°C. For determination of free IsoK only, proceed to step 6. For determination of total (esterified and free) IsoK, add 1 mL methanol solution and 1 mL 0.4 *N* potassium hydroxide solution for each 50 mg of protein in sample. Incubate at room temperature for two h.
4. After base hydrolysis, add 20 mL of ethanol solution, vortex, and centrifuge at 2000*g* for 10 min at 4°C.
5. Discard supernatant, add 20 mL Folch solution, resuspend pellet, and centrifuge at 2000*g* for 5 min. Discard supernatant, add 20 mL methanol, resuspend pellet, and centrifuge at 2000*g* for 5 min. Resuspend in 3 mL PBS for each mg protein.
6. Add 10 ng each of RSB STD and LTM STD to sample. For samples with very small amounts of IsoK, less standard should be used to ensure that the sample peak area is at least 10% of the standard peak area.
7. Heat sample to 95°C for 10 min. Allow to cool to room temperature. Add 1 mg of Pronase for each mg of protein in sample. Incubate at 37°C for 24 h while shaking.
8. Add 1 μL of aminopeptidase *M* for each mg protein in sample. Incubate at 37°C for 24 h while shaking.
9. Sample is loaded on appropriately sized Oasis column. For tissue where starting protein is greater than 200 mg, at least one 1 g Oasis column is required. Oasis column is prequilibrated using 10 mL methanol, then 10 mL water. Sample is loaded and then washed with at least 10 mL water. Sample is eluted with 10 mL of methanol. For tissue where starting protein is less than 200 mg, a 60 mg Oasis column is used, as in step 1.
10. Dry eluate under nitrogen until less than 100 μL remains. Add 1 mL of HPLC solvent A. Inject the eluant into C18 RP-HPLC gradient system at 1 mL/min beginning at 100% HPLC solvent A, then ramp gradient to 40% C over 5 min, followed by a second gradient ramp to 100% C over the next 15 min, then held at 100% C for an additional 12 min. Fractions are collected at 1-min intervals and 100 μL of each fraction is counted by liquid scintillation. Fractions containing radioactivity are combined and dried under nitrogen until only about 20 μL remains. An equivalent volume of methanol is added.
11. Sample is then analyzed by LC–ESI/MS-MS. Liquid chromatography is performed using C8 HPLC column at 50 μL/min starting at 100% HPLC Solvent D to 100% Solvent E over 7 min and held at 100% Solvent E for an additional 2 min. We use a Finnigan TSQ-7000 (San Jose, CA) triple quadrupole mass spectrometer equipped with a standard API-1 electrospray ionization source outfitted with a 100 μm I.D. deactivated fused silica capillary. Nitrogen is used for both the sheath and auxiliary gas. The sheath gas is operated at a

pressure of 60 psi and the auxiliary gas flow is set to 10 units. The mass spectrometer is operated in the positive ion mode and the electrospray needle is maintained at 4.0 kV. The heated capillary is operated at 20 V and 200°C and the tube lens voltage is set to 80 V. The mass spectrometer is operated in the selected reaction monitoring (SRM) mode. Ions are collisionally activated at an indicated argon pressure of 2.5 mT. To improve sensitivity, the instrument resolution is degraded so that the peak width of the precursor ion at one-half maximum height is approx 2.4 amu, and the peak width of the product ion at one-half maximum height is approx 1.45 amu. Mass transitions at the specified collision energy (*m/z* 479.4 to *m/z* 84.1, –36 eV and *m/z* 479.4 to *m/z* 332.1, –28 eV), (*m/z* 485.4 to *m/z* 89.1, –36eV and *m/z* 485.4 to *m/z* 332.1, –28 eV), (*m/z* 467.4 to *m/z* 321.1, –28 eV), and (*m/z* 473.4 to *m/z* 32.1, –28 eV) are monitered for lysyl-lactam adduct, LTM STD, reduced Schiff base adduct, and RSB STD, respectively.

5. ANALYSIS

Reduced Schiff base adducts elute as a single peak in LC–ESI/MS-MS at R_T 6.1 min (Fig. 3A). The amount of Schiff Base adduct in the sample is calculated as (area of *m/z* 467.4 to *m/z* 321.1 peak/area of *m/z* 473.4 to *m/z* 321.1 peak) × (ng RSB STD added in step 6). The lactam adducts elute as a doublet at R_T 6.3 min (Fig. 3B). To confirm that peaks arise from IsoKs and not from non-specific sample contaminants, peaks for *m/z* 479.4 to *m/z* 84.1 are compared to those for *m/z* 479.4 to *m/z* 332.1. The efficiency of the *m/z* 479.4 to *m/z* 332.1 product formation is about ten times lower than that of the *m/z* 479.4 to *m/z* 84.1 product, so that in samples with very low amounts of IsoKs, peaks in this channel may be below the level of detection. The amount of lactam adducts in the sample is calculated as (area of appropriate *m/z* 479.4 to *m/z* 84.1 peaks/area of the *m/z* 485.4 to *m/z* 89.1 peak) × (ng LTM STD added in step 6). Isotopic contamination from the [$^{13}C_6$][^{3}H] lysine standards at the *m/z* 479.4 and 467.4 is generally about 1% of the *m/z* 485.4 and 473.4, so that standards alone should be injected on LC–ESI/MS-MS to determine the appropriate background subtraction.

6. DISCUSSION

Elucidation of the potential role for IsoKs in the pathogenesis of disease requires accurate quantification of adduct formation in control vs diseased tissue. A finding that IsoK protein adducts are increased in diseased tissue forms the basis for studies exploring the functional consequences of adduct formation in vitro. If there is a specific protein of interest, this protein may be immunoprecipitated to determine if that protein contains IsoK adducts.

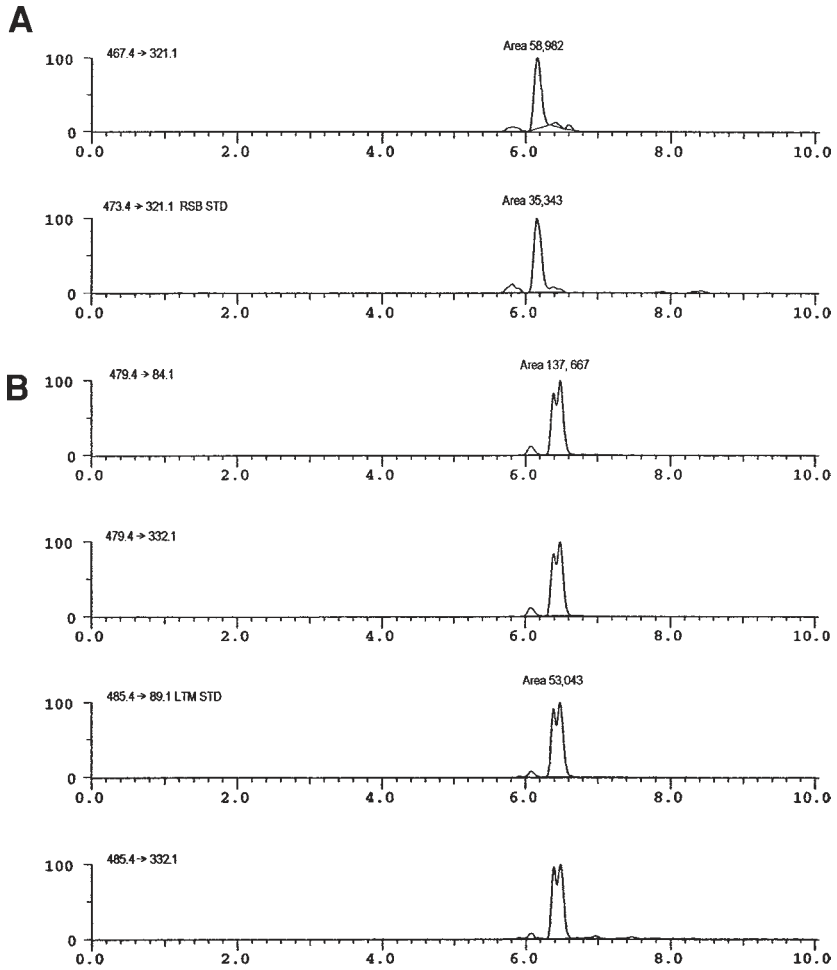

Fig. 3. Stable isotope dilution LC—ESI/MS-MS for lysyl-isoketal adducts. **(A)** Multiple reaction monitoring chromatographs of the mass transitions from 467.4 to 321.1 and 473.4 to 321.1 for the measurement of lysyl-reduced Schiff base adducts and [^{13}C] lysyl-reduced Schiff base internal standard, respectively. **(B)** Multiple reaction monitoring chromatographs of the mass transitions from 479.4 to 84.1 and to 332.1 and from 485.4 to 89.1 and 332.1 for the measurement of lysyl-lactam adduct and [^{13}C] lysyl-lactam internal standard, respectively.

The protein can then be adducted with IsoK in vitro to assess whether this alters the function of the protein. At present, we are working on methodology to identify unknown proteins that contain IsoK adducts by developing antibodies to IsoK adducts, which can be used for Western-blot analysis,

and also using mass spectrometric methods. However, this methodology is currently only in the developmental stages.

It should be mentioned that the level of reduced Schiff base and lactam adducts measured are an underestimate of the total adducts present in tissues. This is because IsoKs exhibit a unique proclivity to form protein cross-links, which are resistant to enzymatic hydrolysis. Currently, there is no approach available to measure IsoK adducts in cross-linked proteins.

In addition to elucidation of a potential role of IsoKs in oxidant injury in disease states, measurement of both Schiff base and lactam adducts may provide both temporal and spatial information about lipid peroxidation events in disease. As mentioned, a finding of increased levels of Schiff base adducts suggests ongoing acute lipid peroxidation whereas a finding that lactam adducts are selectively increased over Schiff base adducts suggests a more chronic level of ongoing lipid peroxidation. In addition, measurement of IsoK adducts may eventually provide spatial information that localizes lipid peroxidation. Reactive aldehydes that are formed as scission products of lipid peroxidation, e.g., HNE and malondialdehyde (MDA), are much less reactive than IsoKs, allowing them to diffuse from their site of formation. However, IsoKs, owing to their remarkable reactivity, are rapidly trapped by their immediate reaction with adjacent proteins at sites where they are formed. Therefore, as methodology becomes available to identify specific proteins than contain IsoK adducts, it may provide an insight into the subcellular localization of lipid peroxidation.

REFERENCES

1. Brame, C. J., Salomon, R. G., Morrow, J. D., and Roberts, L. J. 2nd. (1999) Identification of extremely reactive gamma-ketoaldehydes (isolevuglandins) as products of the isoprostane pathway and characterization of their lysyl protein adducts. *J. Biol. Chem.* **274,** 13,139–13,146.
2. Bernoud-Hubac, N., Davies, S. S., Boutaud, O., Montine, T. J., and Roberts, L. J. 2nd. (2001) Formation of highly reactive gamma-ketoaldehydes (neuroketals) as products of the neuroprostane pathway. *J. Biol. Chem.* **276,** 30,964–30,970.
3. Iyer, R. S., Ghosh, S., and Salomon, R. G. (1989) Levuglandin E2 crosslinks proteins. *Prostaglandins* **37,** 471–480.
4. Boutaud, O., Brame, C. J., Salomon, R. G., Roberts, L. J. 2nd, and Oates, J. A. (1999) Characterization of the lysyl adducts formed from prostaglandin H2 via the levuglandin pathway. *Biochemistry* **38,** 9389–9396.
5. Murthi, K. K., Salomon, R. G., and Sternlicht H. (1990) Levuglandin E2 inhibits mitosis and microtubule assembly. *Prostaglandins* **39,** 611–622.
6. Foreman, D., Levison, B. S., Miller, D. B., and Salomon, R. G. (1988) Anhydrolevuglandin D2 inhibits the uterotonic activity of prostaglandins F2 alpha and D2. *Prostaglandins* **35,** 115–122.

7. Hoppe, G., Subbanagounder, G., O'Neil, J., Salomon, R. G., and Hoff, H. F. (1997) Macrophage recognition of LDL modified by levuglandin E2, an oxidation product of arachidonic acid. *Biochim. Biophys. Acta.* **1344,** 1–5.
8. Schmidley, J. W., Dadson, J. , Iyer, R. S., and Salomon, R. G. (1992) Brain tissue injury and blood-brain barrier opening induced by injection of LGE2 or PGE2. *Prostaglandins Leukot. Essent. Fatty Acids* **47,** 105–110.
9. Salomon, R. G., Miller, D. B., Raychaudhuri, S. R., Avasthi, K., Lai, K., and Levison, B. S. (1984) *J. Am. Chem. Soc.* **106,** 8296–8298.
10. Boutaud, O., Brame, C. J., Chaurand, P., et al. (2001) Characterization of the lysyl adducts of prostaglandin H-synthases that are derived from oxygenation of arachidonic acid. *Biochemistry* **40,** 6948–6955.

16

Bioassay of 2'-Deoxyguanosine/8-Hydroxy-2'-Deoxyguanosine by HPLC With Electrochemical/ Photodiode Array Detection

Kelly S. Williamson, Kenneth Hensley, Quentin N. Pye, Scott Ferrell, and Robert A. Floyd

1. INTRODUCTION

Living organisms exposed to reactive oxygen species (ROS) on a continual basis will promote oxidative stress, thereby forming mutations in DNA and damage to cells. As an end result, it has been shown that modified forms of damaged DNA can lead to mutagenesis, carcinogenesis, degenerative diseases, cancer, diabetes, and aging *(1–16)*. With this in mind, the DNA nucleoside 2´-deoxyguanosine (dG) undergoes a hydroxylation reaction at the C-8 position to yield a useful biomarker, 8-hydroxy-2´-deoxyguanosine (8-OH-dG) that has been employed to measure oxidative damage as illustrated in Fig. 1. Other disease/nondisease related events resulting in the formation of this oxidation product, 8-OH-dG, are reported by Möller et al. (5). There have been a wide variety of assays used in the detection of free radical-mediated DNA oxidation products such as: high performance liquid chromatography coupled with electrochemical and ultraviolet detection (HPLC–ECD and HPLC–UV) *(2–9,12,13,16–21,24)*, liquid and gas chromatography-mass spectrometry (LC–MS and GC–MS) *(4,10,12,22–27)*, postlabeling techniques (^{32}P-HPLC *[5]*, ^{32}P-TLC [thin-layer chromatography] *[30–33]*, or fluorescent probe-HPLC *[34]*), antibody assays *(35–37)*, and lastly, HPLC using tandem mass spectrometry (HPLC–MS-MS) *(1,23,25,26,28,29)*. R. A. Floyd, H. Kasai, and others *(9,17,18,38,39)* were some of the early pioneers for accurately measuring DNA oxidation adducts

From: *Methods in Pharmacology and Toxicology: Methods in Biological Oxidative Stress*
Edited by: K. Hensley and R. A. Floyd

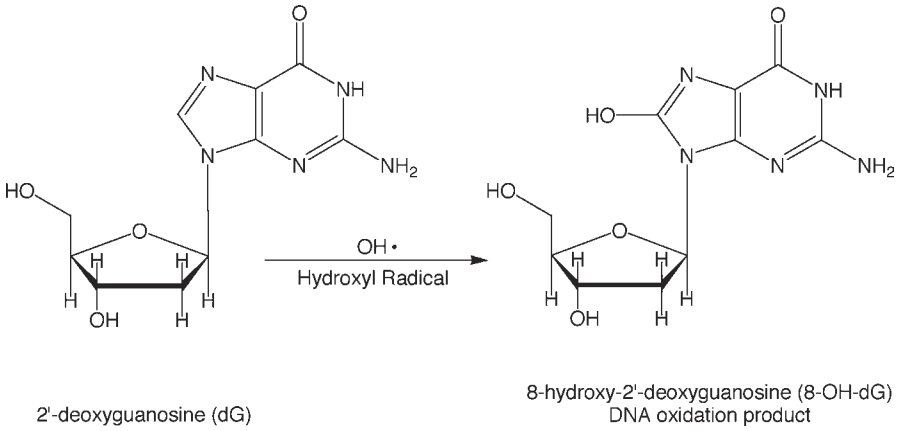

Fig. 1. The hydroxylation reaction of dG to yield the 8-OH-dG oxidation product as discussed in the text.

using HPLC in series with electrochemical, spectrophotometric, or fluorometric detection in order to determine the level of oxidative DNA damage in cells. The focus of this publication is to demonstrate the following methods: (A) The isolation and digestion of salmon-sperm DNA (ssDNA) treated with methylene blue (MB) plus light in order to generate oxidative stress (singlet oxygen is produced as reported by Schneider et al. *[40]*) forming the biomarker, 8-OH-dG. (B) Employing HPLC–ECD-PDA (photodiode array) as a bioanalytical technique in the characterization and quantification of DNA homologs, such as 8-OH-dG (hydrolyzed form) and dG (native form) using the aforementioned light-exposed, MB-treated ssDNA. A dose-response curve depicting the formation levels of 8-OH-dG/10^5 dG vs increasing MB concentrations is also illustrated.

2. MATERIALS

Unless otherwise stated, all reagents and HPLC-grade solvents were purchased from Fisher Scientific (Pittsburgh, PA), Sigma-Aldrich Chemical Company (St. Louis, MO), or Roche Molecular Biochemicals (Indianapolis, IN).

1. ssDNA from salmon testes (cat. no: D 1626, Type III sodium salt, Sigma-Aldrich).
2. DNA isolation reagents, MB light exposure conditions, and equipment: Refer to the protocol described by Schneider et al. *(40)* and Sambrook et al. *(41)* for additional information about Subheading 3., Methods, steps 1–3, regarding isolating the light-exposed, MB-treated ssDNA.

Table 1
Optimal Cell Potentials for Electrochemical Array Detection of DNA Adducts Using a 12-Channel Instrument

Cell number	Cell potential (mV)	Cell number	Cell potential (mV)
1	200	7	650
2	250	8	675
3	300	9	700
4	350[a]	10	750[b]
5	400	11	825
6	500	12	900

[a]Optimal cell potential for 8-OH-dG.
[b]Optimal cell potential for dG.

3. DNA digestion reagents and equipment: refer to the procedure illustrated by Maidt and Floyd *(9)*, in Subheading 3., Methods, step 4 for reagents/equipment used in digesting the light-exposed, MB-treated ssDNA.
4. Methylene blue: prepared at a 2 m*M* concentration using millipore-filtered water.
5. Vortex-Genie (Scientific Industries, Inc., Bohemia, NY).
6. Beckman Coulter™ Du® 640B UV Spectrophotometer (Beckman Coulter, Fullerton, CA).
7. Mobile phase: 50 m*M* sodium acetate, 8% HPLC-grade methanol, 50 µL/L of the bacteriocide, Reagent MB (ESA, Chelmsford, MA), pH 5.1.
8. Beckman microfuge 11 (Beckman Coulter, Fullerton, CA).
9. 13-mm, 0.2 µm Pall Gelman® LC PVDF acrodisk syringe filters.
10. Standards. dG was purchased from Sigma-Aldrich and 8-OH-dG (Cayman Chemical Co, Ann Arbor, MI) were prepared at a stock concentrations of 1 m*M* in millipore-filtered water, and checked by UV spectrophotometry using a molar extinction coefficient of 12,300 $M^{-1}cm^{-1}$ at 247 nm for dG and 8-OH-dG, respectively *(9)*.
11. HPLC-ECD/PDA equipment: ESA Model 5600 CoulArray HPLC (ESA, Chelmsford, MA) that is equipped with a binary gradient elution system (only an isocratic system was needed), 84-vial autosampler with a column oven, and 12 electrochemical cells operating in the oxidative mode. Table 1 lists the optimal cell potentials for chromatographic analysis using HPLC–ECD/PDA detection. The PDA used was a Waters 996 PDA detector (Waters Corporation, Milford, MA) equipped with its own data-acquisitioning system and connected upstream from the electrochemical detector. The software used to acquire and process chromatograms for this application was the Millenimum 32, version 2.10. The dG/8-OH-dG standards used to determine the assignment of chromatographic peaks, as well as the optimal oxidation potential for dG (R_t: ~14.0 min) and 8-OH-dG (R_t: ~19.0 min) were 750 mV and 350 mV, respectively. The optimal wavelength for each DNA product (dG and 8-OH-dG) was measured at 247 nm.

3. METHODS

1. The MB-treated ssDNA (exposed to light) preparation/quantification method is as follows in steps 1–3. (Refer to the protocol illustrated by Schneider et al. *[40]* and Sambrook et al. *[41]* for additional information.) ssDNA was dissolved in millipore-filtered water at a concentration of 1 mg/mL (5 mL final volume) and was stirred overnight at ambient temperature to help solubilize the DNA. Fragmentation of the ssDNA solution prior to exposure of MB plus light was accomplished by rapidly passing it 20 times through a 18-gage needle/syringe in order to shear the ssDNA. This enables the MB to intercalate throughout the DNA for maximum exposure to dG as well as for optimal production of 8-OH-dG.
2. Formation of 8-OH-dG was initiated by transferring the prepared reagents (230 µL of ssDNA (1 mg/mL), 70 µL millipore-filtered water, and 100 µL of 4X MB solution) into a 24-well plate to yield a final volume of 400 µL. All samples were done in triplicate and in one-half serial dilutions. The final concentrations consisting of MB were 0 µ*M*, 0.625 µ*M*, 1.25 µ*M*, 2.50 µ*M*, 5.00 µ*M*, and 10.0 µ*M*, respectively. One ssDNA control was prepared, processed and analyzed in the same manner as the samples were but no MB was added for background determination. The microplate was placed on top of a pool of water supported by a glass plate and was held in place by surface tension. Light exposure time for the MB-treated ssDNA samples was 30 min, the distance between the samples/light source was approx 18 cm, and the light source used was a 100-W (Sylvania Tungsram E27, GE-Europe, Hungary) light bulb. For additional information regarding exposure conditions, refer to Schneider et al. *(40)*.
3. After the samples were exposed to 30 min of light, the samples were transferred from the microplate wells into labeled, 1.7-mL microfuge tubes. To each tube, 30 µL of 3 *M* sodium acetate and 400 µL of 4°C isopropyl alcohol was added. Precipitation of the samples was accomplished by inverting the microfuge tubes several times followed by vortex mixing. All of the samples were placed in the –20°C freezer for overnight storage. Light-exposed, MB-treated ssDNA samples were pelleted the following day by employing a high-speed microfuge for 15 min at approx 10,000*g*. After centrifugation, the supernatant was discarded. Light-exposed, MB-treated ssDNA pellets from each sample were allowed to air-dry at ambient temperature, and the pellets were reconstituted in TE buffer (10 m*M* Tris, 1 m*M* EDTA, pH 8.0) at a final volume of 250 µL and stored at –20°C prior to initiation of the digestion protocol depicted below in Subheading 3., Methods, step 4. Quantification of the isolated MB- treated ssDNA was obtained spectrophotometrically, as described by Maidt and Floyd *(9)*.
4. The light-exposed, MB-treated ssDNA digestion method is as follows. (Refer to the protocol illustrated by Maidt and Floyd *[9]* for additional information.) Because the DNA is already solubilized in TE buffer, aliquot known amounts (~200 µg of DNA) into a series of labeled centrifuge vials, add 25 µL of 0.50 *M* sodium acetate, pH 5.1, and 2.75 µL of 1 *M* $MgCl_2$. Heat the samples

at 100°C in water for approx 5 min to cause the DNA to become single-stranded, then immediately cool the samples on ice for 5 min. Add 10 µg of nuclease P_1 and incubate for 1 h at 37 °C. Aliquot out 8 µL of 1 *M* Tris base for each sample to manually adjust the pH to 7.8. Add 2 µL of alkaline phosphatase and incubate samples for 1 h at 37 °C. Lastly, precipitate the enzymes by aliquoting 4 µL of 5.8 *M* acetic acid, vortex mix briefly, and filter each sample thorough a 13-mm, 0.2-µm HPLC acrodisk LC PVDF syringe filter prior to HPLC–ECD/PDA analysis.

4. ANALYSIS

The optimized HPLC-ECD/PDA parameters used are as follows:

- Column: Microsorb-MV, C_{18}, 3 µm, 4.6 × 100 mm.
- Flow rate: 0.250 µL/min.
- Injection volume: 60 µL.
- Column temperature: ambient.
- Autosampler temperature: ambient.
- Run time/sample: 30 min.

All other chromatographic conditions were previously mentioned in the HPLC–ECD/PDA equipment section. DNA oxidation products were identified based on their respective retention times and the method quantitation limit (MQL) for the dG/8-OH-dG components were carried out by generating a series of calibration curves using a standard mix containing both adducts, prepared at concentrations ranging from 0.5 n*M*–1000 n*M*. The MQL was determined to be in the low femtomole levels by HPLC–ECD (dG/8-OH-dG) and low picomole levels by HPLC–PDA (dG/8-OH-dG). Linearity of each DNA congener was established and the regression coefficients were greater than 0.999 as shown in Fig. 2A,B. The DNA homologs were quantified by measuring the peak heights of the DNA samples relative to the peak heights of the standard calibration curve previously generated. Figures 3 and 4 depict a standard mix of a typical HPLC–ECD/PDA chromatogram of dG and its DNA oxidation product, 8-OH-dG. Figures 5 and 6 show representative sample HPLC–ECD/PDA chromatograms of the 10 µ*M* light-exposed, MB-treated ssDNA. As reported by Maidt and Floyd *(9)*, the 8-OH-dG content of the hydrolysated DNA can be depicted as the number of 8-OH-dG present per 100,000 normal deoxyguanosines. This was determined by dividing the concentration (n*M*) of 8-OH-dG vs the concentration (n*M*) of dG and multiplying by 100,000 dG residues. Therefore, an example calculation for 8-OH-dG per 100,000 dG in a 60 µL injection of light-exposed, MB-treated, hydrolyzed

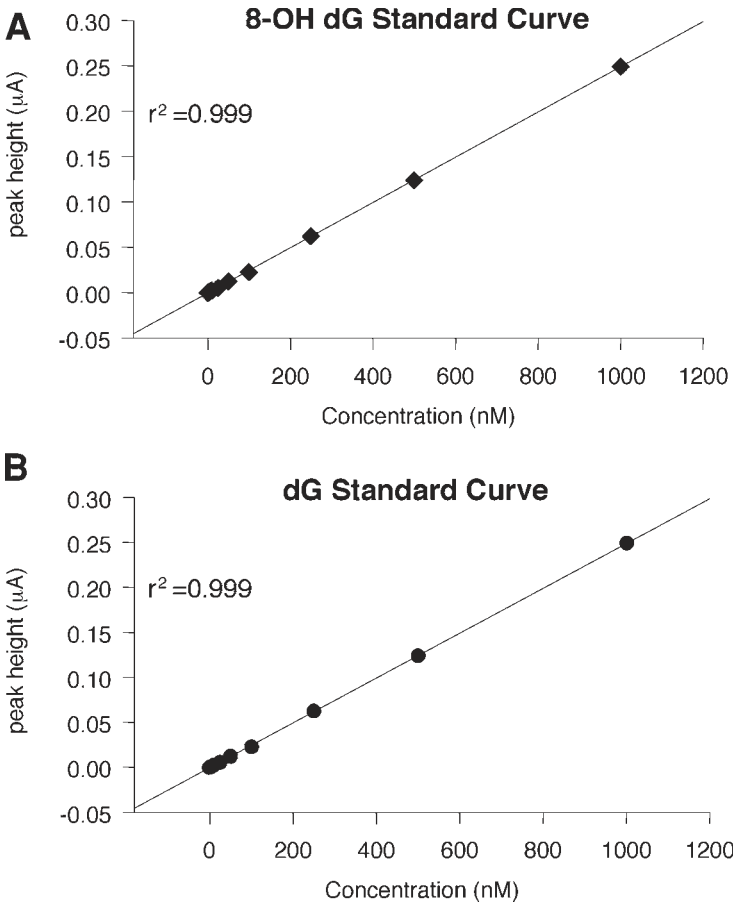

Fig. 2. **(A)** Representative calibration curve for 8-OH-dG via HPLC–ECD/PDA. **(B)** Representative calibration curve for dG via HPLC–ECD/PDA.

ssDNA cells is depicted in Equation (1) and the mean values for 8-OH-dG/10^5 dG are summarized in Table 2:

Sample: Vial replicate #1, ssDNA – 10 μ*M* MB

8-OH-dG: 1284 n*M*

dG: 30369 n*M* (Eq. 1)

1284 n*M*/30369 n*M* × 100,000 = 4228 (8-OH-dG/100,000 dG)

Table 2
Average Mean Calculation (Summarized) of Light-Exposed, MB-Treated ssDNA Samples Employed in Determining the Ratio 8-OH-dG/10^5 dG Residues by HPLC–ECD

Sample I.D.	MB concentration (μ*M*)	8-OH-dG/10^5 dG (avg mean)
Vial #1 (DNA Ctrl[a])	N/A	1113
Vial #1–3	0.00	1147
Vial #1–3	0.625	1805
Vial #1–3	1.25	2110
Vial #1–3	2.50	2846
Vial #1–3	5.00	3265
Vial #1–3	10.0	4382

[a]Only one DNA control sample without MB added was used for this project.

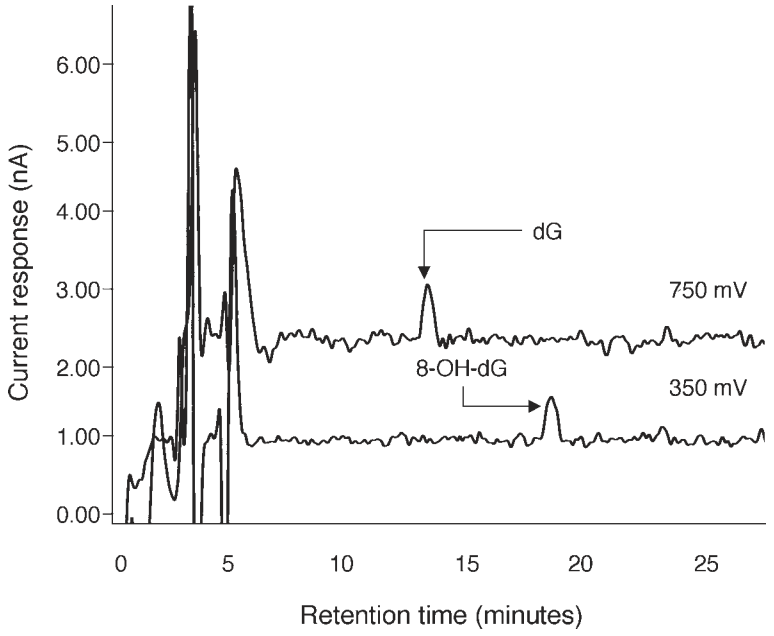

Fig. 3. Representative HPLC–ECD chromatogram of a 2.5 n*M* dG/8-OH-dG standard mix.

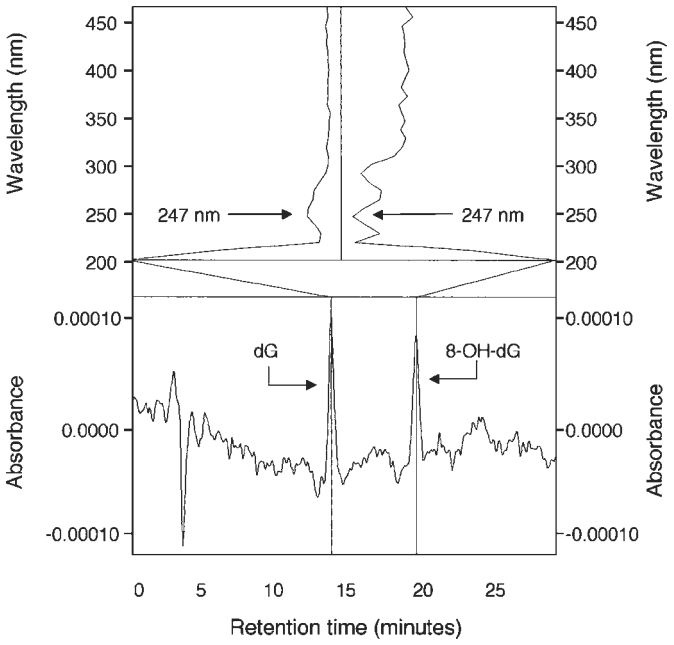

Fig. 4. Representative HPLC–PDA chromatogram of a 25 n*M* dG/8-OH-dG standard mix.

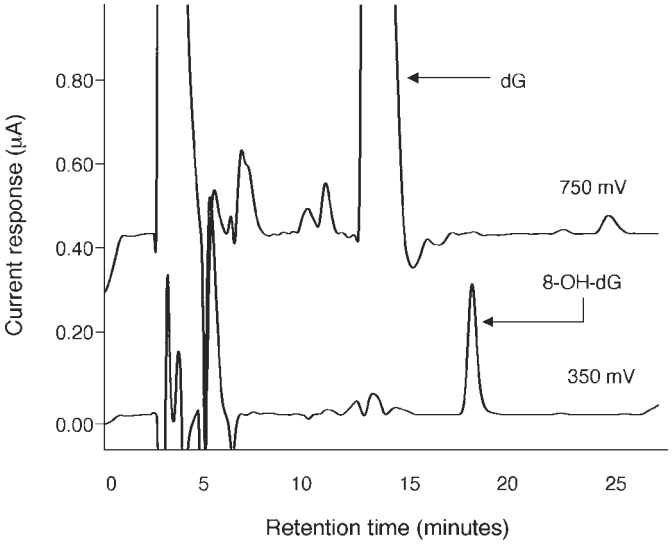

Fig. 5. Representative HPLC–ECD chromatogram of a 10 μ*M* light-exposed, MB-treated ssDNA sample.

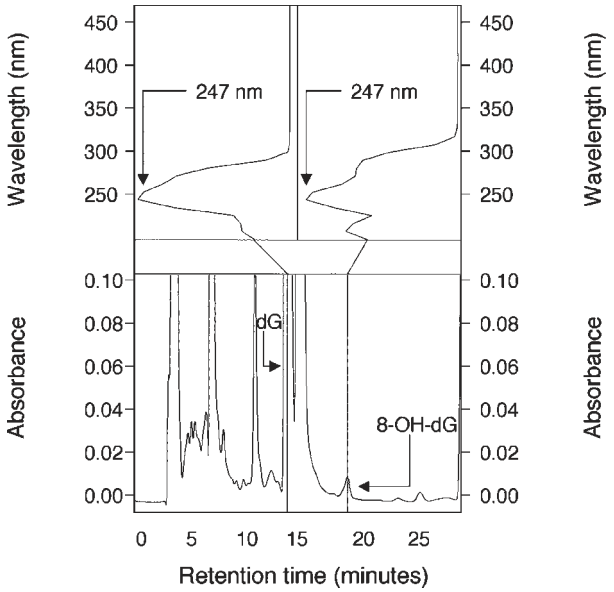

Fig. 6. Representative HPLC–PDA chromatogram of a 10 μ*M* light-exposed, MB-treated ssDNA sample.

5. DISCUSSION

For brevity's sake, only the HPLC–ECD results will be discussed and reported. The objectives of this publication were demonstrated by initiating oxidative stress using light-exposed, MB-treated ssDNA to form the biomarker, 8-OH-dG from dG. The protocols used in the formation, isolation, digestion, characterization, and quantitation of DNA congeners, 8-OH-dG/dG residues by HPLC-ECD/PDA are also reported. A dose-response curve depicted in Fig. 7 is based on the data in table II via HPLC-ECD and was generated for this project to clearly illustrate that as the 8-OH-dG/10^5 dG ratio increases, the MB concentration increases as the ssDNA is exposed to light. This bioanalytical technique is both sensitive and selective, however, HPLC–ECD is much more sensitive/specific than HPLC–PDA. Low femtomole levels can be easily attained by HPLC–ECD (dG/8-OH-dG), whereas samples quantified at the picomole levels by HPLC–PDA (dG/8-OH-dG) will enable the user some freedom and flexibility, but there are some limitations as well. Other bioanalytical methods previously mentioned in this chapter, have been used in the detection/quantification of 8-OH-dG and dG, however this bioassay still proves to be a reliable technique in the assessment of oxidative stress to cellular DNA.

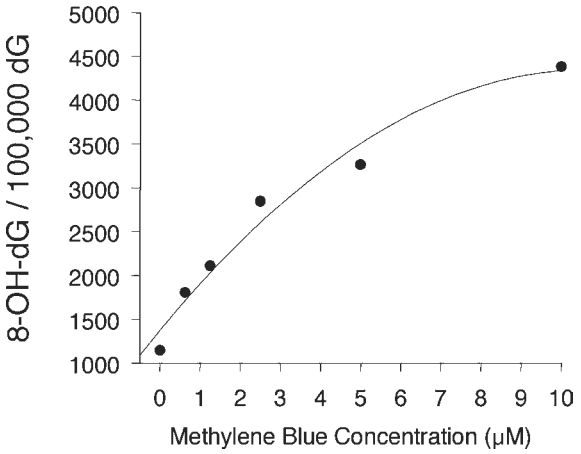

Fig. 7. Dose-response curve depicting the formation levels of 8-OH-dG/10^5 dG residues vs increasing MB concentrations employing light-exposed, MB-treated ssDNA.

ACKNOWLEDGMENTS

This work was supported by the National Institutes of Health (NIH NS35747) and the Oklahoma Center for the Advancement of Science and Technology (OCAST H967067).

REFERENCES

1. Podmore, I. D., Cooper, D., Evans, M. D., Wood, M., and Lunec, J. (2000) Simultaneous measurement of 8-oxo-2'-deoxyguanosine and 8-oxo-2'-deoxyadenosine by HPLC-MS/MS. *Biochem. Biophys. Res. Commun.* **277,** 764–770.
2. Halliwell, B. and Gutteridge, J. M. C. (1999) *Free Radicals in Biology and Medicine*, 3rd ed., Oxford University Press, Oxford, UK, pp. 388–393.
3. Beckman, K. B., Saljoughi, S., Mashiyama, S. T., and Ames, B. N. (2000) A simpler, more robust method for the analysis of 8-oxoguanine in DNA. *Free Radic. Biol. Med.* **29,** 357–367.
4. Douki, T. and Cadet, J. (1999) Modification of DNA bases by photosensitized one-electron oxidation. *Int. J. Radiat. Biol.* **75,** 571–581.
5. Möller, L., Hofer, T., and Zeisig, M. (1998) Methodological considerations and factors affecting 8-hydroxy-2'-deoxyguanosine analysis. *Free Radic. Res.* **29,** 511–524.
6. Loft, S., Deng, X. S., Tuo, J., Wellejus, A., Sorensen, M., and Poulsen, H. E. (1998) Experimental study of oxidative DNA damage. *Free Radic. Res.* **29,** 525–539.

7. Hofer, T. and Möller, L. (1998) Reduction of oxidation during the preparation of DNA and analysis of 8-hydroxy-2'-deoxyguanosine. *Chem. Res. Toxicol.* **11,** 882–887.
8. Möller, L. and Hofer, T. (1997) [^{32}P]ATP mediates formation of 8-hydroxy-2'-deoxyguanosine from 2'-deoxyguanosine, a possible problem in the ^{32}P-postlabeling assay. *Carcinogenesis* **18,** 2415–2419.
9. Maidt, M. L. and Floyd, R. A. (1996) in *Free Radicals: A Practical Approach.* (Punchard, N. A. and Kelly, F. J., eds.), Oxford University Press, London, 14, 201–209.
10. Douki, T., Delatour, T., Bianchini, F., and Cadet, J. (1996) Observation and prevention of an artefactual formation of oxidized DNA bases and nucleosides in the GC-EIMS method. *Carcinogenesis* **17,** 347–353.
11. Ames, B. N., Shigenaga, M. K., and Hagen, T. M. (1993) Oxidants, antioxidants, and degenerative diseases of aging. *Proc. Natl. Acad. Sci. USA* **90,** 7915–7922.
12. Ravanat, J.-L., Turesky, R. J., Gremaud, E., Trudel, L. J., and Stadler, R. H. (1995) Determination of 8-oxoguanine in DNA by gas chromatography-mass spectrometry and HPLC-electrochemical detection: overestimation of the background level of the oxidized base by the gas chromatography-mass spectrometry assay. *Chem. Res. Toxicol.* **8,** 1039–1045.
13. Haegele, A. D., Briggs, S. P., and Thompson, H. J. (1994) Antioxidant status and dietary lipid unsaturation modulate oxidative DNA damage. *Free Radic. Biol. Med.* **16,** 111–115.
14. Tesfamariam, B. (1994) Free radicals in diabetic endothelial cell dysfunction. *Free Radic. Biol. Med.* **16,** 383–391.
15. Hayakawa, M. and Kuzuya, F. (1990) Free radicals and diabetes mellitus. *Nippon Ronen Igakkai Zasshi.* **27,** 149–154.
16. Ramon, O., Wong, H.-K., Joyeux, M., Riondel, J., Halimi, S., Ravanat, J.-L., et al. (2001) 2'-deoxyguanosine oxidation is associated with the decrease in the DNA-binding activity of the transcription factor SP1 in liver and kidney from diabetic and insulin-resistant rats. *Free Radic. Biol. Med.* **30,** 107–118.
17. Floyd, R. A., Watson, J. J., Wong, P. K., Altmiller, D. H., and Rickard, R. C. (1986) Hydroxyl free radical adduct of deoxyguanosine: sensitive detection and mechanisms of formation. *Free Radic. Res. Commun.* **1,** 163–172.
18. Kasai, H., Tanooka, H., and Nishimura, S. (1984) Formation of 8-hydroxyguanine residues in DNA by x-irradiation. *Gann* **75,** 1037–1039.
19. Evans, M. D. (2000) Measurement of 8-oxo-2'-deoxyguanosine in cellular DNA by high performance liquid chromatography-electrochemical detection, in *Measuring In Vivo Oxidative Damage: A Practical Approach.* (Lunec, J. and Griffiths, H. R., eds.), Wiley, NY, pp. 53–61.
20. Helbock, H. J., Beckman, K. B., Shigenaga, M. K., Walter, P. B., Woodall, A. A., et al. (1998) DNA oxidation matters: The HPLC-electrochemical detection assay of 8-oxo-deoxyguanosine and 8-oxo-guanine. *Proc. Natl. Acad. Sci. USA* **95,** 288–293.
21. Shigenaga, M. K., Aboujaoude, E. N., Chen, Q., and Ames, B. N. (1994) Assays of oxidative DNA damage biomarkers of 8-oxo-2'-deoxyguanosine and 8-oxo-

guanine in nuclear DNA and biological fluids by high-performance liquid chromatography with electrochemical detection. *Methods Enzymol.* **234,** 16–33.
22. Halliwell, B. and Dizdaroglu, M. (1992) The measurement of oxidative damage to DNA by HPLC and GC/MS techniques. *Free Radic. Res Commun.* **16,** 75–87.
23. Serrano, J., Palmeria, C. M., Wallace, K. B., and Kuehl, D. W. (1996) Determination of 8-hydroxydeoxyguanosine in biological tissue by liquid chromatography/electrospray ionization-mass spectrometry/mass spectrometry. *Rapid Commun. Mass Spectrom.* **10,** 1789–1791.
24. Douki, T., Delatour, T., Paganon, F., and Cadet, J. (1996) Measurement of oxidative damage at pyrimidine bases in γ-irradiated DNA. *Chem. Res. Toxicol.* **9,** 1145–1151.
25. Ravanat, J.-L., Duretz, B., Guiller, A., Douki, T., and Cadet, J. (1998) Isotopic dilution high-performance liquid chromatography-electrospray tandem mass spectrometry assay for the measurement of 8-oxo-7,8-dihydro-2'-deoxyguanosine in biological samples. *J. Chromatogr. B.* **715,** 349–356.
26. Renner, T., Fechner, T., and Scherer, G. (2000) Fast quantification of the urinary marker of oxidative stress 8-hydroxy-2'-deoxyguanosine using solid-phase extraction and high-performance liquid chromatography with triple-stage quadruple mass detection. *J. Chromatogr. B.* **738,** 311–317.
27. Dizdaroglu, M. (1994) Chemical determination of oxidative DNA damage by gas chromatography-mass spectrometry. *Methods Enzymol.* **234,** 3–16.
28. Poulsen, H. E., Weimann, A., and Loft, S., (1999) Methods to detect DNA damage by free radicals: Relation to exercise. *Proc. Nutr. Soc.* **58,** 1007–1014.
29. Kasai, H. (1997) Analysis of a form of oxidative DNA damage, 8-hydroxy-2'-deoxyguanosine, as a marker of cellular oxidative stress during carcinogenesis. *Mutat. Res.* **387,** 147–163.
30. Randerath, K., Reddy, M. V., and Gupta, R. C. (1981) ^{32}P-Labelling test for DNA damage. *Proc. Natl. Acad. Sci. USA* **78,** 6126–6129.
31. Gupta, R. C., Reddy, M. V., and Randerath, K. (1982) ^{32}P-Postlabelling analysis of nonradioactive aromatic carcinogen-DNA adducts. *Carcinogenesis* **3,** 1081–1092.
32. Beach, A. C. and Gupta, R. C. (1992) Human biomonitoring and the ^{32}P-postlabelling assay. *Carcinogenesis* **13,** 1053–1074.
33. Devanaboyina, U. and Gupta, R. C. (1996) Sensitive detection of 8-hydroxy-2'-deoxyguanosine in DNA by ^{32}P-postlabeling assay and the basal levels in rat tissue. *Carcinogenesis* **17,** 917–924.
34. Sharma, M., Box, H. C., and Paul, C. R. (1990) Detection and quantitation of 8-hydroxydeoxyguanosine 5'-monophosphate in X-irradiated calf thymus by fluorescent postlabeling. *Biochem. Biophys. Res. Commun.* **167,** 419–424.
35. Degan, P., Shigenaga, M. K., Park, E.-M., Alperin, P. E., and Ames, B. N. (1991) Immunoaffinity isolation of urinary 8-hydroxy-2'-deoxyguanosine and 8-hydroxy-guanine and quantitation of 8-hydroxy-2'-deoxyguanosine in DNA by polyclonal antibodies. *Carcinogenesis* **12,** 865–871.
36. Musaratt, J. and Wani, A.A. (1994) Quantitative immunoanalysis of promutagenic 8-hydroxy-2'-deoxyguanosine in oxidized DNA. *Carcinogenesis* **15,** 2037–2043.

37. Yarborough, A., Zhang, Y. J., Hus, T. M., and Santella, R. M. (1996) Immunoperoxidase detection of 8-hydroxydeoxyguanosine in aflatoxin B_1 treated rat liver and human mucosal cells. *Cancer Res.* **56,** 683–688.
38. Kasai, H. and Nishimura, S. (1986) Hydroxylation of guanine in nucleosides and DNA at the C-8 position by heated glucose and oxygen radical-forming agents. E*nviron. Health Perspect.* **67,** 111–116.
39. Kasai, H., Hayami, H., Yamaizumi, Z., Saito, H., and Nishimura, S. (1984) Detection and identification of mutagens and carcinogens as their adducts with guanosine derivatives. *Nucleic Acids Res.* **12,** 2127–2136.
40. Schneider, J. E., Jr., Pye, Q. N., and Floyd, R. A. (1999) Qβ bacteriophage photoinactivated by methylene blue plus light involves inactivation of its genomic RNA. *Photochem. Photobiol.* **70,** 902–909.
41. Sambrook, J., Fritsch, E. F., and Maniatis, T. (1989) *Molecular Cloning: A Laboratory Manual.* 2nd ed., Cold Spring Harbor Laboratory Press, Cold Spring Harbor, New York.

17

HPLC With Electrochemical Detection Analysis of 3-Nitrotyrosine in Human Plasma

Kelly S. Williamson, Kenneth Hensley, and Robert A. Floyd

1. INTRODUCTION

Analytical methodologies used to study protein nitration products in biological matrices have evolved over the last few years. Consequently, instrumental methods for measuring nitrated proteins and amino acids have been applied to a wide variety of sample matrices, including cerebral microvessels *(1)*, cell culture *(2)*, brain tissue/serum matrices *(3–7)*, atherosclerotic tissue *(8)*, and Alzheimer's diseased tissue *(3,9)*. The most commonly measured compounds of interest are 3-NO_2-Tyr (3-nitrotyrosine), as well as the tyrosine congeners such as those depicted in Fig. 1. High-performance liquid chromatography coupled with electrochemical detection (HPLC–ECD) is an extremely versatile and reliable chromatographic technique employed to facilitate selectivity and reproducibility of, and to accurately measure, tyrosine homologs. This bioanalytical assay enables the user to generate chromatograms based on its electrochemical rather than optical properties. The principles and methodologies of HPLC–ECD have been previously discussed *(1,11)*. The primary focus of this chapter is to discuss the bioanalytical methodologies and techniques used to analyze 3-NO_2-Tyr and its tyrosine variants in human plasma samples using direct HPLC–ECD. Other available bioanalytical methods used in the isolation, characterization, and quantitation of 3-NO_2-Tyr, and are discussed in greater detail by Herce-Pagliai et al. *(10)* and also by Hensley et al. *(11)*.

From: *Methods in Pharmacology and Toxicology: Methods in Biological Oxidative Stress*
Edited by: K. Hensley and R. A. Floyd

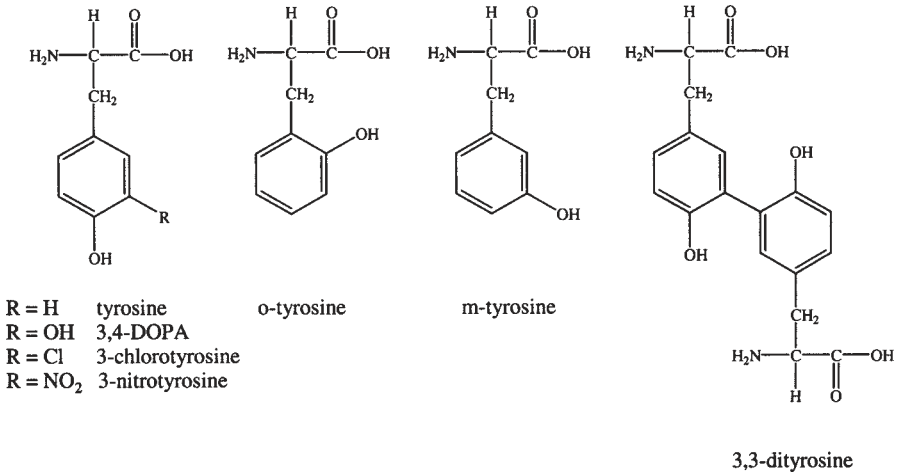

Fig. 1. The chemical structures of the different tyrosine derivatives discussed in the text.

2. MATERIALS

Unless otherwise stated, all reagents and HPLC-grade solvents were purchased from Fisher Scientific (Pittsburgh, PA) or Sigma Chemical Company (St. Louis, MO).

1. Aliquot 60 mL of trichloroacetic acid into a 100-mL container, add 40 mL of millipore-filtered water, mix well, and allow to cool before using.
2. IEC HN-SII benchtop centrifuge (International Equipment Co., Needham Hts., MA).
3. Vortex-Genie (Scientific Industries, Inc., Bohemia, NY).
4. 13-mm, 0.2-μm Pall Gelman® Acrodisks LC PVDF syringe filters.
5. Sonicator: Branson Sonifier Model 250, (Branson Ultrasonics Corp., Danbury, CT).
6. Mobile Phase:
   a. Reservoir A: 58 m*M* Lithium Phosphate, 0% HPLC-grade Methanol, 1 mL/L of a 3 mg/mL lithium dodecylsulfate (LDS) solution was added, pH 3.18, and 50 μL reagent MB was added as a bacteriocide (ESA, Chelmsford, MA) – for 1 L preparation.
   b. Reservoir B: 58 m*M* Lithium Phosphate, 20% HPLC-grade Methanol, 1 mL/L of a 3 mg/mL lithium dodecylsulfate (LDS) solution was added, pH 3.18, and 50 μL reagent MB was added as a bacteriocide (ESA, Chelmsford, MA) – for 1 L preparation.
7. Standards. 3-nitro-L-tyrosine, tyrosine, ortho-tyrosine, and meta-tyrosine were purchased from Sigma and prepared at a stock concentration of 1 m*M*. Serial

dilutions of mix standards were prepared by aliquoting all tyrosine homologs at varying concentrations for a six-point calibration curve to demonstrate instrument efficiency and linearity.

8. HPLC–ECD Equipment: Instrumentation consisted of an ESA Model 5600 CoulArray HPLC (ESA) that is equipped with a binary gradient elution system, 84 vial autosampler with a column oven, and 12 electrochemical cells operating in the oxidative mode. Cell potentials were assigned and are illustrated in Table 1. Hydrodynamic voltammograms were generated for each standard to determine the assignment of chromatographic peaks, as well as determining the optimal oxidation potential for each analyte. This was done by preparing a plot of the fractional percentage of the cumulative current response versus the cell potential (mV). Fig. 2 illustrates a representative hydrodynamic voltammogram for 3-nitrotyrosine. Analyte separation was conducted on a TosoHaas (Montgomeryville, PA) reverse-phase (RP) ODS-TM C_{18} analytical column (4.6 × 250 mm, 5-μm particle size). Other HPLC–ECD methods have been used/modified previously but this particular method provides the user with another avenue for analyzing tyrosine variants in human plasma samples. Fig. 3 depicts a typical HPLC–ECD chromatogram of tyrosine and its oxidation and nitration products *(1–3,11)*. The optimized HPLC–ECD parameters utilized are discussed in Subheading 4, Analysis. Fig. 4 illustrates 3-NO_2-Tyr resolved in a sample of presumptively normal human plasma.

3. METHODS

1. Aliquot 0.500 mL of human plasma into a 15-mL centrifuge tube and sonicate sample on ice (approx 20 dips with the sonicator tip). Vortex mix each sample for approx 1 min and minimize light exposure as much as possible.
2. Add 0.050 mL of 60% TCA to each sample, sonicate again as in step 1, and vortex mix each sample.
3. Centrifuge plasma samples at 4,000 rpm on a IEC HN-SII benchtop centrifuge, at ambient temperature for 20 min. Remove each supernant, filter (*see* next step), and transfer into labeled, individual 1.7 mL eppendorf microcentrifuge tubes.
4. Filter each sample through a 0.2-μm, 13-mm PVDF filter prior to HPLC–ECD analysis. This is done to remove any particulate matter that might obstruct the HPLC–ECD system.
5. As previously stated, standard mixes consisting of 3-nitro-L-tyrosine and the oxidation and nitration products were prepared. Dissolution of these products is facilitated by using a slightly acidic medium (e.g., water adjusted to pH 3.0 works well or mobile-phase reservoir A). Calibration standards are randomly interspersed among the plasma samples for HPLC–ECD autoanalysis.

NOTE: Minimize prolong storage after the addition of 60% TCA prior to HPLC–ECD analysis of 3-NO_2-Tyr.

Table 1
Assigned Cell Potentials in the Oxidative Mode
(ESA Model 5600 CoulArray HPLC Detector)

Channel number	Cell potential (mV)
1	200
2	300
3	400
4	525
5	600
6	625
7	650[a]
8	675
9	700[b]
10	750
11	825
12	900

[a]Optimal potential for tyrosine and *o*-tyrosine.
[b]Optimal potential for 3-nitro-L-tyrosine.

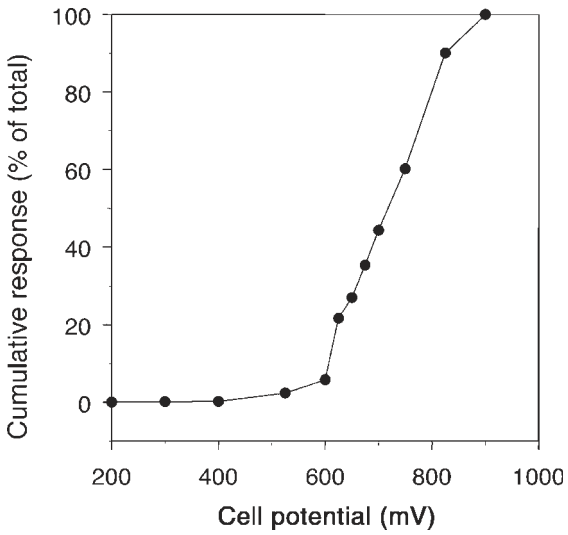

Fig. 2. Hydrodynamic voltammogram of 3-NO_2-Tyr obtained on a 12-channel coulometric array.

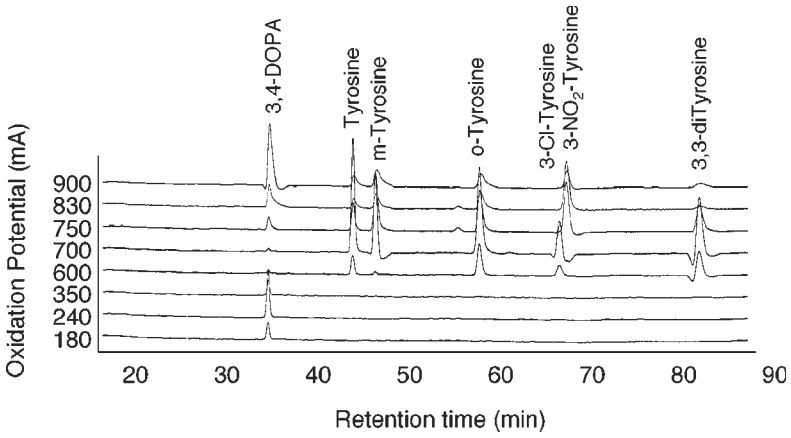

Fig. 3. Typical HPLC–ECD chromatogram of tyrosine and its variants using an 8-channel ECD array.

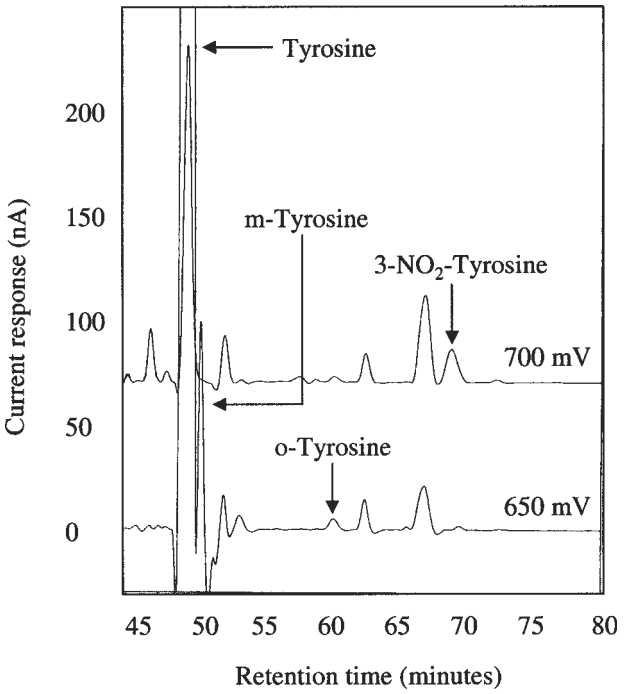

Fig. 4. Typical chromatogram of a representative plasma sample submitted for HPLC–ECD analysis.

Table 2
Gradient Program Used in the Isolation, Characterization, and Quantitation of Tyrosine Analytes

Run time (minutes)	%A Mobile phase	%B Mobile phase
0.00	100	0
20.0	100	0
30.0	50	50
40.0	50	50
55.0	25	75
80.0	25	75
90.0	0	100
110.0	0	100
115.0	100	0
120.0	100	0

4. ANALYSIS

The optimized HPLC–ECD parameters used are as follows:

- Flow rate: 0.6 mL/min.
- Injection volume: 60 μL.
- Column temperature: ambient.
- Autosampler temperature: 4°C.
- Run time/sample: 120 min.

All other chromatographic conditions were previously mentioned in the HPLC–ECD equipment section. Table 2 illustrates the optimized gradient program employed for chromatographic separation of the tyrosine analytes. Fig. 4 illustrates an actual HPLC–ECD chromatogram of 3-NO_2-Tyr from human plasma. The ratio of 3-NO_2-Tyr/tyrosine should be reported for each sample analyzed. Values on the order of 1:10,000–1:1000 are typical for this ratio in normal human tissue.

5. DISCUSSION

HPLC coupled with electrochemical detection is an effective, quantitative method used to study protein nitration products in biological matrices such as plasma samples. In particular, 3-NO_2-Tyr has shown promise as an index of nitrative stress that can be measured in human plasma or other tissue. The detection limits for 3-NO_2-Tyr and the other tyrosine congeners are in the low picomole range, thus far surpassing ultraviolet (UV)-visible sensitivity. This bioanalytical method has been employed as a biomarker indicating an inflammatory condition, and has wide applicability to basic, applied, and clinical research.

ACKNOWLEDGMENTS

This work was supported by the National Institutes of Health (NIH NS35747) and the Oklahoma Center for the Advancement of Science and Technology (OCAST H967067).

REFERENCES

1. Hensley, K., Williamson, K. S., Maidt, M. L., Gabbita, S. P., Grammas, P., and Floyd, R. A. (1999) Determination of biological oxidative stress using high performance liquid chromatography with electrochemical detection (HPLC–ECD). *J. High Res. Chromatogr.* **22,** 429–437.
2. Hensley, K., Maidt, M. L., Pye, Q. N., Stewart, C. A., Wack, M., Tabatabaie, T., and Floyd, R. A. (1997) Quantitation of protein-bound 3-nitrotyrosine and 3,4-dihydroxyphenylalanine by high-performance liquid chromatography with electrochemical array detection. *Anal. Biochem.* **251,** 187–195.
3. Hensley, K., Maidt, M. L., Yu, Z. Q., Sang, H., Markesbery, W. R., and Floyd, R. A. (1998) Electrochemical analysis of protein nitrotyrosine and dityrosine in the Alzheimer brain reveals region-specific accumulation. *J. Neurosci.* **18,** 8126–8132.
4. Salman-Tabcheh, S., Guerin, M. C., and Torreilles, J. (1995) Nitration of tyrosyl residues from extra and intracellular proteins in human whole blood. *Free Radic. Biol. Med.* **19,** 695–698.
5. Maruyama, W., Hashizume, Y., Matsubara, K., and Naoi, M. (1996) Identification of 3-nitro-L-tyrosine, a product of nitric oxide and superoxide, as an indicator of oxidative stress in the human brain. *J. Chromatogr. B. Biomed. Appl.* **676,** 153–158.
6. Shigenaga, M. K. (1999) Quantitation of protein-bound 3-nitrotyrosine by high-performance liquid chromatography with electrochemical detection. *Methods Enzymol.* **301,** 27–40.
7. Kaur, H., Lyras, L., Jenner, P., and Halliwell, B. (1998) Artefacts in HPLC detection of 3-nitrotyrosine in human brain tissue. *J. Neurochem.* **70,** 2220–2223.
8. Evans, P., Kaur, H., Mitchinson, M. J., and Halliwell, B. (1996) Do human atherosclerotic lesions contain nitrotyrosine? *Biochem. Biophys. Res. Commun.* **226,** 346–351.
9. Smith, M. A., Richey Harris, P. L., Sayre, L. M., Beckman, J. S., and Perry, G. (1997) Widespread peroxynitrite-mediated damage in Alzheimer's disease. *J. Neurosci.* **17,** 2653–2657.
10. Herce-Pagliai, C., Kotecha, S., and Shuker, D. E. (1998) Analytical methods for 3-nitrotyrosine as a marker of exposure to reactive nitrogen species: a review. *Nitric Oxide* **2,** 324–336.
11. Hensley, K., Williamson, K. S., and Floyd, R. A. (2000) Measurement of 3-nitro-tyrosine and 5-nitro-γ-tocopherol by high-performance liquid chromatography with electrochemical detection. *Free Radic. Biol. Med.* **28,** 520–528.

III

Reactive Oxygen Species and Reactive Nitrogen Species

18

Protein Carbonyl Levels—An Assessment of Protein Oxidation

Alessandra Castegna, Jennifer Drake, Chava Pocernich, and D. Allan Butterfield

1. INTRODUCTION

Oxidative stress may be a hallmark of several neurodegenerative disorders, including Alzheimer's disease (AD), Huntington's disease (HD), and Parkinson's disease (PD), as well as Creutzfeldt-Jakob disease (CJD), frontotemporal dementia, and amyotrophic lateral sclerosis (ALS) *(1)*. Oxidative stress occurs when the formation of reactive oxygen species (ROS) increases, or when scavenging of ROS or repair of oxidatively modified molecules decreases *(2,3)*. ROS are highly reactive, toxic oxygen moieties, such as hydroxyl radical, peroxyl radical, superoxide anion, and hydrogen peroxide. Collectively, ROS can lead to oxidation of proteins and DNA, peroxidation of lipids, and, ultimately, cell death. To counteract these damaging radicals, antioxidant systems have been developed. Among these are enzymes, such as glutathione peroxidase, glutathione reductase, superoxide dismutase (SOD), and catalase, among others; and small, nonprotein, cellular antioxidants such as, glutathione, vitamin C, vitamin E, and uric acid.

Oxidative stress has been shown to increase protein oxidation *(2–6)*, and has been reported in AD *(7)*, animal models of AD *(8)* and HD *(9,10)*, rheumatoid arthritis (RA) *(11)*, respiratory distress syndrome *(12)*, PD *(13)*, atherosclerosis *(14)*, and accelerated aging *(15)*. One way to measure protein oxidation is to determine levels of protein carbonyls. Protein carbonyls can result from oxidative cleavage of the protein backbone, direct oxidation of amino acids such as lysine, arginine, histidine, proline, glutamic acid, and threonine, or by the binding of aldehydes produced from lipid peroxidation

From: *Methods in Pharmacology and Toxicology: Methods in Biological Oxidative Stress*
Edited by: K. Hensley and R. A. Floyd

such as 4-hydroxynonenal (HNE) or acrolein *(2,3)* (Fig. 1). In addition, carbonyl groups may be introduced into proteins by reactions with reactive carbonyl derivatives generated as a consequence of the reaction of reducing sugars or their oxidation products with lysine residues of proteins, glycation, or glycoxidation reactions *(16,17)*.

The assay of carbonyl groups in proteins provides a convenient technique for detecting and quantifying oxidative modification of proteins. 2,4-dinitrophenylhyrdazine (DNPH) reacts with protein carbonyls to produce hydrazones (Fig. 2). Hydrazones can be detected spectrophotometrically at an absorbance of 370 nm or by fluorescence (18). Western- or slot-blotting techniques are also used for sensitive and specific detection of the protein-2,4-dinitrophenyl hydrazone moiety *(19)*.

2. MATERIALS

1. 0.2% (w/v) DNPH prepared in 2 *N* HCl.
2. 6 *M* guanidine hydrochloride dissolved in 20 m*M* sodium phosphate buffer with a pH of 6.5.
3. 100% (w/v) tricholoroacetic acid.
4. Ethanol/ethyl acetate solution (1:1 v/v).
5. 200 m*M* DNPH stock solution prepared in 100% trifluroacetic acid (TFA).
6. 12% (w/v) Sodium dodecyl sulfate (SDS).
7. Neutralization solution (2 *M* Tris/30% glycerol/ 19% 2-mercaptoethanol).
8. Primary antibody to the 2,4-dinitrophenylhydrazone protein moiety, available from Sigma (St. Louis, MO, D-8406) or Intergen (Purchase, NY, OxyBlot Kit #S7150).
9. Labeled secondary antibody to the species of the primary antibody appropriate for the method of detection (chemiluminescence, fluorescence, colorimetry).
10. Biological sample to be assayed for protein carbonyl determination. Protein concentration is determined by the Pierce BCA method.

3. METHODS

3.1. Spectrophotometric Assay

1. Sample derivatization. Two 1-mg aliquots are needed for each sample to be assayed. Samples are extracted in a final concentration of 10% (w/v) TCA. The precipitates are treated with 500 µL of 0.2% DNPH or 500 µL of 2 *N* HCl. Samples are incubated at room temperature for 1 h with vortexing at 5-min intervals. The proteins are then precipitated by adding 55 µL of 100% TCA. The pellets are centrifuged and washed three times with 500 µL of the ethanol:ethyl acetate mixture. The pellet is then dissolved in 600 µL of 6 *M* guanidine hydrochloride.

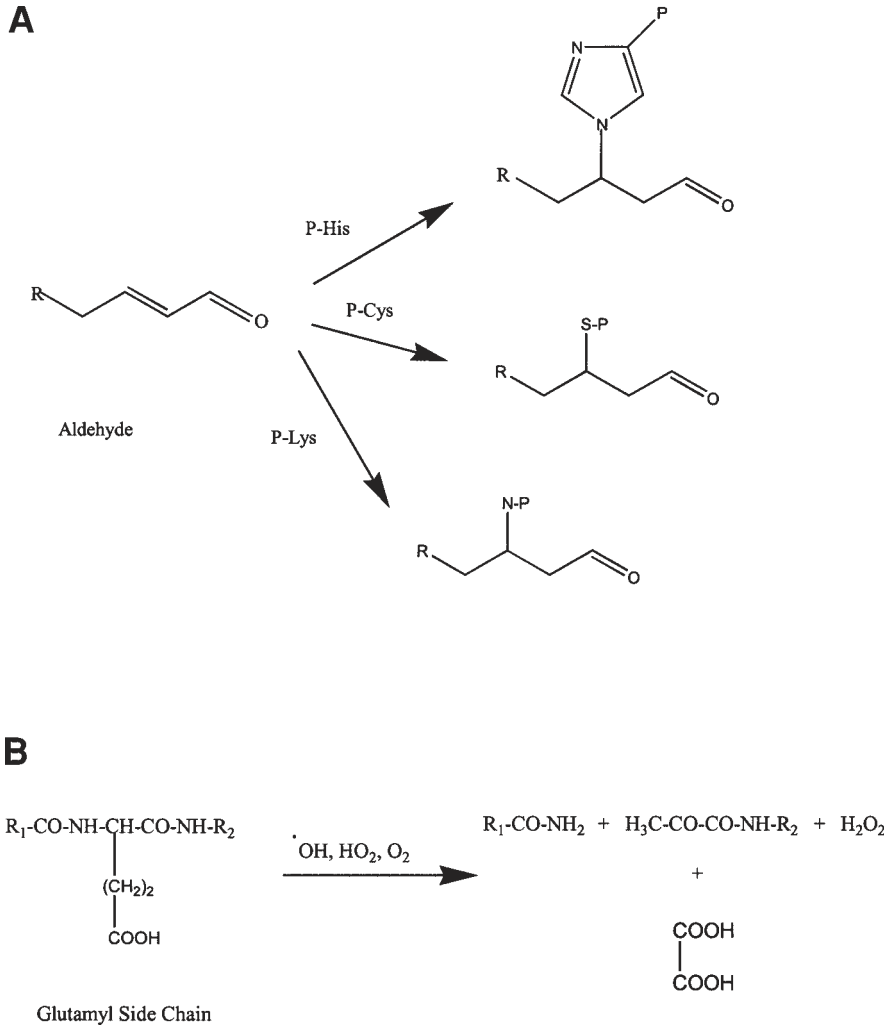

Fig. 1. (**A**) Michael addition of an aldehyde to protein lysine (P-lys), histidine (P-His), or cysteine (P-Cys) residues resulting in the addition of carbonyl groups to the protein. (**B**) Oxidation of the glutamyl side chain leads to formation of a peptide in which the N-terminal amino acid is blocked by an α-ketoacyl derivative.

2. The carbonyl content is determined by reading the absorbance at the optimum wavelength (λ = 360–390 nm) of each sample against its appropriate blank

3.2. Immunodetection Methods

1. Sample derivatization. 200 m*M* DNPH stock solution is diluted 10 times with water. Five μL of sample is incubated at room temperature with 5 μL of 12%

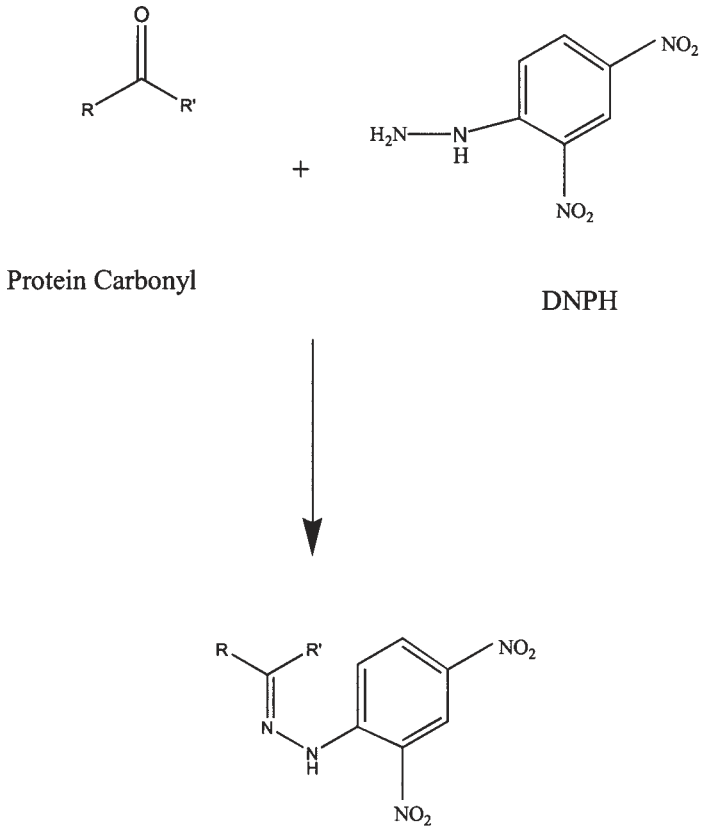

Fig. 2. Dinitrophenylhydrazine (DNPH) reacts with protein carbonyl groups producing a protein-DNP hydrazone moiety that can be detected spectrophotometrically or by immunochemical techniques.

SDS and 10 μL of the diluted DNPH for 20 min with vortexing. The samples are neutralized with 7.5 μL of the neutralization solution.

2. Western blotting. 5–15 μg of the sample solution is loaded onto a gel and electrophoresed according to the Laemmli method *(20)*. The proteins on the gel are then transferred to nitrocellulose paper and standard immunodetection techniques are performed *(21)*.
3. Slot blotting. 250 ng of the sample solution is loaded into the wells of the slot blot apparatus. Proteins are transferred directly to the nitrocellulose paper under vacuum pressure and standard immunodetection techniques are performed.

4. ANALYSIS

For the spectrophotometric assay, 2,4-dinitrophenylhydrazone protein adducts are calculated using the millimolar adsorptivity of 21.0 mM^{-1} cm^{-1} for aliphatic hydrazones. Results are reported as nmol of DNPH incorporated per mg of protein. The carbonyls detected in the immunodetection methods can be reported either by comparing to a standard with an amount of 2,4-dinitrophenylhydrazone protein adducts as determined by the spectrophotometric method or by comparing the density to the control sample density employing suitable imaging software.

5. DISCUSSION

The method chosen for analysis depends on the sample and the needs of the researcher. The spectrophotometric method actually quantitates the 2,4-dinitrophenylhydrazone protein adducts and is therefore useful for comparing samples that will be collected and quantitated at different times. However, because a large amount of sample is required for analysis, it may be inappropriate for samples such as cerebrospinal fluid (CSF) where protein concentration is limited. For samples with limited protein concentration, the slot blot technique is appropriate, because for as little as 0.5 nanograms of protein can be loaded (Fig. 3). Slot-blot analyzes the total protein oxidation whereas Western-blot analysis allows for the comparison of individual proteins that may be oxidized. Two-dimensional (2D) gel electrophoresis followed by identification of the position of an individual protein with specific antibodies and immunoblot analysis for protein carbonyls have been shown to be a potential method to identify specifically oxidized proteins in situ *(22,23)*.

Proteomics may also offer tools to perform such identification in an automated procedure. By observing the total protein profile as well as the oxidized protein profile with 2D-gel electrophoresis, it is possible to select proteins showing higher levels of carbonyls vs control. The spot corresponding to the protein of interest is then excised and submitted for proteomics analysis. Chemical modification and protein digestion with a sequence-specific protease precede the extraction of the proteolytic digestion and the mass spectrometric (MS) analysis of the peptides. On-line HPLC-MS connection offers the possibility of direct mass detection during HPLC separation of the peptides. The masses of a proteolytic digestion are highly characteristic of a protein and represent an important means to identify unknown oxidized proteins utilizing suitable protein databases.

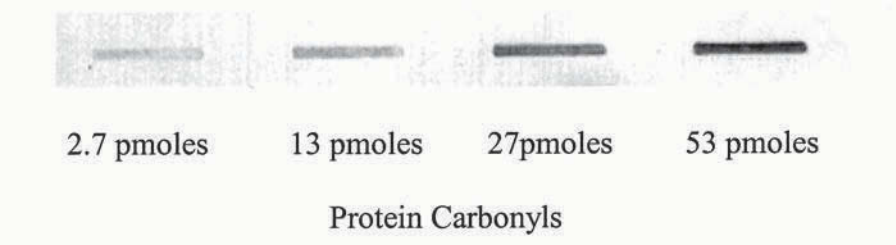

Fig. 3. Sample slot blot of bovine serum albumin (BSA) oxidized by hydroxyl radicals, produced by Fe^{2+} and H_2O_2, and reacted with DNPH, demonstrating sensitivity as low as picomolar levels of protein carbonyls.

The whole procedure potentially allows automated identification of several oxidized proteins at the time, yet some problems can occur. First, reproducibility of 2D-gel analysis, which is crucial for control-sample spot comparison, might be reduced by the instability of pH-gradients in the first dimension (isoelectric focusing; IEF). To circumvent this limitation, the use of immobilized pH gradients (IpHGs) may be suitable *(24)*. IpHGs are formed by copolymerization of buffering and titrant groups of acrylamido-derivatives into a polyacrylamide gel matrix, assuring a steady-state focusing and a consequent high reproducibility of the spot position.

In addition, oxidative modification may result in altering, even slightly, the electrophoretic properties of a protein and its migration with respect to the unmodified one. This problem can be overcome *(22,25)*, especially with the help of specific 2D-gel softwares, which increase the resolution and the possibility of spot crossmatching.

This automated method of proteomic analysis is in its infancy with respect to neurodegenerative diseases, but is under investigation in our laboratory *(26,27)*.

ACKNOWLEDGMENTS

This work was supported in part by grants from NIH.

REFERENCES

1. Butterfield, D. A. and Kanski, J. (2001) Brain protein oxidation in age-related neurodegenerative disorders that are associated with aggregated proteins. *Mech. Ageing Dev.* **122,** 945–962.

2. Stadtman, E. R. (1992) Protein oxidation and aging. *Science* **257,** 1220–1224.
3. Butterfield, D. A. and Stadtman, E. R. (1997) Protein oxidation processes in aging brain. *Adv. Cell Aging Gerontol.* **2,** 161–191.
4. Howard, B. J., Yatin, S., Hensley, K., Allen, K. L., Kelly, J. P., Carney, J. M., and Butterfield, D. A. (1996) Prevention of hyperoxia-induced alterations in synaptosomal membrane-associated proteins by N-tert-butyl-α-phenylnitrone (PBN) and 4-hydroxy-2,2,6,6-tetramethylpiperidine-1-oxyl (Tempol). *J. Neurochem.* **67,** 2045–2050.
5. Aksenov, M. Y., Aksenova, M. V., Mrkesbery, W. R., and Butterfield, D. A. (1998) Amyloid β-peptide (1-40)-mediated oxidative stress in cultured hippocampal neurons. *J. Mol. Neurosci.* **10,** 181–192.
6. Koppal, T., Drake, J., Yatin, S., Jordan, B., Varadarajan, S., Bettenhausen, L., and Butterfield, D. A. (1999) Peroxynitrite-induced alterations in synaptosomal membrane proteins: Insight into oxidative stress in Alzheimer's disease. *J. Neurochem.* **72,** 310–317.
7. Hensley, K., Hall, N., Subramaniam, R., Cole, P., Harris, M., Aksenov, M., et al. (1995) Brain regional correspondence between Alzheimer's disease histopathology and biomarkers of protein oxidation. *J. Neurochem.* **65,** 2146–2156.
8. Yatin, S. M., Link, C. D., and Butterfield, D. A. (1999) In-vitro and in-vivo oxidative stress associated with Alzheimer's amyloid β-peptide. *Neurobiol. Aging* **20,** 325–330.
9. LaFontaine, M. A., Geddies, J. W., Banks, A., and Butterfield, D. A. (2000) 3-Nitropropionic acid induced in-vivo protein oxidation in striatal and cortical synaptosomes: insights into Huntington's disease. *Brain Res.* **858,** 356–362.
10. LaFontaine, M. A., Geddies, J. W., Banks, A., and Butterfield, D. A. (2000) Effect of exogenous and endogenous antioxidants on 3-nitropropionic acid-induced in-vivo oxidative stress and striatal lesions: insights into Huntington's disease. *J. Neurochem.* **75,** 1709–1715.
11. Chapman, M. L., Rubin, B. R., and Gracy, R. W. (1989) Increased carbonyl content of proteins in synovial fluid from patients with rheumatoid arthritis. *J. Rheumatol.* **16,** 15–19.
12. Gladstone, I. M. and Levine, R. L. (1994) Oxidation of proteins in neonatal lungs. *Pediatrics* **93,** 764–768.
13. Yoritaka, A., Hattori, N., Uchida, K., Tanaka, M., Stadtman, E. R., and Mizuno, Y. (1996) Immunohistochemical detection of 4-hydroxynonenal protein adducts in Parkinson disease. *Proc. Natl. Acad. Sci. USA* **93,** 2696–2701.
14. Uchida, K., Toyokumi, S., Kishikawa, S., Oda, H., Hiaia, H., and Stadtman, E. R. (1994) Michael addition-type 4-hydroxy-2-nonenal adducts in modified low-density lipoproteins: markers for atherosclerosis. *Biochemistry* **33,** 12,487–12,347.
15. Butterfield, D. A., Howard, B. J., Yatin, S., Allen, K. L., and Carney, J. M. (1997) Free radical oxidation of brain proteins in accelerated senescence and its modulation by N-tert-butyl-α-phenylnitrone. *Proc. Nat. Acad. Sci. USA* **94,** 674–678.
16. Berlett, B. A. and Stadtman, E. R., (1997) Protein oxidation in aging, disease, and oxidative stress. *J. Biol. Chem.* **272,** 20,313–20,316.

17. Wondrak, G. T., Varadarajan, S., Butterfield, D. A., and Jacobson, M. K. (2000) Formation of a protein-bound pyrazinium free radical cation during glycation of histone H1. *Free Radic. Biol. Med.* **29,** 557–567.
18. Reznick, A. Z. and Packer, L. (1994) Oxidative damage to proteins: spectrophotometric method for carbonyl assay. *Methods Enzymol.* **233,** 357–363.
19. Levine, R. L., Williams, J. A., Stadtman, E. R., and Shacter, E. (1994) Carbonyl assays for determination of oxidatively modified proteins. *Methods Enzymol.* **233,** 346–357.
20. Laemmli, U. K. (1970) Cleavage of structural proteins during the assembly of the head of bacteriophage T4. *Nature* **227,** 680–685.
21. Glenney, J. R. (1986) Antibody probing on western blots have been stained with India Ink. *Anal. Biochem.* **156,** 315–318.
22. Aksenov, M., Aksenova, M., Butterfield, D. A., and Markesbery, W. R. (2000) Oxidative modification of creatine kinase BB in Alzheimer's disease brain. *J. Neurochem.* **74,** 2520–2527.
23. Aksenov, M. Y., Aksenova, M. V., Butterfield, D. A., Geddes, J. W., and Markesbery, W. R. (2001) Protein oxidation in the Alzheimer's disease brain. *J. Neurosci.* **103,** 373–383.
24. Molloy, M. P. (2000) Two-dimensional electrophoresis of membrane proteins using Immoblized pH Gradients. *Anal. Biochem.* **280,** 1–10.
25. Talent, J. M., Kong, Y., and Gracy, R. W. (1998) A double-stain for total andoxidized proteins from two-dimensional fingerprints. *Anal. Biochem.* **263,** 31–38.
26. Castegna, A., Aksenov, M., Aksenova, M., et al. (2002) Proteomic identification of oxidatively modified proteins in Alzheimer's disease brain. Part I: creatine kinase BB, glutamine synthase, and ubiquitin carboxy-terminal hydrolase L-1. *Free Radic. Biol. Med.* **33,** 562–571.
27. Castegna, A., Aksenov, M., Thongboonkerd, V., et al. Proteomic identification of oxidatively modified proteins in Alzheimer's disease brain. Part II: dihydropyrimidinase-related protein 2, α-enolase and heat shock cognate 71. *J. Neurochem.* **82,** 1524–1532.

19

Fluorogenic Analysis of H_2O_2 in Biological Materials

Kenneth Hensley, Kelly S. Williamson, and Robert A. Floyd

1. INTRODUCTION

The biological importance of hydrogen peroxide and other "reactive oxygen species" (ROS) has become greatly appreciated in recent years. It has become apparent that certain ROS, in particular hydrogen peroxide (H_2O_2) and nitric oxide (•NO), are ubiquitously used as intra- or intercellular messengers *(1)*. Because these ROS are short-lived in vivo, their steady-state concentrations remain low, and their accurate quantitation poses a significant technical challenge. Moreover, it is often necessary to monitor changes in ROS in real time, for instance during the time course of hormonal stimulation of cultured cells *(2)*. The most common methods of measuring H_2O_2 rely upon peroxide-dependent oxidation of reduced xanthene dyes such as 2',7'-dichlorodihydrofluorescein (H_2DCF, also called dichlorofluorescin) or dihydrorhodamine 123 (H_2RD123) (Fig. 1). These dyes were originally used to measure peroxidase activities *(3)* but the assays were easily modified to allow peroxide determination *(2,4–7)*. Although the reduced dyes are not highly fluorescent, their oxidation products are, and can be monitored continuously using a fluorescence spectrometer, microplate reader, or confocal microscope. Although flexible and convenient, the fluorogenic determination of H_2O_2 must be performed with due consideration of factors that may interfere with the chemistry of the assay.

From: *Methods in Pharmacology and Toxicology: Methods in Biological Oxidative Stress*
Edited by: K. Hensley and R. A. Floyd

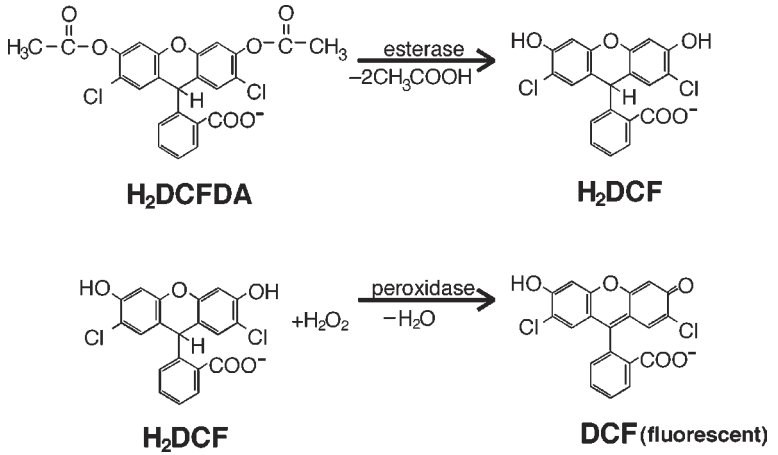

Fig. 1. Chemistry of H_2DCFDA oxidation using H_2O_2 as a terminal electron acceptor.

2. MATERIALS

1. 2',7'-dichlorodihydrofluorescein diacetate (H_2DCFDA) or H_2RD123, dissolved to 10 m*M* final concentration in DMSO. Ethanol may be substituted for DMSO.
2. 2,7-dichlorofluorescein (DCF) or rhodamine 123 (RD123), dissolved to 10 m*M* in dimethyl sulfoxide (DMSO) or ethanol.
3. Calcein acetoxymethyl ester (calcein-AM), dissolved to 10 m*M* in DMSO or ethanol.
4. Horseradish peroxidase (HRP), dissolved to 2 mg/mL in aqueous buffer, pH 7.2. The buffer of choice can be selected to match the requirements of the biological components within the sample to be assayed. Thiol compounds should be omitted from the assay buffer. A 10 m*M* sodium acetate buffer is recommended for the assay of peroxide-generating enzymes such as xanthine oxidase; phenol-free cell-culture medium can be used with adherent or suspended cells. For the study of mitochondria, the buffer of choice is KHP (20 m*M* 4-(2-hydroxyethyl)-piperazineethanesulfonic acid [HEPES], 80 m*M* KCl, 5 m*M* KH_2PO_4, 2 m*M* EGTA, pH 7.2).
5. Nargase (type XXVII) protease dissolved to 5 mg/mL in the buffer of choice.
6. Biological sample to be assayed for H_2O_2 generation. 50 μL of tissue homogenate at 1 mg/mL total protein is generally recommended for assays of substrate-linked peroxide generation. Alternatively, 20 μL of isolated brain or liver mitochondria may be used at a concentration of 4 mg/mL. If adherent cells are assayed, cultures should be grown to confluence in 96-well clear

microplates (>50,000 cells/well). Suspended cells should be assayed at >200,000 cells/mL or 1 mg/mL total cellular protein, in phenol-free medium or isotonic phosphate. Care should be taken to omit thiols or strong reducing agents from the cell culture medium during the peroxide assay.

7. Stimulating agent (oxidizable substrate or cell stimulant). For enzyme assays, this should be the enzyme substrate dissolved to 10X final concentration in the buffer of choice. For example, mitochondria can be stimulated with NADH or succinate (dissolved to 10 m*M* in KHP).
8. Authentic H_2O_2. Actual concentration can be determined using an extinction coefficient of 40 $M^{-1}cm^{-1}$ at 240 nm.
9. Fluorescence microplate reader and clear 96-well microplates.

3. METHODS

1. Generation of H_2O_2 from isolated enzymes or tissue preparation (e.g., mitochondria). In each well of the microplate, mix the following reagents in the following order: 120 μL buffer, 50 μL biological sample, 10 μL HRP, 2 μL H_2DCFDA or H_2RD123. For assays using H_2DCFDA to probe samples with very low esterase activity or variable esterase activity (such as a purified enzyme preparation), also add 5 mL nargase. Esterase activity is determined by substituting calcein-AM for the H_2DCFDA or H_2RD123 and reading the kinetics of substrate hydrolysis at 485 nm excitation and 538 nm emission wavelengths, using DCF as a standard. An esterase activity greater than 20 nmoles calcein-AM hydrolyzed/mg min is considered sufficient. Incubate samples 5 mins at ambient temperature before proceeding.
2. Generation of H_2O_2 from cells. Wash cells with saline or phenol-free tissue-culture medium and incubate cells for 5 min with 190 μL medium, 10 μL HRP, and 2 μL H_2DCFDA or H_2RD123.
3. Initiate the H_2O_2 generation by adding 20 μL of stimulant (enzyme substrate or cell stimulator).
4. Fluorescence of the reaction incubates can be read at 488 nm excitation and 538 nm emission (fluorescein filters) regardless of whether H_2DCFDA or H_2RD123 is being used as an indicator dye.

4. ANALYSIS

The reaction should be monitored continuously for a length of time sufficient to generate an accurate linear regression. The rate of H_2O_2 generation is calculated by comparison with a standard curve constructed from serial dilutions of DCF or RD123. Each experiment should be designed to include appropriate controls, for instance, by omitting enzyme substrates or cell stimulants. The net rate of peroxide increase with stimulation can then be reported in units of pmoles DCF (or RD123) generated/mg protein/min.

5. DISCUSSION

The oxidation of either H_2DCFDA or H_2RD123 in the presence of H_2O_2 provides a sensitive means of measuring the peroxide in aqueous solutions near neutral pH (Fig. 2). The decision to use H_2DCFDA vs H_2RD123 as a probe depends on the particular needs of the researcher. In general, H_2DCFDA provides a greater dynamic range of assay sensitivity and greater assay linearity than does H_2RD123 (Fig. 2A). On the other hand, H_2DCFDA must be enzymatically hydrolyzed to the phenolic form before reaction with peroxide is possible (Fig. 2B). H_2RD123 oxidation is not dependent upon esterase activation (Fig. 2B). If the analyst chooses to use H_2DCFDA as a probe, he must therefore control for variations in esterase activity among his samples. This can easily be done by measuring esterase activity fluorometrically or by adding an excess quantity of exogenous esterase.

An artifact may arise if the fluorogenic peroxide assay is performed in the presence of strong reducing agents such as thiols (e.g., glutathione, N-acetylcysteine, mercaptoethanol, or dithiothreitol; DTT). The artifact arises because thiol compounds react with photochemically excited xanthene dyes to generate π radical anions *(8)* and, indirectly, peroxides (Fig. 3). Fig. 4 illustrates that inclusion of either reduced or oxidized glutathione (GSH or GSSG, respectively) in the DCF assay accelerates H_2DCF oxidation, and this effect is most apparent when adequate peroxidase activity was present (Fig. 4). The analyst therefore may consider controlling for variations in thiol content among his/her samples, which, although possibly indexing the general oxidation state of the tissue sample, might preclude accurate determination of specific H_2O_2 flux. As a practical matter, these caveats are relatively insignificant in systems such as isolated mitochondria, which generate profligate quantities of H_2O_2 (on the order of 100 pmole/mg/min protein), but become more important as the rate of DCF formation decreases toward the detection limits of the assay.

ACKNOWLEDGMENTS

This work was supported by the National Institutes of Health (NIH NS35747) and the Oklahoma Center for the Advancement of Science and Technology (OCAST H97067).

REFERENCES

1. Sen, C. K. and Packer, L. (1996) Antioxidant and redox regulation of gene transcription. *FASEB J.* **10,** 709–720.

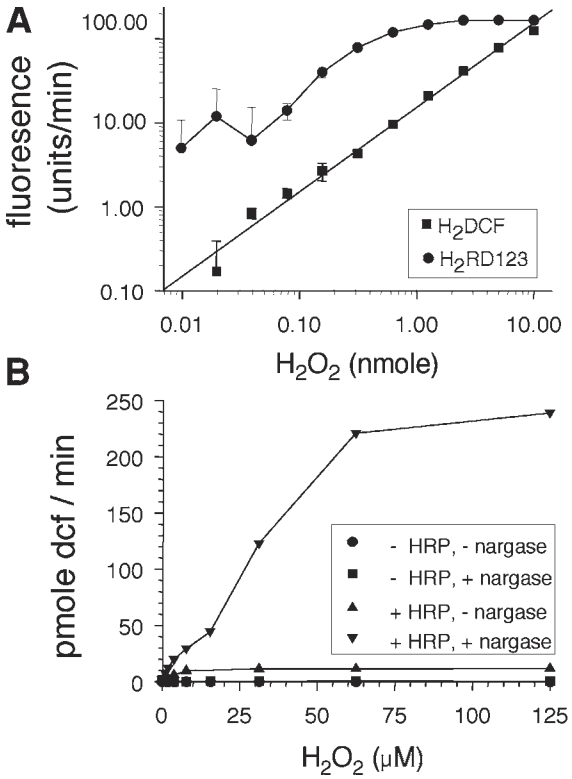

Fig. 2. **(A)** Comparison of 2',7'-dichlorodihydrofluorescein (H_2DCF) and dihydrorhodamine 123 (H_2RD123) reagents as oxidizable substrates for determination of H_2O_2. Assays were performed as described in Methods. **(B)** Demonstration of the need for both esterase and peroxidase activity to enable efficient oxidation of H_2DCFDA. HRP = horseradish peroxidase.

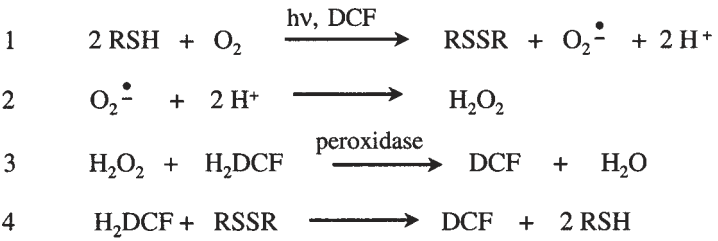

Fig. 3. Proposed mechanism of H_2DCF oxidation in the presence of thiol-reducing agents, an initial catalytic quantity of DCF, and peroxidase. The photochemical reduction of DCF has been characterized elsewhere *(8)*.

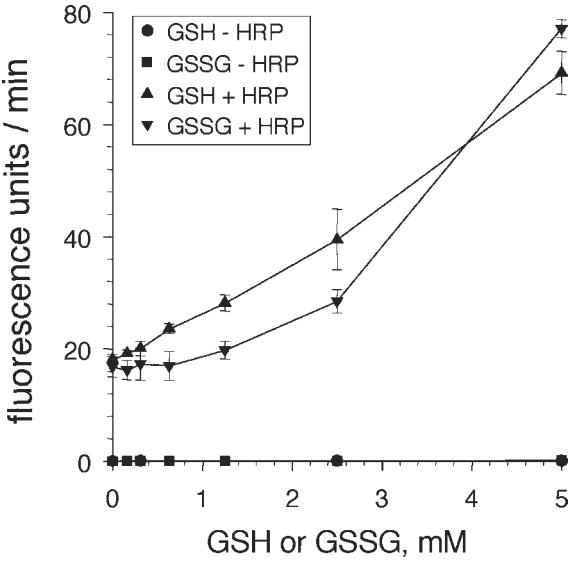

Fig. 4. Acceleration of H_2DCFDA oxidation by glutathione. Reactions were conducted as described in Methods, except that GSH or GSSG were included in the mixture. GSSG contained approx 1% GSH contaminant as assessed by HPLC with electrochemical detection. Error bars indicate standard error.

2. Robinson, K. A., Stewart, C. A., Pye, Q. N., Nguyen, X., Kenney, L., Salzman, S., et al. (1999) Redox-sensitive protein phosphatase activity regulates the phosphorylation state of p38 protein kinase in primary astrocyte culture. *J. Neurosci. Res.* **55,** 724–732.
3. Brandt, R. and Keston, A. S. (1965) Synthesis of diacetyldichlorofluorescin: A stable reagent for fluorometric analysis. *Anal. Biochem.* **11,** 6–9.
4. Loschen, G., Azzi, A., and Flohe, L. (1973) Mitochondrial H_2O_2 formation: Relationship with energy conservation. *FEBS Lett.* **33,** 84–88.
5. Baggiolini, M., Ruch, W., and Cooper, P. H. (1986) Measurement of hydrogen peroxide production by phagocytes using homovanillic acid and horseradish peroxidase. *Methods Enzymol.* **132,** 395–400.
6. LeBel, C. P., Ischiropoulos, H., and Bondy, S. C. (1992) Evaluation of the probe 2',7'-dichlorofluorescin as an indicator of reactive oxygen species formation and oxidative stress. *Chem. Res. Toxicol.* **5,** 227–231.
7. Royall, J. A. and Ischiropoulos, H. (1993) Evaluation of 2',7'-dichlorofluorescin and dihydrorhodamine as fluorescent probes for intracellular H_2O_2 in cultured endothelial cells. *Arch. Biochem. Biophys.* **302,** 348–355.
8. Ajtai, K. and Burghardt, T. P. (1992) Luminescent/paramagnetic probes for detecting order in biological assemblies: transformation of luminescent probes into π-radicals by photochemical reduction. *Biochemistry* **31,** 4275–4282.

20

Detection of Reactive Oxygen Species by Flow Cytometry

Alexander Christov, Ladan Hamdheydari, and Paula Grammas

1. INTRODUCTION

Reactive oxygen species (ROS) are a family of molecules including molecular oxygen and its derivatives produced in all aerobic cells. Extensive production of ROS has been implicated in the oxidation of biological macromolecules, such as DNA, proteins, carbohydrates, and lipids. This condition has commonly been referred to as oxidant stress. Oxidant stress is involved in the pathogenesis of many cardiovascular diseases and is closely related to vascular endothelial dysfunction *(1)*. Endothelial dysfunction includes altered anticoagulant and antiinflammatory properties of the endothelium, impaired modulation of vascular growth, and dysregulation of vascular remodeling *(2)* .

The ROS group includes free radicals, such as super oxide anion ($O_2^{-\bullet}$), nitric oxide (NO^-), and lipid radicals, hydrogen peroxide (H_2O_2), peroxynitrite ($ONOO^-$), and hydrochlorous acid (HOCl). Major sources of ROS in vascular cells are mitochondrial respiration, arachidonic acid pathway enzymes lipooxygenase and cyclooxygenase, xanthine oxidase, NO synthase, NADH/NADPH oxidase, peroxidase, among others.

ROS interact with signaling systems in controlling vascular functions. As the levels of ROS increase, they participate in pathophysisolgical responses, such as attenuation of vasodilator mechanisms and promotion of adhesion protein expression. High levels of ROS can overwhelm cellular antioxidant systems, triggering apoptotic and necrotic cellular death *(3)*.

From: *Methods in Pharmacology and Toxicology: Methods in Biological Oxidative Stress*
Edited by: K. Hensley and R. A. Floyd

The technique for automatic separation of suspended living cells using intracellular fluorescence and light scattering (LS), known as flow cytometry and cell-sorting, or FACS (fluorescence activated cell sorter) analysis, originated during the years 1968–1969 *(4)*. The essential elements of FACS, a laser and two light detectors (one for fluorescence and one for LS) remain unchanged to this day. Improvements in this methodology result from the development of new fluorescent probes capable of targeting specific sites or processes in living cells *(5)*. One of these fluorescent markers is carboxy-H_2DCFDA (5-[and-6]-carboxy 2',7'dichlorodihydrofluorescein diacetate). Carboxy-H_2DCFDA, when delivered to the cellular interior, specifically labels intracellular ROS.

Endothelial dysfunction caused by elevated ROS levels has been implicated in hypercholesterolemia, atherosclerosis, hypertension, diabetes, and heart failure. Recent studies have also linked ROS-induced vascular endothelial dysfunction to neuronal degeneration, cognitive impairment, and development of Alzheimer's disease. As the role of ROS-triggered endothelial dysfunction in the development and progression of these disorders becomes more clear, new therapeutic methods may be discovered and introduced for treatment.

In-vitro injury-induced production of ROS has been studied in different model cell systems, among them endothelial cells originating from rat brain vessels *(6)*, endothelial cells from porcine aorta *(7)*, bovine pulmonary artery *(8)*, bovine aorta *(9)*, and human umbilical vein *(10)*. In this study we report injury-induced production of ROS in rat brain resistance vessel-derived endothelial cells. The brain endothelial cell culture system was originally developed in 1993 *(11)* and since has proven to be a reliable model system to study brain endothelial cell responsiveness *(12–16)*.

Circulating oxidized low-density lipoprotein (OxLDL) particles are a major factor in blood vessel endothelial dysfunction in vivo and play a critical role in atherogenesis. OxLDLs are known to alter the balance between pro- and antioxidant activity in endothelial cells. In our experiments we have induced brain endothelial cell injury by treatment with LDL particles modified with 4-hydroxy 2-nonenal (4-HNE), a major byproduct of lipid peroxidation. This form of modified LDL is similar to the form of lipids (OxLDL) associated with atherosclerotic lesions *(17)*.

Flow cytometry is a widely used experimental technique. In the current study, this method has been successfully adapted for studying levels of ROS in cultured endothelial cells under basal conditions and in response to OxLDL injury.

2. MATERIALS AND METHODS

2.1. Materials

1. LDL was obtained from Sigma-Aldrich (St. Louis, MO).
2. 4-HNE was purchased from Cayman (Ann Arbor, MI).
3. Biotin hydroxytoluene (BHT) was purchased from Cayman (Ann Arbor, MI).
4. 5-(and-6)-Carboxy-2',7'dichlorodihydrofluorescein diaceate (carboxy H_2DCFDA) was obtained from Molecular Probes (Eugene, OR).
5. Glutathione and diamide (Sigma-Aldrich, St. Louis, MO).

2.2. Procedure for Modification of LDL

LDL (1 mg/mL in sodium phosphate buffer) was modified by treatment of 1 m*M* HNE for 24 h at 37°C *(18)*.

2.3. Endothelial Cell Culture

Endothelial cell cultures derived from rat brain resistance vessels were established, as previously described *(11–16)*.

Cells were maintained in Dulbecco's modified Eagle's medium (DMEM; Gibco, Grand Island, NY), containing 10% fetal calf serum (FCS), supplemented with 1% glutamine, and 1% antibiotics in a humidified 5% CO_2–, 95% air incubator at 37°C. Cells between passages 8 and 9 were used in these experiments.

2.4. Labeling with Carboxy-H_2DCFDA

The culture medium was replaced with DMEM containing 300 μ*M* 5-(and-6)-carboxy-2',7'dichlorodihydrofluorescein diacetate (carboxy-H_2DCFDA) and incubated for 30 min. The carboxy-H_2DCFDA-containing medium was prepared by adding an aliquot of 20 μL from a 15 m*M* stock solution of carboxy-H_2DCFDA in DMSO (dimethylsulfoxide) to 1 mL of DMEM. Carboxy-H_2DCFDA is an acetate ester of the fluorescent indicator 5-(and-6)-carboxy-2',7'dichlorodihydrofluorescein, cell membrane-permeable, and nonfluorescent until hydrolyzed. Once inside cells, the acetate groups are cleaved by nonspecific esterases, resulting in a charged form that is membrane impermeable, binds to ROS, and fluoresces after excitation.

2.5. Induced ROS Production and Preparation for Analysis

ROS normally exist in living cells at a background level. An increase in ROS levels usually reflects changes in cell metabolism closely related to cellular dysfunction or a response to cell injury. Treatment of cells with reductive or oxidative agents can also change intracellular ROS levels. In this study, glutathione and diamide were used as reductive and oxidizing,

respectively, reference agents. Glutathione (GSH) is a tripeptide thiol that has facile electron-donating capacity, linked to its sulfhydryl (-SH) group. GSH is an important water-phase antioxidant and essential cofactor for antioxidant enzymes. Its high electron-donating capacity, combined with its high intracellular concentration, endows GSH with great reducing power that is used to regulate the complex thiol-exchange system (-SH ⇔ -S-S-). The reducing power of GSH is a measure of its free-radical scavenging, electron-donating, and sulfhydryl-donating capacity. Diamide is a small thiol oxidant that specifically oxidizes the glutathione. It is a powerful oxidant probe that perturbs the redox balance of cells. In these experiments HNE-modified LDL, glutathione, and diamide were used to provoke changes in the ROS content in the endothelial cells as follows. The carboxy-H_2DCFDA-containing medium was replaced by DMEM containing either 10 mg/mL HNE-LDL *(19)*, 100 m*M* glutathione, or 10 m*M* diamide, and the cells were incubated for 1 h at 37°C in the dark.

From this step, light must be limited to avoid photobleaching of the fluorescent probe.

1. To remove endothelial cells from culture plates 1 mL Versene-Trypsin (0.025%) was added, and cells incubated for 10 min at 37°C. Suspended endothelial cells were then collected and transferred into a 5 mL centrifuge tube containing 1 mL FCS.
2. Cells were centrifuged at 200*g* for 5 min and the endothelial cell pellet resuspended in Hank's balanced salt solution (HBSS). This wash step was performed twice.
3. After the final wash, endothelial cells were resuspended for flow cytometry.

2.6. Detection of ROS by Flow Cytometry

1. Endothelial cell suspensions were gently passed through a 40 μm nylon mesh filter to remove large aggregates.
2. ROS content in the endothelial cells was measured by the fluorescence intensity of carboxy-H_2DCFDA excited at 488 nm following the standard operational procedure for the FACS Callibur Automated Benchtop Flow Cytometer (Beckton Dickinson).

3. ANALYSIS AND DISCUSSION

Our results indicated that flow cytometry was an easy and reproducible method for the detection of ROS in cultured cells. Using brain endothelial cells labeled with carboxy-H_2DCFDA, we detected changes induced by treatment with HNE-modified LDL in the intracellular ROS content (Figs. 1 A,B). Background ROS content in cultured endothelial cells was demonstrable in unlabeled endothelial cells which autofluoresce (with a mean value of about 2

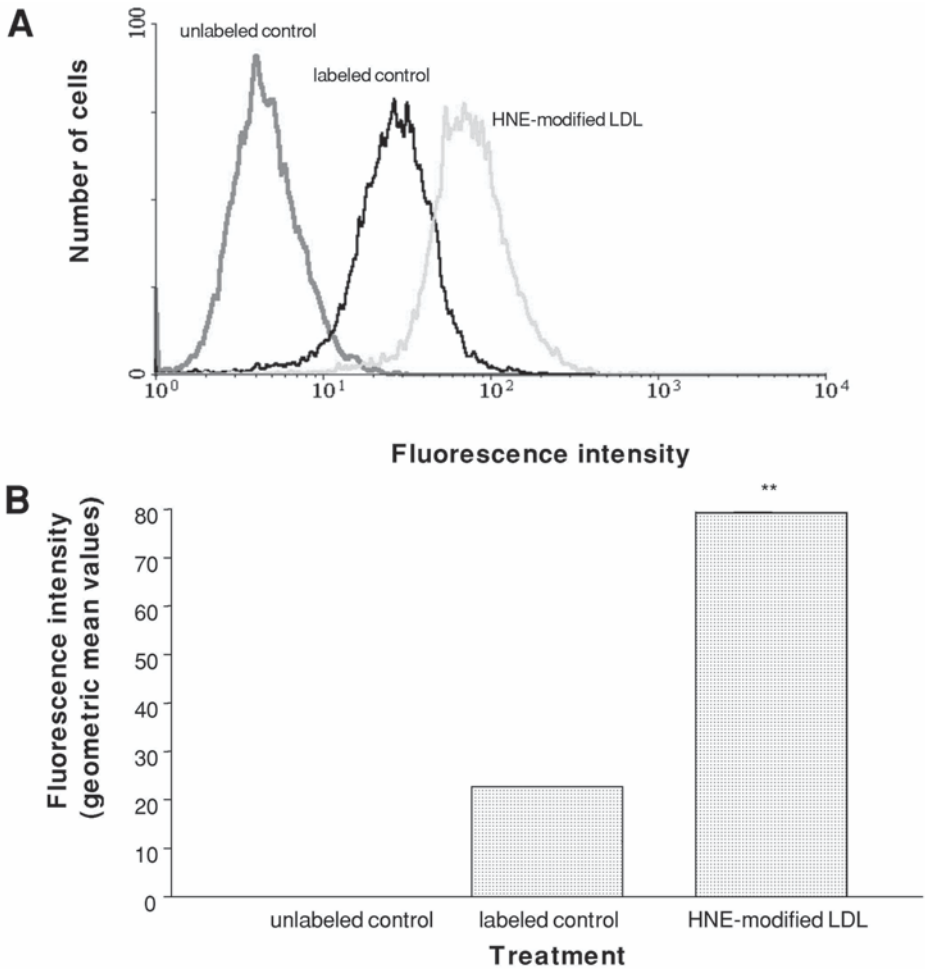

Fig. 1. Brain endothelial cells were labeled with carboxy-H_2DCFDA and either untreated (labeled control) or treated for 24 h with HNE-modified LDL (HNE-modified LDL). Fluorescence intensity (relative units) emitted from untreated and treated endothelial cells was excited with 488 nm laser light. **(A)** Actual spectra from a representative single experiment. **(B)** Comparison of fluorescence intensity per individual cell (mean ± standard error values from three experiments) emitted from untreated and treated endothelial cells. **, $P<0.01$, significantly higher than for the labeled control.

to 3 relative units on our scale) because of naturally existing fluorophores (proteins and lipids), also named "native fluorophores" *(20)*, when exposed to the laser light of 488 nm (Fig. 1A). The endothelial cells exposed to HNE-modified LDL showed a significantly ($P < 0.01$), increased amount of ROS,

approximately 3-fold, compared to untreated cells (Fig. 1B). To examine the accuracy of these experimental results, we analyzed the effect of treatment with the reference agents (glutathione and diamide) on the intracellular level of ROS in endothelial cells (Fig. 2). Treatment with glutathione reduced the amount of intracellular ROS while diamide did not significantly alter ROS levels. However, there was a significant ($P<0.01$) difference between ROS levels, as assessed by mean fluorescence emission intensity, between glutathione and diamide-treated cells.

Flow cytometry and 2',7'-dichlorofluorescein diacetate have also been utilized by other investigators to study changes in endothelial-cell ROS levels in response to ischemia *(8)*, hypoxia *(10)*, transformation *(21)*, apoptosis *(22,23)* and signaling cascade activation *(7)*. Although 100 μ*M* carboxy-H_2DCFDA is commonly used *(24)*, this concentration was insufficient for labeling brain endothelial cells. Because our experiments required 300 μ*M* carboxy-H_2DCFDA to optimally label brain endothelial cells in suspension, we performed experiments to determine whether the higher level of DMSO that is present at this concentration of carboxy-H_2DCFDA would affect endothelial cell viability. Our results indicate that based on the similarity of the light scattering pattern from unlabeled and labeled control samples (Figs. 3A,C), the amount of DMSO present during labeling was not harmful.

In our previous studies we have focused on possible links between brain endothelial cell injury and age-related degenerative disorders, especially neurodegenerative diseases *(25)*. In the current study we report that oxidized LDLs raise brain endothelial cell ROS levels and therefore could be important mediators of endothelial cell injury in several disease states where these lipid species are elevated.

4. CONCLUSION

Based on the results of this study and others, we conclude that detection of ROS in cultured endothelial cells by flow cytometry is an easy-to-apply, accurate and dependable experimental method.

REFERENCES

1. Cai., H. and Harrison, D. G. (2000) Endothelial dysfunction in cardiovascular diseases: the role of oxidant stress. *Circ. Res.* **87,** 840–844.
2. Gimbrone, M. A., Jr. (1995) Vascular endothelium: an integrator of pathophysiologic stimuli in atherosclerosis. *Am. J. Cardiol.* **75,** 67B–70B.
3. Wolin, M. S. (2000) Interactions of oxidants with vascular signaling systems. Arterioscler. *Thromb. Vasc. Biol.* **20,** 1430–1442.

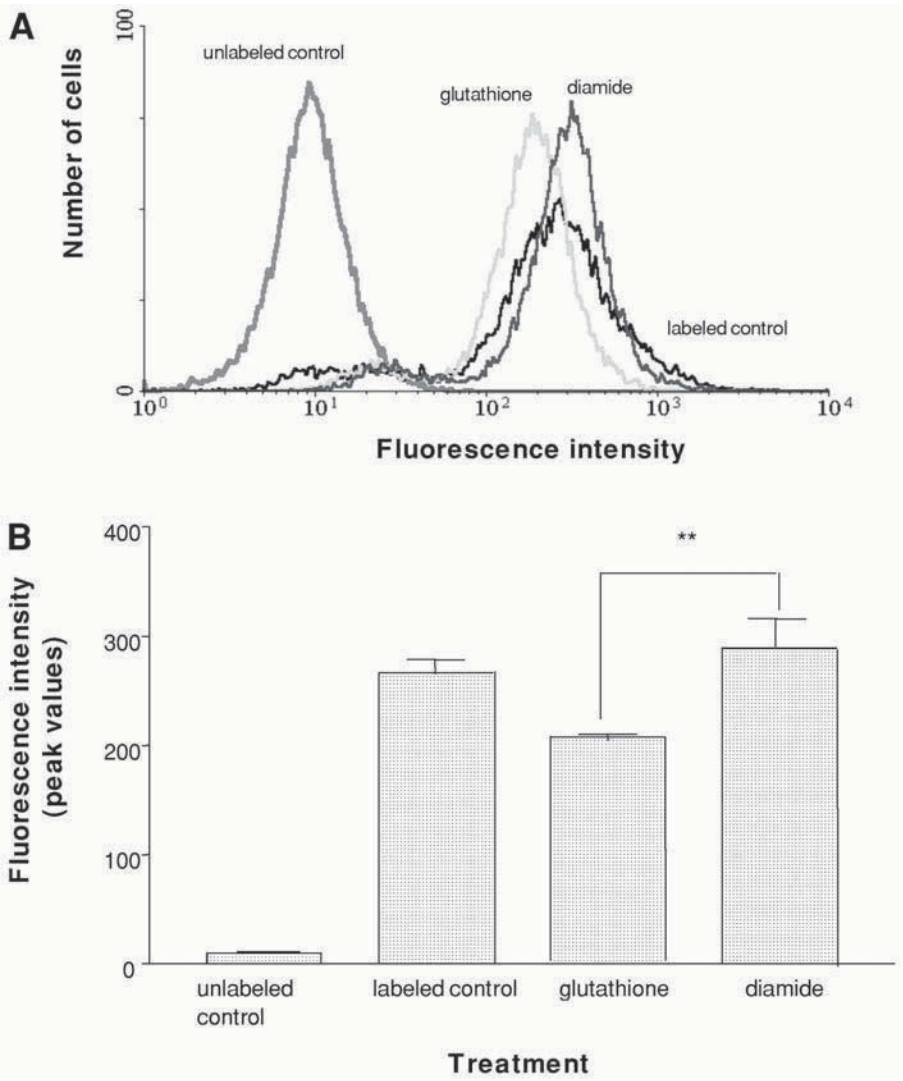

Fig. 2. Brain endothelial cells were labeled with carboxy-H_2DCFDA and either untreated (labeled control) or treated for 24 h with glutathione (glutathione) and diamide (diamide). Fluorescence intensity (relative units) emitted from untreated and treated endothelial cells was excited with 488 nm laser light. **(A)**Actual spectra from a representative single experiment. **(B)** Comparison of fluorescence intensity per individual cell (mean ± standard error values from three experiments) emitted from untreated and treated endothelial cells. **, $P<0.01$, significantly higher than for glutathione.

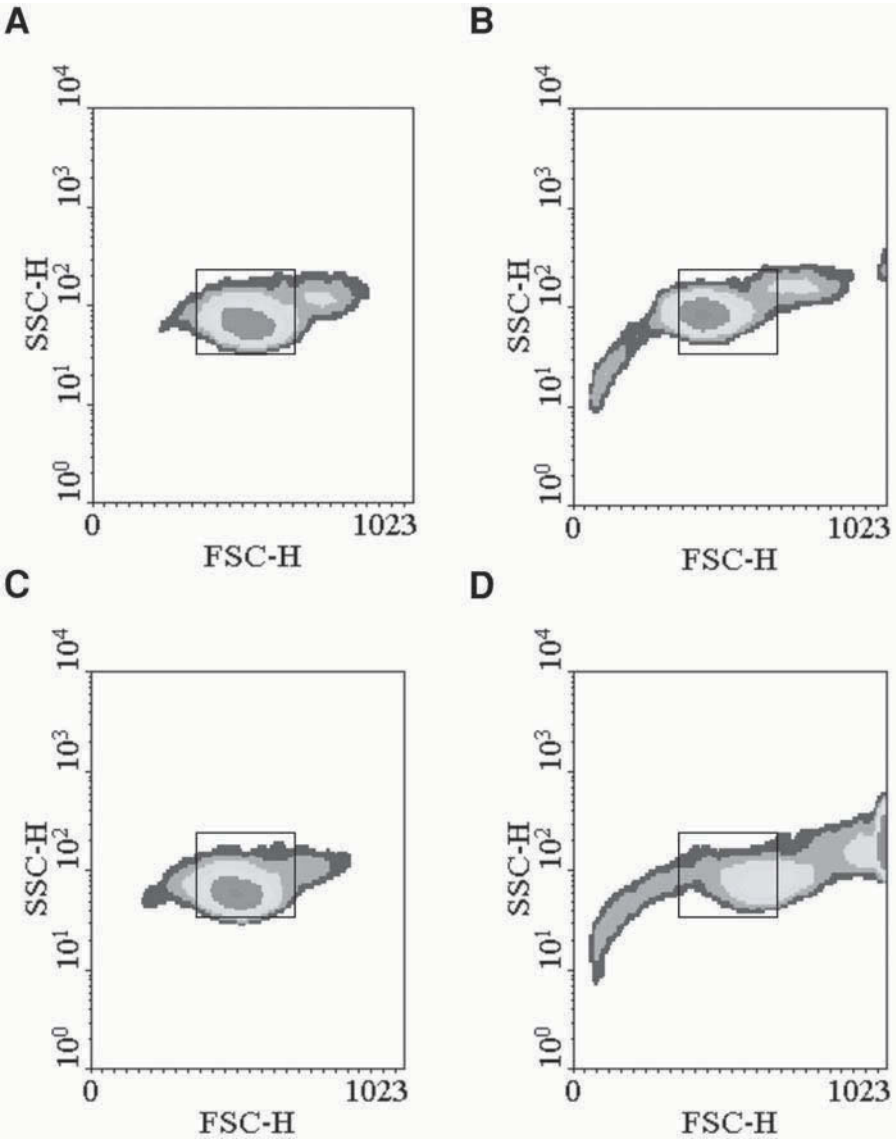

Fig. 3. Density plots of forward (FSC-H) vs side (SSC-H) scattering of the laser light produced by unlabeled **(A)**, labeled **(B)** with 100 μ*M* carboxy-H_2DCFDA, labeled with 300 μ*M* carboxy-H_2DCFDA **(C)**, and labeled with 500 μ*M* carboxy-H_2DCFDA **(D)** brain endothelial cells.

4. Herzenberg, L. A., De Rosa, S. C., and Herzebberg, L. A. (2000) Monoclonal antibodies and the FACS: complementary tools for immunobiology and medicine. *Immuno. Today* **21,** 383–390.
5. Herzenberg, L. A. Parks, D., Sahaf, B., Perez, O., Roederer M., and Herzenberg L. A. (2002) The history and future of Fluorescence Activated Cell Sorer and Flow Cytometry: A view from Stanford. *Clin. Chem.* **48,** 1819–1827.
6. Strasser, A., Stanimirovic, D., Kawai, N., McCarron, R. M., and Spatz M. (1997) Hypoxia modulates free radical formation in brain microvascular endothelium. *Acta. Neurochir. Suppl.* **70,** 8–11.
7. Colavitti, R., Pani, G., Bedogni, B., Anzevino, R., Borrello S., Waltenberger J., and Galeotti T. (2002) Reactive oxygen species as downstream mediators of angiogenic signaling by vascular endothelial growth factor receptor-2/KDR. *J. Biol. Chem.* **277,** 3101–3108.
8. Wei, Z., Al-Mehdi, A. B., and Fisher, A. B. (2001) Signaling pathway for nitric oxide generation with simulated ischemia in flow-adapted endothelial cells. *Am. J. Physiol. Heart Circ. Physiol.* **281,** H2226–H2232.
9. Burlacu, A., Jinga, V., Gafencu, A. V., and Simionescu, M. (2001) Severity of oxidative stress generates different mechanisms of endothelial cell death. *Cell Tissue. Res.* **306,** 409–416.
10. Ali, M. H., Schlidt, S. A., Chandel, N. S., Hynes, K. L., Schumacker, P. T., and Gewertz, B. L. (1999) Endothelial permeability and IL-6 production during hypoxia: role of ROS in signal transduction. *Am. J. Physiol.* **277,** L1057–1065.
11. Diglio, C. A., Liu, W., Grammas, P., Giacomelli, F., and Wiener J. (1993) Isolation and characterization of cerebral resistance vessel endothelium in culture. *Tissue. Cell* **25,** 833–846.
12. Grammas, P., Botchlet, T., Fugate, R., Ball, M. J., and Roher, A. E. (1995) Alzheimer disease amyloid proteins inhibit brain endothelial cell proliferation in vitro. *Dementia* **6,** 126–130.
13. Grammas, P., Moore, P., Cashman, R. E., and Floyd, R. A. (1998) Anoxic injury of endothelial cells causes divergent changes in protein kinase C and protein kinase A signaling pathways. *Mol. Chem. Neuropathol.* **33,** 113–124.
14. Kanmogne, G. D., Grammas, P., and Kennedy, R. C. (2000) Analysis of human endothelial cells and cortical neurons for susceptibility to HIV-1 infection and co-receptor expression. *J. Neurovirol.* **6,** 519–528.
15. Grammas, P. and Ovase, R. (2002) Cerebrovascular transforming growth factor-beta contributes to inflammation in the Alzheimer's disease brain. *Am. J. Pathol.* **160,** 1583–1587.
16. Rajah, T. T. and Grammas, P. (2002) VEGF and VEGF receptor levels in retinal and brain-derived endothelial cells. Biochem. *Biophys. Res. Commun.* **293,** 710–713.
17. Chen, Q., Esterbauer, H., and Jurgens, G. (1992) Studies on epitopes on low-density lipoprotein modified by 4-hydroxynonenal. Biochemical characterization and determination. *Biochem. J.* **288,** 249–254.
18. Uchida, K., Toyokuni, S., Nishikawa, K., Kawakishi, S., Oda H., Hiai, H., and Stadtman, E. R. (1994) Michael addition-type 4-hydroxy-2-nonenal adducts in

modified low-density lipoproteins: markers for atherosclerosis. *Biochemistry* **33,** 12,487–12,494.

19. Galle, J., Heinloth, A., Schwedler S., and Wanner C. (1997) Effect of HDL and atherogenic lipoproteins on formation of O_2^- and renin release in juxtaglomerular cells. *Kidney Int.* **51,** 253–260.
20. Richards-Kortum, R. and Sevick-Muraka, E. (1996) Quantitative optical spectroscopy for tissue diagnosis. *Annu. Rev. Phys. Chem.* **47,** 555–606.
21. Sheehan, J. P., Swerdlow, R. H., Miller, S. W., Davis, R. E., Parks, J. K., Parker, W. D., and Tuttle, J. B. (1997) Calcium homeostasis and reactive oxygen species production in cells transformed by mitochondria from individuals with sporadic Alzheimer's disease. *J. Neurosci.* **17,** 4612–4622.
22. Deshpande, S. S., Angkeow, P., Huang, J., Ozaki, M., and Irani, K. (2000) Rac1 inhibits TNF-alpha-induced endothelial cell apoptosis: dual regulation by reactive oxygen species. *FASEB J.* **14,** 1705–1714.
22. Assaly, R., Olson, D., Hammersley, J., Fan, P. S., Liu, J., Shapiro, J. I., and Kahaleh, M. B. (2001) Initial evidence of endothelial cell apoptosis as a mechanism of systemic capillary leak syndrome. *Chest* **120,** 1301–1308.
24. Geller, H. M., Cheng, K. Y., Goldsmith, N. K., Romero, A. A., Zhang, A. L., Morris, E. J., and Grandison L. (2001) Oxidative stress mediates neuronal DNA damage and apoptosis in response to cytosine arabinoside. *J. Neurochem.* **78,** 265–275.
25. Grammas, P. (2000) A damaged microcirculation contributes to neuronal cell death in Alzheimer's disease. *Neurobiol. Aging* **21,** 199–205.

21

Nitrite Determination by Colorimetric and Fluorometric Griess Diazotization Assays

Simple, Reliable, High-Throughput Indices of Reactive Nitrogen Species in Cell-Culture Systems

Kenneth Hensley, Shenyun Mou, and Quentin N. Pye

1. INTRODUCTION

Reactive nitrogen species (RNS) are generated as part of inflammatory reactions, mostly as a consequence of inducible nitric oxide synthase (iNOS) (reviewed in refs. *1–3*). Typically, nitric oxide (•NO) is produced by macrophage-type cells or, in the central nervous system (CNS), by reactive microglia. The iNOS enzyme catalyzes the oxidative conversion of arginine to citrulline, plus •NO free radical. Normally, iNOS activity is high and sustained irrespective of cytosolic Ca^{2+} levels. This contrasts sharply with the activity of constitutively expressed forms of nitric oxide synthase (NOS), such as neuronal NOS (nNOS) or endothelial NOS (eNOS), which normally generate only small bursts of •NO in response to transient Ca^{2+} currents *(2)*. Under some circumstances, constitutive forms of NOS may generate profligate quantities of •NO. For instance, eNOS can be phosphorylated by a protein kinase B (AKT)-dependent pathway, after which the phosphorylated enzyme loses Ca^{2+} dependence and becomes a copious producer of RNS *(4–5)*. •NO *per se* is a vasodilator and neurotransmitter, but likely not a major toxin. The •NO free radical is relatively unstable in the biological milieu, reacting via complex pathways to yield secary and tertiary RNS, such as peroxynitrite ($ONOO^-$) and $•NO_2$ free radical. These products may be much more deleterious than the original •NO radical (reviewed in ref. *1*).

It is often desirable to have a simple, reliable indicator of RNS production in cell-culture systems, or to have a simple quantitative index of

From: *Methods in Pharmacology and Toxicology: Methods in Biological Oxidative Stress*
Edited by: K. Hensley and R. A. Floyd

cytokine stimulation. Frequently this goal can be accomplished using a straightforward assay for nitrite (NO_2^-) production, which is readily adaptable to measure nitrate (NO_3^-) after chemical or enzymatic reduction to nitrite. Both nitrite and nitrate are formed by autoxidation of •NO (Fig. 1). Hence these anions are suitable, stable analytes indicative of cumulative •NO flux.

The chemical basis for NO_2^- determination is the Griess diazotization assay, first described in the 19th century *(6)* and recently adapted to a variety of colorimetric, fluorometric, and amperometric protocols *(7–11)*. In the typical Griess assay, NO_2^- is allowed to react with an aromatic amine in acidic medium to yield a colored or fluorescent azo derivative (Fig. 1). The reaction may be direct or indirect (Fig. 1). Two of the more reliable variants of the Griess assay are described below (fluorometric and colorimetric protocols in Subheading 3., Methods, with an illustrated application to the determination of RNS production by microglial cells in culture. Both assays are suitable for microplate-based experimental designs and high-throughput analyses.

2. MATERIALS

1. Sodium nitrite ($NaNO_2$) stock solution, 10 m*M* in H_2O (stable for at least 1 mo at 4°C).
2. 1% sulfanilamide, in 10% HCl (LabChem, Pittsburgh, PA, or other supplier).
3. 0.1% aqueous N-1(naphthylethyl)ethylenediamine dihydrochloride (LabChem or other supplier).
4. Diaminonapthalene (DAN), 100 m*M* in dimethyl sulfoxide (DMSO) (for fluorometric NO_2^- assays only; Molecular Probes, Eugene OR).
5. 2 *N* NaOH (for fluorometric NO_2^- assays only).
6. Phenol red-free cell culture medium (usually Dulbecco's modified Eagles' Medium [DMEM], but any phenol red-free formulation will be adequate subject to the constraints of the investigator's particular cell-culture needs).
7. Recombinant murine TNF-α (Calbiochem, San Diego, CA) or other cell stimulus.
8. MTS tetrazolium viability reagent (CellTiter AqueousOne® Solution, Promega, Madison WI).

3. METHODS

3.1. Cell Cultures

The particular paradigm used for treatment of cells will need to be optimized for the purposes of the individual researcher. A useful positive control consists of RAW macrophages or Walker EOC-20 microglia (American Type Culture Collection, ATCC, Rockville MD). EOC-20 cells in particular

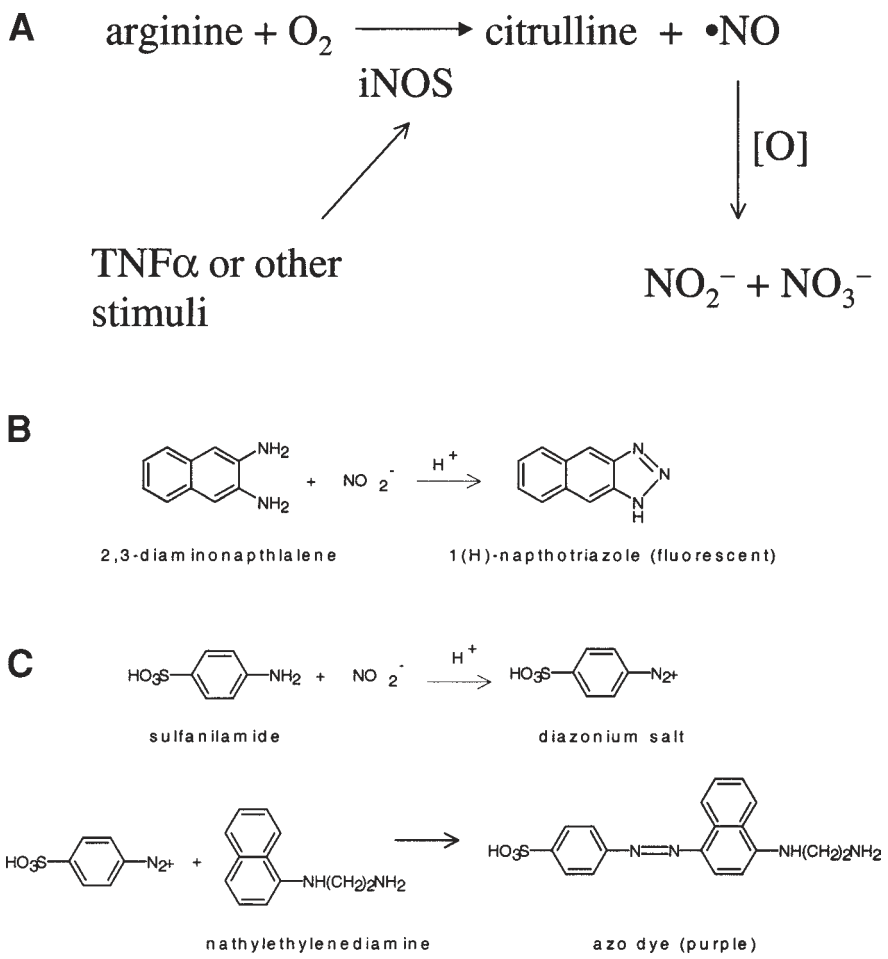

Fig. 1. **(A)** Biochemistry of NO_2^- production in immune cells experiencing a pro-inflammatory challenge. **(B)** Chemistry of diazotization reaction (Griess reaction) using the colorigenic compound (napthyl)ethylenediamine or (**C**) the fluorogenic compound diaminonapthalene.

grow very rapidly and respond aggressively to model stimuli, especially tumor necrosis factor alpha (TNFα). EOC-20 cells are a characterized, nonvirus-transformed, colony-stimulating factor 1 (CSF-1) dependent mouse microglial cell line that expresses IgG receptors FcγRI and II; Mac-1, Mac-2, Mac-3, CD45, CD80, and major histocompatibility complex (MHC-I) constitutively and expresses MHC-II in response to interferon-γ (IFN-γ) *(12)*. EOC-20 cells therefore closely resemble macrophages and primary microglial insofar as they have been characterized.

Typically, EOC-20 cells are grown in 75cm^2 cell culture flasks until passaged into 24-well cell culture plates. Cells are easily maintained in DMEM medium supplemented with 10% fetal calf serum (FCS) and 20% L292 fibroblast-conditioned medium. L292 cells (also available through ATCC) are a transformed cell line that secretes copious quantities of colony-stimulating factor 1 (CSF-1), which promotes proliferation of the EOC-20 cells. Proliferation rate can be modified by varying the percentage of L292-conditioned medium in the mixture.

Cells are typically stimulated as in the following example. Cells are grown to confluence and medium replaced with fresh medium. Stimulus (e.g., TNF-α dissolved and diluted in saline plus 4% pyrogen-free bovine serum albumin [BSA]) is added to the cells in a concentration of 1–20 ng/mL. Cells are placed in a standard incubator for 24 at which time the Griess assay is performed.

3.2. Nitrite Standard Curve

$NaNO_2$ is diluted 1:100 from the 10 m*M* stock solution into EOC-20 cell culture medium. Serial $^1/_2$ dilutions are made to yield final NO_2^- concentrations of 100 μ*M*, 50 μ*M*, 25 μ*M*, 12.5 μ*M*, 6.25 μ*M*, 3.13 μ*M*, and 1.57 μ*M*. A blank is prepared that consists of fresh EOC-20 medium only.

3.3. Colorimetric Nitrite Assay

Immediately before the assay, Griess reagent is made by combining equal volumes of the two components, N-1(naphthylethyl)ethylenediamine and sulfanilamide. 100 μL of sample (i.e., cell-culture medium or standard) is placed in appropriate wells of a 96-well clear microplate. If the medium is extremely proteinaceous or contains suspended cells, it may be necessary to centrifuge the sample prior to this step. To each well of the microplate, 100 μL of Griess reagent is then added. After 3–5 min, the optical density (OD) is measured at 560 nm and compared to the external standard curve. A typical standard curve is illustrated in Fig. 2.

3.4. Fluorometric Nitrite Assay

The typical fluorometric Griess assay is performed in a very similar fashion. 100 μL of sample is placed in each well of a 96-well microplate. Diaminonapthalene is diluted to 10 m*M* in water from the original 100 m*M* DMSO stock solution, and 1% HCl is added to the aqueous mixture to yield a working solution of DAN. 100 μL of DAN is added to each sample. After 10 min, an additional 100 μL of 2 *N* NaOH is added. The fluorescence intensity is then recorded at an excitation wavelength of 355 nm and an emission wavelength of 460 nm. A typical standard curve is illustrated in Fig. 3.

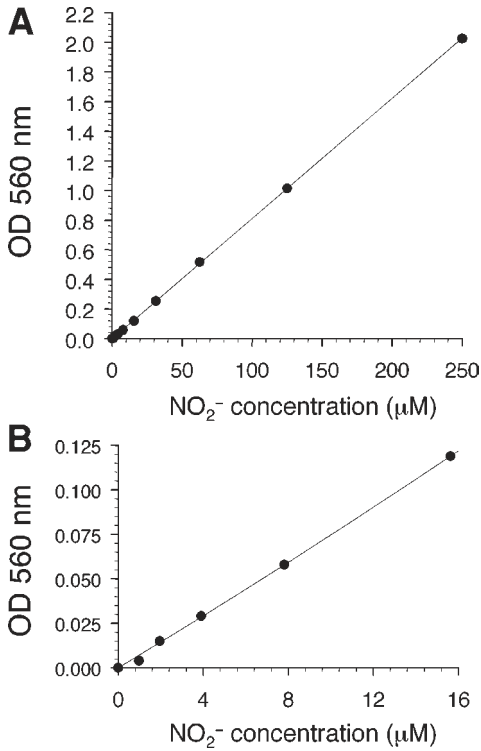

Fig. 2. Standard curves obtained for NO_2^- in Dulbecco's minimal essential medium (DMEM) containing phenol red. Each point is the mean of duplicate samples. In both (**A**) and (**B**), a linear curve fit is indicated ($r^2 = 0.99$). The acidity of the Griess reagent causes a pH shift and obviates most absorbance from the phenol red in the medium, so that phenol red is generally not a consideration in cell culture assays employing the NO_2^- assay.

3.5. Nitrite Plus Nitrate

If the researcher desires to measure NO_2^-, the sample must be reduced prior to the Griess assay. This can be done with NADPH plus NO_3^- reductase or by some inorganic catalysts, though the conversion efficiencies are often low *(7,9–11)*. In most cell systems, NO_2^- and NO_3^- correlate very well so that NO_2^- determination is a very accurate index of the magnitude of RNS production.

3.6. Viability Assays

It is often desirable to ascertain the viability of cells after recording nitrite levels in the medium. For this purpose, medium is removed and replaced with

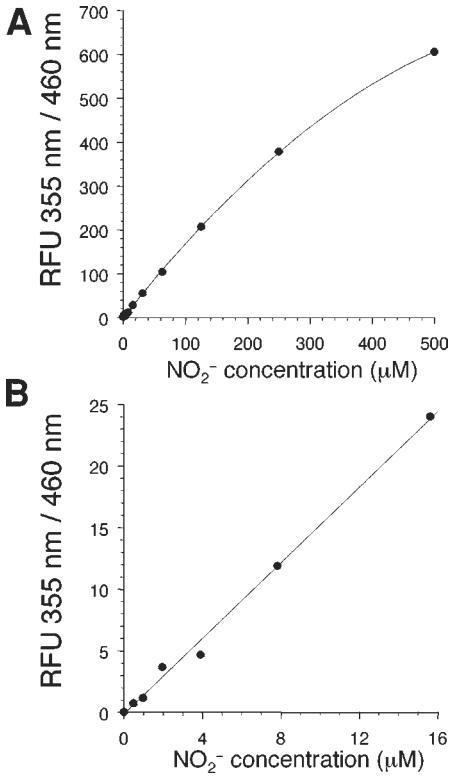

Fig. 3. Standard curves obtained for NO_2^- diluted into DMEM, using the fluorometric Griess assay with diaminonapthalene as the derivatizing reagent. The data indicate a mean of duplicate samples, fitted using a quadratic regression for the broad concentration range **(A)** or a linear regression for the narrower, low concentration range **(B)**.

phenol-free medium (usually DMEM) containing 2% MTS viability reagent (3-[4,5-dimethylthiazol-2-yl]-5-[3-carbosymethonyphenol]-2-[4-sulfopheyl]-2H-tetrazolium, inner salt), freshly diluted prior to the assay. Cells are placed at 37°C for 30 min to 1 h, after which time 200 μL of medium is removed and the OD measured at 540 nm. A blank is prepared containing viability reagent not exposed to cells; this is equivalent to 0% viability.

4. DISCUSSION

The Griess assay is a convenient, robust, and inexpensive assay for indexing a pro-inflammatory stimulus impinging upon an RNS-producing

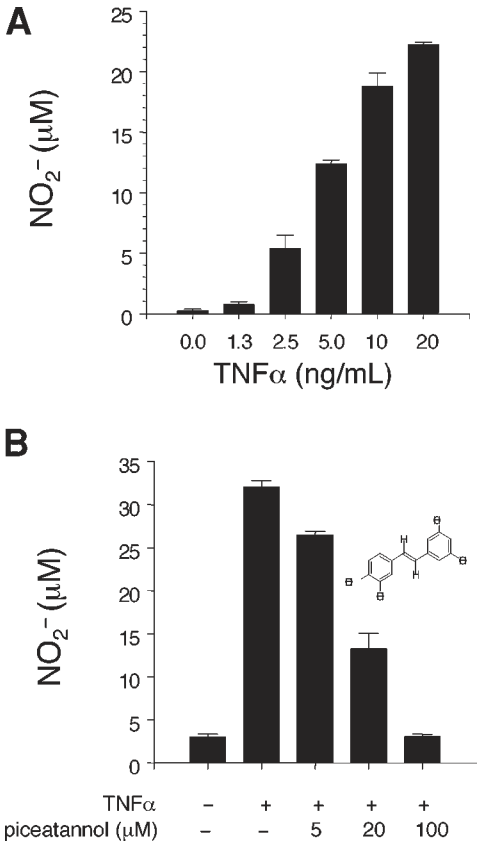

Fig. 4. NO_2^- production in EOC-20 microglial cells as a function of TNF-α concentration **(A)** and dose-dependent inhibition of the stimulus by piceatannol **(B)**; structure, inset). Data bars indicate mean ± standard deviation for four wells of a 24-well plate of cells.

cell. As an illustration, Fig. 4 demonstrates the dose-dependent stimulation of EOC-20 microglia by TNF-α as determined by the colorimetric Griess technique. Figure 4 further illustrates the dose-dependent inhibition of this stimulation by piceatannol, a polyphenolic anti-inflammatory compound and tyrosine kinase inhibitor.

In general, the colorimetric Griess assay is sensitive and precise enough to allow quantitative determination of the cellular response to a pro-inflammatory ligand, as well as the evaluation of inhibitory agents. The detection limit for the colorimetric Griess assay is typically 1 μ*M*, although this varies somewhat with the exact diamine used in the assay; N-1(naphthylethyl)ethylenediamine is one of the more sensitive commercially available diazotization agents available for

this purpose. The fluorometric Griess assay is somewhat more sensitive with detection limits of 0.2–0.5 μ*M* when diaminonapthalene is used as the derivatizing reagent. Both techniques yield linear responses in the range of 5–50 μ*M*, although a quadratic curve fit to a broad calibration curve is usually the best model for the standard curve (*see* Figs. 2–3).

The Griess assay can be used conveniently with most cell-culture media, including medium that contains phenol red. The acidity of the Griess reagent causes a pH shift that nullifies the absorbance of phenol red at 560 nm. Of course, for maximum accuracy, the external NO_2^- standard curve should be generated in the same medium used for culturing and stimulating the cells. Contrastingly, viability measurements must be performed in phenol red-free medium, to avoid interference between the phenol red and the reduced formazan produced by live cells as they metabolize the tetrazolium reagent.

ACKNOWLEDGMENTS

This work was supported by the National Institutes of Health (NIH NS35747), the American Heart Association (AHA0051176Z) and the Oklahoma Center for the Advancement of Science and Technology (OCAST HR02149R).

REFERENCES

1. Hensley, K., Williamson, K. S., and Floyd, R. A. (2000) Measurement of 3-nitrotyrosine and 5-nitro-γ-tocopherol by high-performance liquid chromatography with electrochemical detection. *Free Radic. Biol. Med.* **28,** 520–528.
2. Fukuto, J. M. and Chaudhuri, G. (1995) Inhibition of constitutive and inducible nitric oxide synthase: potential selective inhibition. *Annu. Rev. Pharmacol. Toxicol.* **35,** 165–194.
3. Maxwell, A. J. (2000) Mechanisms of dysfunction of the nitric oxide pathway in vascular diseases. *Nitric Oxide* **6,** 101–124.
4. Fulton, D., Gratton, J. P., McCabe, T. J., Fontana, J., Fujio, Y., Walsh, K., et al. (1999) Regulation of endothelium-derived nitric oxide production by the protein kinase Akt. *Nature* **399,** 597–601.
5. Dimmeler, S., Fleming, I., Fisslthaler, B., Hermann, C., Busse, R., and Zeiher, A. M. (1999) Activation of nitric oxide synthase in endothelial cells by Akt-dependent phosphorylation. *Nature* **399,** 601–605.
6. Griess, J. P. (1879) *Ber. Deutsch. Chem. Ges.* **12,** 426–428.
7. Archer, S. (1993) Measurement of nitric oxide in biological models. *FASEB J.* **7,** 349–360.
8. Misko, T. P., Shilling, R. J., Salvemini, D., Moore, W. M., and Currie, M. G. (1993) A fluorometric assay for the measurement of nitrite in biological samples. *Anal. Biochem.* **214,** 11–16.

9. Tsikas, D., Gutszki, F.-M., Rosa, S., Bauer, H., Neuman, C., Dockendorff, K., et al. (1997) Measurement of nitrite and nitrate in biological fluids by gas chromatography-mass spectrometry and by the Griess assay: problems with the Griess assay: solutions by gas chromatography-mass spectrometry. *Anal. Biochem.* **244,** 208–220.
10. Borcherding, H., Leikefeld, S., Frey, C., Diekmann, S., and Steinrucke, P. (2000) Enzymatic microtiter plate-based nitrate detection in environmental and medical analysis. *Anal. Biochem.* **282,** 1–9.
11. Sohn, O. S. and Fiala, E. S. (2000) Analysis of nitrite/nitrate in biological fluids: denitrification of 2-nitropropane in F344 rats. *Anal. Biochem.* **279,** 202–208.
12. Walker, W. S., Gatewood, J., Olivas, E., Askew, D., and Havenith, C. E. G. (1995) Mouse microglial cell lines differing in constitutive and interferon-gamma-inducible antigen-presenting activities for naïve and memory CD4+ and CD8+ T cells. *J. Neuroimmunol.* **63,** 163–174.

22

Protein Carbonyl Determination Using Biotin Hydrazide

Kenneth Hensley and Kelly S. Williamson

1. INTRODUCTION

Protein oxidation is a recognized component of aging and a consequence of severe or prolonged exposure to reactive oxygen species (ROS). Direct attack of protein by ROS causes formation of protein-bound carbonyl groups *(1)*. These carbonyl functions represent a variety of site-specific modifications, most particularly adipic and glutamic acid semialdehydes *(2)*. Additionally, numerous lipid oxidation products, including α,β-unsaturated γ-hydroxyalkenals can attack proteins yielding protein-bound aldehydes *(3)*. Furthermore, nonemzymatic glycation can yield protein-bound carbonyl functionalities *(4)*. Thus, protein carbonyls represent a possibly convenient indicator of oxidative stress. A variety of techniques have been introduced to measure protein carbonyls in tissue extracts, where they are found to increase exponentially as a function of organism aging *(5)*. All the extant techniques for protein carbonyl determination rely upon reductive amination between the carbonyl group and a probe, typically dinitrophenylhydrazine (DNPH) *(5–6)*. Antibodies specific to the probe can then be used to visualize protein carbonyls.

There are some serious shortcomings in the use of DNPH to measure protein carbonyls. The derivitization chemistry is more cumbersome and less efficient than might be desired, but most importantly, the technique requires the use of primary and secary antibodies that are not perfectly specific. Moreover, the need for secary antibodies in most Western-blot applications renders the DNPH method unsuitable for matrices containing high levels of intrinsic immunoglobulin G (IgG), such as serum or liver tissue. To circumvent these difficulties, we have developed a technique that uses biotin

From: *Methods in Pharmacology and Toxicology: Methods in Biological Oxidative Stress*
Edited by: K. Hensley and R. A. Floyd

hydrazide rather than DNPH as the carbonyl-reactive probe. The reaction chemistry is direct and does not require catalysts or reducing agents. Derivatized proteins can be visualized using streptavidin-conjugated peroxidase or, alternatively, can be captured on a monomeric avidin column for subsequent concentration and analysis.

2. MATERIALS

1. Biotin hydrazide: Dissolve to 50 m*M* in dimethyl sulfoxide (DMSO) and freeze at –20°C (stable for at least 6 mos).
2. Streptavidin-conjugated horseradish peroxidase: Stock solution made to 0.5 mg/mL in sterile saline and frozen in aliquots at –20°C; stable for at least 3 mos).
3. N-Morpholino-ethanesulfonate (MES buffer): 20 m*M* in water, adjusted to pH 5.5.
4. Butylated hydroxytoluene (BHT) 100 m*M* in absolute ethanol.
5. Ferrous sulfate ($FeSO_4$).
6. Desferroxamine mesylate (DFO), an iron chelator, 100 m*M* in saline.
7. Ascorbic acid, 100 m*M* in water, pH 7.2.

3. METHODS

1. In vitro oxidation of tissue homogenate. The following procedure has been adapted for oxidation of central nervous system (CNS) tissue homogenates, but may be used in other applications. Tissue is lysed in any desired buffer containing protease inhibitors; a typical buffer is 10 m*M* sodium acetate, pH 7.2, plus 0.1% triton X-100. The lysate is clarified by centrifugation and the supernatant removed for protein concentration analysis, then adjusted to 4 mg/mL.
2. Aliquots of protein extract are prepared for in vitro oxidation. Typically, 0.5-mL aliquots are prepared for each reaction but the reaction size may be scaled according to the needs of the researcher. The following treatments are prepared:
   a. Control: 0.5 mL protein extract, 30 μL saline.
   b. Ascorbic acid control: 25 μL ascorbic acid.
   c. Iron gradient samples: 25 μL ascorbic acid plus 5 μL of 100X concentrated Fe^{2+} solution. Copper tends to be more redox-active, but the choice of metal should be empirically determined based on the investigator's individual needs. Typically, the final concentration of iron should span a range from 1 to 200 m*M*.

   Samples are incubated for 60 min at room temperature with gentle agitation. Reactions are terminated by addition of 1/10 volume of 100 m*M* DFO and 25 μL of ethanolic BHT. When iron is used as the redox active metal, the investigator may also add 1 m*M* desferoxamine mesylate to chelate the metal. Samples are diluted 1:1 in 20 m*M* MES buffer, pH 5.5. For brain-tissue lysates, the aforementioned procedure is sufficient to ensure protein oxidation *(7)*. For pure proteins, the researcher may desire to add an additional 1 m*M* H_2O_2 to intensify the oxidation reactions.

3. Alternative protocol for preparation of experimental tissue. If carbonyls are to be compared between experimental groups of animals, the tissue is removed and rapidly lysed in 20 m*M* MES buffer, pH 5.5, containing 0.1% triton X-100 and standard protease inhibitors. Ethanolic BHT is added to a final concentration of 1 m*M* and the sample is clarified by centrifugation, then adjusted to 2 mg/mL total protein concentration.
4. Labeling. To each volume of lysate, biotin hydrazide is added to a final concentration of 5 m*M*. Tissue is incubated for 8 h at room temperature with gentle agitation. The researcher may wish to optimize time of labeling for his/her specific purposes.
5. Western blot development. Typically, the labeled sample is mixed 1:1 with standard sodium dodecyl sulfate (SDS)-loading buffer (5% SDS, 4% mercaptoethanol, 50% glycerol, 0.01% bromophenol blue, 0.2 *M* tris) and electrophoresed using appropriate polyacrylamide gels. After transfer to PVDF membrane, the sample is blocked for 2 h in 3% bovine serum albumin (BSA). The blot is then probed for 1 h with 0.1 mg/mL streptavidin-horseradish peroxidase (HRP) in 3% BSA plus 1.5% Tween-20. The blot is then washed thoroughly in 1.5% Tween-20 and developed using peroxidase substrates of choice. Usually, enhanced chemiluminescence reagents are preferable.
6. Analysis. For most applications, densitometry can be performed to quantify differences in protein carbonyl levels among experimental groups. If desired, protein standard of known oxidation level can be used as an internal control for densitometric applications. The technique can be adapted for one- or two-dimensional (1D/2D) gels, or for dot blots. Alternatively, protein can be captured on a monomeric avidin column and eluted with 5 m*M* biotin for subsequent proteomic or enzymological analysis.
7. Controls for specificity. In some cases, it is possible, that proteins may be visualized nonspecifically through the interaction of the streptavidin-HRP with endogenous biotin or other structures. To control for this possibility, subsitute biotin for biotin hydrazide in the labeling reaction and develop as described in step 6. Nonspecific proteins will remain during the substitution; specifically carbonylated proteins will be visualized only in the presence of the biotin hydrazide derivatizing agent.

4. DISCUSSION

Biotin hydrazide reacts exclusively with carbonyl groups at pH 5.5, as illustrated in Fig. 1. This reaction facilitates the use of biotin hydrazide in the ultrasensitive detection of carbonylated (oxidized) proteins in biological samples (Fig. 2). A convenient control can be performed by substitution of biotin for biotin hydrazide, therefore determining specificity of the labeling reaction. Proteins labeled with biotin hydrazide are suitable for subsequent protein studies after purification over standard monomeric avidin affinity columns.

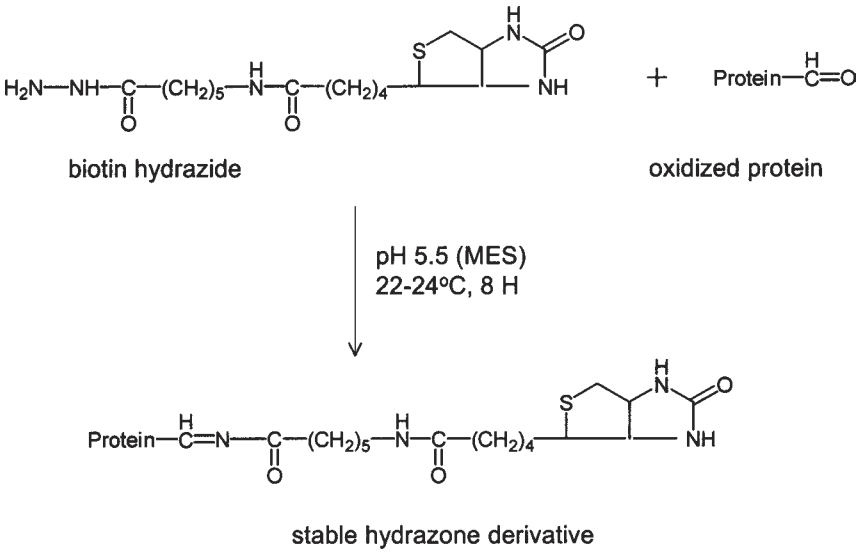

Fig. 1. Chemistry of biotin hydrazide reaction with protein carbonyls to yield a stable hydrazone derivative.

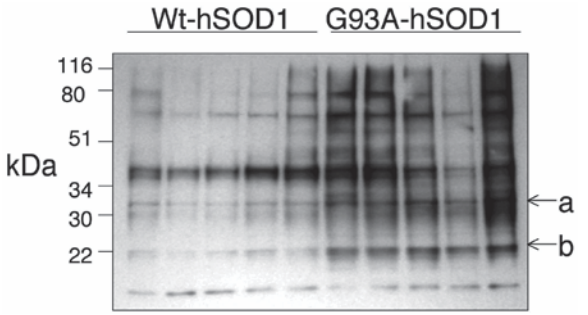

Fig. 2. Protein oxidation in biological tissues as visualized using the biotin hydrazide method. Spinal cord protein extracts were prepared from mice expressing human wild-type superoxide dismutase 1 (SOD1), or mice expressing equivalent copy numbers of mutant SOD1 containing a Gly to Ala substitution at residue 93 (G93A-SOD1). The mutant SOD1 expressing animals develop symptoms of amyotrophic lateral sclerosis (ALS), a degenerative motor neuron disease, and experience age-related spinal cord protein oxidation *(8)*. All samples were collected from 120–130 D mice and processed as described in the text. Note the specifically increased carbonylated proteins at 32 kDa **(A)** and 20 kDa **(B)** apparent molecular weight. The 20 kDa band has been identified as SOD1 *(8)*.

ACKNOWLEDGMENTS

This work was supported by the National Institutes of Health (NIH NS35747), the American Heart Association (AHA0051176Z), and the Oklahoma Center for Neurosciences.

REFERENCES

1. Stadtman, E. R. and Levine, R. L. (2000) Protein oxidation. *Ann. NY Acad. Sci.* **899,**191–208.
2. Requena, J. R., Chao, C. C., Levine, R. L., and Stadtman, E. R. (2001) Glutamic and aminoadipic semialdehydes are the main carbonyl products of metal-catalyzed oxidation of proteins. *Proc. Natl. Acad. Sci. USA* **98,** 69–74.
3. Esterbauer, H., Schaur, R. J., and Zollner, H. (1991) Chemistry and biochemistry of 4-hydroxynonenal, malonaldehyde and related aldehydes. *Free Radic. Biol. Med.* **11,** 81–128.
4. Baynes, J. W. and Thorpe, S. R. (2000) Glycoxidation and lipoxidation in atherogenesis. *Free Radic Biol. Med.* **28,** 1708–1716.
5. Smith, C. D., Carney, J. M., Starke-Reed, P. E., Oliver, C. N., Stadtman, E. R., Floyd, R. A., and Markesbery, W. R. (1991) Excess brain protein oxidation and enzyme dysfunction in normal aging and in Alzheimer disease. *Proc. Natl. Acad. Sci. USA* **88,** 10540–10543.
6. Levine, R. L., Wehr, N., Williams, J. A., Stadtman, E. R., and Shacter, E. (2000) Determination of carbonyl groups in oxidized proteins. *Methods Mol. Biol.* **99,** 15–24.
7. Hensley, K., Carney, J. M., Hall, N., Shaw, W., and Butterfield, D. A. (1994) Electron paramagnetic resonance investigations of free radical induced alterations in neocortical synaptosomal membrane protein infrastructure. *Free Radic. Biol. Med.* **17,** 321–331.
8. Andrus, P. K., Fleck, T. J., Gurney, M. E., and Hall, E. D. (1998) Protein oxidative damage in a transgenic mouse model of familial amyotrophic lateral sclerosis. *J. Neurochem.* **71,** 2041–2048.

23

Real-Time, In-Vivo Measurement of Nitric Oxide Using Electron Paramagnetic Resonance Spectroscopic Analysis of Biliary Flow

Kenneth Hensley, Yashige Kotake, Danny R. Moore, Hong Sang, and Lester A. Reinke

1. INTRODUCTION

The nitric oxide free radical (•NO) is formed by the enzymatic oxidation of arginine in a reaction catalyzed by various isoforms of the enzyme nitric oxide synthase (NOS). •NO serves myriad physiologic functions, including actions as a vasodilator. Under conditions of inflammation, macrophages (and certain other permissive cell types) synthesize copious quantities of •NO through the expression of an inducible isoform of NOS (iNOS). •NO may serve a defensive function against pathogens, acting as a microbial toxin. Combination of •NO with the superoxide radical anion ($O_2 \cdot^-$), also syntheisized by activated immune cells, leads to the formation of the highly reactive oxidant peroxynitrite ($ONOO^-$). •NO and its redox congeners have received much attention as pathophysiologic agents in both acute and chronic inflammation, septic shock, cardiovascular biology, and neurodegenerative disorders. The bioanalysis of •NO is complicated by the relative instability of this species in a biological mileu, where the •NO radical can decompose through oxygen-dependent pathways or alternatively be consumed through reaction with thiol moieties and heme groups. A method to continuously monitor the •NO level in anesthetized rats, using an in vivo trapping reaction of NO by iron-dithiocarbamate complex, is shown in this chapter.

•NO reacts with certain metal complexes to form very stable adducts detectable by electron paramagnetic resonance (EPR) spectroscopy (Fig. 1)

From: *Methods in Pharmacology and Toxicology: Methods in Biological Oxidative Stress*
Edited by: K. Hensley and R. A. Floyd © Humana Press Inc., Totowa, NJ

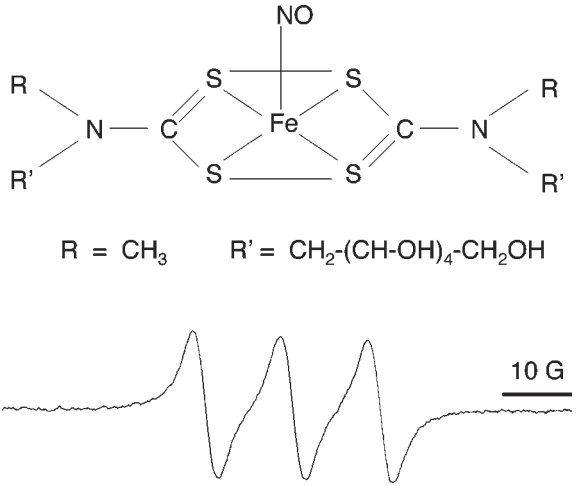

Fig. 1. Structure of the MGD-Fe-nitrosyl complex and its EPR spectrum (approx 10 m*M*).

(1,2). The formation of a nitrosyl adduct with dithiocarbamate-iron complexes has been used to monitor •NO production in cell culture *(3)*, in models of septic shock *(4–6)*, and in brain and heart tissue ex vivo *(7–8)*. We have adapted this technique to allow continuous monitoring of •NO in anesthetized but otherwise physiologically competent rats, that do not have a gall bladder and therefore continuously secrete bile into the duodenum *(9)*. The real-time analysis of •NO flux is accomplished by cannulation of the bile duct and flowing the bile directly through the EPR sample cell (Fig. 2). A complex of D-N-methylglucamine dithiocarbamate with iron (MGD-iron) is administered intravenously by means of a continuous saline drip. The EPR signal from MGD-Fe-NO formed in vivo is continuously monitored in bile effluent over the course of several h. The MGD-Fe-NO formation rate, measured by this technique, has been shown to respond vigorously to experimental manipulations such as the administration of an archetypical inflammatory stimulus (bacterial lipopolysaccharide, LPS) *(9)*. At the discretion of the researcher, N,N-diethyldithiocarbamate (DETC) may be substituted for MGD as an iron chelator *(9,10)*.

2. MATERIALS

1. Adult male Sprague-Dawley rats, 300–400 g in weight.
2. LPS (*Escherichia coli*).

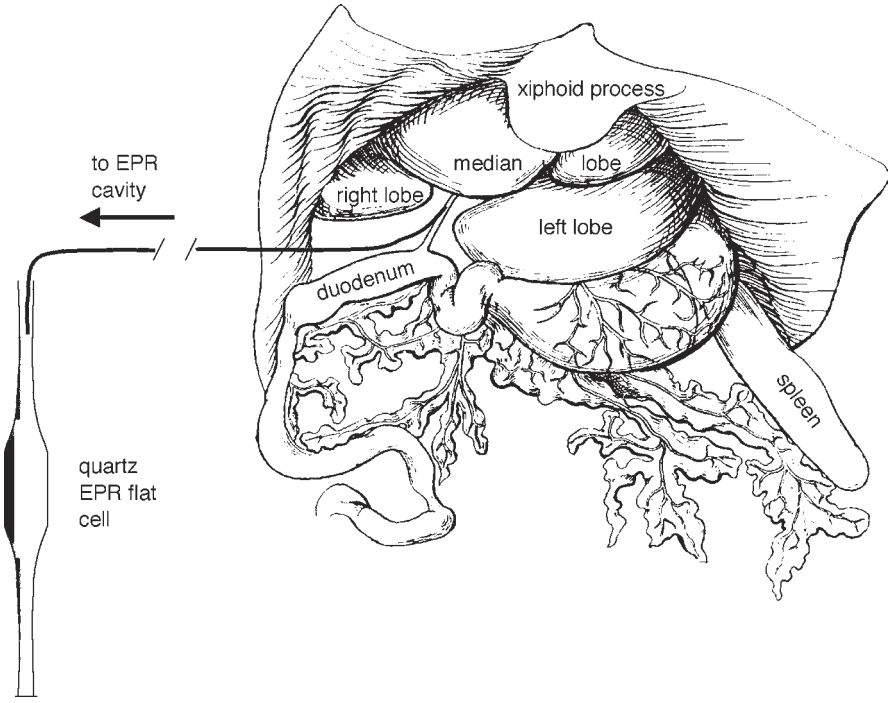

Fig. 2. Illustration of the surgical area used during in vivo cannulation of the rat bile duct.

3. Nω-nitro-L-arginine methyl ester (L-NAME) (a NOS inhibitor) and L-arginine (a NOS substrate).
4. Sodium MGD or DETC.
5. Ferrous sulfate [$FeSO_4 \cdot 7H_2O$].
6. Ketamine anesthetic, PE-10 polyethylene tubing, and standard surgical kit.
7. EPR flat cell (type WG814, Wilmad Glass, Buena, NJ) and EPR spectrometer (Bruker 300 E, Karlsruhe, Germany).
8. Syringe pump (type 22, Harvard Apparatus, South Natick, MA).

3. METHODS

1. Animal preparation and bile-duct cannulation. In order to induce continual and pronounced •NO generation in vivo, animals are treated by intraperitoneal injection of LPS at a dose of 3 mg/kg. Other stimulation paradigms may be utilized according to the needs of the individual researcher. Two h after LPS administration, animals are anesthetized with ketamine (70 mg/kg, i.p.). The experimental animal is placed on its back and the abdomen opened with a longitudinal excision. The bile duct is cannulated with PE-10 tubing (Fig. 2).

The animal is placed on a platform above the cavity of the EPR spectrometer and the end of the PE-10 tubing distal to the animal is inserted into the EPR flat cell, within the EPR cavity. Throughout the experiment, the animal is illuminated with a 200 W tungsten lamp to maintain body temperature while the abdomen is covered with saline-wetted sterile cotton gauze to prevent desiccation. The temperature of the peritoneal cavity is monitored with a contact thermometer.

2. I.V. cannulation and MGD-Fe administration. The inferior vena cava is exposed and cannulated with sterile polyethylene tubing and a three-way stopcock is inserted into the I.V. line. An aqueous solution of MGD (160 mg/kg, 0.52 mole/kg) and iron sulfate (16 mg/kg, 0.056 mole/kg) is infused through the I.V. line. Subsequently, physiologic saline with 10 m*M* MGD plus 1 m*M* iron sulfate is continuously infused through the I.V. line at a rate of 20 μL/min using a syringe pump.
3. Administration of test compounds. •NO formation can be pharmacologically modulated, for instance by addition to the animal of NOS inhibitors or by experimental compounds. As an archetype for pharmacologic inhibition of •NO flux, L-NAME is administered into the I.V. drip at a dose of 200 mg/kg. Other test compounds can be similarly administered.
4. EPR monitoring of •NO flux in bile effluent. The bile flow is adjusted to a constant rate by moving the end of the polyethylene (PE) tubing with respect to the flat cell until a rate of approx 120 μL/min is achieved. The EPR signal from the MGD-Fe-NO complex is obtained at approx 2400 G by setting instrumental parameters as follows: Field scan = 100 G; scan rate = 100 G/80 s; time constant = 0.16 s; field modulation = 100 kHz; modulation amplitude = 2 G; microwave power = 20 mW. For continuous monitoring of the MGD-Fe-NO signal, the magnetic field is fixed at the center of the first peak of the nitrosyl signal and the instrument is switched from the field scan mode to the time-scan mode.
5. Estimation of •NO concentration in bile effluent. Authentic MGD-Fe-NO is synthesized by adding a known amount of •NO gas (Alphagaz, Walnut Creek, CA)-saturated water (1.9 m*M* at 20°C) to a solution containing 100 m*M* MGD plus 10 mM ferrous sulfate. This standard solution is then diluted 1/20 in bile collected from untreated rats, and the EPR spectrum of the standard MGD-Fe-NO preparation is collected as previously described.

4. ANALYSIS

By setting the EPR instrument in the time-scan mode, a continuous trace is obtained illustrating the MGD-Fe-NO spectral intensity as a function of time (Fig. 3). Administration of pharmacologic inhibitors or stimulants of •NO production causes readily apparent deflection of the trace (Fig. 3). The data can be expressed as the average rate of MGD-Fe-NO formation, measured in arbitrary intensity units/time, or as μmoles of the MGD-Fe-NO complex formed per hour after comparison to an external MGD-Fe-NO standard.

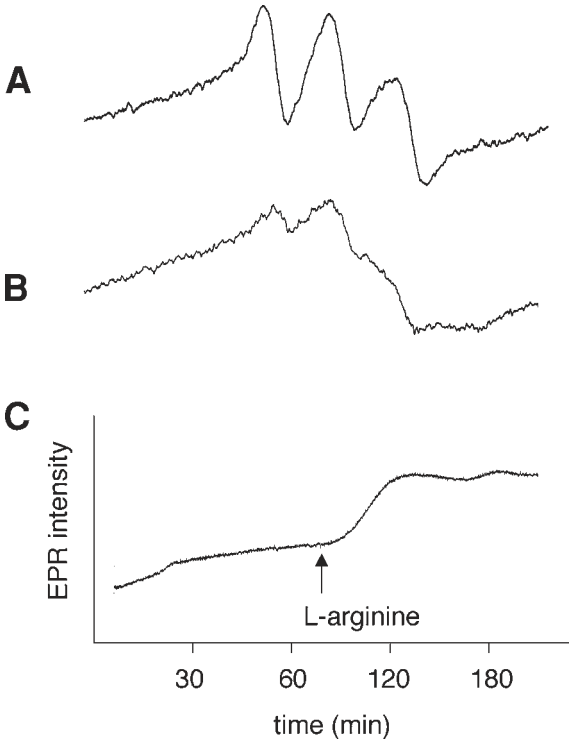

Fig. 3. EPR spectra (X-band) in bile recorded with the direct introduction of bile into the EPR sample cell. A rat was treated with saline or LPS (3 mg/kg) and in 0.5 h the bile duct was cannulated under ketamine anesthesia. **(A)** MGD-Fe-NO signature obtained from the bile 2 h after LPS administration. **(B)** MGD-Fe-NO signature obtained from the bile of a rat injected with vehicle only (saline), 2 h after administration. **(C)** Time-scan trace of MGD-Fe-NO signal obtained from the bile of an LPS treated rat, demonstrating acceleration of •NO flux induced by administration of the NOS substrate L-arginine (250 mg/kg bolus, I.V.).

5. DISCUSSION

The EPR spectrum of MGD-Fe-NO complex obtained from bile effluent is shown in Fig. 3. In addition to the three-line EPR signature characteristic of the MGD-Fe-NO complex ($g = 2.04$, $a_N = 12.6$ G), one can also observe a single broad EPR line attributable to the copper complex of MGD *(9)*. As the MGD-Fe-NO complex grows in intensity, the copper signal becomes less significant. Also, some background level of MGD-Fe-NO is observed even in normal, unstimulated animals, presumably owing to the action of constitutive NOS or to reduction of nitrite (NO_2^-). The signal intensity from

normal, unstimulated animals is very small and remains essentially unchanged over at least a 2-h period of cannulation. As shown in Fig. 3, the rate of •NO generation is sensitive to the concentration of the NOS substrate L-arginine and also to pharmacological inhibitors such as L-NAME *(9)*. Thus, the measurement of •NO flux using MGD-Fe as a trapping agent provides a reliable tool for basic research as well as a means for screening of iNOS inhibitors using a relevant *in vivo* model for acute inflammation.

ACKNOWLEDGMENTS

This work was supported by National Institutes of Health grant GM54878.

REFERENCES

1. Mordvintcev, P., Mulsch, A., Busse, R., and Vanin, A. (1991) On-line detection of nitric oxide formation in liquid aqueous phase by electron paramagnetic resonance spectroscopy. *Anal. Biochem.* **199,** 142–146.
2. Fujii, S. and Yoshimura, T. (2000) Detection and imaging of endogeously produced nitric oxide with electron paramagnetic resonance spectroscopy. *Antioxid. Redox. Signal* **2,** 879–901.
3. Kotake, Y. (1996) Continuous and quantitative monitoring of rate of cellular nitric oxide generation. *Methods Enzymol.* **228,** 222–229.
4. Wallis, G., Brackett, D., Lerner, M., Kotake, Y., Bolli, R., and McCay, P. B. (1996) In vivo spin trapping of nitric oxide generated in the small intestine, liver, and kidney during the development of endotoxemia: a time-course study. *Shock* **6,** 274–278.
5. Reinke, L. A., Moore, D. R., and Kotake, Y. (1996) Hepatic nitric oxide formation: spin trapping detection in biliary efflux. *Anal. Biochem.* **243,** 8–14.
6. Miyajima, T. and Kotake, Y. (1995) Spin trapping agent, phenyl N-tert-butyl nitrone, inhibits induction of nitric oxide synthase in endotoxin-induced shock in mice. *Biochem. Biophys. Res. Commun.* **215,** 114–121.
7. Zweier, J. L., Wang, P., and Kuppusamy, P. (1995) Direct measurement of nitric oxide generation in the ischemic heart using electron paramagnetic resonance spectroscopy. *J. Biol. Chem.* **270,** 304–307.
8. Suzuki, Y., Fujii, S., Numagami, Y., Tominaga, T., Yoshimoto, T., and Yoshimura, T. (1998) *In vivo* nitric oxide detection in the septic rat brain by electron paramagnetic resonance. *Free Radic. Res.* **28,** 293–299.
9. Kotake Y., Moore D. R., Sang H., and Reinke L. A. (1999) Continuous monitoring of in vivo nitric oxide formation using EPR analysis in biliary flow. *Arch. Biochem. Biophys.* **3,** 114–122.
10. Tominaga S., Sato T., Ohnishi T., and Ohnishi S. T. (1994). Electron paramagnetic resonance (EPR) detection of nitric oxide produced during forebrain ischemia of the rat. *J. Cereb. Blood Flow Metab.* **14,** 715–722.

Index

From: *Methods in Pharmacology and Toxicology: Methods in Biological Oxidative Stress*
Edited by: K. Hensley and R. A. Floyd © Humana Press Inc., Totowa, NJ

METHODS IN PHARMACOLOGY AND TOXICOLOGY
Mannfred A. Hollinger, PhD, Series Editor

Methods in Biological Oxidative Stress

Edited by

Kenneth Hensley and Robert A. Floyd
Free Radical Biology and Aging Research Program, Oklahoma Medical Research Foundation, Oklahoma City, OK

Free radicals and reactive oxidizing agents are now recognized as causes or contributing factors in inflammation and other disease states and have become a major focus of interest in pharmacology, toxicology, physiology, and biochemistry. In *Methods in Biological Oxidative Stress*, expert researchers detail their best experimental methods for detecting free radicals and reactive oxygen species or their byproducts. The techniques range from established standard protocols to advanced methodologies using HPLC, mass spectrometry, and electron paramagnetic resonance. The HPLC techniques are applied to the electrochemical measurement of protein oxidation products, particularly nitrotyrosine and dityrosine, and to the electrochemical detection of DNA oxidation products. There are also mass spectrometry methods for measuring lipid oxidation products. Each technique is described in step-by-step detail to ensure robust results, with many presented by the experimenters who have led their development. Useful notes explain the pitfalls to avoid and the chemical principles underlying each method.

Authoritative and highly practical, *Methods in Biological Oxidative Stress* provides laboratory researchers and technicians a unique collection of standard, easy-to-use experimental methods for oxidative stress bioanalysis, plus cutting-edge instrumental techniques using HPLC, mass spectrometry, and EPR spectrometry.

- **Standard methods plus cutting-edge instrumental techniques using HPLC, MS, and EPR**
- **Explanation of the chemical principles behind the methods**
- **Electrochemical techniques for measuring nitration products**
- **Mass spectrometry techniques for measuring lipid oxidation products**

Contents

Methods in Pharmacology and Toxicology™
Methods in Biological Oxidative Stress
ISBN: 0-89603-815-7 E-ISBN: 1-59259-424-7
humanapress.com

ISBN 0-89603-815-7
9 780896 038158 90000